Università degli Studi di Ferrara

DOTTORATO DI RICERCA IN
"SCIENZE DELL'INGEGNERIA"

CICLO XXVIII

COORDINATORE Prof. Stefano Trillo

EXPERIMENTAL ANALYSIS AND NUMERICAL SIMULATION OF A FLAT-PANEL GROUND HEAT EXCHANGER

Settore Scientifico Disciplinare ING-IND/10

Dottorando	**Tutore**
Dott. Bortoloni Marco	Prof. Piva Stefano

Anni 2013/2015

To my father

Abstract

Worldwide, the innovation and environmental policies for energy saving in buildings and the reduction of greenhouse gas emissions have widely supported renewable energy technologies. Ground-source heat pumps (GSHPs) are regarded as a reliable technology and may represent an efficient and cost-effective solution for space heating and cooling, when the investment for ground heat exchangers is reasonable. In ground-coupled heat pump (GCHPs), a subset of GSHPs, a ground heat exchanger is required to thermally couple a heat pump with the ground. The ground heat exchanger usually consists of a piping system installed in vertical boreholes or in shallow diggings. Vertically coupled heat pumps benefit from the relatively stable temperature in the deep ground and uses geothermal energy from the earth. A horizontally coupled heat pump uses the seasonal heat storage in shallow soil therefore, the performance of horizontal ground heat exchangers (HGHEs) is strongly dependent on climatic conditions due to the low installation depth.

A considerable amount of research has been devoted to the performance optimisation of GCHPs, in the last decades. More recently, a number of studies have dealt with the development of new configurations and new geometries for HGHEs, aiming to improve their efficiency. As part of these efforts, this thesis was dedicated to an innovative HGHE, called Flat-Panel, which was invented and developed at the University of Ferrara. This study dealt with the experimental analysis and the numerical simulation of Flat-Panels and it was intended to provide guidance on the behaviour and the performance of this novel HGHEs.

The experimental analysis was carried out by means of a dedicated experimental setup equipped with two Flat-Panel prototypes. Tests were conducted simulating the operation of a GCHP in different operating conditions (heating and cooling) and modes (continuous, discontinuous and pulsed). Very good performance was reached for both heating and cooling mode in comparison with the widespread installations of straight pipes or slinky coils. The performance was higher in heating mode due to the higher temperature difference between the working fluid and the undisturbed soil in summer. Moreover, according to other studies, seasonal thermal drifts were not measured for HGHEs, regardless of the amount of energy exchanged.

The numerical analysis dealt with the simulation of heat transfer in soil due to Flat-Panels. A finite element numerical code was applied solving the unsteady-state heat transfer problem in a 2D domain. In view of this, the Flat-Panel shape was modelled as a boundary condition. In order to further delve into particular aspects of HGHEs behaviour, the different heat transfer processes at the ground surface were modelled on the basis of the surface properties and a comprehensive weather dataset. Furthermore, the effect on numerical simulation of HGHEs of different boundary conditions at the ground surface was analysed. The ground surface ener-

gy balance model (GSEB), the equivalent surface heat flux and temperature were assigned as boundary conditions of the 1st, 2nd and 3rd kind in three different simulations, respectively. The results indicate that the use of the GSEB model is the preferable approach to the problem, not affecting the calculation time. The equivalent surface temperature could be considered as a reasonable simplification, although its correct estimation is a major issue.

The results of the numerical simulation were compared with multiple experimental data sets in different operating conditions. Overall, the model produced a good agreement in terms of ground temperature variation due to the combined effect of the HGHE operation and the heat transfer process at the ground surface. In addition, a sensitivity analysis was carried out to evaluate the effect of variations in soil thermal conductivity.

Abstract

Le recenti politiche ambientali, volte alla riduzione del fabbisogno energetico in edilizia ed alla riduzione delle emissioni di gas clima alteranti, hanno supportato il diffondersi delle tecnologie ad energia rinnovabile. Tra queste, le pompe di calore geotermiche si sono affermate come soluzione alternativa ai tradizionali sistemi per il riscaldamento e raffrescamento degli edifici, in virtù della loro provata affidabilità e dell'elevata efficienza.

Sono attualmente disponibili diverse tipologie di pompa di calore geotermica che possono essere in primo luogo classificate in due sottocategorie: a circuito aperto e a circuito chiuso. Le pompe di calore geotermiche a circuito chiuso sono maggiormente diffuse e sono termicamente accoppiate al terreno, che è la sorgente/pozzo termico, per mezzo di scambiatori geotermici. Questi sono generalmente costituiti da un sistema di tubazioni in materiale plastico, che può essere installato in perforazioni verticali (fino a 200 m di profondità) o in posizione orizzontale all'interno di appositi sbancamenti e trincee superficiali (solitamente fino a 2 m).

Le pompe di calore geotermiche accoppiate a scambiatori verticali beneficiano della favorevole temperatura del terreno alle basse profondità. All'incirca a 10 m dalla superficie infatti il terreno ha una temperatura quasi costante pari alla temperatura media annuale dell'aria, che aumenta all'aumentare della profondità secondo il gradiente geotermico locale. Al contrario, nel caso di scambiatori orizzontali, la pompa di calore è accoppiata termicamente ad una sorgente (il terreno superficiale) la cui temperatura oscilla stagionalmente al variare delle condizioni ambientali. In virtù di ciò, gli scambiatori verticali offrono prestazioni mediamente migliori, tuttavia l'elevato costo, rende comunque competitiva la più economica soluzione orizzontale per applicazioni residenziali di piccola taglia.

Negli ultimi decenni, un considerevole sforzo è stato fatto per l'ottimizzazione delle prestazioni delle pompe di calore geotermiche, sia in ambito accademico che industriale. Di recente sono state sviluppate nuove configurazioni e geometrie per gli scambiatori orizzontali con l'obiettivo di aumentarne l'efficienza di scambio termico. Questa tesi si inserisce in questo ambito, essendo dedicata ad un innovativo scambiatore geotermico di tipo Flat-Panel, inventato e sviluppato presso l'Università degli Studi di Ferrara.

L'analisi delle prestazioni di scambiatori Flat-Panels è stata condotta sia per via sperimentale sia impiegando tecniche di modellazione numerica, nell'intento di fornire indicazioni approfondite sul loro utilizzo in accoppiamento a pompe di calore geotermiche. Allo scopo è stato allestito un apparato sperimentale equipaggiato con due prototipi di Flat-Panel, presso il Dipartimento di Architettura dell'Università di Ferrara. Sono stati condotti diversi test simulando il funzionamento di una pompa di calore geotermica in differenti condizioni operative (riscaldamento e raffrescamento) e in diverse modalità (funzionamento continuo, disconti-

nuo e pulsato). Con rifermento ai più comuni scambiatori orizzontali, il Flat-Panel ha fornito prestazioni molto buone sia in riscaldamento che raffrescamento. In particolare, un'ottima prestazione è stata ottenuta durante i test estivi, in virtù della maggiore differenza di temperatura tra il fluido termovettore ed il terreno termicamente indisturbato. Come riportato in letteratura in merito agli scambiatori orizzontali, anche per i Flat-Panels non sono stati osservati fenomeni di deriva termica nel terreno superficiale, indipendentemente dall'energia scambiata.

L'analisi numerica ha riguardato la modellazione dello scambio termico nel terreno per mezzo di scambiatori di tipo Flat-Panel. Allo scopo è stato impiegato un modello numerico agli elementi finiti risolvendo lo scambio termico in regime transitorio in un dominio bidimensionale. Nel dominio di calcolo la particolare geometria del Flat-Panel è stata ricondotta ad una condizione al contorno. È stato inoltre sviluppato un modello del bilancio di energia alla superficie del terreno (condizione al contorno del terzo tipo) al fine di simulare dettagliatamente la variazione giornaliera e stagionale della temperatura del terreno superficiale, che è determinante per le prestazioni degli scambiatori orizzontali. In considerazione di ciò, l'analisi è stata approfondita con ulteriori simulazioni per valutare l'effetto sulla soluzione numerica di differenti condizioni al contorno alla superficie del terreno: il modello del bilancio di energia, un flusso termico equivalente ed infine una temperatura superficiale equivalente. I risultati indicano che l'utilizzo del modello del bilancio di energia è l'approccio da preferirsi, senza che questo comporti un particolare aggravio in termini di tempo di calcolo. L'utilizzo di una temperatura equivalente è una ragionevole semplificazione, sebbene la sua stima corretta sia piuttosto complessa.

I risultati del modello numerico proposto sono stati confrontati con i dati sperimentali ottenuti durante i test in diverse condizioni operative. Complessivamente il modello si è dimostrato affidabile nel calcolo della variazione di temperatura nel terreno determinato dall'effetto combinato dello scambio termico alla superficie del terreno e allo scambiatore. Infine, è stata svolta un'analisi di sensitività per valutare l'effetto della variazione della conduttività termica del terreno.

TABLE OF CONTENTS

LIST OF TABLES

x

LIST OF FIGURES

Nomenclature

Acronyms

ASHP	Air-source heat pump
DXHP	Direct-exchange heat pumps
FP	Flat-Panel
GCHP	Ground-coupled heat pump
GHE	Ground heat exchanger
GSEB	Ground surface energy balance
GSHP	Ground -source heat pump
GWHP	Ground-water heat pump
HGHE	Horizontal ground heat exchanger
RHT	Rate of heat transfer
RTD	Resistance temperature detectors
SCW	Standing column well
SWHP	Surface-water heat pump
TRT	Thermal response test
VGHE	Vertical ground heat exchanger

Symbols

A	annual amplitude of the air temperature	(°C)
c_p	specific heat at constant pressure	(J/kgK)
d	zero plane displacement height	(m)
D_0	Julian day with the minimum temperature	
DD	degree days	
D_h	hydraulic diameter	(m)
e_a	actual vapour pressure	(kPa)
$\dot{E}_{in}$	rate of energy transfer into a control volume	(W)
$\dot{E}_{out}$	rate of energy transfer out of control volume	(W)
EP	standardised energy requirement	(W/m^3)
e_s	saturation vapour pressure	(kPa)
ET_0	reference crop evapotranspiration	(mm/day)
F_c	heat pump part load factor for cooling	
F_h	heat pump part load factor for heating	
G	soil heat flux	(W/m^2)
G	soil heat flux density	(MJ/m^{2}day)
h	convection heat transfer coefficient	(W/m^{2}K)
H	sensible energy flux	(W/m^2)
h	specific enthalpy	(kJ/kg)

hh	daily operating hours of heating/cooling system	(h)
k	thermal conductivity	(W/mK)
k	von Karman constant	
K_c	crop coefficient	
LE	latent energy flux	(W/m^2)
l_h	latent heat of evaporation	(kJ/kg)
$L_{h,p}$	overall lengths of pipe for heating	(m)
$L_{h,p}$	overall lengths of pipe for cooling	(m)
$\dot{m}$	mass flow rate	(kg/s)
P_m	coefficient related to the pipe diameter	
Q	heat transfer rate	(W)
$Q_{g,cD}$	power for cooling	(W)
$Q_{g,hD}$	power for heating	(W)
R	net radiative energy flux	(W/m^2)
r	ratio of the plenum to the total building volume	
r_a	aerodynamic resistance to heat transfer	(s/m)
R_e	Reynolds number	
R_g	ground resistance	(mK/W)
R_{ld}	downward longwave solar radiation	(W/m^2)
R_n	net radiation at the crop surface	(MJ/m^{2}day)
R_p	pipe resistance	(mK/W)
R_s	shortwave solar radiation	(W/m^2)
S	heat transfer surface	(m^2)
S/V	building shape ratio	(m^{-1})
s_f	calibration coefficient of shading	
S_m	coefficient related to the distance between the trenches	
t	time	(s)
T	temperature	(K)
$T_{g,H}$	maximum ground temperature at the average depth of the GHE (cooling)	(°C)
$T_{g,L}$	minimum ground temperature at the average depth of the GHE (heating)	(°C)
T_{wi}	design temperature of the working fluid entering into the GHE	(°C)
T_{wo}	design temperature of the working fluid leaving the GHE	(°C)
$\hat{U}$	overall heat transfer coefficient	(W/m^{2}K)
u_2	wind speed at 2 m	(m/s)
u_z	wind speed at height z	(m/s)
V	fluid velocity	(m/s)
v	mean fluid velocity	(m/s)
V	total building volume	(m^3)

$\dot{W}$	rate at wich work is performed	(W)
z	height of measurement above the ground surface	(m)
z_h	height of humidity measurements	(m)
z_m	height of wind measurements	(m)
z_{oh}	roughness length for transfer of heat and vapour	(m)
z_{om}	roughness length for momentum transfer	(m)

Greek Letters

μ	dynamic viscosity	(kg/s·m)
Δ	slope vapour pressure curve	(kPa/°C)
α	themal diffusivity	(m^2/s)
α	albedo	
ε_s	surface emissivity	
ρ	density	(kg/m^3)
σ	Stefan-Boltzmann constant	(W/m^{2}K^4)

1.   INTRODUCTION

1.1   Ground Source Heat Pumps

Nowadays, the reduction of greenhouse gas emissions and the rational use of energy have become a major issue. Worldwide, the great opportunity for energy saving in the buildings sector has been recognised. For the above reasons, recent environmental policies have promoted the energy efficiency of buildings and the spread of renewable energy technologies. Among them, ground source heat pumps (GSHPs) (also referred to as geothermal heat pump systems or earth energy systems) are regarded as a viable and environmentally-friendly energy source if carefully designed for residential and commercial heating and cooling applications.

The first heat pump using the ground as a heat source dates back to a Swiss patent (Heizverfahren, CH59350) issued in 1912 (Zoelly, 1912). However, research on this technology intensified after the Second World War, both in the US and the EU. At that time, the basic analytical theory for a GSHP system (Ingersoll & Plass, 1948) was developed applying the line source model to the design of a ground heat exchanger and thus laying the foundations for some future design models. The commercial use of GSHPs began after the oil crisis in 1973 in the US and in Northern Europe, driven by the advances in heat pump efficiencies and operating ranges. These systems are being increasingly applied in recent years, as an alternative to conventional heating systems (electricity or gas boilers) with significant savings in terms of primary energy. Moreover, a single heat pump can provide thermal energy for space heating/cooling and domestic hot water production, without the need for separate systems. One of the major advantages of GSHPs is their worldwide applicability and versatility related to the use of the ground as a heat source. What's more, they do not require fractured rock and water as for a conventional geothermal reservoir.

GSHPs rely on the thermal energy availability in the shallow ground, which is related to the ground temperature and its heat capacity. In terms of temperature, three different ground zones can be distinguished (Popiel, et al., 2001): *surface zone*, *shallow zone* and *deep zone*. In the shallow zone (up to a depth of 1 m), the ground temperature is very sensitive to short time changes of weather conditions. Up to a depth of about 10 m and depending on the geological conditions, the ground temperature shows daily and seasonal fluctuations related to air temperature variations. Moreover, the ground surface cover (e.g. bare ground, lawn, snow) also has a significant effect on the temperature at shallow depth.

As depth increases, the effect of temperature fluctuations of the ground is reduced. Below 10 m and up to a depth of 20 m the temperature remains relatively constant throughout the year, due to high thermal inertia of the soil. The annual average temperature differs depending on the location and it is approximately equal to the average annual air temperature (Hart & Couvillion, 1986). In northern

Italy, the temperature of the ground at depths between 10 m and 20 m is nearly constant and equal to 13-15 °C. Below this zone, the temperature begins to rise according to the natural geothermal gradient, on average by about 3 °C every 100 m (Grant, et al., 1982). The natural temperature distribution at shallow depths is shown in Fig. 1.1.

For the above reasons, if compared to the widespread air source heat pump (ASHP) systems, the GSHP technology can achieve higher energy efficiency because the ground, used as a heat source/sink, provides more favourable temperature and fewer fluctuations than ambient air temperature. Additionally, in GSHP systems the thermal energy is usually transferred through water, which is a more desirable heat transfer medium than air. However, GSHPs have higher purchase and installation cost than air-source systems due to the cost of the ground heat exchanger.

GSHP systems consist mainly of three components: the heat and cooling distribution system on the building side, the heat pump, and the coupling with the ground. In the last decades several typologies of GSHPs have been developed to use the ground, ground water or surface water as a heat source and sink. Depending on the ground-coupling, GSHPs have been basically classified by ASHRAE (1999) in three categories, ground-coupled heat pumps (GCHPs), surface-water heat pumps (SWHPs) and ground-water heat pumps (GWHPs), as shown in Fig. 1.2. The latter, also referred to as open loop systems, uses the ground-water as the working fluid which is pumped directly from a water well to the heat pump and then reinjected to the aquifer via a second well. GWHPs first appeared in the 1940s and thereafter have been installed successfully due their simplicity and efficiency.
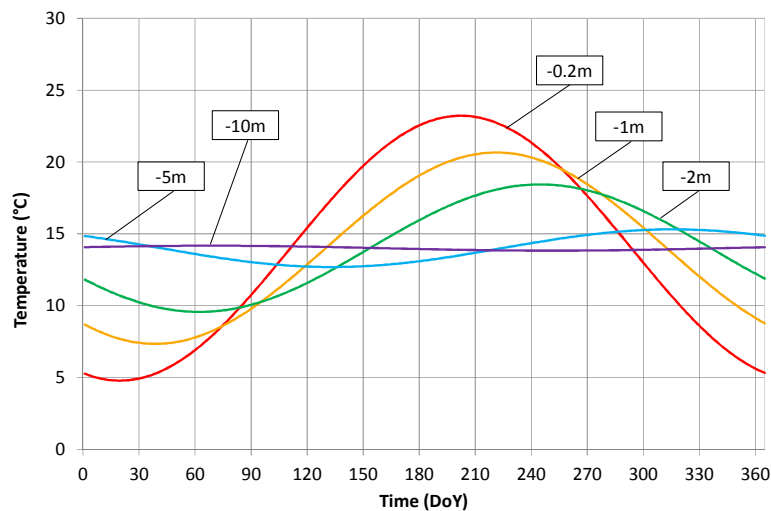
Fig. 1.1 Natural near-surface temperature variation at depth.

Ground-Coupled Heat Pumps
closed loop

vertical   horizontal

Ground-Water Heat Pumps
open loop

Dispose
to pond,
lake, river

Surface-Water Heat Pumps
lake or pond loop

indirect   direct

pond   pond
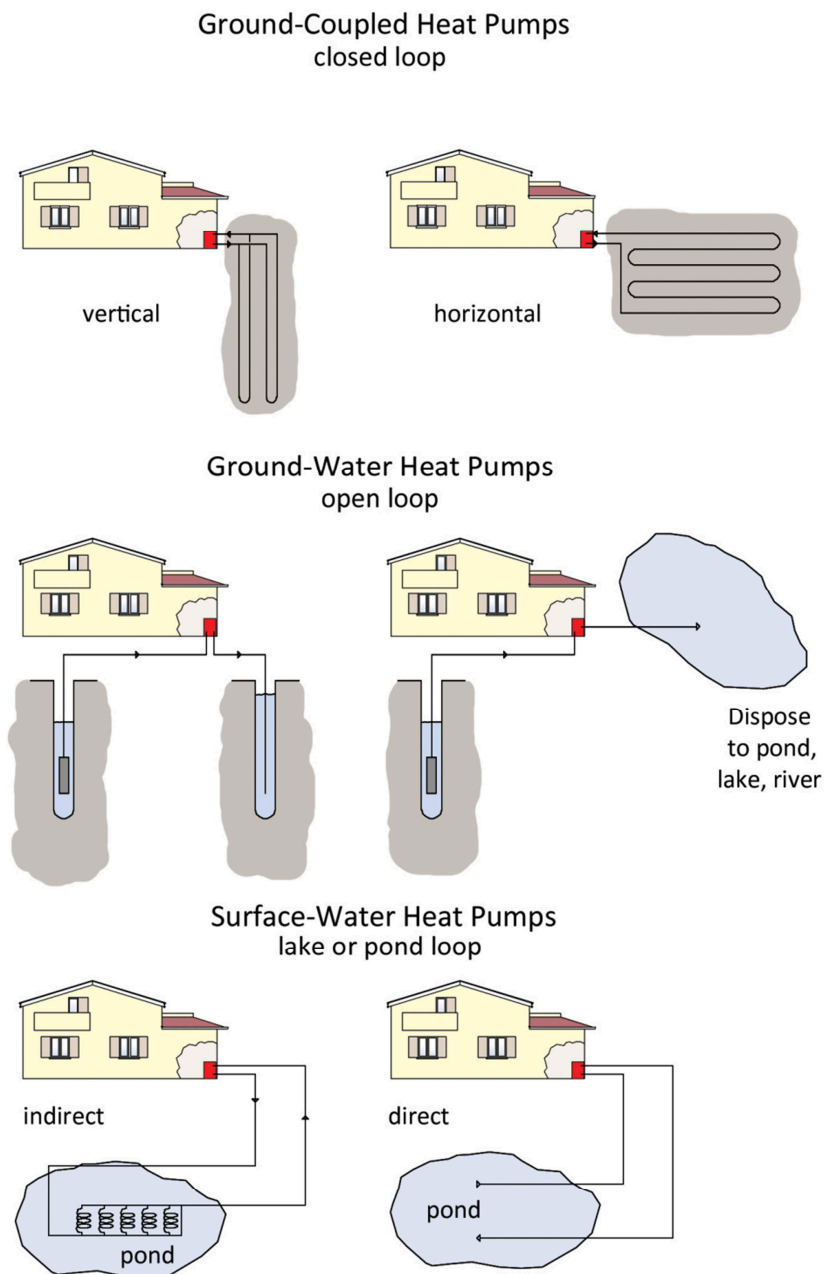
Fig. 1.2 Typologies of ground source heat pumps.

These systems have some advantages over other GSHPs, such as the low initial cost. However, their applicability depends on the availability and chemical quality of ground-water, and also it might be limited by the local environmental regulations. A different typology of GWHPs named standing column well (SCW) are receiving increasing attention although the applicability is limited by the need of a large amount of ground water supply. In these systems, the water is drawn from the bottom of a standing column of water and returns to the top of the same well. Conversely, GCHPs and SWHPs are closed loop systems, in which the heat transfer fluid (usually water or a water/antifreeze solution) flows in a loop of pipes buried in the ground or submerged in the water of a lake or pond.

Most of the GSHPs installed at present are GCHPs and this technology is also prevailing in the market due to their widespread applicability. Moreover, a growing interest among researchers is focused on the ground heat exchangers (GHEs), which are recognized as the least efficient component of these systems, and as the one with the highest effect on the initial cost.

1.2   Ground Coupled Heat Pumps

GCHP systems consist of a water-to-air or a water-to-water heat pump, which is thermally coupled with the ground by means of a ground heat exchanger (GHE). The thermal mass of the ground is used as a heat source or sink, without underground water extraction. Compared to GWHPs, the GCHPs do not have environmental problems due to ground water quality and availability and also require much less pumping energy. GCHP systems are easily applicable and can be installed almost at any location where drilling or earth trenching is feasible. The GHEs usually consists of a piping system buried in the earth through which a heat transfer fluid circulates. The working fluid pumped in the closed loop is either pure water or an antifreeze solution (usually water/glycol). A GHE typically operates from 0°C to 35°C, thus an antifreeze solution will be required to prevent freezing in the heat pump heat exchanger during the heating period. However, the use of glycol has some drawbacks related to its toxicity in case of seepage in to soil and to the viscosity at low temperatures resulting in higher energy consumption for pumping.

The piping system of the GHE is usually made of high-density polyethylene (HDPE) installed in vertical boreholes drilled down up to a hundred meters depth or in shallow horizontal trenches a few meters below the ground surface. Thus, the ground heat exchangers in GCHPs are divided in VGHEs and HGHEs according to their arrangement, as discussed in sections 1.2.1 and 1.2.2, respectively. The GHE accounts for a great portion at the total cost of a GCHP and primarily drives the energy performance of the system. Therefore, the configuration of the GHEs must be chosen, and then sized accurately, taking into account the peak heating and cooling loads, the annual energy balance and the capacity of the ground to absorb or provide heat. If the thermal load in winter (or in summer) is prevalent, the over-

sizing of the ground heat exchanger may be necessary to avoid the progressive cooling (or heating) of the ground and thus a decrease in the system performance.

In order to reduce the initial cost, the integration of the ground heat exchangers with structural pile foundations have been recently tested. In these systems, named energy piles, the working fluid circulates in pipes embedded in the concrete structural element which is in direct contact with the ground. With energy piles the investment for the GHEs is reduced. However, the applicability of this technology is limited only to new buildings, and the system design is significantly complicated in comparison with other GSHPs.

For small size systems, direct-exchange heat pumps (DXHPs) have been diffused as an alternative typology of GCHPs. In these systems the refrigerant is distributed through a copper tube that is buried in the ground in a horizontal or vertical configuration. DXHPs rely on a single heat transfer stage and do not need a circulating pump. However, the heat pump requires a larger compressor than traditional GCHPs. Although these systems perform better in moist soils, they cannot be installed in corrosive soil.

1.2.1 Vertical Ground Heat Exchangers

Among the GHE configurations available for GCHPs, the vertical one is the most widespread installation in central and northern Europe, and in the US as well. The vertical configuration takes advantage of the relatively constant year-round temperature of soil at a depth of 10-15 m below the ground surface, and from the local geothermal gradient below this depth. In vertical GCHP systems, the ground heat exchanger configurations typically consist of one or more boreholes within which the closed-loop plastic pipes are installed. After the pipe is installed, the borehole is backfilled with a cement-bentonite grouting that prevents the migration of contaminants into the ground water system and ensure the optimal thermal contact with the ground.

The depth of the vertical GHEs (VGHEs) depends on the specific geological, hydrological, and spatial characteristics. Boreholes are typically drilled 50 m to 350 m deep with a diameter ranging from 100 mm and 200 mm. Several arrangements have been tested and used for the pipes within the boreholes, as shown in Fig. 1.3. The widespread typologies of VGHEs are:

• U-tubes (single or double): two straight pipes are connected at the bottom with a U-bend. In double U configurations two single U-tubes are inserted in a single borehole. Typical U-tubes are made of high-density polyethylene (HDPE) and have a diameter in the range of ¾ in. (19 mm) to 1 ½ in. (38 mm).
• Coaxial tubes: two pipes of different diameter installed in each other. The working fluid circulates to the ground in the annulus and returns to the heat pump thorough the inner pipe.

The U-tubes solution (both single and double) is the most reliable and commonly used in the market. A borehole with double U-tubes has a lower thermal resistance than a single one, but also higher thermal interference between flow and return pipes. Coaxial tubes are not widespread and the technology is still under development. However, this GHE configuration is promising because it would allow a borehole length reduction and thus reduce the overall cost of the system (Raymond, et al., 2015). While the installation of a U-tube is achievable with current tools and expertise, that of coaxial configuration is difficult and requires further investigation.

A single borehole might be adequate for residential applications with small heating/cooling loads. Multiple boreholes are generally required for larger loads. Multiple geothermal wells are arranged in grids with an adequate separation distance (Kavanaugh & Rafferty, 1997) (not less than 4.5 m) to reduce the thermal interactions between single boreholes. Large thermal interaction can result in a reduced efficiency of the GHEs and thus increasethe total borehole length needed for a given heat load profile.

Drilling inclined boreholes has recently been proposed as a possible solution to reduce the thermal interference. The inclined configuration can improve the energy performance of GHEs especially for the GCHP systems with imbalanced annual loads (Ping, et al., 2006). Moreover, where the land surface for installation is limited, with inclined arrangements a single shallow plumping manifold is possible for several boreholes.
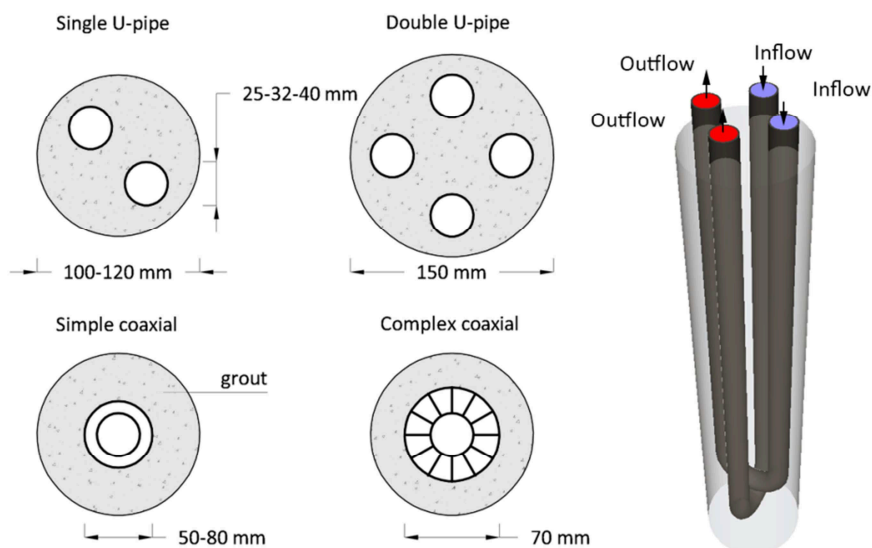
Fig. 1.3 Cross-sections of different types of borehole heat exchangers.

The proper sizing of the ground heat exchanger length is a fundamental task in the design of a reliable and effective GCHP system. In GCHP systems the closed-loop is the most expensive component and there is little economy of scale unlike the heat pump equipment (Kavanaugh & Rafferty, 1997). For years, the practice of oversizing has been applied to avoid the GHEs not fulfilling their design loads after the first few years of operation. This has decreased the competitiveness of GCHPs in comparison with conventional heating and cooling systems. In the last few decades, research efforts have produced several methods and commercially available design software tools for the sizing of GHEs based on principles of heat transfer: (Ingersoll & Zobel, 1954); (Kavanaugh, 1984); (Eskilson, 1987) (IGSHPA, 1991); (Spitler, et al., 1996); (Kavanaugh & Rafferty, 1997).

The design of vertical ground heat exchangers is complicated by a variety of factors. The thermal performance of VGHEs are strongly affected by the local geological formations and the properties of different soil layers. However, a proper sub-surface characterization is not always economically feasible. Moreover, the presence of ground-water flows makes the design more complex and should be considered. Although in general the ground-water flow affects positively the thermal performance of GCHP systems, it could increase the thermal interactions in a multiple borehole GHEs.

A fundamental task in the design of VGHEs is the proper assessment of seasonal heating and cooling loads. A substantial difference between the heat released and extracted annually to and from the ground may result in a temperature rise or fall in the ground over a number of years, and thus in an efficiency reduction of the system.

Another challenge in the design of GCHP systems arises from the fact that most commercial and institutional buildings, even in moderate climates, are generally cooling dominated and therefore give more heat to the ground than they extract over the annual cycle. This load imbalance may require the heat exchanger length to be significantly greater than the length required if the annual loads were balanced. This has given rise to the concept of "supplemental heat rejecters" or so-called "hybrid GSHP systems". Supplemental heat rejecters have been integrated into building designs to effectively balance the ground loads and therefore reduce the necessary length of the ground-loop heat exchanger. In cases where the excess heat cannot be used beneficially, conventional cooling towers can provide a cost-effective means to reduce heat exchanger length although, the design of these supplemental components adds to the challenge of designing the overall hybrid GCHP system (Chiasson, 1999).

1.2.2 Horizontal Ground Heat Exchangers

Horizontal ground heat exchangers are the primary focus of this thesis. Therefore, the topic will be addressed in detail in the following sections of this chapter,

with particular attention to the new challenges that this promising technology is facing, laying the foundation for the purpose of this study.

In horizontal GCHPs, the ground heat exchanger is installed in the upper 2 m of the ground soil. In most cases they are used in small scale systems (single/ two family houses) as well as small industrial applications.

The horizontal ground heat exchanger typically consists of a series of parallel pipes, laid in dug trenches or horizontal boreholes. Anyway several different pipe arrangements are possible, as illustrated in Fig. 1.4. The simplest, but also the least-efficient, is a single pipe (or multiple pipe, up to six) embedded in a linear trench. This solution, however, requires a large land area and for this reason it has been used mainly in North America. In Europe, due to restrictions in the available area, the pipes are usually laid in a relatively dense pattern, connected either in a series or parallel. In the series connection, a single closed-loop is embedded in the ground according to a predetermined path. In the parallel connection, the supply and return pipes of the individual pipe loops are combined in collecting and distribution manifolds and routed to the heat pump. The pipes are usually laid at distances of 0.5 m to 0.8 m, according to the pipe diameter and thermal load. Typically, about 35 to 55 m of pipe are installed per kW of heating and cooling capacity. When the land area is limited, the required total length of trench can be reduced of 20 % (Canada), by fitting the pipe as a series of overlapping coils (sometimes referred to as a slinky). The slinky coils are usually placed vertically in a narrow trench or horizontally at the bottom of a wider trench. This arrangement reduces the amount of land used but requires more pipes (up to double), which may result in additional costs. In order to increase the heat transfer surface, the installation of capillary tube mats has been recently introduced, in analogy with that used in radiant floor systems. These collectors are suited for heat pump systems for heating and cooling, where natural recharge of the ground is not vital.

In the first applications, a metallic piping was used but, it has been progressively abandoned due to the high cost and corrosion problems. A copper-clad plastic is still in use for direct expansion horizontal systems (12 mm - 15 mm in diameter). High-density polyethylene is commonly used, because it is flexible and can be joined by heat fusion. The pipe diameter is usually from 20 mm to 40 mm, large enough to avoid pressure drop resulting in higher costs for pumping. Since the heat transfer rate for GHEs is usually low, the low thermal conductivity of these materials is not particularly disadvantageous.

The GCHP systems coupled with HGHEs use the shallow soil mainly as a seasonal source/ sink of heat. In winter, when the solar radiation is reduced and air temperature is low, the GCHP systems need the highest energy output (and vice versa in summer). Their performances are thus strongly affected by the climatic conditions, due to the low installation depth of the ground heat exchanger. In fact, at a depth between 1 m and 2 m, the temperature of the soil can in fact vary of course also of $\pm$ 5 °C, as shown in Fig. 1.1.

Straight pipe in trench
(single)

Straight pipes in trench
(multiple)

Straight pipes
(connection in series)

Straight pipes
(connection in parallel)

Slinky coils
(horizontal or vertical)

Trench collector
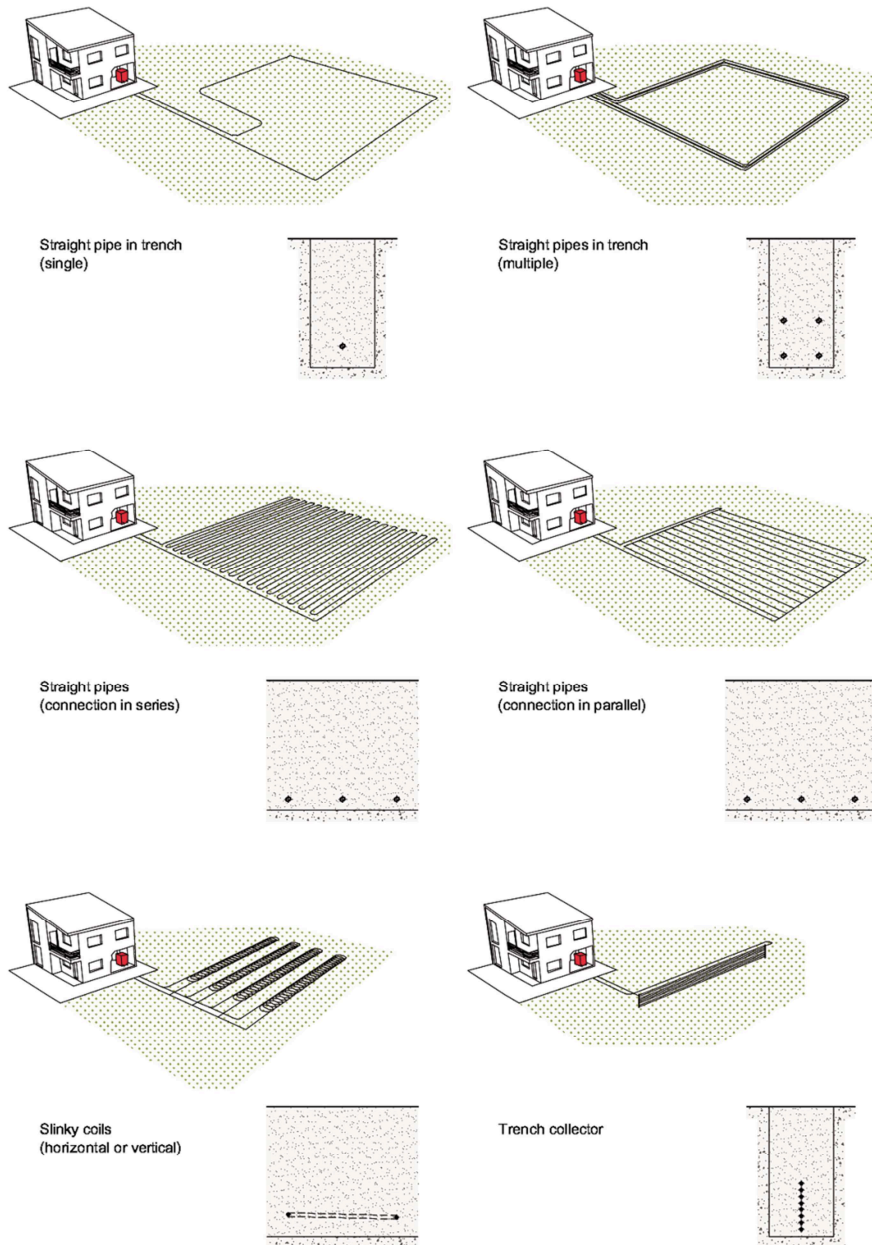
Fig. 1.4 Various configurations of Horizontal Ground Heat Exchanger (HGHE)

The seasonal variation of the soil temperature can lead to unfavourable working conditions and, consequently, to an efficiency reduction. Nevertheless, the close dependence on environmental conditions allows avoiding ground thermal drifts after long-term operations for shallow HGHEs (Gan, 2013). Among other factors in fact, solar radiation is the main source of seasonal recharge of energy in the ground, being absorbed by approximately 46 % by the earth and thus it almost deletes the effect of the horizontal heat exchangers. Moreover, the soil moisture content (via natural groundwater, rain or melting snow) also has a significant effect as dry, loose soil has a lower thermal conductivity than moist, packed soil. Consequently, the horizontal solution is not feasible under buildings or in covered areas.

For these reasons, the sizing of horizontal ground heat exchangers is a difficult task. The ground loop must be sized to meet the peak thermal load (in heating and cooling) and the thermal load seasonal trend. The length of pipe required depends also on the structure and physical properties of soil and on the loop configuration. In horizontal systems, the more pipe is buried per unit length of trench (e.g. slinky coil), the greater is the energy output, due to the higher heat transfer surface. But this also results in an increased thermal interference between the pipes. The performance of a ground heat exchanger is usually expressed as the amount of thermal power exchanged with the ground per unit of length : as a function of pipe length for horizontal loops or of trench length for slinky coils. The heat exchanged will essentially depend on the temperature difference between the working fluid and the natural ground temperature at the average depth of the GHE. An accurate sizing is usually performed with specific dynamic simulation software, the accuracy of which have been verified using monitored data. However, for small to medium size systems there are simplified and reliable methods. The Italian guidelines on the sizing of horizontal ground heat exchanger (UNI 11466, 2012) are detailed in the following paragraph 1.3.

The horizontal installation holds some advantages in terms of costs and installation. Despite the large area required, the excavation process remains fairly straightforward, local operators can usually be employed and the excavated soil can be directly used for backfilling. Moreover, since HGHEs are installed at shallow depths, the geologic characterisation is relatively easy. On the contrary, vertical exchangers are more expensive than horizontal but have higher thermal efficiency and require less pipe and pumping energy. Anyway, an over-conservative design approach is feasible for horizontal systems, due to the relatively low installation cost of the embedded piping. A comparison between HGHEs and VGHEs is reported in Tab. 1-1. Horizontal ground heat exchangers have received much less attention than verticals with respect to research efforts last decades. This may be related to the fact that in large applications VGHEs are preferred due to the less ground area required. Anyway, as regards the horizontal technology, new arrangements for the widespread slinky coils and a number of exchangers with novel shapes have been recently proposed (e.g. baskets, radiators).

Tab. 1-1 Comparison between horizontal and vertical installation.

	Horizontal GHE	Vertical GHE
Performance	↓	↑
Building cost	↑	↓
Building equipment	–	↓
Maintenance	↑	–
Building permission	↑	–
Soil use restriction	–	↑
Ground water contaminant risk	↑	–
Design	↓	–
Number of Installations	↓	↑

These innovative solutions aim to achieve higher performance than the wide-spread installation of straight pipes, basically increasing the heat transfer surface with the same trench length. This thesis is focused on a new type of horizontal heat exchanger, invented and patented in 2012 at the University of Ferrara.

1.3   The Design and Modelling of Horizontal Ground Heat Exchangers

An horizontal GCHP systems share some issues in terms of design approach with the vertical ones. The application of horizontal heat exchangers is mainly dedicated to heating/cooling systems for residential or commercial buildings of a small size, due to the large ground area required to cover a given heat load. As a consequence, a complete and detailed thermal analysis is not always economically feasible during the design phase.

The correct design approach for the horizontal heat exchangers should take into account for several factors, among which the characteristics of the installation site are particularly important.

Firstly, the weather variables (i.e. the local climate), lead the temperature trend of the shallow ground layers. Among these, the effect of incident solar radiation at the ground surface is the most significant heat gain. Its effect is related to the morphological characteristics of the site: open or shaded, flat or inclined. Furthermore, it is dependent on the surface covering that will be maintained on site after the GHE installation.

Rainfall also has a significant influence on the HGHE performance, because the moisture content increases the effective heat capacity and changes the thermal conductivity of shallow soils. Even wind conditions affect the ground temperature of the ground, although its effect is complex to estimate, particularly with a grass surface cover. In general terms, temperate climate, which is characterised by the

absence of extremes of temperature in both winter and summer, is the most favourable for horizontal applications.

Secondly, the thermo-physical properties of the soil (i.e. effective heat capacity and thermal conductivity) affect the performance of horizontal exchangers. Shallow soil in fact, is an heterogeneous compound of rock particles, organic matter and water, contrary to rocks. Furthermore, the solid part can vary significantly in composition and particle size, especially in historically inhabited areas. This aspect affects the ability of the soil to retain moisture and allow its migration through the solid particles. The higher the water content, the higher the heat capacity and thermal conductivity of the soil, since the air content is reduced. The presence of groundwater flow at shallow depths greatly improves the heat transfer. What's more, the organic matter component can further improve the thermal properties of the soil if the conditions are damp or saturated, although its thermal properties are poor when dry.

Horizontal ground heat exchangers are usually installed on land which can be easily dug and moved, such as loamy and sandy soils. These soils are not particularly favourable for heat transfer and their thermal properties improve significantly if the water content increases. Considering all these factors, the type of ground cover plays an important role in regulating both the content of water in the soil and the effect of weather variables on the temperature of the ground.

For systems designed to satisfy both the energy requirement for heating and cooling, the most important feature of the ground cover is the permeability to water and moisture. Soil moisture in fact, naturally tends to move to areas at lower temperature and pressure. Consequently, when the ground heat exchanger is used to provide cooling (so heating the ground), the ground around it tends to dry out thus reducing the GHE performance. Grass and low vegetation are commonly used as ground cover, and no evidence has been found of an interference between the operation of HGHEs and vegetated surfaces.

On the other hand, an important aspect is the choice of the configuration of the ground heat exchanger. Contrary to vertical installation in fact, there are several possible configurations for shallow exchangers (e.g. straight pipes or slinky coils) as reported in Fig. 1.4, and their performance varies considerably (Chiasson, 2006). As a consequence, the overall length of GHE needed to satisfy a specific energy requirement will be higher or lower according to the considered configuration.

The starting point of the design procedure is the calculation of both heating and cooling loads, and clearly the GHE must be sized to cover the highest among them. In addition, the load factor must be considered in the design, intended as the heat pump running hours on a daily basis.

For a given energy demand and HGHE length, the near to one is the load factor, the higher the thermal solicitation on the ground. As a consequence, the heat exchanger should be properly sized to maintain favourable working conditions in terms of the temperature of the working fluid.

As for vertical ground exchangers, simplified methods are available for a preliminary design of the horizontal ground heat exchanger in small scale GCHP systems by means of monograms and tables. The monogram provided by the Swiss Society of Engineers and Architects (SIA) and reported in Reuss & Sanner (2001) is shown in Fig.1.5. It allows the preliminary calculation of the total pipe length for heat pumps up to 20 kW. Depending on the soil type and the exposure to solar radiation of the site, the heat extraction rates are expressed for ground surface area unit and vary from 10 W/m^2 to 40 W/m^2. In recent years, multiple-pipe configurations installed in horizontal trench have received more attention. Although requiring more length of pipe, this configuration requires less ground area and diggings, and therefore frequently less cost. As reported in DOE (2001) the trench lengths can range from 8.7 m/kW to 34.6 m/kW, depending on soil characteristics and moisture content, and the number of pipes in the trench.

These data and methods should not be used for the final and precise design of the HGHEs, because they are based on local experience and therefore they are not directly applicable to different climatic conditions and soils.

In November 2012, Italian legislation on the design and sizing requirements for GSHP systems was published (UNI 11466, 2012). As regards the design of horizontal ground heat exchangers, it refers to the method recently provided by the International Ground Source Heat Pump Association (IGSHPA, 2009). The design method is a simplification of that presented in Kavanaugh & Rafferty (1997) for VGHE, which is based on the solution of the equation for heat transfer from a cylinder buried in
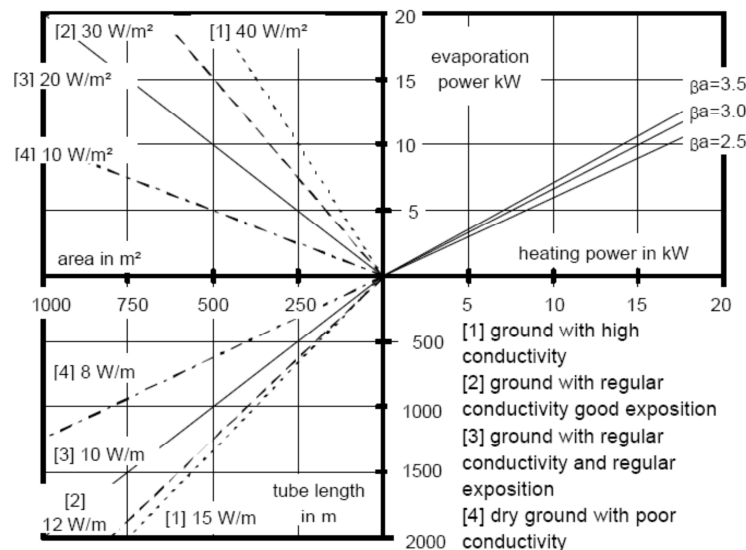
Fig. 1.5 Nomogram for sizing horizontal ground loops (SIA, 1996) (Reuss & Sanner, 2001)

the ground, developed by Carslaw & Jaeger (1947) and firstly suggested by (Ingersoll & Zobel, 1954) as an appropriate method of sizing ground heat exchangers. For horizontal exchangers in fact, the method does not take into account an eventual long-term effect on the ground thermal field due to a thermal imbalance between the heat extracted from the ground and the heat rejected to the ground. The analytical approach is useful to calculate the overall length of pipe to be installed in ground heat exchangers according to different arrangements (e.g. straight pipes and slinky coils) with a trench installation. In these cases, calculations are performed for extreme circumstances, called the "design conditions", when the heating/cooling loads are maximum and the ground temperatures are minimum/maximum respectively. In Southern Europe, these conditions usually occur in January/February and July/August, according to the local climate.

The design lengths for the heating and for the cooling season, are defined as:

$$L_{h,p} = \frac{\dot{Q}_{g,hD} \cdot \left(R_p + R_g \cdot P_m \cdot S_m \cdot F_h\right)}{T_{g,L} - \left(\dfrac{T_{wi} + T_{wo}}{2}\right)_{hD}} \tag{1.1}$$

$$L_{c,p} = \frac{\dot{Q}_{g,cD} \cdot \left(R_p + R_g \cdot P_m \cdot S_m \cdot F_c\right)}{T_{g,L} - \left(\dfrac{T_{wi} + T_{wo}}{2}\right)_{cD}} \tag{1.2}$$

where:

$L_{h,p}$ and $L_{c,p}$ are the overall lengths of pipe for heating and cooling respectively (m)
$Q_{g,hD}$ and $Q_{g,cD}$ are the power for heating and cooling (W)
R_p the pipe resistance (mK/W)
R_g the ground resistance (mK/W)
P_m coefficient related to the pipe diameter (diameter different of ¾ '')
S_m coefficient related to the distance between the trenches
F_h and F_c are the heat pump part load factor for heating and cooling respectively
$T_{g,L}$ minimum ground temperature at the average depth in heating season (°C)
$T_{g,H}$ maximum ground temperature at the average depth in cooling season (°C)
T_{wi} design temperature of the working fluid entering into the GHE (°C)
T_{wo} design temperature of the working fluid leaving the GHE (°C)

The values of R_p, R_g, P_m and S_m are determined from physical and geometrical considerations and depend on the considered configuration of the ground heat exchanger, which are listed in tables provided by the Standard.

One of the key parameters is the undisturbed ground temperature. The design method in fact, requires knowledge of the minimum and maximum ground temperature at the HGHE depth. The annual variation of daily average soil temperature at different depths can be estimated using a sinusoidal function (UNI 11466, 2012). The method is based on the correlation firstly developed by Kusuda & Achenbach

(1965) under the assumptions that the ground can be considered a semi-infinite solid, and that the surface boundary condition can be described by a sinusoidal temperature variation. This approach is frequently used by commercial software dedicated to the sizing of the geothermal exchangers. Sometimes, it has been applied as a boundary condition to carry out simulations by means of numerical codes, which aimed at the study of the HGHE performance. However, the approach is based on some simplifying assumptions limiting its accuracy: the ground surface temperature is equal to that of the air and has sinusoidal evolution; the effect of solar radiation is negligible.

The temperature of the working fluid is also a critical parameter in the design and performance of the ground heat exchangers. On the one hand, a high difference between the average temperature of the working fluid and the undisturbed temperature of the ground allows a reduction in the dimensions of the geothermal heat exchanger. On the other hand, this could lead to a higher and faster alteration in the thermal field of the surrounding ground and consequently to a decrease of the efficiency of the heat pumps. On the contrary, a low difference between them allows higher efficiency of the heat pump and lower energy consumption, but it will result in a bigger ground heat exchanger, which is among the most expensive components of a GCHP system. Moreover, the minimum and maximum fluid temperature at the HGHE outlet are limited in range for practical constraints of the heat pumps. In order to obtain a properly sized HGHE and an high heat pump efficiency, a difference in the range of $6 \div 11$ K between temperature of the fluid leaving the HGHE and the undisturbed soil temperature is recommended by ASHRAE (2007) and in UNI 11466 (2012) in the heating season. The recommended range for the cooling operation is higher and varies within the range $11 \div 17$ K.

Although widely applied, one of the limitations of this approach is related to the theory of the cylindrical source, which makes it directly applicable only to straight pipes configurations of HGHE. It has been extended to slinky coils by means of an equivalence with one of the provided configurations. However, new concepts of horizontal ground heat exchangers have been developed in recent years in order to increase the heat exchange surface per unit of trench length.

Moreover, the behaviour of an horizontal GCHP system is relatively complex and is time and temperature dependent. As a consequence, for detailed analysis and simulation purposes, these dependencies require a dynamic modelling approach using relatively short time steps.

In recent decades, the development of numerical codes based on the methods of finite differences (FDM), finite volume (FVM) and finite element (FEM), in parallel to the increase in computing power, made it possible to perform more accurate simulations of horizontal ground heat exchangers. By contrast, the numerical approach requires a high amount of input data, which are not always available. Moreover, it takes longer calculation time compared to analytical solutions.

Research into horizontal ground heat exchangers was the "ground coil program" started in 1980 at Oak Ridge National Laboratory (Mei, 1986), which aimed to develop new models to better predict ground coil performance and thus go beyond the limitations of line-source theory. Three numerical models for horizontal pipes were developed applying an explicit finite difference scheme. The first model was developed to analyse the effect of soil moisture freezing around a single coil. The bi-dimensional model assumes a radially symmetrical temperature profile from inside the pipe, with a far-field boundary condition based on the correlation of Kusuda & Achenbach (1965). The inlet fluid temperature is used as input in order to calculate the amount of heat exchanged between the coil and the ground around it. Since the performance of the horizontal ground heat exchangers is affected by the seasonal temperature variation of the shallow soil, a second model was developed including this phenomenon. In this case, the heat transfer was assumed radially symmetrical up to the coil outside wall only, and unlike in the first model, the far-field boundary condition was a function of both time and depth. Finally, a third model was developed to study the problem of the thermal interference between two pipes buried close to each other. The multiple solution in fact, showed better performance than the single one. The results of each model were compared to experimental data in terms of daily energy absorbed from the ground with a conservative average error of 16%.

Based on the Mei model, a more detailed approach to the modelling of horizontal ground heat exchangers was presented in Piechowski (1998) and (1999), which describe the model validation and theoretical development, respectively. The model of Piechowski involves both heat and mass transfer taking into account the moisture diffusion through the soil due to temperature gradient for a more precise calculation of the soil temperature field and the working fluid temperature. In order to maintain an acceptable simulation time, the mass transfer is only modelled at the interface between soil and pipe, where higher variations occur in both temperature and moisture gradients. Therefore, the heat transfer is simulated over a larger 3D finite difference domain by adopting a dual coordinate system. The results have been compared against experimental data and the model had proved to accurately predict the performance of an horizontal GHE. It was found that the type of soil and its moisture content are the parameters that most affect the performance of a HGHE. Therefore, a proper initial estimate of the soil thermophysical properties is important for an accurate design and simulation. However, the inclusion of moisture mass transfer component has not been shown to significantly increase the accuracy, due to the moderate operating temperature of a HGHE.

The recent spread of commercial numerical codes (albeit expensive), has made this task easier by reducing the time previously required to develop a model although this need skilled personnel to be operated. Anyway, the use of such instru-

ments has allowed the numerical study of new concepts and shapes of horizontal ground heat exchangers, which are discussed in paragraph 1.4.1 and 1.4.2.

1.4   Recent and Current Research on Horizontal Ground Heat Exchangers

The GCHP technology has been shown to be technically reliable and economically attractive in many applications. The horizontal solution has received less attention than the vertical one. Moreover, compared to this, it actually had a lower penetration in the market of the GCHP systems, which developed mainly in Northern Europe and North America. However, a renewed interest in the horizontal solution had recently led to a variety of laboratory testing, field testing and theoretical analysis, in an attempt to overcome the performance limits of this technology and maintain its advantages.

This paragraph traces the latest research in the field of horizontal ground heat exchangers through a comprehensive bibliography collection. The first part is dedicated to the conventional types HGHE, with a single or multiple straight pipe configuration and the more efficient slinky coil configuration. In the second part (paragraph 1.4.1) the new concepts and shapes of HGHE that have been recently developed are treated.

From the second half of the 2000s, some researchers have turned their attention to horizontal ground heat exchangers, in order to study their application in the Mediterranean area. The performance of a horizontal GCHP has been studied experimentally in Turkey by Esen, et al. (2007). The heat exchanger consists of a single-pass straight pipe with a diameter of 16 mm, buried at the relatively shallow depth of 1 m, where the yearly average ground temperature is around 16 °C. They found that the overall coefficient of performance of the system was 3.2 on average, with a minimum value of 2.7. This value appeared to be relatively low due to the design of the heat exchanger which was installed at a low depth. Moreover, a numerical model based on the finite difference approximation was developed and compared with experimental data, in order to calculate the ground temperature field around the pipe. The finite difference method was used to solve a comprehensive heat transfer model of parallel pipes HGHE in Demir, et al. (2009), taking into account the effect of the energy balance at the ground surface due to weather variables. The results have been compared with the Mei model and checked against experimental data obtained by means a dedicated real scale GCHP, showing a maximum difference of 10%. Subsequently, the same experimental setup was amended, in order to study the performance of a thin aluminium pipe (13 mm inner diameter) in comparison with the traditional polypropylene pipes previously installed, as reported in Koyoun, et al. (2009). They reported a better performance in terms of heat exchanged per unit mass of working fluid (kJ/kg·s) with aluminium pipe (26% higher than with PP pipe). An experimental analysis of a horizontal GHE for Northern Tunisia has been presented by Naili, et al. (2012). The HGHE consists

of a multiple HDPE pipes configuration (16 mm inner diameter) with a distance between the pipes of 0.3 m. Similarly to Esen, et al. (2007) it was buried at a depth of 1m. An average heat exchange rate of 26 W/m for unit length of dig was measured during the test, which has been conducted in cooling season. The effect of pipe spacing has been analysed by means of a commercial finite element code by Benazza, et al. (2011). A quasi-3D domain has been simulated in steady state under a typical cooling season condition. A reduction of the space between the pipes increases the length of pipe available per unit of ground surface, resulting in an increase of the heat transfer. However, this relationship is not linear and stabilizes as the spacing tends to 0.5 m due to thermal interference between the pipes.

Nowadays, commercial software are available, which allow the detailed simulation of the heat transfer in soil due to ground heat exchangers. However, this approach could often result in the need for high calculation power and time. In order to overcome this drawback, an in-house finite volume numerical code has been developed by Gan (2013) to analyse the transient heat transfer through a straight pipe HGHE, taking into account the interactions between the environmental conditions and the soil. The model has been used to evaluate the effect of installation depth and operating time for the heating operation. Finally, the accuracy of the model has been tested in comparison with the commercial code FLUENT. One study by Simms, et al. (2014) examined the impact of soil heterogeneity on the performance of HGHE, using an in-house finite element model. In the model domain, heterogeneous soil frames have been generated with a spatial correlation parameter. The analysis showed that the effect of soil heterogeneity is limited in determining the mean soil thermal conductivity. Therefore, they conclude that the assumption of soil homogeneity is an acceptable simplification in modelling HGHE. Recently, Kupiec, et al. (2015) have developed a mathematical model of a HGHE based on the one dimensional unsteady heat conduction equation with an internal heat source. The soil domain has been assumed as an infinite slab affected by a periodical temperature at the upper layer and a constant temperature at the lower one. A new model of horizontal GHE has been presented in Sofyan, et al. (2015), following a new approach to include the seasonal variation in soil temperature, which has been included as an internal source term instead of comprehensive energy balance at the ground surface. The model has been validated against the data from a dedicated experimental setup and then it has been used for a sensitivity analysis of the pipe length, flow rate, inlet temperature and burial depth. Although the installation depth seems to have little effect, this result could be due to the short period simulated, therefore, according to the authors it should be further investigated for longer operating periods.

Together, these studies indicate that research in the field of HGHE with traditional configurations are still ongoing. Two important topics emerge from the studies discussed so far. On the one hand, the horizontal exchangers may be applied in warm climates (e.g. Mediterranean countries), as an economically feasible alterna-

tive to air-source heat pumps. However, the use of HGHE in cooling dominated locations presents different issues in comparison with the European and North American applications, due to the different climatic and soil conditions. Consequently, further research is needed, also testing different and more efficient HGHE configurations. On the other hand, the modelling of horizontal exchangers has been further detailed, although previous existing models can be considered reliable. Moreover, the simple geometry of straight pipe configurations has allowed the development of new approaches to HGHE simulation by means of in-house numerical codes, in order to carry out precise simulations with reasonable computing times.

Among the widespread configurations of horizontal GHE, "slinky coils" have received increasing attention. The "slinky coil" GHE consists in overlapped circular coiled polyethylene pipes instead of straight pipes. This geometry gathers the heat transfer surface into a ground smaller volume, therefore, the expected heat exchange rate is higher resulting in less ground area and shorter trenching. Although, an interesting and detailed installation guide of slinky coils has been published by IGSHPA (Jones, 1994), the slinky coil GHEs performance needs further investigation in terms of heat exchange capacity and long-term performance (Fujii, et al., 2010). Moreover, the lack of an appropriate design method, often resulted in oversized or undersized exchangers. For these reasons, research has been conducted in recent years, both performing intensive field tests and detailed numerical analysis. In some studies, the simulations were carried out mainly by means of commercial codes, which allow easier modelling of complex geometries such as the slinky.

One study by Wu, et al. (2010) used the commercial CFD software FLUENT to simulate the performance of Slinky coil HGHEs in a 3D domain for short term operation. Computer simulations proved to be useful to perform sensitivity analysis of different coil diameters and pitches. Moreover, the results of two months period of monitoring of a GCHPs system were also presented and compared with simulation results. The efficiency of the system decreased over time due to the gradual decrease in temperature of inlet and outlet. During the test, the average COP of the system was 2.5. Simulations of three different HGHE geometry configurations (straight single pipe, slinky and helical) were performed by means of the numerical code FLUENT as presented in Congedo, et al. (2012). The different solutions have been compared in terms of heat exchange performance and tested for different working conditions by varying the installation depth, the flow rate and the soil thermal conductivity. The innovative helical configuration showed the best performance, although it requires more excavation than the others. Both previous models were used to simulate full-detail 3D geometries of horizontal exchangers. Although this approach allows a more precise study of interference between the coils, it is very demanding in terms of computing power required for the simulations. As a consequence, a simplified geometry could be necessary in order to simulate a full-scale HGHE.

A significant experimental analysis on the subject was presented by Fujii, et al. (2010). TRT and long-term field tests were carried out for two types of slinky coil installations in shallow trenches (vertical and horizontal arrangement). On short-term tests, the horizontal installation has demonstrated a higher efficiency in heat exchange, due to the more stable ground temperature at a constant depth of 1.5 m. The horizontal configuration has also been tested for a long-term period (more than 50 days) and showed an average heat exchange rate of 25.5 W/m, which was significantly lower than on short-term tests. The Authors pointed out that the performance of HGHE "can drastically change with the change in ground temperature". The experimental data has been used as a reference in the following research by Fujii, et al. (2012) , in order to improve the design approach of horizontal HGHE. They analysed the performance of a simplified shape of slinky-coil HGHE by means of a commercial FEM code, FEFLOW, taking into account the time-dependent heat flux at the ground surface due to weather conditions. This numerical model was then modified in a further work (Fujii, et al., 2013), to take into account the effect of the snow coverage on the performance of HGHEs. A recent study by Adamovsky, et al. (2015) reports a comparative experimental analysis of linear and a Slinky horizontal ground heat exchangers. Long-term tests have been conducted under the same operating conditions for both exchangers, during the heating period. The linear exchanger showed a higher heat extraction rate in comparison with the Slinky one. This result is in contrast with previous studies, in which it was stated that the Slinky configuration had a higher performance. Although this aspect requires further investigation, the main limitation of this study is that it compared two configurations that differ not only in geometry, but also in installation depth, pipe diameter and overall pipe length, which are in favour of the linear exchanger.

Finally, Xiong, et al. (2015) have developed a simplified Slinky GHE model, adopting a dedicated thermal response function (similar to that used in VGHEs modelling) for the first time in a horizontal exchangers simulation. The model has been validated against the experimental data provided by Fujii, et al. (2012), and it has been adopted to be integrated in building simulation programs.

1.4.1   New Concepts of Horizontal Ground Heat Exchangers

Over the last decade and particularly in the last five years, some studies have attempted to develop new and more efficient concepts of horizontal ground heat exchangers. Research has led to interesting developments and progress is still on-going. Although the horizontal installation is both inexpensive and simple to realise in comparison to VGHE, it requires a significant land area. Moreover, the HGHE of conventional type showed a rather low efficiency in heat transfer. However, the horizontal exchangers have some significant advantages. With the dual aim of improving their performance and reducing installation costs, new arrangements for

conventional pipe exchangers have been studied in recent years. Additionally, installation at shallow depths allows considerable freedom in the design of the exchanger geometry, contrary to the vertical GHE. Taking advantage of this aspect, new shapes have been proposed in order to maximise the heat exchange area in relation to the volume of ground used, making more competitive horizontal exchangers.

In 2010, an experimental geothermal field with 10 horizontal boreholes was built in Stillwater, Oklahoma (USA). Directional drilling was considered a viable option, especially for retrofit installations of GCHP systems, without disturbing the ground surface. The vertical-like boreholes were drilled horizontally at a depths ranging between 2 m and 3.4 m, each housing a high density polyethylene U-tube. In-situ thermal response tests (TRTs) were carried out for each borehole in 2010 and 2012, in order to evaluate the eventual variation in the ground thermal conductivity and in the borehole resistance. As reported in Beier & Holloway (2015), a reduced ground thermal conductivity and an increased borehole thermal resistance were observed in the second session of TRTs (in drought conditions) for shallower boreholes.

A research project sponsored by the Building Technologies Program (U.S. Department of Energy) and developed by Oak Ridge National Laboratory investigated the opportunity of reducing the installation cost of conventional straight pipe HGHE by installing them in existing construction excavations (around the basement walls, below the basement floor, utility trenches), and when required in auxiliary trenches as shown in Fig. 1.6 a). Therefore, without the need for dedicated excavation, the installation cost can be significantly reduced. This approach applies to recent high energy standard homes, with reduced heating/cooling energy demand, which allows a significant reduction in the ground heat exchanger size. A comprehensive report of the project was published by Hughes & Im (2012) and it is based also on other publications where the project's technical work is presented in depth. The project developed successful energy performance models and design tools for this innovative ground heat exchanger, also referred to as foundation heat exchanger (FHX). Moreover, two real-scale research houses were constructed to provide experimental data in order to validate the model. The results showed that the excavation cost for ground heat exchangers can be significantly reduced since up to 60% of the total ground loop can be installed in existing construction excavations in the case of high energy standard houses. A different concept of foundation heat exchangers has been investigated by Nam & Chae (2014). The foundations of big commercial and residential buildings usually lie at a depth of up to 10 m, where the ground temperature is nearly constant. A conventional straight pipe HGHE can be installed within concrete foundations, which serves as a heat source or sink for a GCHP system. Numerical simulations have been performed by means of the commercial FEM code FEFLOW to define the optimum design of these type of exchanger. The numerical results have been compared with experimental data provided by

Hwang Kwang-il, et al. (2007), which reports the seasonal performance analysis of a large scale HGHE installed into the foundation slab of a building in Seoul. Numerical simulation confirmed that this foundation-exchanger is not particularly energy efficient. In the best case, with the pipes installed between foundations and soil, the average heat exchange rate is 14 W/m.

A further study by Fujii, et al. (2013) investigated both experimentally and via numerical simulation the performance of a double-layer Slinky coil HGHE, one placed above the other in horizontal position at a depth of 1 m and 2 m respectively. The tests data showed a higher heat exchange rate for unit ground area for the dual layer Slinky HGHE in comparison with the single one since the total heat exchange surface is almost twice in the first case. The numerical model is based on that reported in Fujii, et al. (2012) and it has been modified to set the sol-air temperature (SAT) trend as boundary conditions at the ground surface. It has been applied to perform sensitivity analysis for the optimum depth of the upper layer and the preferable flow direction.

In recent years, helical pipes have been mainly applied in vertical position for applications in energy-piles exchanger. However, this configuration showed interesting potential in terms of performance if installed in horizontal position, as showed in a work of Congedo, et al. (2012), where the slinky configuration was compared with an innovative helical heat exchanger by means of a CFD numerical model. This configuration showed interesting potential in terms of performance, thus reducing installation cost. Recently, Yoon, et al. (2015) have performed experimental tests to evaluate the heat exchange efficiency of a small-scale horizontal helical heat exchanger against conventional Slinky coil and U-tube exchangers. A dedicated steel-box mock-up has been used to carry out TRTs for 30 h, for different spiral and coil pitches. In overall terms the helical GHE has shown an heat exchange rate per pipe length the 30-40% higher than the Slinky one, due to the lower thermal interference between pipes. Following a similar approach to Congedo, et al. (2012), the numerical code FLUENT has been used by Dasare & Saha, (2015) to develop a design method for horizontal ground heat exchangers, for a given ground area and thermal load. Three different configurations were simulated and compared, including the helical one. Given the complex geometry, only a portion of 5 m was modelled for each exchanger. In addition, in order to maximize the heat transfer, the HGHE were tested with a double layer arrangement. The results showed that this configuration has better performance, similar to what was observed by Fujii, et al. (2013).

A variant of the HGHE with spiral configuration are the energy baskets (cylindrical or conical), as shown in Fig. 1.6 b). Although the baskets are installed in a vertical position; they are designed to be installed at a depth between 1 m and 4 m. Energy baskets are regarded as horizontal ground heat exchangers in terms of thermal behaviour. Their singular shape allows the installation of a greater pipe length per unit of ground area, thus increasing the available heat transfer surface.

However, a basket GHE should be installed at a distance of about 4-5 m from another one, due to the considerable volume of soil involved in heat exchange.

a) Foundation Heat Exchanger

(Hughes & Im, 2012)

b) Basket heat exchanger

(Erdwärmekorb, Uponor)

C) Compact collector modules

(IVT Industrier AB)

Fig. 1.6 New concepts of horizontal ground heat exchangers.

Depending on the height of the basket, the overall length of the pipe can vary from 75 m to 150 m, with a rate of heat transfer around 10-15 W/m per unit of pipe length. This shape has not been well investigated in research. Anyway, the cooling performance of basket heat exchangers have been recently tested by Boughanmi, et al. (2015) in hot climatic conditions.

In 2002 a project was started by IVT (a heat pump producer) with the aim of designing a new type of GHE for shallow applications, as illustrated by Wärnelhöf & Kronström (2007). A compact and modular geothermal collector has been developed, which consists of a number of 40 mm pipes connected at the top and the bottom by U-bends, as shown in Fig. 1.6 c). The single modules can be installed in a series, both in a vertical and horizontal position. The compact geometry and the higher heat transfer surface per unit of trench length reduce the total installation cost for a given heating or cooling load, therefore a shorter pay-back time is expected. A study of Cauret & Bernier (2009) has been dedicated to examine the performance of compact collectors by means of a full scale geothermal field equipped with such collectors. Moreover, they developed and validated against experimental data a dedicated design tool, which is based on the finite line source method with spatial superposition to obtain specific g-functions.

Overall, there seems to be some evidence to indicate that horizontal exchangers have excellent potential in coupling with GSHP systems. Although the horizontal GHEs have been always compared with the vertical ones, these two solutions work in substantially different ways. Furthermore, the differences between them are significant also in terms of costs and installation requirements. On balance, horizontal exchangers are particularly suitable for small scale residential applications and represent an effective solution in the temperate climate, where the ground surface does not approach to freezing conditions.

In recent years, many researchers have turned their attention to horizontal exchangers with the aim of studying their behaviour in depth, to increase their performance and reduce their drawbacks at the same time. Two important themes emerge from the studies discussed so far: many studies have focused on new arrangements and configurations for HGHE based on round pipes (e.g. Slinky, Helical, Baskets, etc.), whereas a few of them have followed a more innovative approach, developing new shapes of HGHE. Contrary to VGHE, opportunity for improvement in performance is still remarkable for HGHE. Their installation is easy and in fact, it allows a free approach to the design of the heat exchanger.

1.5   The Flat-Panel Shape.

An innovative horizontal ground heat exchanger, called Flat-Panel (FP), has been developed recently at the University of Ferrara, which applied for a patent in 2012 (Bottarelli, 2013). Today, the Flat-Panel shape is a European Patent Pending (EP 24184392A3). It was designed to be installed in shallow trenches, with the orig-

inal flat and thin shape, aiming to increase the heat exchange surface area per unit length of the trench, as shown in Fig. 1.7.

The first prototype consists of a rectangular shaped panel, 3 m long and 1 m high. Two sheets of polypropylene (PP) 4 mm thick spaced by 20 mm are welded in order to form a cavity where the working fluid flows. Despite the small thickness of the cavity, a FP contains a considerable volume of fluid (up to 60 L), thus increasing the thermal inertia of the system. Within the cavity, a labyrinth has been designed as a series of rectangular channels with a high base/height ratio (2 mm/16.7 mm). Consequently, the overall length of the working fluid circulation path is equal to 6.1 m per unit length of heat exchanger (i.e. trench). The fluid flows for most of the length in a vertical direction, in order to avoid thermal stratification due to buoyancy forces. In addition, the labyrinth has been designed to reduce the stagnation areas where the fluid flows at low speed.

The geometry of the Flat-Panel is illustrated in Fig. 1.8. Despite these positive aspects, the geometry needs particular care during the installation. The procedure to flush air from the heat exchanger, called "power flushing", has been revealed to be onerous and it must be performed with a high flow rate and pressure. If a certain quantity of air is trapped in the exchanger, the fluid circulation is penalised thus reducing the available heat transfer surface and consequently the performance of the exchanger.
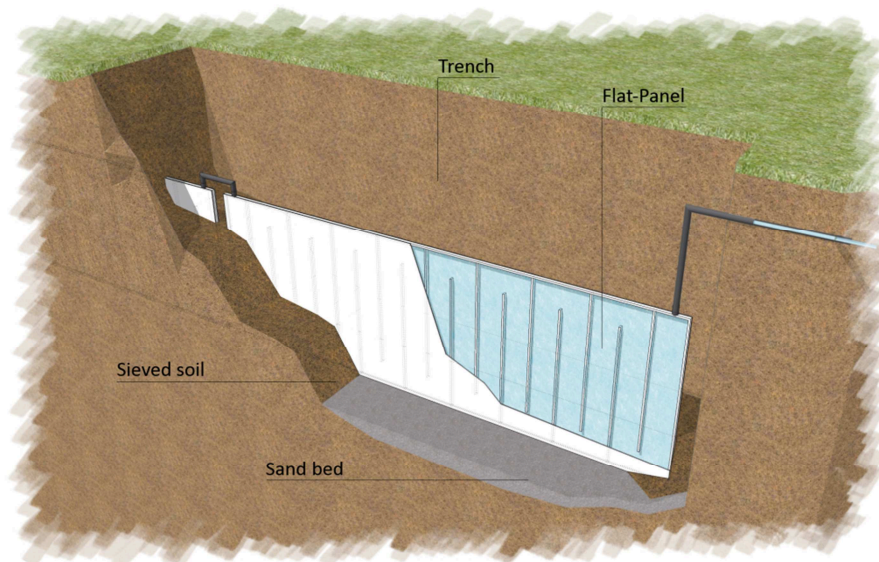
Fig. 1.7 Flat-Panel installation scheme.
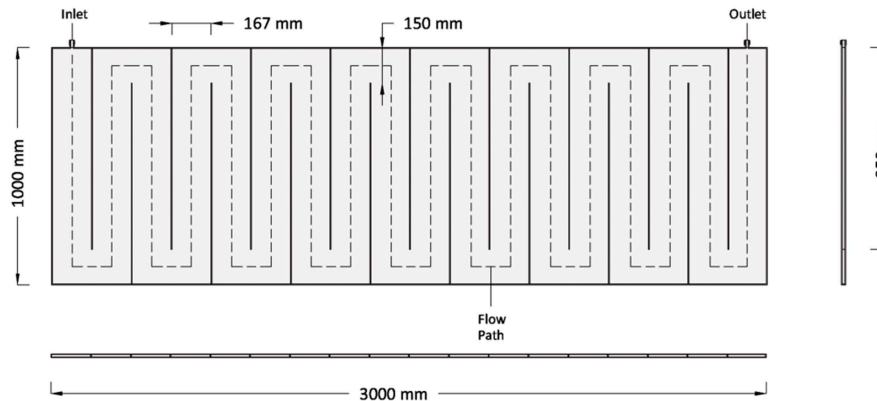
Fig. 1.8 Geometry of a Flat-Panel.

Two hand-crafted prototypes were initially built and installed in an experimental setup dedicated to the study of their behaviour and performance. The experimental setup and the results of the tests are described in Chapter 2. The advantages and disadvantages emerged during the study, besides the specific requirements of the production process, and provide the evidence base for the subsequent industrialization of the Flat-Panel.

1.6   Thesis motivation and objectives.

This research deals with a novel shape of horizontal ground heat exchangers, which has been designed for small scale ground-coupled heat pumps. A review of the literature shows that these systems have a great potential for development. The strengths and weaknesses of the technology have been widely discussed in the introduction. In recent years, a number of studies have been devoted to the development of new configurations and new geometries for ground heat exchangers with horizontal installation, with the aim of optimizing their performance.

This thesis therefore, fits into this context as part of these efforts. The thesis is dedicated to an innovative HGHE called Flat-Panel, which has been invented and developed at the University of Ferrara.

The first part of the thesis involves the experimental analysis of the performance of a ground heat exchanger equipped with Flat-Panels. A number of tests have been conducted by means of a dedicated experimental setup, in different operating conditions (heating and cooling) and for different operating modes (continuous, discontinuous and pulsed).

Secondly, the thesis deals with the numerical simulation of the Flat-Panel. The main objective is to simulate the ground thermal response due to different heat injection or extraction rate by HGHEs. Moreover, the heat transfer processes at the

ground surface will be included in detail. The heat transfer process in the shallow soil depends on several factors therefore, it is considerably complicated. Among these factors, the energy balance at the soil surface has a decisive role in determining the temperature of the soil. A numerical model of a 2D Flat-Panel is developed by means of the commercial finite element code COMSOL Multiphysics. To simulate in detail the soil temperature, an energy balance at the ground surface is proposed as a boundary condition in the model. The model is calibrated with respect to the experimental data. In addition, a sensitivity analysis mainly focused on the thermal conductivity of the ground, which is a key parameter in soil heat transfer, was is carried out.

This research will be helpful in providing guidance on the operation and performance of the Flat-Panel. More generally, this thesis is intended to gain additional information about HGHE, which may be used for the performance optimization of horizontal GCHP systems.

2.   EXPERIMENTAL ANALYSIS

2.1   Introduction

This Chapter provides an overview of the tests that have been carried out to study the performance of Flat-Panels and the effect the Flat-Panels would have on the ground temperature field. The Flat-Panel, a novel shape of ground heat exchanger, has been described in paragraph 1.5 of Chapter 1. A description of the experimental setup, its location, and of the monitoring system, precedes the results of the experimental analysis.

The data analysed in this chapter is related to the whole experimental activity, which started in 2011 and ended in December 2014; the experimental setup is still in service. The author has been involved on the experimental activity since the beginning and has chosen to include in this thesis also the results obtained with tests preceding the beginning of his Ph.D., in January 2013. The reason for this choice was the opportunity to better assess the evolution of the ground temperature during the test sequence, and how the performance of the ground heat exchanger are affected by the heat exchanged previously. The heat transfer in the ground is indeed a slow phenomenon, due to the low thermal diffusivity, so the "thermal anomaly" caused during a test could still be detectable after months and could affect the following test. A preliminary data analysis was presented in Bottarelli & Bortoloni (2013).

Anyway, the experimental setup and the monitoring system have been improved over the years. Moreover, the experimental setup has required several maintenance procedures due to repeated failures, caused by the difficult operating conditions. For this reason, the analysis regarding the performance of the heat exchangers is focused on the last four tests, the last of which ended in December 2014.

2.2   The Experimental Setup at the Department of Architecture

The experimental setup was built at the Department of Architecture, the University of Ferrara (Italy) in 2011. The complex of buildings is located in an historic urban quarter of the city. As shown in Fig.2.1, the experimental setup was built in a portion of the garden, in the courtyard of the Department. The geographical coordinates are (44°49'43.88N; 11°37'20.00E), 12 m above sea level.

The local climate of the Po valley has been classified as Cfa (Humid Subtropical) in the Köppen-Geiger climate classification system but it is usually referred to as a humid continental climate. The winter is harsh and humid, and the temperature often decreases below 0 °C. The summer is hot and muggy, with high temperature (greater than 35 °C) during the day.
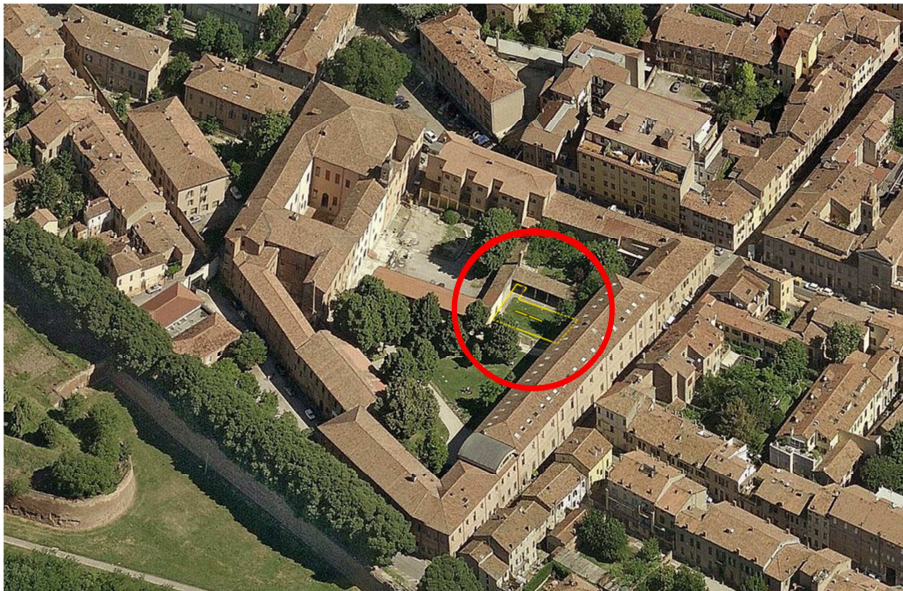
Fig. 2.1 Location of experimental setup, in the garden of Department of Architecture in Ferrara.

According to the Climate Normal, a reference on the thirty-year average of 1961-1990, the minimum value of the monthly average temperature is 1.6 °C and the maximum 24.0 °C. However, a growing trend of temperature was observed over the last years, as evidenced by the difference of 2.0 °C between the mean annual temperature for the period 1961-1990 (13.4 °C) and that for the period 1991-2008 (15.4 °C) reported in ARPA Emilia-Romagna, Servizio Idro-Meteo-Clima (2009).

As regards the recent reference period of fifteen years (1991-2005) the monthly average temperature had a minimum value of 4.6 °C in January and a maximum of 27.4 °C in August. The monthly average solar radiation is minimum in December, in its direct and diffuse component equal to 2.1 MJ/m^2 and 1.3 MJ/m^2 respectively, and maximum in July with an overall monthly average value of 23.9 MJ/m^2. The average annual rainfall is around 650 mm with a minimum in winter and moderate peaks in spring and autumn. No significant variations have been observed over the last decades. The monthly average temperature, solar radiation (direct + diffuse) and rainfall are reported in Fig. 2.2. All weather data has been provided by ARPA-EM (the meteorological service of Emilia-Romagna region) and the Italian regulation UNI-10349. Finally, the average wind speed is low intensity in Ferrara, almost lower than 2.5 m/s at the reference height of 10 m. In winter and autumn, the prevailing direction is from west and north-east; easterly winds are prevailing in spring and summer.
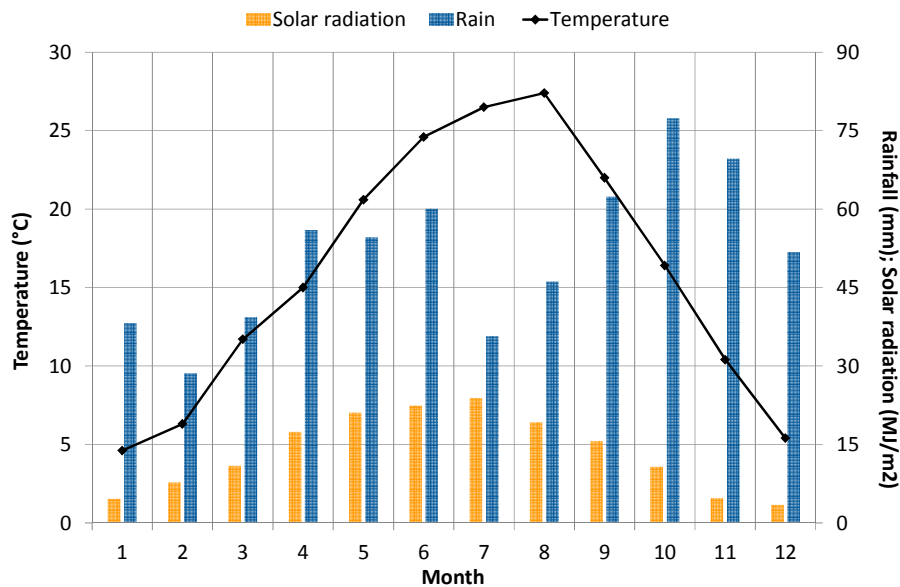
Fig. 2.2 The monthly average temperature, solar radiation and rainfall for the period 1991-2005 in Ferrara.

The experimental setup is located in a sheltered area of the garden, with a low portico at the north-western and north-eastern boundaries, and the main building of the Department (more than 10 m high) on the south-eastern side.

Consequently, the site is characterized by low wind speeds near the ground surface and it is subjected to partial shading during the day due to the adjacent buildings. In order to analyse the actual weather conditions of the site, a weather station was installed as detailed in paragraph 2.2.2 which is dedicated to the monitoring system.

The experimental setup covers a land area of about 320 m^2, 23 m long and 14 m wide. The land is covered with wild grass of different kinds and height, and hosts a young oak-tree near the ground heat exchanger.

Historically, the area was an island on the Po river, the largest river in Italy. The route of the river Po, which nowadays flows some kilometres north, had run near the southern walls of the city until the 12th century. As a consequence the shallow soil (up to a depth of 4-5 m) is partially dry and the groundwater table lies in a sandy geological unit, which is 6 m deep. Moreover, the first human settlement of the town of Ferrara was established in this area. An important fluvial port developed on the island in the middle Ages, and it was a busy crossroads of goods for a long time. Moreover, the ancient convent of S. Antonio in Polesine, founded by the beatified Beatrice II d'Este in the 13th century, is near to the Department of Archi-

tecture, were the experimental setup was built. For these reasons, the ground is frequently mixed with rubble, bricks and pottery up to a depth of 2 m, and the lithology is non-homogeneous.

2.2.1 Description of the Experimental Setup

The experimental system is composed basically of two major parts: a system to heat up or cool down the working fluid and a hydraulic closed-loop connected to a horizontal ground heat exchanger (HGHE).

The former one has been equipped with a plastic open-tank of 0.3 m^3, which is used as an expansion vessel for the hydraulic loop and as thermal storage for the working fluid. The tank has been positioned in a sheltered place under the *portico* and then protected with a thermally isolated wood casing.

In the tank, the working fluid temperature is maintained to a set-point value by means of two joule immersion water heaters (1.5 kW each) which are controlled by an On/Off thermostat. Given their dangerous position, electrical connections have been properly insulated. Anyway, the electric system of the experimental setup has been protected with a number of differential circuit breakers.

The experimental setup was originally designed to work only in heating mode. It was improved in January 2012 by installing a chiller to carry out tests in cooling mode. The unit was hydraulically connected with the tank by means of a secondary hydraulic loop equipped with a dedicated pump. The chiller (Teco TK 3000) was originally designed to maintain the correct water temperature in aquarium tanks and it is suitable for tanks up to 3 m^3. It is equipped with a rotary screw compressor, a coaxial heat exchanger and the loop is charged with refrigerant R410A. A thermostat controls the temperature of the working fluid within the range 0-35 °C. The cooling performance is reported in Tab. 2-1 for two test conditions. The working fluid going to the HGHE flows through a 3-speed circulator pump (Grundfos UPS, series 100), which has been installed on the tank outlet pipe in a horizontal position. The pump is suitable for geothermal heating and cooling systems. Moreover, a micro-meter needle valves has been installed downstream of the pump for precise flow control. To limit and manage the pump operation to user specified periods, the power supply of the pump has been connected to an On/Off time switch.

Tab. 2-1 COP of the chiller.

Outlet temperature (°C)	Air temperature (°C)	Flow rate (l/h)	Thermal load (W/l)	COP
25	30	3000	0.5	2.8
8	30	800	0.1	1.4

The different components of the system for heating up or cooling down the working fluid are shown in Fig. 2.3 and Fig. 2.4.

The ground heat exchanger, it is 6 m long and consists of two Flat-Panel prototypes embedded in the ground through which the heat-transfer fluid (a water/antifreeze mixture) coming from the tank circulates. In order to install the ground heat exchanger, a shallow trench 1.9 m deep has been dug by qualified personnel. The trench was about 0.8 m wide and 6.5 m long. Originally, the trench was 0.4 m wide only; it was successively enlarged for maintenance operations on Flat-Panels.

Fig. 2.3 The tank with the pump and micro-meter needle valves.

Fig. 2.4 The thermally insulated wood casing and the chiller.

During digging operations, the remarkable non homogeneous lithology of the ground was found and samples were collected to study the physical properties of the ground. The Flat-Panels were laid into the trench in a vertical position on a bed of sand and then backfilled with the soil previously dug. The backfill material was screened for stones, bricks and pottery as a precautionary measure to avoid damage and to ensure good long-term thermal contact with the ground. Moreover, during this phase two horizontal temperature probes were installed along the exchanger, as described in paragraph 2.2.2. The different phases of the Flat-Panels installation are shown in Fig. 2.5.

The ground loop was pressure tested after installation and purged of all the air. The closed-loop was connected to the heating/cooling system, and filled with antifreeze which was directly poured into the tank. A dedicated irrigation system was also installed on the top of the trench, to wet the soil on demand. Finally, the trench was covered with a further layer of sieved soil and the ground was levelled. The building site during and after the installation of the ground heat exchanger is shown in Fig. 2.6.

The hydraulic connection between the ground heat exchanger and the closed-loop consists of two systems of multiple valves, as shown in Fig. 2.7. The first one is positioned between the circulator and the first Flat-Panel (FP1); the second one is between FP1 and FP2. The two groups have been installed in two shallow dry wells to easily control the fluid supply to Flat-Panels. It is possible to set the flow direction (from FP1 to FP2, and vice versa), to supply the two Flat-Panels in parallel or in a series and eventually to supply only one Flat-Panel.

More than 40 m of insulated DN20 high-density polyethylene pipe have been used for hydraulic connections. All the piping has been thermally insulated and protected with corrugated pipe.

Finally, the complete layout of the experimental setup is shown in Fig. 2.8.

Fig. 2.5 The installation of Flat-Panels.

Fig. 2.6 The building after during installation and after.
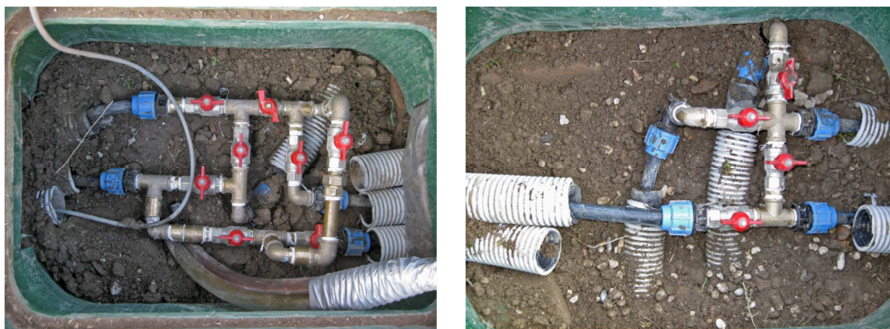
Fig. 2.7 The group of valves between the pump and FP1 (left) and between FP1 and FP2 (right).
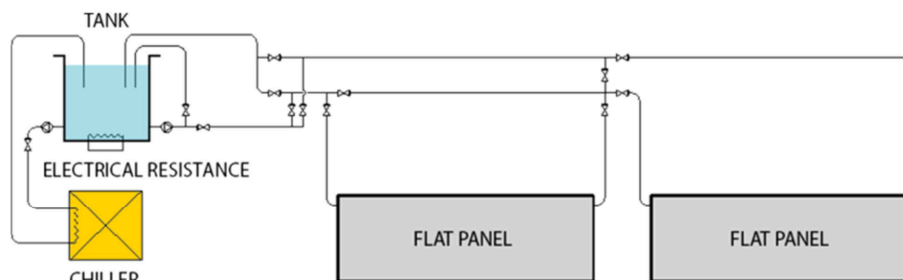
Fig. 2.8 Layout of the experimental setup.

2.2.2 The Monitoring System

The experimental setup has been equipped with a monitoring system, in order to investigate the performance of the Flat-Panels and their effect on the undisturbed temperature distribution in the ground. The monitoring system consisted initially of a network of temperature sensors. These were installed within the tank to measure the flow and return temperature. Moreover, a number of temperature sensors were properly protected and arranged in the ground to monitor the ground temperature. The network was connected to a multiplexer and all the data were recorded and saved in a computer by means of a dedicated software.

In its first configuration, the monitoring system was not equipped with a flow meter; therefore the mass flow rate of the working fluid was measured by direct weighing. The weighing procedure was possible given the low working pressure of the closed loop and the temperature of the working fluid, below 40 ° C. To perform the measurement the return pipe was provided with a tap and valve to stop the fluid supply to the storage tank. The mass flow measurements were performed initially according to the gravimetric method.

The monitoring system was gradually improved by adding new instruments. A thermal energy meter was mounted in January 2012, when the chiller was installed. In February 2012, a weather station was placed to monitor several weather variables. Finally in December 2013, a secondary wireless unit for the weather station was installed with 4 temperature sensors and a moisture sensor to monitor the natural temperature and moisture content of the ground.

In its final configuration, the system was organized in three separate subsystems:

- A *network of resistance temperature detectors (RTD)* to monitor the temperature of ground and working fluid. The network was connected to a computer by means of a multiplexer. In-house software was developed and used for data recording.

- A *compact thermal energy meter* to monitor the mass flow rate and the flow and return temperature. The device was also connected to a computer for remote data recording by dedicated software.

- A *weather station* was equipped with several sensors to monitor the weather variables and the undisturbed temperature of the ground at various depths. The data were recorded and stored by dedicated software.

Relevant maintenance activities have been carried out in recent years to maintain the system efficiently and improve its capability. The monitoring system, as configured, has served to create a comprehensive database of the experimental tests performed.

One of the objectives of the experimental activity is to study the "thermal anomaly" generated by HGHEs in the natural temperature field of the ground, which can be significantly extended. Moreover, the heat transfer phenomenon in the shallow soil related to horizontal ground heat exchangers is of considerable complexity, because many factors are involved in it (e.g. environmental conditions at the ground surface, thermo-physical properties of soils, energy demand). Consequently, the network of temperature sensors was initially designed to meet the need of having several measurement points and a good time resolution.

For this purpose, the monitoring system was equipped with several resistance temperature detectors (RTD). A multipoint probe was adopted, as normally used for temperature detection in silos or sheds for the storage of raw materials (cereals e.g.). The final measurement network was equipped with 11 multipoint probe lines with 7 RTDs each. All the lines were connected (through a three pole shielded cable) to a 8 channels Multiplexer (MUX) that forwarded the several digital input signals into a single line. For this reason, only 8 lines could be read simultaneously. The MUX was connected through a cable for digital data communication in serial network RS485 to a filter converting the signal in USB protocol. Finally, the signal was received by a computer where a dedicated software read and stored the data. The whole system was derived from an industrial application, and modified with the support of experts of the Consiglio Nazionale della Ricerche (CNR). The monitoring system, as configured, has been considered the right choice for the application, in terms of reliability and cost.

The installed temperature sensor was of RTD type produced by SGM LEKTRA s.r.l.. The sensor is mounted on a small electronic card (5 x 30 mm), as shown in Fig. 2.9. The signal is already converted into digital temperature data by the probe, so it is directly readable by the MUX. The sensor originally had a temperature range from -30 °C to +125 °C and a precision of ±0,5K (in the range of -10 °C ÷ +85 °C). However, the manufacturer developed a modified and more accurate version (±0.1 K) upon specific request.

Fig. 2.9 A temperature probe and a shielded temperature probe.

The multipoint temperature probe was protected with a sheath in AISI type 304 stainless steel in the industrial application of temperature detection in silos. However, this solution was not deemed adequate for this application, due to the high thermal conductivity of steel. Moreover, in the original system, the distance between each sensor was much higher (more than 1 m) than that expected in the experimental setup (between 50 to 100 cm). So, a proper mechanic and hydraulic protection for the sensors was developed. Given the difficult operating conditions, the electronic cards were initially protected with heat shrink tubing and then placed into a flexible PVC tube (diameter of 5 mm) sealed with hot melt adhesive, as shown in Fig. 2.9. A total of 10 multipoint temperature probes were installed into the ground around the Flat-Panels, in a horizontal and vertical positions, as shown in Fig. 2.10 and 2.11. Eight probes were installed vertically in the ground up to a depth of 4.5 m at various distances from the exchangers. An Other two were laid horizontally 0.20 m and 0.40 m far from the Flat-Panels, at a depth of 1.15 m and 1.65 m. A further line was installed to monitor the flow and return temperature of the working fluid within the tank, the temperature of the three valves groups, and finally the air and the ground surface temperature. In Fig. 2.10 and 2.11 the positions of the vertical (V) and horizontal (H) probes and their distance from the exchangers are shown. Moreover, the depth of each sensor is also reported.
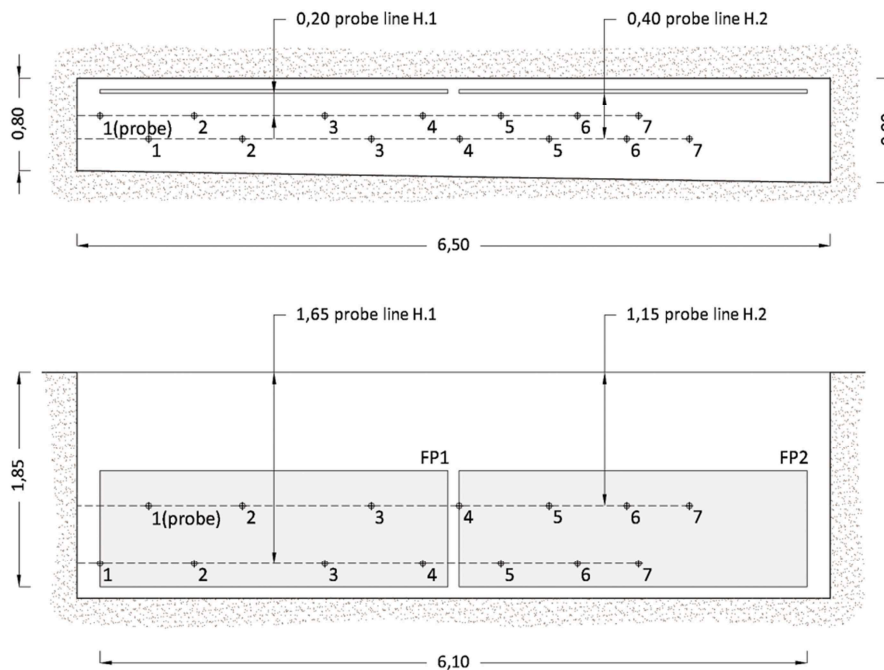
Fig. 2.10 Layout of the horizontal temperature probes.

H	Horizontal probe line ID
V	Vertical probe line ID
1/-1.00	Probe ID / depth (m)
FP1	Flat-panel ID
*	Not available

Plant
probe line
— 1 Air temperature
— 2 Flow temperature
— 3 Group of valves
— 4 Group of valves
— 5 Group of valves
— 6 Return temperature
— 7/*
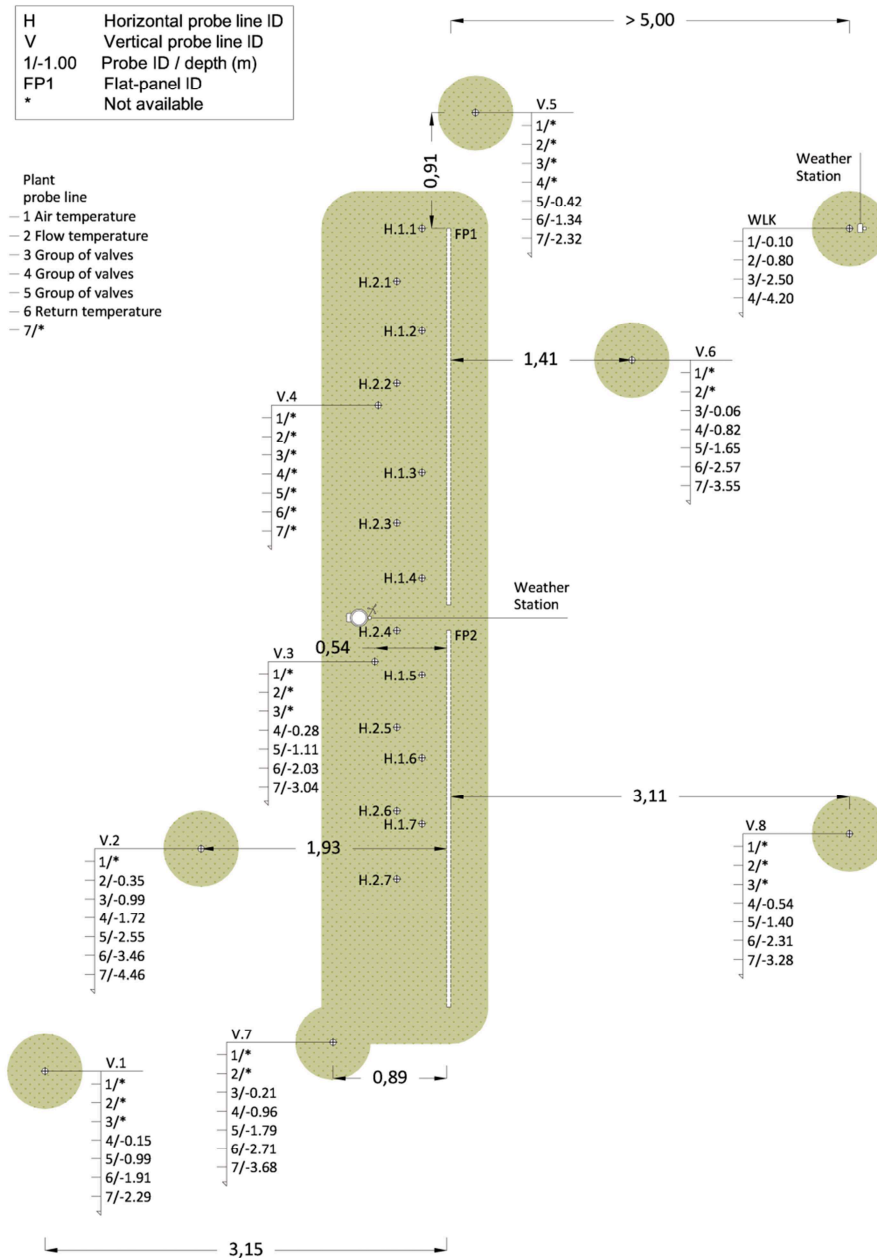
Fig. 2.11 Layout of the vertical and horizontal temperature probes distribution.

The experimental setup was firstly improved in January 2012, when a chiller was installed in order to carry out tests in cooling mode. At the same time, the hydraulic circuit was modified to install a compact heat meter (MicroCLIMA by Maddalena S.p.A.) on the working fluid return pipe in a vertical position. It was designed for heating and cooling applications, with an automatic switch and two separate registers. The heat meter consists of a an electronic unit for the metering of energy consumption, a flow sensor and two temperature sensors, all permanently connected to each other, as shown in Fig. 2.12. The flow rate is gauged by a single jet flow meter without magnets in contact with water. The flow and return temperature are measured by a pair of PT500 platinum temperature probes, diameter 5 mm. The return temperature sensor is directly mounted on the heat meter. The device is certified in accordance with the Directive 2004/22/EC (MID MI004) and the European Standard EN 1434-1:2007, with accuracy class 2.

The heat meter has been provided with an M-Bus communication interface, compliant with Directive 2004/22/EC (standard EN 1434-3) since January 2013. The M-Bus network was managed by a TCP/IP M-Bus master (CMe3000, a level converter by Elvaco AB), which read the data from the electronic unit of the meter. Moreover, the electronic unit of the heat meter was directly powered by the M-Bus network, thus enabling unlimited daily readouts. The data of energy consumption, volume flow, flow rate, power, flow and return temperature, temperature difference were all displayed on the interface and available via LAN. A specific software for level converters (MBSheet, by Relay GmbH) was used on a PC for the readout of M-Bus network and the data storage.

Finally, a wireless weather station (Vantage Pro2 by Davis Instruments) was installed in February 2012, with the aim of collecting weather data and then analysing the relationship between environmental conditions and the performance of the Flat-Panels. The weather station consisted of an intregrated sensor suite (ISS) placed near the ground to collect outside weather data and an indoor console/receiver to display and record in real time the data received from ISS.

Fig. 2.12 The compact heat meter.

A data logger connects the console to a PC where a dedicated software (WeatherLink) allowed the data storage for detailed analysis and graphing. To monitor weather variables, the ISS was equipped with several sensors: a rain collector, anemometer, solar radiation sensor, temperature and humidity sensors, as shown in Fig. 2.13. The temperature and humidity sensors were shielded to minimize the effect of solar radiation on solar readings. The weather station was improved in December 2013 by adding a secondary wireless station (also referred as Soil Station). This secondary unit was placed more than 5 m far from the ground heat exchanger (Fig. 2.13) to measure the natural ground temperature. It was equipped with four temperature probes placed at different depths (0.1, 0.8, 2.5 and 4.2 m) using a self-built drill. The installed sensors (accuracy ±0.5 K), referred to as WLK in the following, were thermistors with stainless steel housing. Moreover a soil moisture sensor was installed to a depth of 0.1 m to measure the moisture content variations in shallow soil due to rainfall and evaporation. The data are stored in a PC by means of a data logger.

The measuring system proved to be quite reliable. However, some problems occurred during testing. The protection made of heat-shrink tubing and a flexible PVC tube, used to install the temperature probes into the ground, was rigorously tested before application. However, in some cases it proved to be inadequate in the long term in terms of hydraulic sealing. As a consequence, the network suffered some sensor failure, due to water infiltration, and some measurement points were lost. Moreover, the M-Bus network suffered communication problem. Nevertheless, a comprehensive data set was collected for the duration of the experimental activity, from 2011 to the end of 2014. The monitoring system is still operating. The data analysis allowed the assessment of the Flat-Panels performance and their effect on the ground temperature field, as described in the following paragraphs.

A complete diagram of the monitoring system is reported in Fig. 2.14.

Fig. 2.13 The integrated sensor suite (ISS) and the soil station.
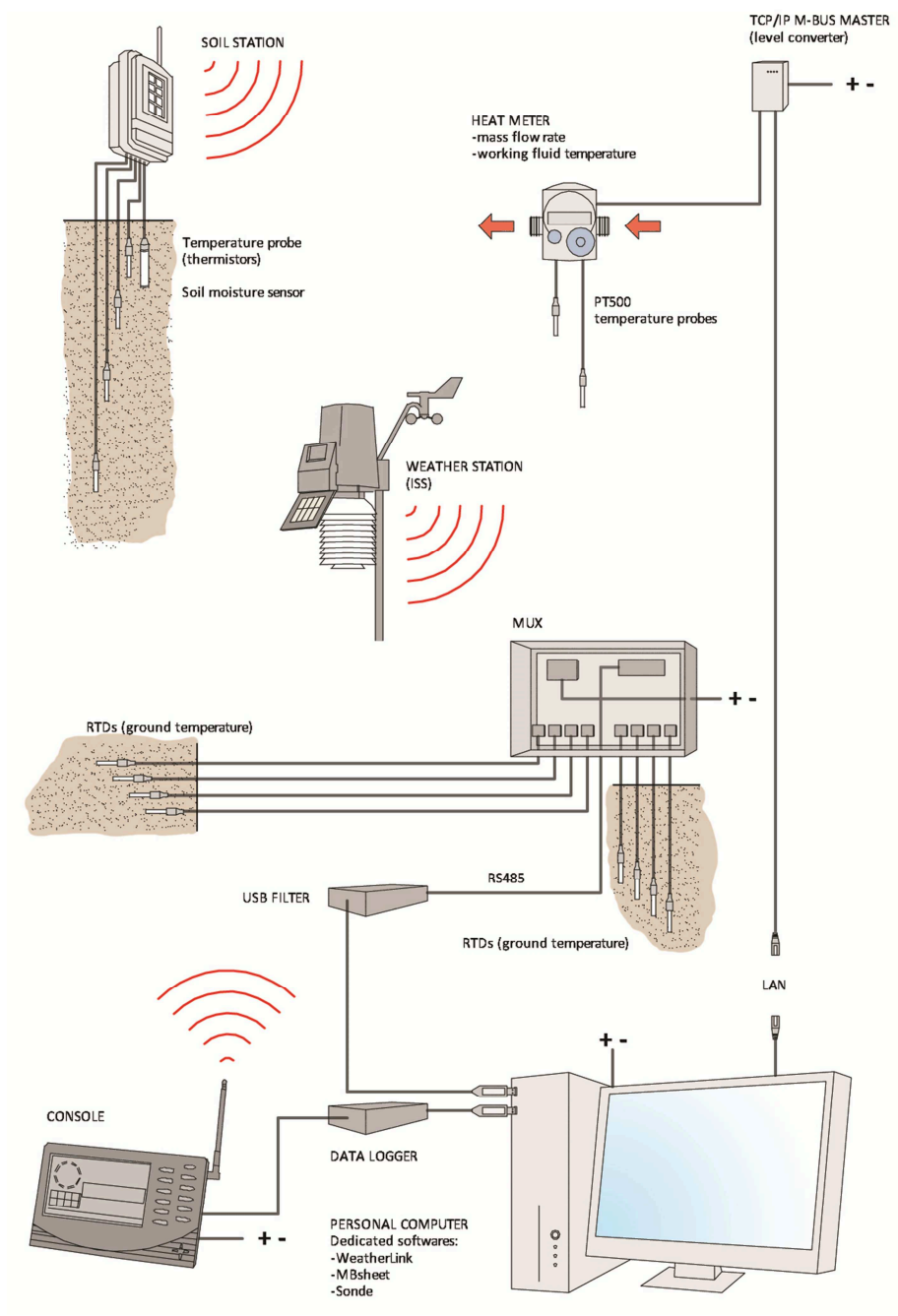
Fig. 2.14 Layout of the monitoring system.

2.2.3 Undisturbed ground temperature

The performance of the horizontal ground heat exchangers are strongly affected by environmental conditions, therefore the knowledge of the shallow soil temperature is important for a detailed characterization of local environmental conditions in designing HGHEs. In addition, the ground temperature can be significantly different between rural and urban areas, where the soil is usually warmer due to the urban heat island. Luo & Asproudi (2015) have analysed data of shallow soil temperature in both rural and urban areas of London: in the last decade at a depth of 1 m an increase of 1.18 °C has been observed in urban ground temperature.

In order to monitor the temperature in the shallow soil at the Dept. of Architecture, the monitoring system was equipped with a Soil Station with 4 ground temperature sensors, placed at different depths. Fig. 2.15 illustrates the evolution of the temperature of the soil at the site, for the years 2014 and 2015. The temperature near the surface (-0.1 m) shows daily and seasonal fluctuations, which are related to the air temperature. Although these variations are reduced at a depth of 0.8 m, they are still detectable. The change between the maximum of temperature in summer and the minimum in winter is considerable, and may exceed 15 °C up to a depth of 1 m (up to 7 °C, at 4.2 m). A certain variability is observable from one year to another, both in terms of minimum and maximum values, and in terms of the duration of the warm and the cold period.
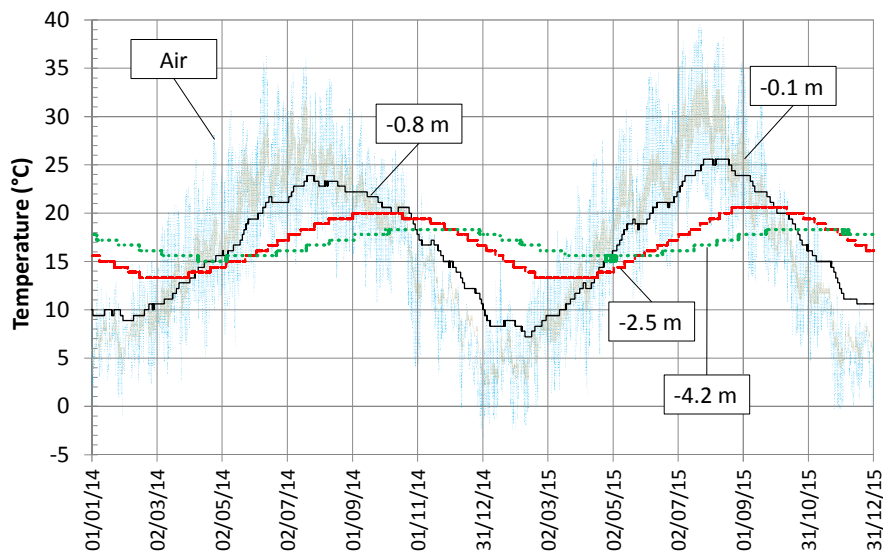
Fig. 2.15 Ground temperature at different depths in 2014 and 2015.

In overall terms, the soil is quite warm at the site, the average temperature of the soil at a depth of 2.5 m was 16.7 °C in 2014, that is 1.4 °C higher than the average air temperature.

The amount of water stored in the soil is another key parameter due to its effect on soil thermal properties and consequently on the heat transfer process at the ground surface. In view of this the measuring system was equipped to measure the water content of the surface layer. In addition, a piezometer was installed to monitor the groundwater level. The groundwater table lies at a depth of 6 m, in a sandy geological unit, therefore the soil moisture content near the surface is mainly affected by temperature, precipitation amounts and evapotranspiration process.

Figure 2.16 shows the moisture content of soil to a depth of 0.1 m. This is calculated through a watermark sensor, which measures indirectly the soil water tension in centibars (cbar). In the graph, values between 0-10 cbar correspond to saturated soil conditions, 30-60 cbar to moist soil and above 100 cbar to partially dry conditions.
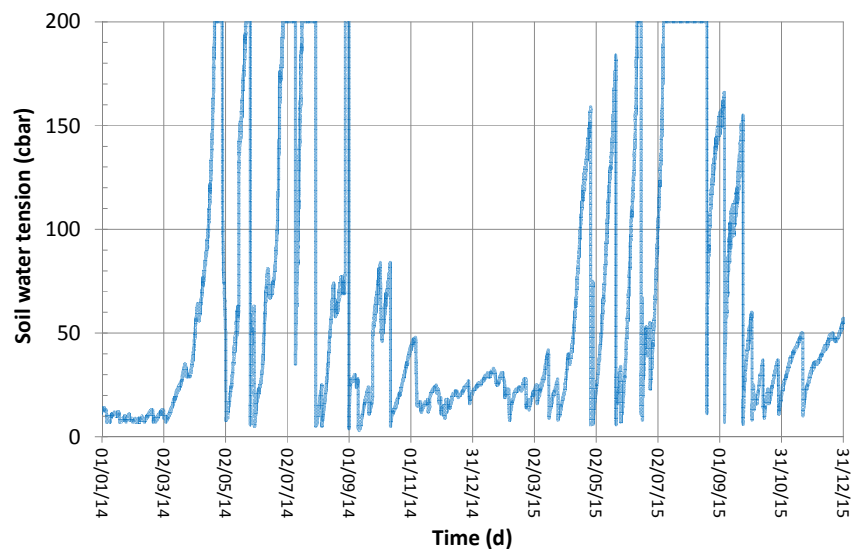
Fig. 2.16 Moisture content of shallow soil, measured at a depth of 0.1 m, in 2014 and 2015.

2.3 Data analysis

2.3.1 Operating modes

The experimental setup was turned on for the first time on March 11th, 2011. The measurements of the ground temperature started earlier; however, the testing

was postponed due to the need to level out the temperature in the soil near the excavation. The air temperature was lower than that of the ground at the excavation depth (between -0.8 and -1.85 m) during the installation of the two ground heat exchangers. As a consequence, the trenching and the following filling significantly altered the natural temperature of the surrounding soil and therefore the test started when the soil temperature measured by the two horizontal lines of sensors arranged near the heat exchangers (H.1 and H.2) was comparable with the undisturbed soil temperature at the same depth (sensor line V.8). The vertical line V.8 was took as the reference among the sensor lines available at that time because it was the farthest from the thermally disturbed area of excavation.

The recording of the data provided by the measurement system started simultaneously with the first experimental test on March 11th. The data recording operations were performed with different time steps, ranging between 60 s and 900 s, according to the specific operating procedures used during the whole experimental activity (2011-2015). Tests were carried out according to three operating modes:

- *Heating mode:* The working fluid was heated to a temperature (up to 35 °C) higher than the average temperature of the shallow ground by the thermal resistance and then pumped in the geothermal closed-loop to simulate the summer working condition of the GCHP.

- *Cooling mode:* The working fluid was cooled down to a temperature (variable between 8 °C and 2 °C) lower than the average temperature of the shallow ground by the chiller and then supplied to the closed-loop to simulate the winter working condition of the GCHP.

- *Free mode:* the working fluid circulated in the closed loop and its temperature was free to vary according to the air temperature and the ground temperature.

Moreover, a timer has been installed to control the system operation to defined periods. The piping of the closed loop was also designed to allow the possible inversion of the flow direction (from FP2 to FP1) and to supply the two Flat-Panels in parallel or in series. In addition it was possible to supply only a Flat-Panel instead of two. Anyway, the Flat-Panels have operated in series since 15th March 2012 with the same flow direction (from FP1 to FP2). The performance analysis of the system has been focused on the tests carried out after that time.

Table 2-2 summarizes the different operating modes and their duration during the experimental activity. It also includes the total length of the ground heat exchanger used in each test.

The data obtained from the field tests are discussed in the following paragraphs 2.3.2 and 2.3.3. The data analysis was firstly focused on the plant with the aim to assess the performance of Flat-Panels. After that, the data of the ground temperature were interpreted to analyse the effect of the system on the ground thermal field.

Tab. 2-2. Operating modes.

Period	Mode	Lenght (m)
11/03/2011→31/05/2011	Heating	3
31/05/2011→20/06/2011	Free	3
14/07/2011→28/09/2011	Heating	6
19/11/2011→31/01/2012	Free	6
31/01/2012→04/04/2012	Cooling	6
24/07/2012→01/10/2012	Heating	6
13/11/2012→10/04/2013	Cooling	6
14/08/2013→23/10/2013	Heating	6
23/10/2013→04/12/2013	Free	6
04/12/2013→03/04/2014	Cooling	6
12/06/2014→12/12/2014	Heating	6

2.3.2 Energy Performance of the Flat Panel Ground Heat Exchanger

In this section, the dataset of the experimental activities is analysed. The purpose of this analysis is the evaluation of the performance of the ground heat exchanger with the Flat-Panel shape.

The first part is dedicated to the results which have been obtained in all the tests performed from 2011 and to the method used to process the data. In the second part, the analysis is focused on tests carried out in 2013 and 2014 (2 tests in cooling mode and 2 tests in heating mode), are described in detail. Since January 2013 in fact, the data recording of the mass flow rate and of the inlet/outlet temperature (measured by the heat meter) has been enabled, thus enhancing the reliability of the monitoring system. Starting from the test in cooling mode carried out in winter 2012-2013 the monitoring system has not been modified anymore.

A heat exchanger may be represented reasonably well as a steady-flow system, where the fluid flows through the control volume steadily. In a steady-flow process, the fluid properties can change from point to point in the control volume but remains constant at any fixed point. Moreover, the thermal interaction between a steady-flow system and its surroundings do not change with time. As regards shallow HGHEs, the heat transfer process is unsteady actually, although these systems, which are composed by the HGHE and the ground volume involved in the process,

have an high thermal capacity. Contrary to VGHEs in fact, the heat transfer process in shallow soil is driven also by the complex heat transfer phenomenon at the ground surface, which occur mainly by convection and radiation. As a consequence, the daily and seasonal variation of the shallow soil temperature affect the performance of an HGHE, due to the low installation depth.

Moreover, the operating mode is of primary importance depending on the design of the GCHPs system. The ground heat exchanger and the ground itself, may be subjected to unsteady heat inputs due to the operation of the heat pump, which can be On/Off or modulating when equipped with an inverter.

The tests were done, as regards the experimental setup, supplying the ground heat exchanger both in continuous and discontinuous mode (with variable intervals). If the closed loop is supplied continuously with a constant mass flow rate and at a constant inlet temperature, the system reaches a near-steady-process condition. In Fig. 2.17, the inlet and outlet temperature are shown for the initial part of the test carried out in heating mode in the summer of 2011. The outlet temperature increases slowly according to the high thermal inertia of the system. However, the difference between the inlet and outlet temperature was stabilised to about 2.5 °C after 20 h from the beginning of the test. The duration of the start-up phase was determined by the thermal inertia of the mass of water contained in the ground heat exchanger (120 l), its emptying time and the thermal inertia of the ground. After this phase, the heat transfer continued in near-steady conditions, and the three dimensional heat diffusion phenomenon was prevailing. The time interval needed to reach the steady-flow condition was relatively short in comparison with the whole duration of the tests, never less than 56 days. However, for long time intervals the heat transfer was affected by the seasonal variation of the ground temperature. In the graph, the small variations in the outlet temperature were related to the mass flow rate which was not perfectly constant.

On the contrary, if the closed loop is supplied with a discontinuous mass flow rate and at constant inlet temperature, the difference in terms of heat transfer rate is significant, as shown in Fig. 2.18. In the graph, the return fluid temperature is indicated with a continuous blue line when the circulator is operating and dotted during the shutdown phase. In addition, the soil temperature near the Flat-Panel (0.4 m away) at a depth 1.15 m is shown as a reference. This test was carried out in heating mode in summer 2012 after the installation of an on/off time switch. The timer was set to supply the ground heat exchanger from 8 AM until 8 PM, from Monday to Friday. In this case, the transient characteristic of the start-up phase is visible at each time interval.

The heat transfer process, for a discontinuous operation, can be described in two distinct stages. In the first phase, called *active heat transfer*, the working fluid flows through the ground heat exchanger and a certain quantity of thermal energy is transferred to the ground.
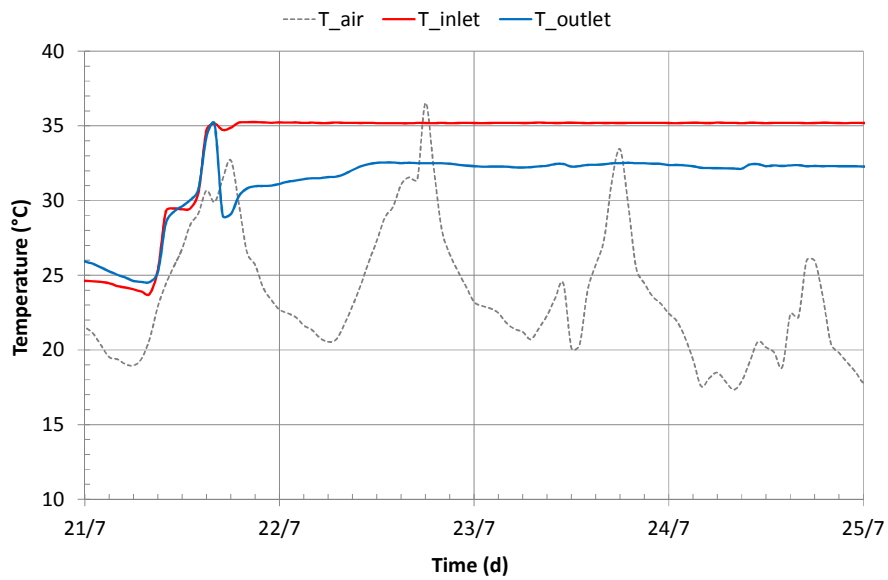
Fig. 2.17 Inlet and outlet temperature in continuous mode.
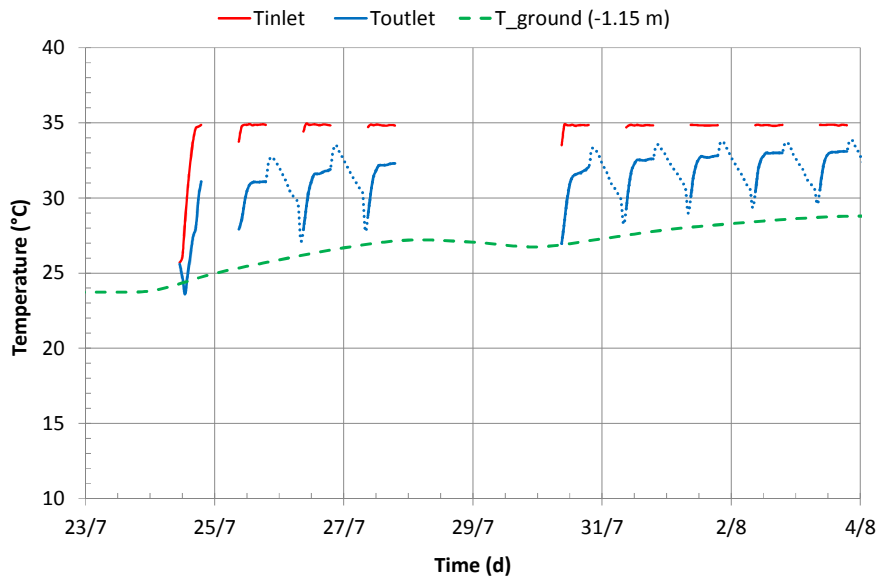
Fig. 2.18 Inlet and outlet temperature in discontinuous mode.

In the second phase, called passive heat transfer, the circulator is Off and the fluid contained within the heat exchanger continues to cool down, tending towards thermal equilibrium with the surrounding soil. For each subsequent start-up in fact, the fluid within the Flat-Panel flows to the outlet section at a temperature significantly lower than the flow temperature, until it finishes the emptying phase. Moreover, the phase of active heat transfer is positively affected by the passive phase, which optimises the heat transfer with the ground over time. The heat transfer in the ground, is usually slow due to the low thermal diffusivity of the soil. However, the temperature difference between inlet and outlet tends to stabilise over time also in this case, but after a significantly greater time than the 20 h of the previous case.

Taking these aspects into consideration, the overall heat transfer rate of the system has been related to the fluid inlet and outlet temperatures and the flow rate in order to calculate the Flat-Panel performance. The relationship has been obtained by applying the energy balance for open systems to the fluid flow through the ground heat exchanger, taken as the control volume. The steady-flow assumption has been considered an acceptable approximation to calculate the overall energy performance of the ground loop in terms of heat injection and extraction rates. In this case, the sections of inlet and outlet of the system correspond to the points at which the inlet and outlet temperature of the working fluid have been measured. As a consequence, the contribution of the horizontal piping connection between the tank and the ground heat exchanger is included.

The general energy balance equation for open systems in rate format is:

$$\frac{dE_{system}}{dt} = \dot{E}_{in} - \dot{E}_{out} + \dot{Q} - \dot{W} \tag{2.1}$$

For a steady process, the amount of energy entering the control volume (heat, work, mass transfer) must be equal to the amount of energy leaving it. Moreover, for an incompressible liquid the volume and the mass of the control volume remain constant, thus the flow work is negligible, given the small pressure variation between the inflow and outflow sections. Equation 2.1 can be applied to the steady-flow system and re-written more explicitly as:

$$\dot{m}\left(h + \frac{V^2}{2} + gz\right)_2 - \dot{m}\left(h + \frac{V^2}{2} + gz\right)_1 = \dot{Q} - \dot{W} \tag{2.2}$$

where the terms within the parentheses are expressed for a unit mass of fluid at the inflow and outflow sections. In this case a further simplification is possible because:

•   The elevation difference between the inlet and outlet of the ground heat exchanger is equal to 0 and therefore, the potential energy term is negligible.

- The variation in the kinetic energy is negligible because the fluid stream in steady flow enters and leaves the system at about the same velocity.

In order to calculate the rate of heat transfer between the control volume and its surrounding the Equation 2.2 is reduced to:

$$\dot{Q} = \dot{m}(h_2 - h_1) \qquad (2.3)$$

where h is the fluid enthalpy (per unit mass). The subscripts 2 and 1 refer to the working fluid at the outlet and inlet sections respectively. Since the working fluid is not undergoing a phase change and constant specific heats are assumed, Equation 2.3 reduces to:

$$\dot{Q} = \dot{m}c_l(T_{out} - T_{in}) \qquad (2.4)$$

where the temperatures in the expression refer to the mean fluid temperatures over the inlet/outlet cross sections at the designated locations, as a further simplification. In heating mode the outlet temperature is lower than the inlet temperature, therefore, the heat transfer rate is negative (and vice versa in cooling mode), according to the sign convention of thermodynamics. In a more general form, Equation 2.4 can be written as:

$$\dot{Q} = \dot{m}c_l\Delta T \qquad (2.5)$$

Equation 2.5 has been applied to calculate the rates of injection and extraction of heat (W/m) of the system and the total amount of energy injected or extracted. During the initial tests (2011), the mass flow rate was measured by direct weighing, since the monitoring system was not equipped with a flow meter in its first configuration. The tests were carried out in heating mode with an inlet temperature of 30 ÷ 35 °C, and thus pure water was used as the working fluid. In order to carry out tests also in cooling mode, the experimental setup has been equipped with a chiller since January 2012.

The working fluid has been replaced with a mixture of water and monoethylenglycol (20 % V/V) with a the freezing point at -9°C. At the same time, the hydraulic circuit has been modified to install the compact heat meter to measure the mass flow rate. The remote recording of measured data recording with a fixed time step of 5 min has been enabled since December 2012 only.

The properties of the working fluid are listed at different values of temperature in Table 2-3. Moreover, the temperature of the working fluid supplied to the closed loop, the mean natural temperature of the ground at the average depth of the ground heat exchanger (1.3 m) and the difference between them are reported in Table 2-4.

Tab. 2-3 Properties of mixture Water and a 20% in volume of Monoethylen-glycol
(Extract from VDI-Warmeatlas, 1991).

Temperature (°C)	Density (kg/m^3)	Specific Heat (kJ/kgK)	Thermal conductivity (W/mK)
-10	1038	3.85	0.498
0	1036	3.87	0.500
20	1030	3.90	0.512
40	1022	3.93	0.521

Tab. 2-4. Average natural ground and average working fluid temperature during tests.

Mode	Natural Soil Temperature (depth: 1.4 m) (°C)	Working Fluid Temperature (°C)	ΔT (°C)
Heating	12 ÷ 22	31 ÷ 35	13 ÷ 23
Cooling	10 ÷ 19	2 ÷ 8	8 ÷ 11
Free	12 ÷ 19	6 ÷ 12	6 ÷ 7

During the tests in the heating mode, the flow temperature was set between 31 °C and 35 °C. These values were significantly higher than the undisturbed temperature of the ground (UNI 11466, 2012). In cooling mode tests, the temperature of the working fluid varied between 8 °C and 2 °C, to maintain an adequate difference with the ground temperature.

Tests were performed for different flow rates, in the range of 80 l/h and 260 l/h. In order to characterize the flow regime within the Flat-Panel, the Reynolds number was calculated for the reference rectangular section (0.15 m x 0.02 m), under the different flow conditions:

$$Re = \frac{\rho v D_h}{\mu}$$

(2.6)

where ρ is the density of the working fluid and v is its mean velocity across the section. Given the hydraulic diameter (D_h) of the rectangular section of 0.035 m and a dynamic viscosity (μ) of the water/glycol mixture of 2.13^{-3} Pa·s at the temperature of 10 °C, the Reynolds number is lower than 2400 and consequently the flow regime is always laminar, as shown in Fig. 2.19.

A comprehensive survey on the flow regime within a Flat-Panel for different sections is reported in Battarra (2013).
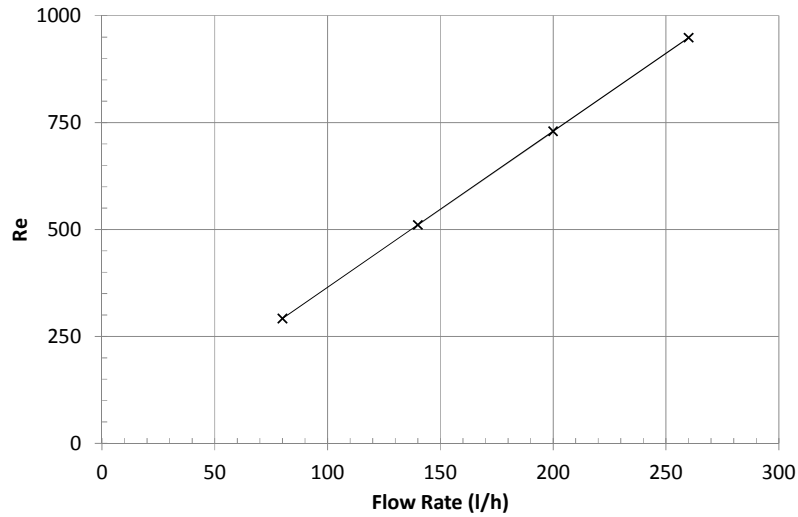
Fig. 2.19 Flow regime for different flow rates.

A summary of the tests which have been carried out since 2011 is reported in Table 2-5. The duration, the total amount of working hours and the total amount of energy extracted/released from/to the ground are reported for each test.

Tab. 2-5 Summary of tests data.

Period	Mode	Lenght (m)	Duration (d)	Time ON (h)	Energy (kWh)
11/03/2011→31/05/2011	Heating	3	161	2907	990
14/07/2011→28/09/2011	Heating	6			
19/11/2011→31/01/2012	Free	6	73	576	41
31/01/2012→04/04/2012	Cooling	6	56	843	225
24/07/2012→01/10/2012	Heating	6	68	591	256
13/11/2012→10/04/2013	Cooling	6	148	1267	367
14/08/2013→23/10/2013	Heating	6	71	1678	590
04/12/2013→03/04/2014	Cooling	6	120	2858	482.3
12/06/2014→12/12/2014	Heating	6	182	1281	919

According to the data reported in Table 2-5, the average heat transfer rate (RHT) of the system was of 45 W/m during the test in cooling mode carried out from January to March 2012. During the test, the system operated both in continuous and discontinuous mode (around the 50% of the time in each mode). The set-point temperature was set to 0 °C, with an average difference between the natural ground temperature and that of the working fluid of 8 - 11 °C, as shown in table 2-5. The set-point temperature in heating mode was set at 35 °C, 13 - 22 °C higher than the natural ground temperature, therefore, higher performance have been obtained. In summer 2012 the average heat transfer rate was 72 W/m. This test was performed with the system operating in discontinuous mode (system turned on from 8 AM to 8 PM every day). Moreover, the system was tested in free mode in winter 2011-2012 showing an average RHT of 12 W/m. In this case the temperature in the tank was variable according to the air temperature.

2.3.3 Test I

The energy performance of horizontal GCHP systems is strongly related to the seasonal temperature variation of the shallow soil, due to the low installation depth of the ground heat exchanger. Moreover, in winter, when solar radiation is reduced and air temperature is low, GCHP systems need the highest energy output from the ground. As a consequence, the natural decrease of the ground temperature can lead to unfavourable working conditions and to an efficiency reduction. In view of this, the testing in cooling mode of the horizontal ground heat exchanger has to deal with a number of issues.

The first test (called Test I) with the experimental setup in its final configuration started on 13th November 2012. The system was set to simulate the winter operation of a GCHP, in order to evaluate the performance of the Flat-Panels in cooling mode. Since January 2013, the values measured by the heat meter have been recorded remotely in a database, with an acquisition time step of 300 s. This dataset has been taken as reference for the performance analysis of the ground heat exchanger. However, the M-Bus interface has suffered of several communication problems with the LAN network. As a consequence, some records have been missed and the large dataset related to the heat meter measurements was incomplete. The electronic unit of the heat meter was equipped with an internal memory and the overall data of each test were saved correctly. Therefore, the data of the total amount of energy and the total volume of working fluid circulated was available for each test. In addition, the network of temperature sensors initially installed (equipped with a sensor line dedicated to the hydraulic loop), worked also after the installation of the heat meter. The simultaneous running of two independent measuring systems allowed collection of a comprehensive dataset. Finally, the reliability of the measuring system has been verified through a comparison between the temperature values measured by the RTD sensors, the heat meter and a further

device. The accurate estimation of the fluid temperature difference (DT) between the inlet and the outlet sections affects the calculation of the overall heat transfer rate of the system through Equation 2.5. Therefore, the DT datasets measured by the heat meter and by the other sensors has been compared in Fig. 2.20. The red line in the graph represents a perfect agreement between the two measuring systems. There is a good positive correlation between the two data sets (R^2 is equal to 0.98). The old measuring system shows the tendency to slightly overestimate the temperature difference in comparison to the heat meter, due to the different installation. The standard deviation is 0.16 °C and 0.33 °C for |DT| lower and higher than 3 °C, respectively. A slight dispersion occurs for |DT| higher than 3 °C, however, this occurs for about the 9% of measurements, therefore it does not significantly affect the relationship.

The return temperature of the working fluid, as measured at the outlet section, has been compared with that measured by a properly installed shielded temperature probe, for further verification. The reference probe was positioned in a dedicated seat in the group of valves, after the FP2. The correlation between the values measured by the two different temperature sensors is reported in Fig. 2.21, from 01/01/2013 to 04/01/2013. There is a good correlation between the two sensors although, the reference one showed slightly higher values of temperature than the PT500 installed on the heat meter. Since the temperature of the working fluid is nearly constant along the connection pipe (highly thermally insulated) between the ground heat exchanger and the heat meter, the heat losses are negligible.
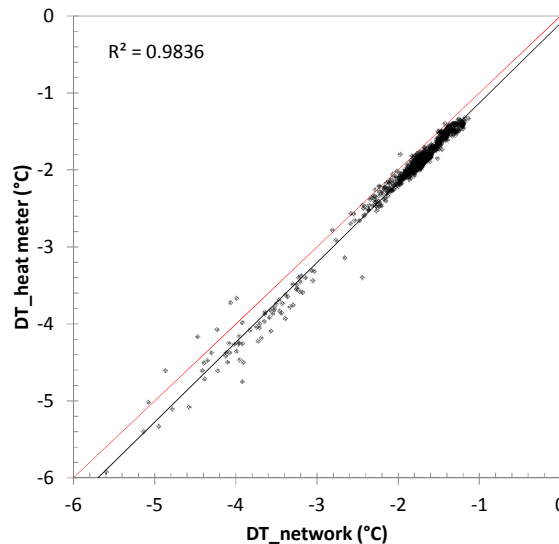
Fig. 2.20 Scatter plot of the difference of temperature between inlet and outlet as measured by the plant probe line (y axis) and the heat meter (x axis).
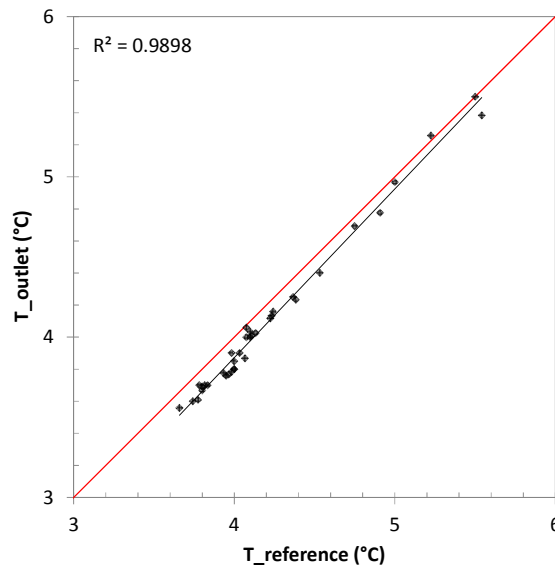
Fig. 2.21 Scatter plot of the outlet temperature (y axis) and the reference (x axis), recorded from 01/01/2013 and 04/01/2013.

The temperature difference between the inlet and outlet sections can be considered as an effect of the thermal coupling with the ground exclusively and therefore it is representative of the GHE performance.

As regards the mass flow rate, the circulator pump was set to maintain a constant flow rate during the whole test. However, variations in mass flow rate up to 10% have been recorded in the long term.

The dataset has been analysed to evaluate the trend of the working fluid temperature during the test, the flow rate, and finally to calculate the RHT of the system and the total amount energy extracted from the ground. These have been further checked with the values of RHT and energy automatically calculated by the heat meter, taking into account the variations of density and specific heat of the water/glycol mixture, due to the temperature variation.

A comprehensive summary of Test I is reported in Table 2-6. The test in cooling mode started in November 2012, with a duration of about 148 days. The working fluid was circulated through FP1 and FP2. Both the circulator pump and the chiller were placed on a timer so that they were turned on from 6 AM to 6 PM, from Monday to Friday. The chiller was initially set to maintain the temperature in the tank at 8 °C, then lowered to 1.5 °C. The initial set-point was chosen to be around 10 °C lower than the natural ground temperature at the mean depth of the ground heat exchanger, as suggested by the Italian regulation on ground heat exchangers (UNI-11466).

Tab. 2-6 Summary of Test I.

Mode	Date		Duration (days)
COOLING	Start: 13/11/2012	End: 10/04/2013	148
Operating Mode			Time ON (hours)
DISCONTINUOS	6 am → 6 pm	Monday → Friday	1267
Inlet temperature Max ÷ Min (°C)	Average ΔT inlet/outlet (°C)	Ground temperature (V.6.5) Initial ÷ Final (°C)	Volume (m^3)
8.0 ÷ 1.5	2.0	17.6 ÷ 9.2	160
Flow rate Min ÷ Max (l/min.)	Average heat transfer rate (W/m)	Max heat transfer rate (W/m)	Energy (kWh)
1.75 ÷ 2.35	48.3	151.3	367

The temperature at the sensor V.6.5 (1.4 m far from FP1, at a depth of 1.65 m) has been taken as the reference.

The circulator and the valve have been initially set to have a flow rate of 3.3 l/min, which was reduced to 2.15 l/min the 15th of November. During the whole test, the experimental setup operated for 1267 h, and a total of 160 m^3 of fluid was circulated, equal to an average flow rate of about 125 l/h.

In overall terms, the ground heat exchanger extracted a total amount of thermal energy of 367 kWh from the ground, equal to 2.4 kWh/day, in discontinuous mode. The average heat transfer rate over the entire period was of 48.3 W/m (with a peak of 150 W/m) which was very similar to that recorded during the preliminary testing activity carried out in cooling mode in the previous winter.

Figure 2.22 illustrates the trend of the average daily temperature of inlet and outlet fluid circulating in the HGHE as measured by the network of sensors during Test I. The daily average temperature of the air and the difference between the temperature of inlet and outlet have been included in the graph. In addition, the simultaneous daily average heat transfer rate (calculated with Eq. 2.5 for unit length of the trench/GHE) is shown in Fig. 2.23 together with the ground temperature trend measured 3 m far from the ground heat exchanger, at a depth of 1 m and 1.9 m with the probes V.1.5 e V.1.6 respectively.

In Test I, the experimental setup was turned on at 11 AM on 13th November, with a set point temperature of 8 °C and a flow rate of 3.3 l/min. However, the flow

rate was corrected to 2.4 l/min after 2 days, in order to maintain a difference (DT) between inlet and outlet fluid temperature of 2 °C. Moreover, the temperature of the fluid flowing to the exchanger was initially lowered to 7 °C around the end of November, then at 4 °C on 3rd December and finally to 2 °C on 14th December, to follow the decreasing trend in the air temperature and in the natural shallow ground temperature, as visible in the graph. These operations allowed the maintenance of an acceptable difference between the fluid temperature and the ground temperature (8 °C), and therefore, an adequate rate of heat transfer for the whole duration of the test.

The temperature difference DT (inlet/outlet), and consequently the rate of heat transfer became almost stable around 2 °C and 45 W/m respectively after the end of January. However, according to the decreasing trend of the undisturbed temperature of the ground, a slight decrease up to about 40 W/m was recorded. Moreover, the discontinuous operation of the experimental setup is shown in Fig. 2.22 and 2.23.

When the circulator and the chiller came into operation, the average working fluid temperature and the average RHT decrease rapidly. The RHT is lower by about 20% after 5 operating days. However, when the system is turned off, the heat transfer between the fluid within the Flat-Panels and the ground continues, and thus an initial recovery is shown at the next system start. At the end of January, the set-point was further lowered to 0 °C, but the chiller was not able to achieve and maintain this temperature in the tank. As a consequence the inlet temperature was higher than 1 °C.

The rate of heat transfer started to increase simultaneously with the increase in soil temperature (at the average depth of the ground heat exchanger) despite this, the temperature in the tank was higher than the set-point due to the increase in air temperature. This indicates that the performance of the ground heat exchanger was influenced by the natural change of temperature of the ground. Therefore, the effect of the seasonal variations of ground temperature should be taken into account for the design of horizontal ground heat exchanger, as reported in (Fujii, et al., 2010). In the final period of the test, the GHE showed an average RHT of about 55 W/m, the 30 % higher than the minimum value at the end of February. Simultaneously the flow rate increased by about 10%.

In analogy with the figures 2.22 and 2.23, the hourly average temperature of the working fluid and the hourly average RHT are shown in Fig. 2.24 and Fig. 2.25 for 2 weeks. The timer was set to supply the ground heat exchanger from 6 AM until 6 PM (from Monday to Friday) with a set-point temperature in the tank of 2 °C. However, the fluid temperature was not constant due to heat losses through the tank envelope when the chiller and the circulator pump were turned off.

The temperature difference between inlet and outlet, and consequently the RHT show high initial values (higher than 4 °C and 80 W/m) at each starting phase, followed by a fast decrease.
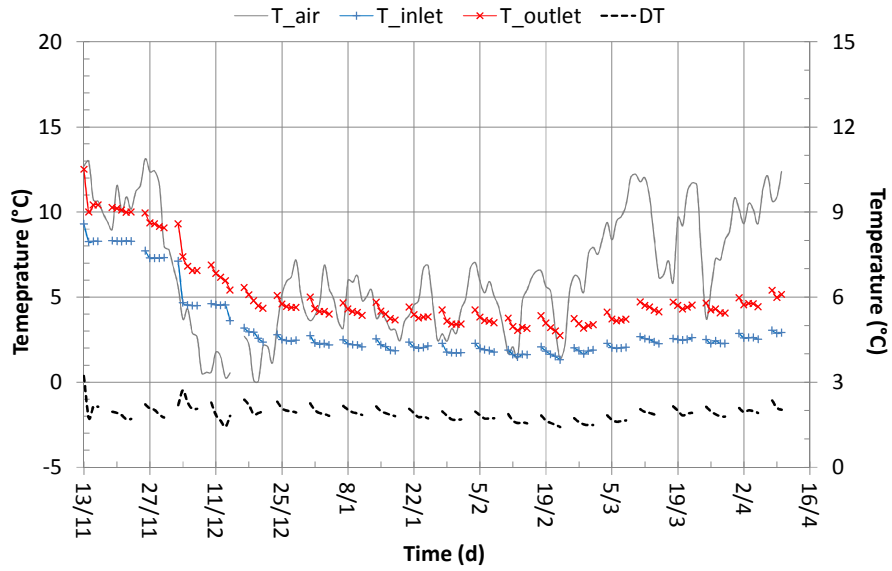
Fig. 2.22 Daily average temperature of the working fluid.
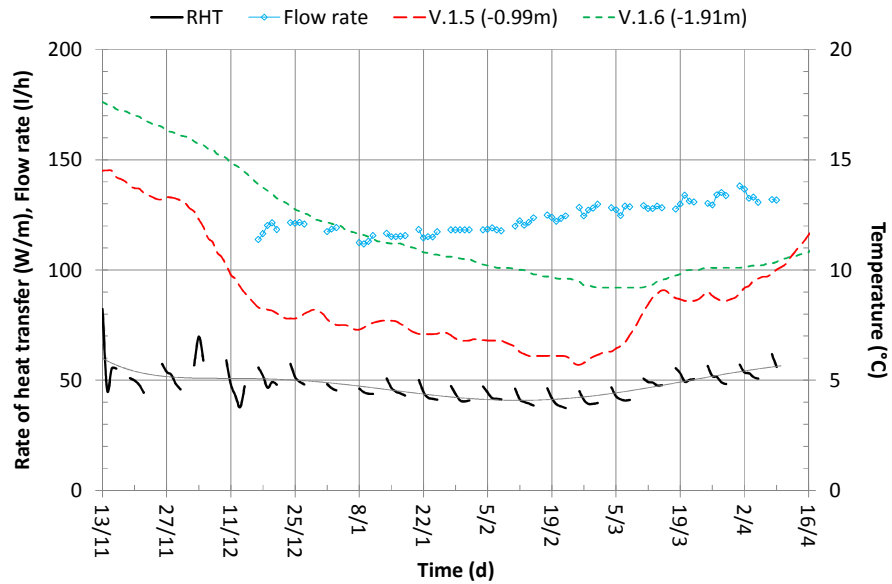
Fig. 2.23 Daily average rate of heat transfer , flow rate and natural ground temperature.
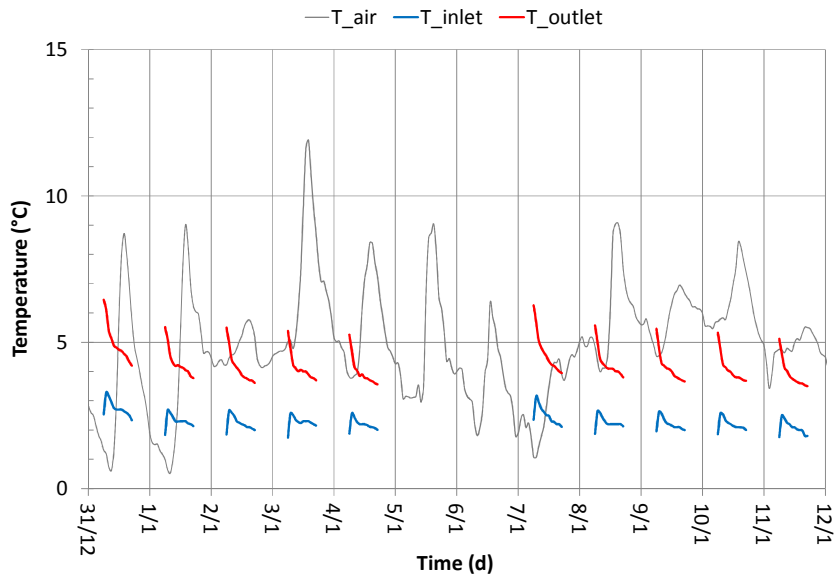
Fig. 2.24 Hourly average temperature of the working fluid from 31th of December to 11th of January.
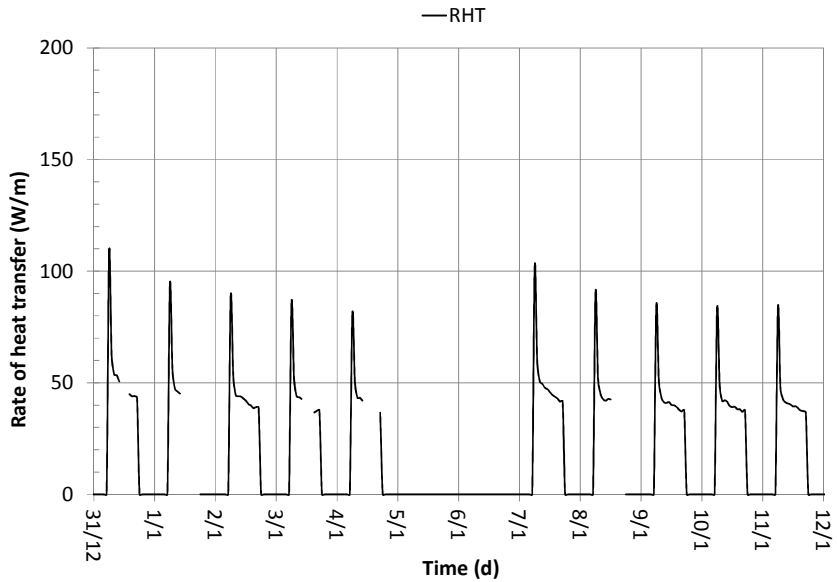
Fig. 2.25 Hourly average rate of heat transfer from 31th of December to 11th of January.

These peaks are strictly related to the passive heat transfer phase when the fluid contained within the Flat-Panels (about 120 L), continues to warm up, tending towards thermal equilibrium with the surrounding soil. Assuming an average flow rate of 2.15 l/min, the circulator pump takes about an hour to change completely the warm fluid contained in the ground loop at each start.

After this phase, the ground heat exchanger completely enters in the active phase. The rate of heat transfer is almost halved after about two hours, and shows a tendency to stabilize at about 40 W/m. In overall terms, both the peaks and the average RHT tend to decrease. However, the process is almost stabilized over time and for small ground temperature variations, as observed between 9th and January 11th when the peak is at 80 W/m and the minimum is 37 W/m.

2.3.4 Test II

One of the most appreciated features of GCHP systems is that they can provide efficiently thermal energy for space heating/cooling, without the need for separate systems. In countries with hot, muggy summers (e.g. Southern Europe), the building energy requirement for cooling can be equivalent, and sometimes greater, than that for heating. In view of this, the testing in heating mode of the horizontal ground heat exchangers is important. Furthermore, the performance of whatever horizontal installation is strongly affected by the natural temperature trend of shallow soil which can have a maximum of between 20 °C and 25 °C at the average depth of installation (approximately between 1 m and 2 m deep).

In August 2013, the experimental setup was set to simulate a summer operation of a GCHP, in order to evaluate the performance of the Flat-Panels in heating mode. The Test II started on 14th August, four months after the end of Test I in cooling mode, in order to have a natural temperature distribution in the shallow ground at the beginning.

Some data recorded by the heat meter was missed due to unresolved problems of communication, similarly to what happened during Test I.

Although the inlet temperature was maintained constant during the test, the measured temperature at the outlet section showed a daily oscillation, up to a maximum of about 0.5 °C. The variation might have been partially related to the heat absorbed by the fluid flowing through the connection piping, due to the effect of solar radiation, as shown in Fig. 2.26. In fact, the terminal part of the connecting pipes (almost 4 m), although thermally insulated and shielded with a double corrugated pipe, was not buried (the excavation near the ancient porch was not allowed). Consequently, it was exposed to the sun.

The temperature difference between the inlet and outlet sections (on average 2°C), therefore, was reduced during the hottest hours of sunny day. As a result, the calculation of the heat transfer rate should be considered as a precautionary approach in this test.
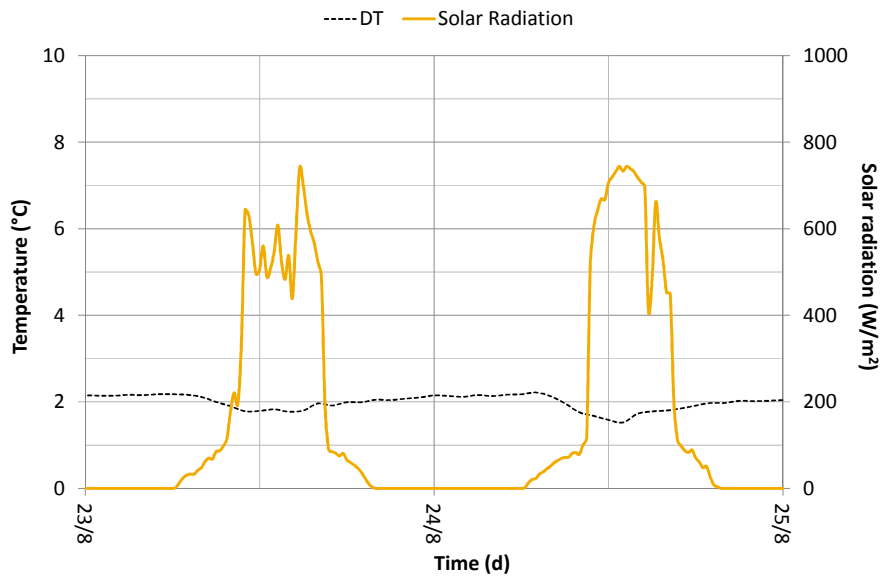
Fig. 2.26 Solar radiation and DT (inlet/outlet) at the end of August 2013, during Test II.

However, the increase of temperature at the outlet section is a temporary phe-nomenon, which negatively affects the performance for a few hours only during the day.

A comprehensive summary of Test II is reported in Table 2-7. Test II (heating mode) started on 14th August 2013, with a duration of about 71 days. The circulator was set to operate in continuous mode, 24 h/day, and 7 days a week. The experi-mental setup was in operation for 1678 h.

In this test, the electric heater integrated into the chiller was used to maintain the working fluid at 35 °C, instead of using the electric heaters installed in the tank. However, the resulting temperature in the tank was initially 33.5 °C due to an error of 1.5 °C in the thermostat reading. The thermostat was then calibrated to obtain the correct reading of the temperature. The initial set-point was chosen to be around 12 °C higher than the natural ground temperature at the mean depth of the ground heat exchanger. Moreover, the test was started with a flow rate of 1.5 l/min, which was significantly lower than in Test I. However, the flow rate was in-creased to 2.15 l/min the 15th of August and it followed an increasing trend (up to 2.9 l/min) during the test. Approximately, 265 m^3 of working fluid circulated through the ground heat exchanger. The system exchanged an amount of 590 kWh with the ground at the end of the test, equal to a daily average of 8.3 kWh. The Flat-Panels showed excellent performance in this case, despite the thermal load being higher than in Test I (more than double).

Tab. 2-7 Summary of Test II.

Mode	Date		Duration (days)
HEATING	Start: 14/08/2013	End: 23/10/2013	71
Operating Mode			Time ON (hours)
CONTINUOS	24h	Monday → Sunday	1678
Inlet temperature (°C)	Average ΔT inlet/outlet (°C)	Ground temperature (V.6.5) Initial ÷ Final (°C)	Volume (m³)
33.5 ÷ 35.0	2.0	21.8 ÷ 22.1	265.3
Flow rate (l/min.)	Average heat transfer rate (W/m)	Max heat transfer rate (W/m)	Energy (kWh)
1.5 ÷ 3.1	58.6	149.9	590.4

The high rate of heat transfer is partially due to the higher temperature difference between the thermally undisturbed soil and the heat transfer fluid. The average heat transfer rate over the entire period was of 58.6 W/m (with a peak of 150 W/m).

As in Test I, the data analysis was used to evaluate the behaviour of the ground heat exchanger during the test, according to the variations in ground temperature and to the changes in operation mode. The trends of the average daily temperature of inlet and outlet during Test II are shown in Fig. 2.27, together with the daily average temperature of the air and the difference between the temperature of inlet and outlet (DT). Moreover, Fig. 2.28 illustrates the simultaneous daily average heat transfer rate (calculated with Eq. 2.5 for unit length of the trench/GHE) together with the flow rate and the ground temperature trend measured 3 m far from the ground heat exchanger, at a depth of 1 m and 1.9 m with the probes V.1.5 e V.1.6 respectively. The test started at 3:40 PM on 14th August, with a flow temperature of 33.5 °C and a flow rate of 1.5 l/min. However, the flow rate increased during the test to a maximum of 3.1 l/min. Moreover, the temperature of the fluid flowing to the exchanger increased to 35 °C after the calibration of the thermostat on 19th August, as visible in the graph. The daily average difference of temperature between inlet and outlet and the average RHT decreased rapidly during the initial phase lasting around 5 days. After this phase, DT was almost stabilised around 2 °C during August. Conversely, the trend of RHT showed variations between 50 W/m and 60 W/m due to variations in flow rate and weather conditions. However, a

slight decreasing trend was recorded until the end of September. Since the middle of September, the rate of heat transfer started to increase according to the decreasing trend of the undisturbed temperature of the ground (at the average depth of the HGHE). Finally, the performance of the GHE increased significantly in the last month to an average value of 72 W/m, with a constant flow rate of 2.9 l/min.

Fig. 2.27 Daily average temperature of the working fluid.
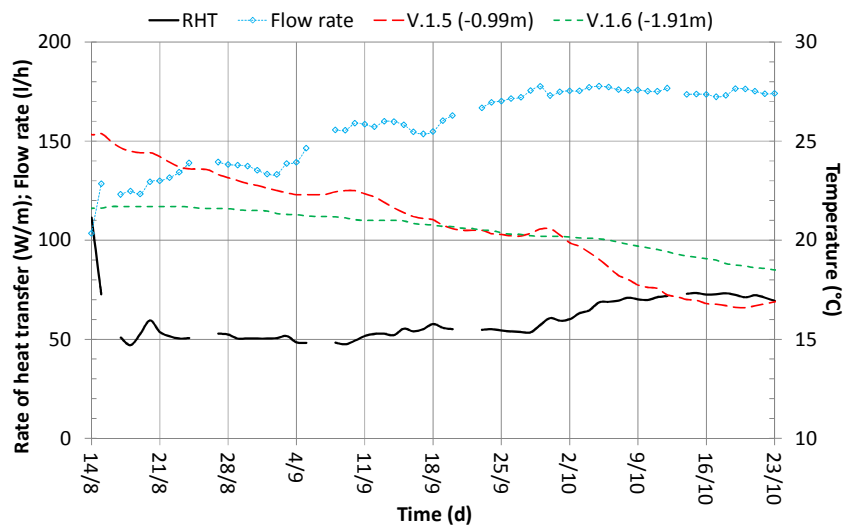
Fig. 2.28 Daily average rate of heat transfer , flow rate and natural ground temperature.

A detail of two weeks is shown Fig. 2.29 and Fig. 2.30 for Test II. The starting phase is clearly visible, when DT is higher than 3 °C and the rate of heat transfer higher than 60 W/m, then followed by a fast decrease. On 19th August, after five full operating days, the daily average RHT was reduced to almost the 30% of the initial peak at 150 W/m. Although the heat transfer process is stable on average terms after the first 15 days, the effect of solar radiation is clearly visible, which involves temporary RHT reductions up to 25%.
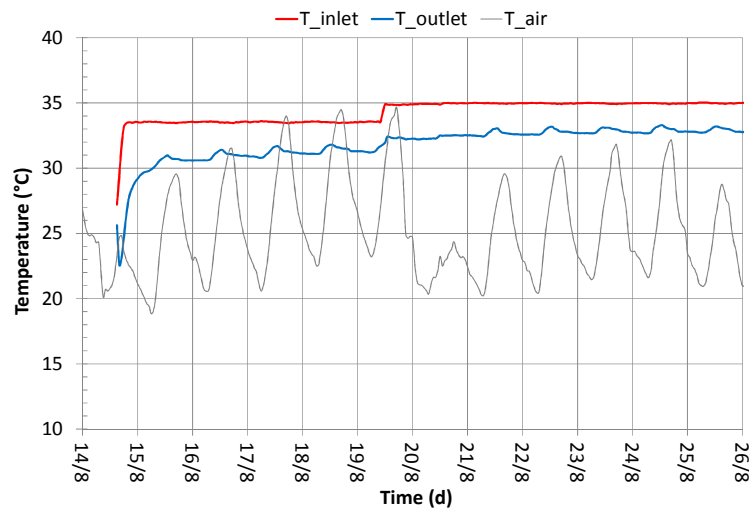
Fig. 2.29 Hourly average temperature of the working fluid from 14th to 28th of August.
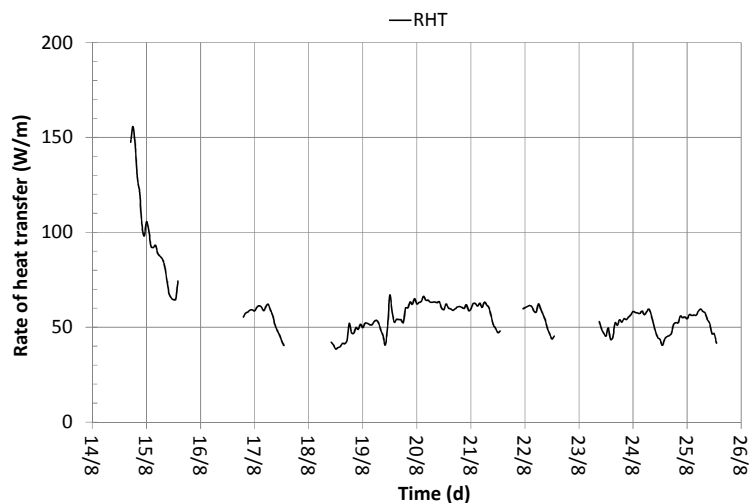
Fig. 2.30 Hourly average rate of heat transfer from 14th to 28th of August.

2.3.5 Test III

Test III began about 45 days after the end of the previous test in heating mode. The circulator had been working after the end of Test II, in order to supply the ground heat exchanger in free mode. At the same time, the experimental setup was subjected to maintenance. During the intervening period a natural uniform temperature distribution was reached around the GHE. The experimental setup was set to operate in cooling and continuous mode. A comprehensive summary of Test I is reported in Table 2-8. This test lasted 120 days, from 4th December 2013 to 3rd April 2014. The chiller was switched on the previous day to lower the working fluid temperature in the tank to 8 °C. On 5th December, the set-point temperature was modulated to 5 °C, in order to obtain a difference of 10 °C between the flow temperature and the natural ground temperature at the mean depth of the ground heat exchanger. The chiller and circulator were set to operate 24 hours a day and 7 days a week. As a consequence, the experimental setup operated for a considerable amount of time (2858 h) in four months. Initially, the flow rate was set to 2.9 l/min, however different flow rate set-points were tested during the course of the test in order to assess the effect of the flow rate on the performance of the ground heat exchanger. A total of 495 m^3 of fluid were circulated, equal to an average flow rate of about 170 l/h. In Test III, the experimental setup extracted an amount of 482 kWh from the ground in continuous operation. This corresponds to a daily heat load of 4 kWh, which is significantly higher

Tab. 2-8 Summary of Test III.

Mode	Date		Duration (days)
COOLING	Start: 04/12/2013	End: 03/04/2014	120
Operating Mode			Time ON (hours)
CONTINUOS	24h	Monday → Sunday	2858
Inlet temperature (°C)	Average ΔT inlet/outlet (°C)	Ground temperature (V.6.5) Initial ÷ Final (°C)	Volume (m^3)
8.0 ÷ 2.0	0.93	15.5 ÷ 10.2	495.2
Flow rate (l/min.)	Average heat transfer rate (W/m)	Max heat transfer rate (W/m)	Energy (kWh)
1.2 ÷ 3.8	28.1	77.9	482.3

than that of the previous cooling Test I (2.4 kWh/day). Therefore, the average heat transfer rate over the entire period was of 28.1 W/m (lower than Test I, in cooling mode), with an initial maximum of 78 W/m and a minimum of 15 W/m.

The performance of the ground heat exchanger during Test III was evaluated through the data analysis, according to the variations in ground temperature and to the changes in operation mode, as shown in Figures 2.31 and 2.32. The trend of the average daily fluid temperature of inlet and outlet, the difference between them and the daily average temperature of the air are shown in Fig. 2.31. In addition, Fig. 2.32 illustrates the simultaneous daily average heat transfer and the ground temperature trend measured 3 m far from the ground heat exchanger, at a depth of 1 m and 1.9 m with the probes V.1.5 e V.1.6 respectively.

Since 27th December the data of the natural ground temperature were measured also with the wireless Soil Station. This secondary unit was placed more than 5 m far from the ground heat exchanger, therefore, no thermal alteration is expected for this sensor. The temperature time series related to the measurements of the sensor placed at a depth of 0.8 m is reported in the Fig. 2.32 (called WLK).

The experimental setup was turned on at 3.30 PM on 4th December, with a set point temperature of 8 °C and a flow rate of 2.9 l/min. However, the temperature set-point was corrected to 5 °C on 5th December, in order to maintain a difference of almost 8 °C between the fluid temperature and the natural ground temperature.

The inlet/outlet temperature difference decreased from 1.4 to 0.7 °C in the following 3 days, according to the high thermal inertia of the system. At the same time, the RHT was almost halved (from 40 W/m to 20 W/m).

After the start-up phase, the heat transfer continued in near-steady conditions. However, a decreasing trend of DT and RHT is visible in the graphs (up to 0.4 °C and 12 W/m respectively), according to natural variation in shallow ground temperature. Such a reduction in the heat transfer rate was related to the low temperature difference between the ground and the working fluid (less than 4.5 °C). The period between 10th December and 20th December in fact, was quite cold, with average air temperature below 4 °C, thus causing a significant cooling of the shallow ground.

A 40 % increase was recorded, up to about 20 W/m, according to the temporary increase in the undisturbed temperature of the ground in the following week. Until the 15th of January, the performance of the ground heat exchanger was stabilised with a DT of about 0.6 °C and a flow rate of 170 l/h.

The temperature of the fluid flowing to the exchanger was initially lowered to 2 °C on 14th of January, in order to enhance the heat transfer, as visible in the graph. The thermostat was calibrated on 22nd January, causing a further decrease of 0.3 °C. At the same time, a decrease of 10-13% in the flow rate was recorded, probably caused by an increase in the viscosity of the water/glycol mixture related to the low temperature. This operation actually resulted in a significant increase in the GHE performance, up to almost 40 W/m.
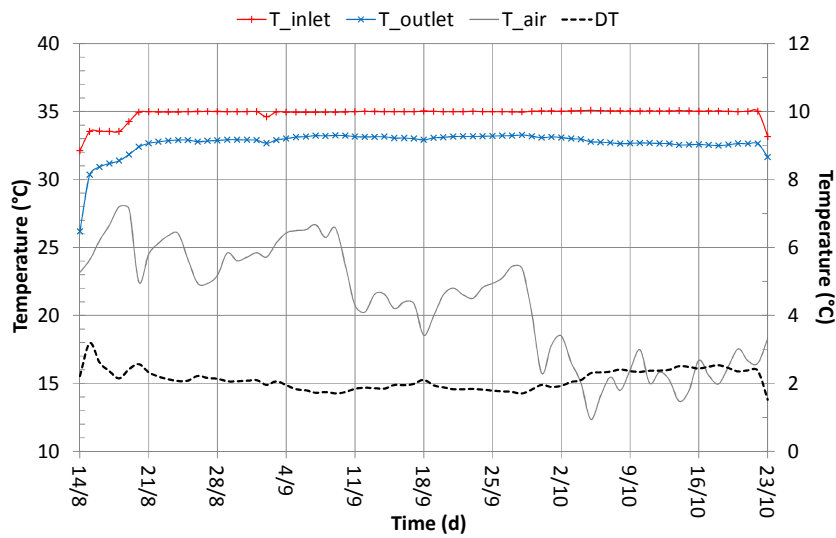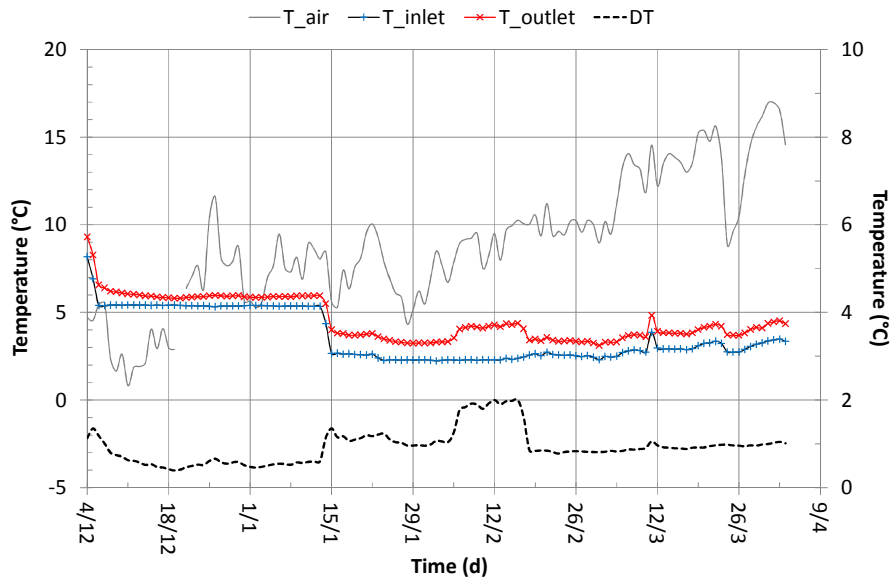
Fig. 2.31 Daily average temperature of the working fluid.
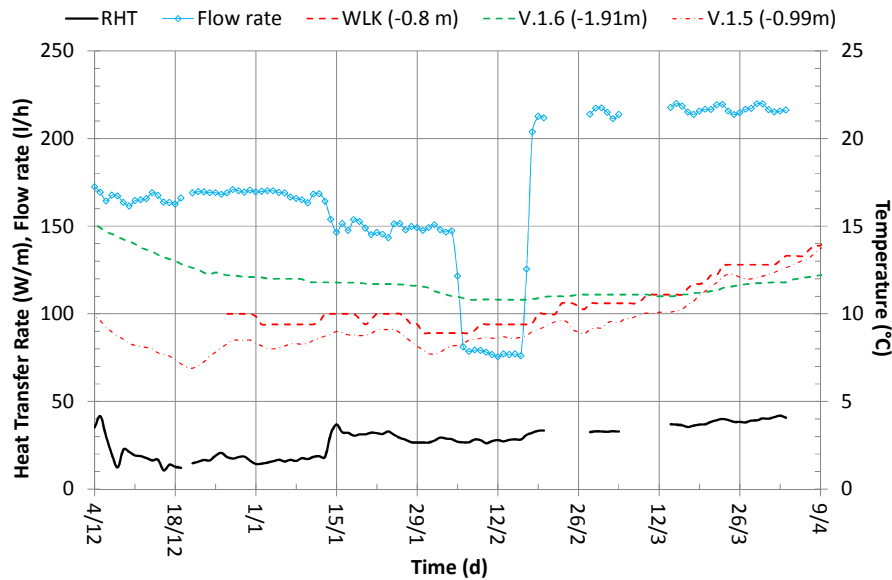
Fig. 2.32 Daily average rate of heat transfer , flow rate and natural ground temperature.

However, a slightly downward trend of RHT and the natural temperature of the ground were observed in the following weeks. Given the near steady operation of the system at this stage, the flow rate was reduced from 145 to 80 litres per hour on 5th of February, in order to analyse the effect of the flow rate on the GHE performance. The temperature difference between inlet and outlet sections of the heat exchanger was increased from 1 °C to 2 °C, because of the increased residence time of the fluid within the ground closed-loop. However, no changes were observed in the rate of heat transfer, which in fact remained constant for the ten trial days at a low flow rate. On 17th February, the flow rate was again increased to 215 l/h, a set-point of the flow rate much higher than the previous one (145 and 80 l/h respectively). A slight and immediate increase in RHT is visible in the graph. Since the beginning of March, the fluid temperature in the tank, and consequently the inlet temperature, have increased beyond the set-point (2 °C), as shown in Fig. 2.33. The chiller cooling capacity in fact, has proved inadequate to balance the warming of the working fluid within the tank. This occurred due to the combined effect of the return fluid (at a temperature higher than the set-point) and of the thermal coupling between the tank and the ambient when the air temperature increased over 10 °C. Therefore, it was not able to maintain the temperature of set-point, despite continuous operation. As a consequence, the fluid temperature at the inlet and the outlet sections showed an oscillatory trend, according to the variations in the air temperature. The experimental set-up suffered a shutdown on 11th March due to an interruption in the power supply which lasted 20 hours. When the test was restarted, a RHT peak of 47 W/m was initially recorded, however, the system took about 24 h to return to the working conditions before the shutdown. The natural ground temperature at shallow depth had generally increased since the beginning of February, due to the changes in local environmental conditions. As a consequence, an increasing trend was recorded in the average rate of heat transfer, independently of the variation of the mass flow. In the period from 17th February (when the mass flow was finally set to 210 l/h) at the end of the test, the average daily RHT increased by 22%.

In analogy with the previous figures 2.29 and 2.30, the hourly average temperature of the working fluid and the hourly average RHT are shown in Fig. 2.33 and Fig. 2.34 for a week. The weekly detail focused on the period between 12th and 19th of January, in order to analyse the effect on the GHE performance of an instantaneous drop of the inlet temperature. The inlet temperature was lowered from 5 °C to 2 °C on 14th of January, in order to enhance the heat transfer in the ground, as visible in the graph 2.33. Before this operation, the Flat-Panels were supplied with a flow rate of 165-170 l/h at a fluid temperature slightly higher than the set-point (5 °C). In these operating conditions, the return fluid temperature was almost constant, 0.6 ° C higher than the flow temperature, resulting in a rate of heat transfer of about 18 W/m. Then, an immediate increase of the RHT was observed contemporary with the lowering of the fluid temperature, due to the higher temperature

difference between the fluid and the ground near the GHE. The temperature difference between inlet and outlet, and consequently the RHT showed high initial values (higher than 1.5 °C and 45 W/m), followed by a decreasing trend for the next 20 hours.
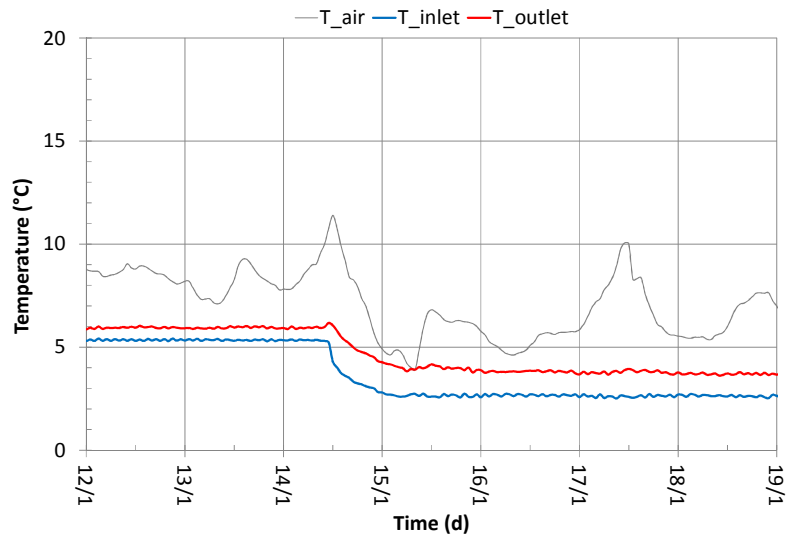
Fig. 2.33 Hourly average temperature of the working fluid from 14th to 28th of August.
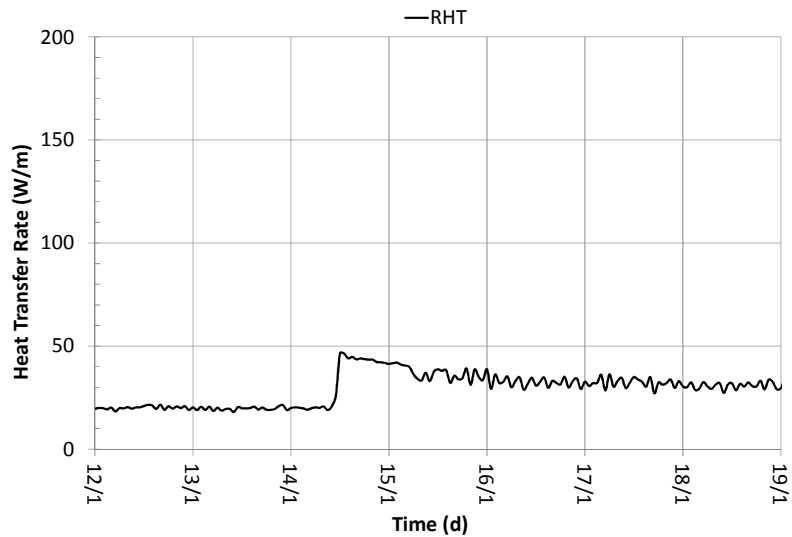
Fig. 2.34 Hourly average rate of heat transfer from 14th to 28th of August.

At the same time, the flow rate decreased from 170 l/h to 145 l/h, due to the variation in viscosity of the working fluid. After this phase, the heat transfer was again stabilised over time at 30-32 W/m, which was 60% higher than the RHT before this operation.

2.3.6 Test IV

In the middle of June 2014, a fourth test (called Test IV) was started in heating mode and under discontinuous operation. In this case, the experimental setup operated for the whole summer, in order to evaluate the performance of the Flat-Panels also early and late in the season. In addition, Test IV was also prolonged until December, when the average daily air temperature was fully below 20 °C. As a consequence, the experimental setup operated under various environmental conditions during the 6 months of test. The previous Test III in cooling mode ended on 3rd April, more than two months before the beginning of Test IV (on 12th June 2014); therefore, the shallow ground had a natural temperature distribution in June.

The experimental setup was operating 24/7, thus, the electric heater controlled by the thermostat maintained a nearly constant temperature in the tank for the whole duration of the test. However, the timer was set to turn on the circulator pump only from 10 AM to 12 AM. Moreover, a short On/Off cycle was programmed within this time interval, in order to simulate the operation of an on/off heat pump. Consequently, the circulator performed an On/Off cycle of 30 min (28 cycles a day), with a run and off time of 15 min each. The initial set-point temperature was fixed to 31.5 °C (3.5 °C lower than the temperature in Test II), in order to obtain a difference of about 14 °C between the fluid temperature and the natural ground temperature at the mean depth of the ground heat exchanger (17 °C at the beginning of Test IV). At the same time the flow rate was set to 3.3 l/min, however it increased during the test to a maximum of 4.3 l/min. A total of 305 m^3 of working fluid were circulated, equal to an average flow rate of about 237 l/h. The M-Bus network, which suffered communication problems during the previous experimental activities, had been finally optimized for this test therefore, a comprehensive database was available. However, while the experimental setup operated during the whole period, the heat meter data recording was interrupted on 28th October due to the failure of an electric component in the network. Unfortunately, the data was available again from the 22nd of November. The total amount of energy and the total volume of working fluid circulated were correctly saved for Test IV, because of the electronic unit of the heat meter was equipped with an internal memory.

During this test, the final part of the hydraulic connection was still exposed to the sun although it was thermally insulated and shielded with a double corrugated pipe. As a consequence, the performance evaluation of the system was affected by

solar radiation as well as in Test II. The temperature difference between the inlet and outlet sections (on average 2.8 °C) was reduced during the hottest hours of a sunny day due to the effect of solar radiation, as shown in Fig. 2.35. There, the temperature distributions of inlet/outlet and the difference between them are reported with respect to the solar radiation measured by the weather station nearby, on the 24th and 25th of June. The 24th of June was a fairly sunny day, therefore, the temporary increase in the return temperature was clear compared to that of the following day. Given that an on/off time schedule was adopted for this test, the temperature of the fluid contained within the pipeline increased during the off-time (lasting 15 min). When the circulation pump restarted, the volume of warm fluid flowed through the outlet section downstream the piping thus reducing and sometimes cancelling the temperature difference between inlet and outlet. However, the portion of piping DN20 exposed to the sun is approximately 4 m long and contains a limited volume of fluid, equal to about 0.0013 m^3. Since the minimum flow rate of about 200 l/h, an emptying time lower than 30 s was estimated. As a consequence, the heating of return fluid significantly affected the measurement for a short time interval only, as visible in the graph, in comparison with an operating time of 900 s for each On/Off cycle.

The increase of the outlet temperature was a temporary phenomenon, which negatively affected the measurements for a few hours only during the day. Moreover, the experimental setup was built in a courtyard therefore, the site is subjected to partial shading during the day due to the adjacent buildings and the piping are completely shaded after 2:30 PM. In order to evaluate the impact of this phenomenon on the measurement of the actual performance of the ground heat exchanger, the trend of the average temperature difference between the inlet and the outlet sections is illustrated in Figure 2.36, during a sunny and a cloudy day.
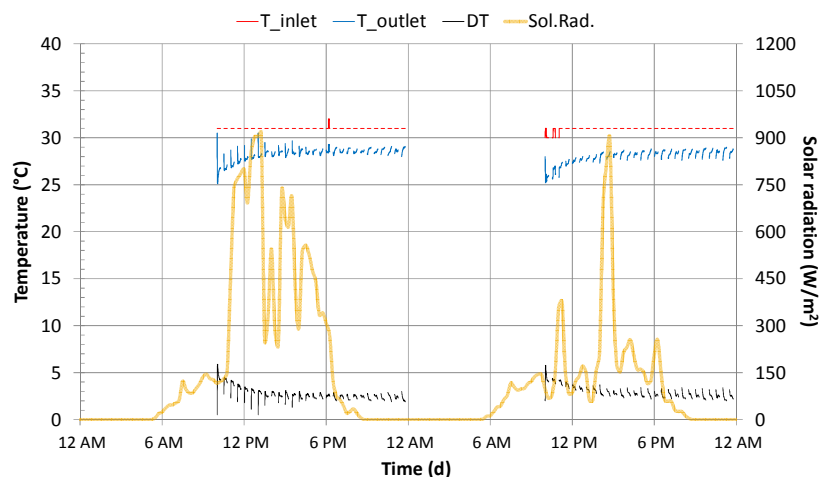
Fig. 2.35 Solar radiation and fluid temperature on 24th and 25th of June 2014.

In addition, the following two days have been added, to improve the reliability of the difference estimate. The 26th of June was partly cloudy like the previous day, though sunny from the afternoon. On the contrary on 27th June the effect of solar radiation on the outlet fluid temperature was comparable to that of 24th. A reduction in the temperature difference was recorded during sunny days. The effect was significant at 1 PM, when the DT measured during sunny days was lower by about 1 °C during than during cloudy days. Starting from the 3 PM the values of temperature were very similar for all the four days which have been considered.

Finally, Fig. 2.36 illustrates the trend of the average rate of heat transfer together with the amount of thermal energy exchanged with the ground during the operating period for the 4 days. Although there was a good correlation between the observed variation in DT and RHT, the second is not entirely attributable to the warming of the fluid within the connecting pipe due to solar radiation. In fact, even the flow rate was subjected to variations during the operating period. A reduction in the rate of heat transfer was observed between 11 AM and 3 PM during sunny days, although the effect was significant only from 12 PM to 2:30 PM. At 1 PM, the difference was 18-20%. Starting from 3 PM the values are very similar for all the four days. Although the reduction in the rate of heat transfer is significant, the phenomenon is limited to approximately 20% of the operating time and only on sunny days. Therefore, the daily energy exchanged with the soil decreased from about 4 kWh to 3.75 kWh for the days considered, corresponding to 6%, which is consistent with that observed during Test II. As a result, the calculation of the heat transfer rate should be considered as a precautionary approach in this Test.
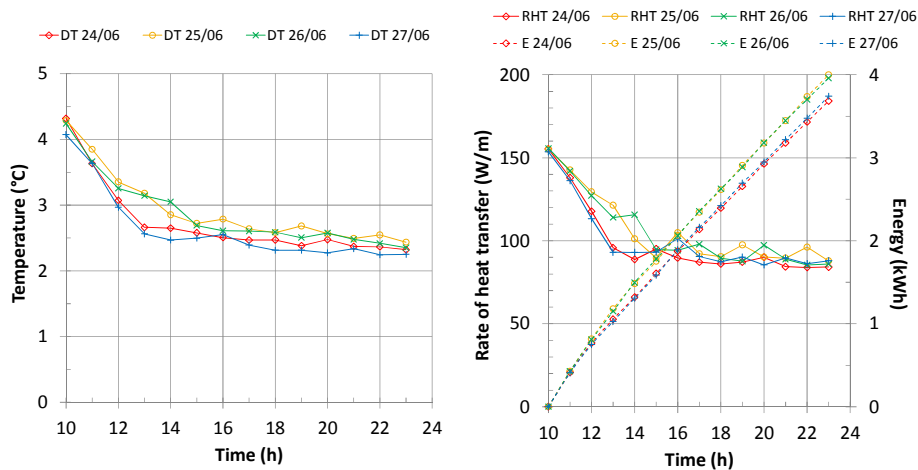
Fig. 2.36 Hourly average DT and overall performance of the system during sunny days (24th and 27th of June) and cloudy days (25th and 26th of June).

Test IV had a duration of 182 days, from 12th June to 12th December. During this period, an amount of 919 kWh of thermal energy was exchanged with the ground by the HGHE, equal to a daily average of 5 kWh. The latter was 8.3 kWh in Test II. The Flat-Panels showed excellent performance in comparison with Test II. The system benefited in terms of heat transfer from the discontinuous operation, which allowed the soil around the ground heat exchanger to cool down after each operating cycle. Moreover, during the passive heat transfer phase, the fluid contained within the heat exchanger continues to cool down, tending towards thermal equilibrium with the surrounding soil. Therefore, the average heat transfer rate over the entire period was of 119 W/m, whereas it was 58 W/m in Test II. What's more, the summer of 2014 was not particularly hot, therefore the average rate of heat transfer was positively affected by the favourable temperature of the ground at shallow depth. A comprehensive summary of Test IV is reported in Table 2-9.

The comprehensive dataset has been analysed in order to evaluate the summer performance of the ground heat exchanger in discontinuous mode. Firstly, Fig. 2.37 illustrates the trend of the average daily temperature of inlet and outlet during Test IV. In addition, the daily average temperature of the air, the difference between the temperature of inlet and outlet (DT) are shown in the graph.

Tab. 2-9 Summary of Test IV.

Mode	Date		Duration (days)
HEATING	Start: 12/06/2014	End: 12/12/2014	182
Operating Mode			Time ON (hours)
DISCONTINUOS PULSED	10 am → 12 Am 15min. ON 15min. OFF	Monday → Sunday	1281
Inlet temperature (°C)	Average ΔT inlet/outlet (°C)	Ground temperature (V.6.5) Initial ÷ Final (°C)	Volume (m^3)
30.0 ÷ 31.5	2.8	17.1 ÷ 18.8	304.7
Flow rate (l/min.)	Average heat transfer rate (W/m)	Max heat transfer rate (W/m)	Energy (kWh)
3.3 ÷ 4.3	119.6	286.6	919.1

Secondly, the simultaneous daily average heat transfer rate and the flow rate are shown in Fig. 2.38 Moreover, the ground temperature trend is also reported for two sensors, 5 m and 3 m far from the ground heat exchanger, at a depth of 0.8 m and 1.9 m respectively.

In Test IV, the experimental setup was turned on at 10:30 PM on 12th June. The fluid temperature in the tank was set at 31 °C, about 14 °C lower than the natural ground temperature measured at a depth of 1.65 m (sensor V.6.5). The flow temperature was subjected to small variations during the test due to the variations of the environmental conditions. At the beginning of the test, the flow rate was 200 l/h; it increased up to a maximum of 240 l/h and finally stabilized at about 215 l/h. These changes of the flow rate over time were caused by variations in the power supply voltage, according to the On/Off cycle of the joule heater, which caused variation in the electrical load.

The test period can be divided into three phases. Firstly, the daily average temperature of the outlet increased rapidly, from an initial 25 °C to about 29 °C after one month. The growth trend was greater in the first week of test, during which the temperature difference inlet/outlet decreased by 3 °C. According to the return temperature of the fluid, the average daily rate of heat transfer decreased up to 120 W/m in the first week and then decreased by another 30% by the middle of July. The start-up phase always benefits from the high temperature difference between the fluid and the ground near the heat exchanger, which gradually warms.

In this case, it lasted about one month, a time significantly longer than in the previous summer test (Test II). Test II in fact, was carried out in continuous mode, while in Test IV the performance of the ground heat exchanger benefited from the discontinuous operation and thus, from the lower energy transferred to the ground on a 24 hours basis. The daily energy exchanged was 8 kWh in Test II and 5 kWh in Test IV; the rate of heat transfer stabilized after an amount of 150 kWh; in the previous case the stabilisation occurred after 50 kWh. At the same time, the temperature of the thermally undisturbed ground was increasing naturally thus, potentially reducing the heat transfer rate. After this phase, the fluid temperature difference between the inlet and the outlet sections was almost stabilised at 2 °C from the second half of July to the first half of August. However, the outlet temperature of return varied within a range of 0.5 °C during this period, as a result of the high temperatures and the effect of solar radiation. As a consequence, the trend of RHT showed variations between 75 and 90 W/m. Since the second half of July, the temperature of the shallow soil at a depth -0.8 m had generally decreased, due to the changes in local environmental conditions. At a greater depth (V.1.6, -1.9 m) the downward trend began with a month of delay, with a good correspondence to what happened the year before (Test II). However, the maximum temperature reached at this depth in 2014 was more than 1 °C lower than in 2013. In this third phase, the performance of the GHE had been positively affected by the natural decreasing trend of the shallow ground temperature.
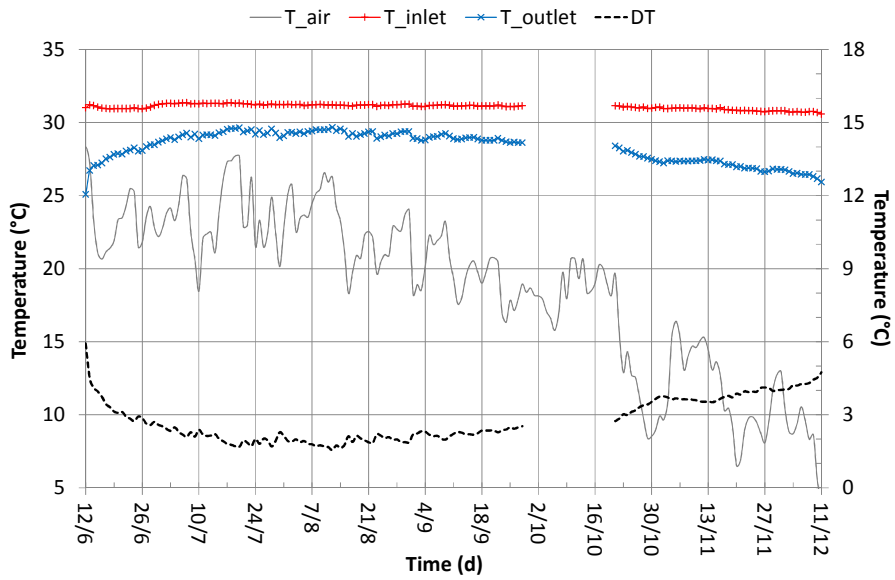
Fig. 2.37 Daily average temperature of the working fluid.
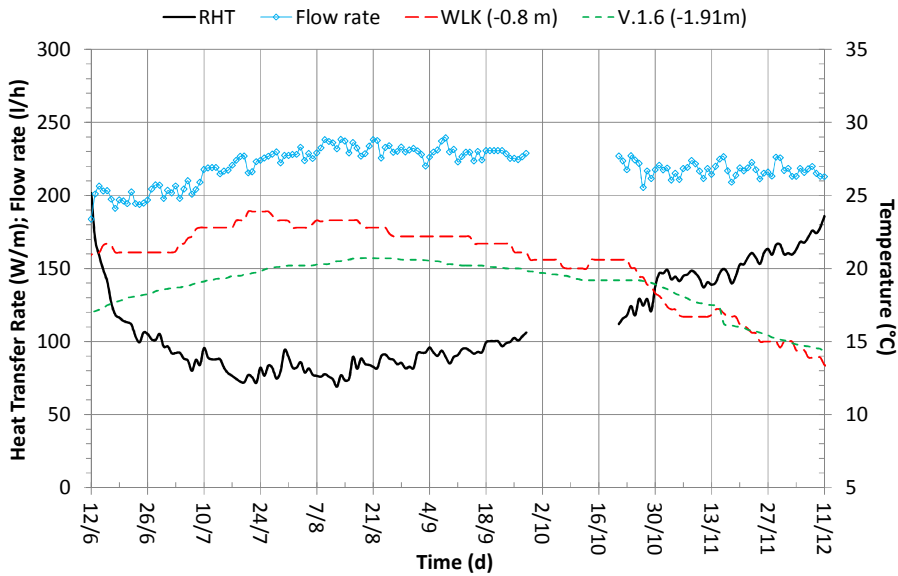
Fig. 2.38 Daily average rate of heat transfer , flow rate and natural ground temperature.

An increasing trend was recorded in the average DT, starting from mid-August. Before the end of September and after more than three months, the fluid flowed out the ground heat exchanger at a temperature 2.5 °C lower than the inlet temperature, a value of DT that was recorded only until the beginning of July. At the same time the rate of heat transfer started to increase with an inversely proportional relationship with the ground temperature. On balance then, there is a strong relationship between the performance of horizontal ground heat exchangers and the seasonal variation of environmental conditions. What's more, this relationship is stronger for discontinuous heat loads, because the contribution of the energy balance at the ground surface is prevailing in this case. Taking these aspects into consideration, a ground thermal drift is not expected after long-term operation. Moreover, horizontal GCHPs have a high efficiency also in mid-season, taking advantage of more favourable working conditions.

Finally, Test IV was extended until 12th December, however, the data recording was interrupted on 28th October and it was available again from the 22nd November. Although the system had worked for six months (in discontinuous mode) the final values of DT and RHT were very similar to the initial ones, more than 4 °C and 160 W/m, respectively. Figure 2.39 illustrates the hourly average temperature of the working fluid (temperature at the inlet and outlet sections) and the hourly average air temperature for a period of two weeks. In addition, the daily temperature of the ground near the ground heat exchanger (sensor H.1.3, located at a depth of -1.65 m and only 0.2 m far from GHE) has been included in the graph, as a reference. The corresponding rate of heat transfer is shown in the Fig. 2.40. The graphs are focused on the initial phase of Test IV, between 12th and 26th of June, in order to analyse the behaviour of the GHE under discontinuous operation.

The timer was set to supply the ground heat exchanger from 10 AM until 12 PM seven days a week with a fluid at 31 °C. The daily operating periods are both clearly evident in the figures. However, it is possible to recognize a first phase of about 3 h, during which the temperature difference inlet/outlet reduces very quickly, and a second one during which the trend is slower. The alternation of these two phases is repeated each time the experimental system is turned on. Firstly, the outlet fluid temperature is conditioned by the fact that the fluid contained in the underground hydraulic circuit continues to cool down during the passive heat transfer phase. Therefore, the fluid is near the thermal equilibrium with the soil at each new daily start. However, the emptying time is very short for a flow rate of about 200 l/h, thus, the initial phase is characterized by an extremely rapid increase of the outlet temperature and consequently by a rapid decrease in the rate of heat transfer. In the following phase, the outlet temperature and RHT decrease slowly due to the progressive warming up of the soil around the ground heat exchanger. Although this resulted in a gradual loss of performance during the initial period of Test IV, the heat transfer tended to level off about 10 days after.
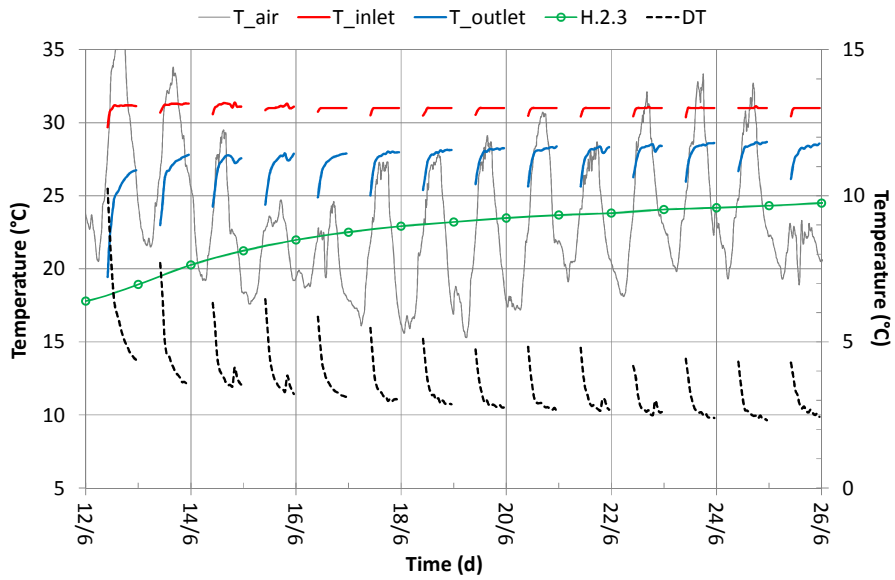
Fig. 2.39 Hourly average temperature of the working fluid from 12th to 26th of June.
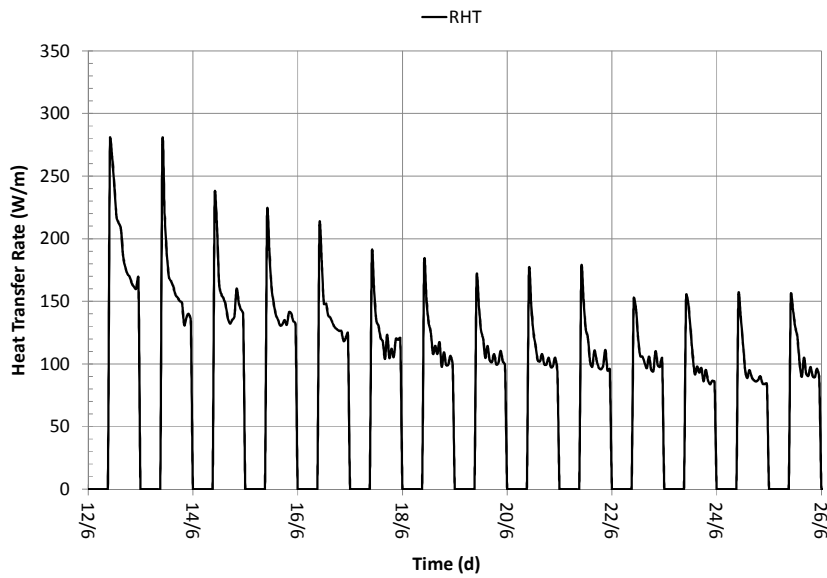
Fig. 2.40 Hourly average rate of heat transfer from 12th to 26th of June.

2.3.7   Data Analysis of the Ground Temperature

In this section, an analysis of trends in soil temperature during the experimental activities is presented starting from 2011. The purpose of this analysis was the evaluation of the thermal field evolution in the soil due to the heat transfer of the two ground heat exchangers. This analysis could also provide useful recommendations about the proper installation of shallow ground heat exchangers, in particular the Flat-Panel type.

In the following figures (Fig. 2.41-2.43), the time series of the daily average temperature are shown for a number of sensors, chosen among those available, in order to highlight the operating modes of the system and the resulting changes in the temperature of the ground. The time series of the daily average temperature for sensors V.3.5, H.2.4 and V.7.4 are shown in Fig. 2.41. The first two sensors were placed 0.4 m and 0.54 m far from the ground heat exchanger respectively, as shown in the monitoring system layout (Fig. 2.11). The depth of V.3.5 and H.2.4 is comparable (-1.11 m and -1.15 m, respectively). The third sensor was positioned 0.89 m away and at a depth of 0.96 m, in front of the second Flat-Panel (FP2). In the graph, the time series of the air temperature measured by the sensor V.4.1 were also included.

The experimental setup was powered up on 11th March 2011 for reliability testing. It worked firstly in heating mode, with a temperature set-point of 30 °C and a flow rate of 3.2 l/min. Initially, the working fluid flowed only into the first Flat-Panel (FP1). At the end of April, the set-point was raised to 35 °C, the working fluid supply to FP1 was stopped and then opened to FP2. The system was turned off at the end of May for maintenance, and finally reactivated on 14th July. These operations caused a quick drop and a subsequent increase in the ground temperature near the exchangers (sensors V.3.5 and H.2.4), as shown in Fig. 2.41. A significant difference of 2.2°C was recorded between the maximum temperature measured by probe H.2.4 (near FP1) and V.3.5. As regards the probe V.7.4, located in a decentralized position, the effect of the heat transfer of the system is less clear. Here, the maximum temperature is 4.5 °C lower in comparison with that of H.2.4. The first test in heating mode finished on 28th September 2011. After 15 days the temperature values measured by the three sensors became similar and then they decreased in accordance with the air temperature trend. In all the three probes, the fluctuations of the air temperature were visible, albeit with a reduced amplitude.

A second test in cooling mode started in February 2012, with duration of about 60 days (set-point of 0 °C, at the chiller). In this case, the working fluid was circulating in both FP1 and FP2. Although the "thermal anomaly" was evident, it was interesting to highlight that the temperature had an increasing trend for all the probes throughout the whole test, in agreement with the trend of the air temperature and despite the heat transfer performed by the system. Also in this case, the values of

the temperature were homogeneous after 15 days from the end of the test (4th April 2012).

   An intermittent working mode was adopted in the next two tests in summer and winter, to simulate a real GCHP system. The first test was carried out from the 24th July 2012 to 1st October 2012 in the heating mode, with a fixed set-point of 35 °C. A timer was set to control the operating time of the supply pump and the joule heater with a daily working interval from 8 AM to 8 PM, from Monday to Friday. In the second test, the system worked in cooling mode from the 13th November 2012 to 10th April 2013, with a time schedule from 6 AM to 6 PM, from Monday to Friday. In this case the flow temperature was initially set to 8 °C and subsequently lowered to 0 °C, according to the environmental conditions. As shown in Fig.2.41, the "intermittent" heat transfer is clearly visible in probe H.2.4 records. In the summer of 2013, a test was carried out in continuous heating mode, by maintaining the supply pump and the electric heaters active 24 hours a day, and a set-point of 35 °C. The experimental setup was turned on in late summer (14th August), when the average daily air temperature began to drop. The ground temperature recorded by the probe close to the Flat-Panels (H.2.4) started to rise quickly, reaching the same maximum value of the previous year, albeit with different working conditions. The fast increase of the ground temperature was related to the high quantity of energy (8.3 kWh/day) exchanged with the ground in a relatively short period. Conversely, the effect of the heat transfer was almost negligible for the probe V.7.4.
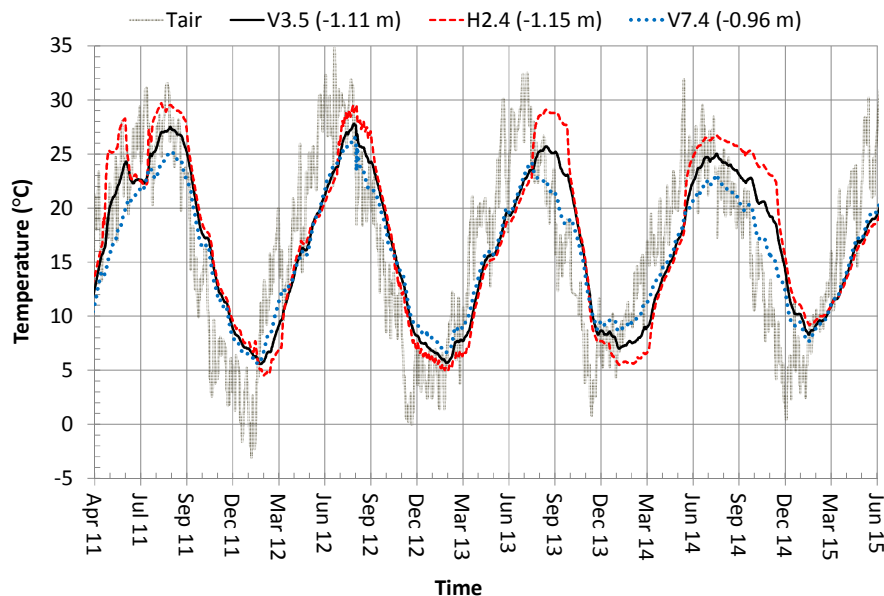
Fig. 2.41 Temperature time series for different sensors (1m deep).

The last test in cooling mode was started on 4th December 2013, with a continuous operation. Initially the set-point was set to 8 °C on the chiller, similarly to the previous winter. Following the gradual cooling of the ground surrounding the heat exchanger, the flow temperature was lowered to 2 °C on 14th January 2014, to maintain an adequate heat transfer rate (Tground-Tinlet). The average daily air temperature started to rise significantly at the end of January. Even with the system operating in cooling mode, the soil temperature at a depth of 1.15 m increased (probes H.2.4 and V.3.5), with a lag of about a week in comparison to the undisturbed ground temperature trend. The test ended on the 3rd April 2014. A fast temperature increase was recorded and after only 40 days the temperature difference between the three probes was less than 1 °C.

Finally, a further test was carried out in heating mode. The experimental setup worked from 10 AM to 11 PM seven days a week. Moreover, the timer was set to perform on/off cycles lasting 15 min each, simulating the "pulsed" operation of a non-modulating GCHP. The flow temperature was fixed to 32 °C. The test lasted five months, starting from 12th June 2014. The initial ground thermal response was fast, less than 24 h 0.40 m away from the Flat-Panels (H.2.4) and 48 h at a distance of 0.55 m (V.3.5). The maximum ground temperature was 26.7 °C, measured after two months by the probe H.2.4. This value is 2.3 °C lower than the peak in the previous summer. From the middle of August, even though the Flat-Panels were still operating, the ground temperature decreased according to the air temperature and the environmental conditions. The system was shut down on 12th December. In comparison with the other tests and in relation to the amount of energy exchanged with the ground (920 kWh), the temperature values for the three probes returned to a uniform level after 75 days.

The time series of the daily average temperature for the probes deep in the soil are shown in Fig. 2.42, similarly to Fig. 2.41. The probes H.1.4 and V.6.5 are at a depth of 1.65 m and at a distance from the Flat-Panels of 0.2 m and 1.4 m, respectively. Two further time series have been reported in the graph. The probe V.6.6 is 2.57 m deep and has been compared with the natural ground temperature at the same depth for the available period (probe WLK.3).

The ground temperature variation recorded for the probe H.1.4 was similar to that of the probe H.2.4. The effect of the heat transfer of the HGHE was clearly visible for all the test periods. However, in this case the peak values of the temperature were slightly smoothed in comparison with that measured by probe H.2.4. Moreover, the fluctuations in the ground temperature related to changes in air temperature were smoothed due to the depth. The "thermal anomaly" was also visible by observing the time series of sensor V.6.5, located at a distance of 1.4m from the Flat-Panels and at the same depth of H.1.4. The ground temperature at this distance was affected by the system operation; it was repeatedly observed that comparable values were always reached during the periods between the tests, despite the significant amounts of energy exploited.
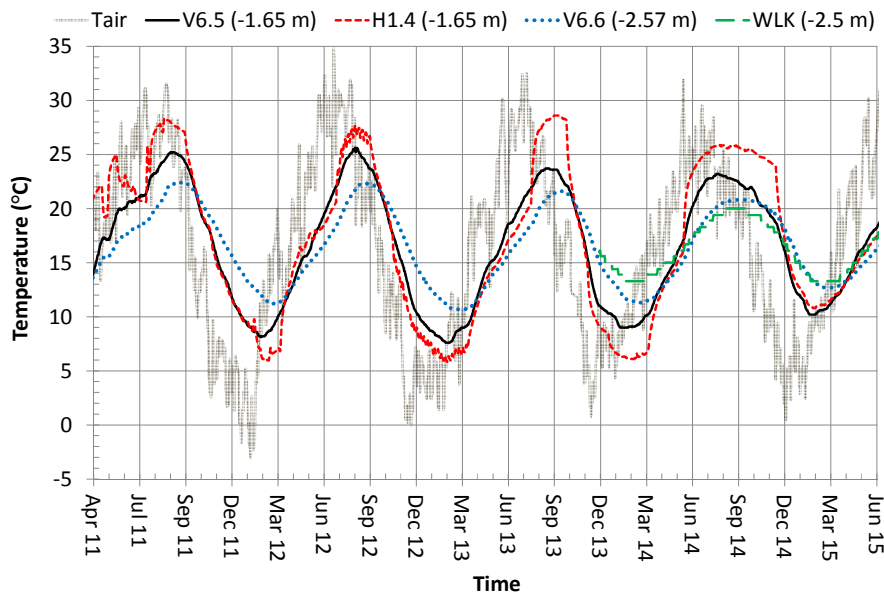
Fig. 2.42 Temperature time series for different sensors (1.65m and 2.5m deep).

A temperature of 15 °C was reached in mid-May in all the years of experimental activity (within a range of about a week). Similarly, the temperature dropped to 15 °C at the end of November. The exceptions were in May 2011 and November 2014, when the system was working for tests in heating mode. The temperature fluctuations are reduced to a depth of 2.5m (V.6.6), but the effect of the heat transfer is still evident in the comparison with the temperature of the undisturbed ground (WLK).

In view of this, some general observations are proposed in the following. Several tests were conducted in different modes of operation, both in heating and in cooling mode. Depending on the operating mode, different thermal gradients were established in the ground surrounding the HGHE. The ground thermal response is related both to the amount of energy and to the heat transfer rate. During the test in heating mode carried out in the summer of 2012, the experimental setup worked for five days a week only (from Monday to Friday). On the contrary, during the tests of summer 2013 and 2014 the experimental setup worked for the whole week. As a consequence, the relative differences of temperature measured by the probes V.3.5, and V.7.4 H.2.4 were appreciably higher in 2013 and 2014.

Finally, a gradual reduction of the maximum ground temperature in the summer was observed, year by year, for all the probes, starting from 2013.

Similarly, a progressive increase of the minimum ground temperature was observed in winter. The phenomenon was related to the different environmental

conditions which occurred during the testing activities, as confirmed by the data analysis of the ground temperature in the shallow layers reported in Fig. 2.43. The daily average temperature of the air and of the ground at a depth of 0.2 m (probe V.7.3) and 0.8 m (probe WLK) had also a smoothing of the peaks, in comparison with the deeper probes near the heat exchanger. This confirmed that the ground temperature in the proximity of the Flat-Panels was determined by the complex interaction between two heat transfer phenomena (the heat transfer by the ground heat exchanger and the energy balance at the ground surface). Such inter-action was also a function of the distance from the heat exchanger and the depth. The exception was the winter between 2014 and 2015. The ground temperature was higher than in the previous winter, although the winter of 2015 was colder than 2014. However, the test started in the summer of 2014 was extended until 12th December and the system continued to warm up the soil. Moreover, the ener-gy transferred to the ground during the summer test of 2014 was much higher than in the previous tests. Consequently, the temperature increase had to be attributed to the system operation.

In Fig. 2.44 and Fig. 2.45 the time series of daily average temperature are shown for the sensor V.3.5 and V.3.6. In addition, the air temperature is included in Fig. 2.44, as a benchmark.
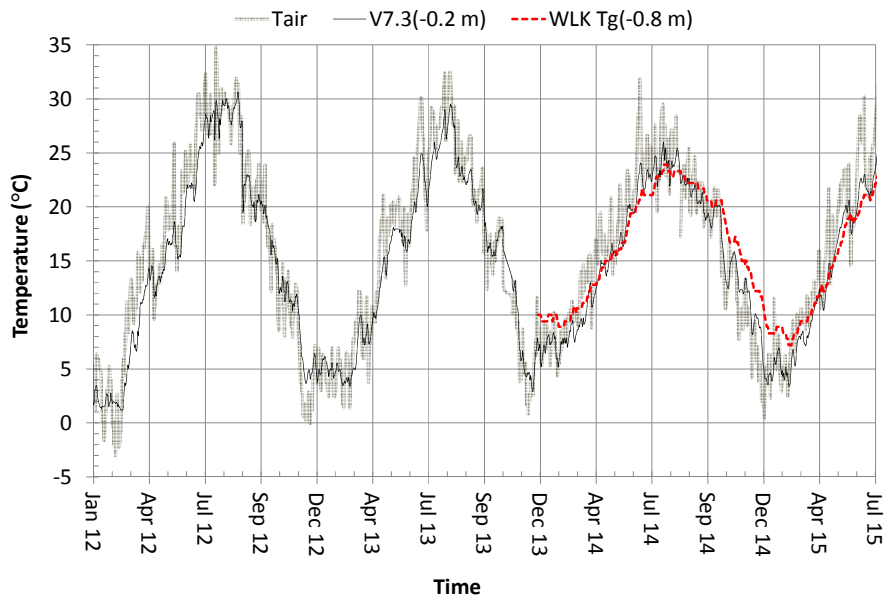
Fig. 2.43 Temperature time series for different shallow probes and the air temperature.

In these figures, the data recorded in four years of experimental activity (2012, 2013, 2014 and 2015) have been superimposed. The graph allows an indirect assessment of the combined effect of the heat transfer and environmental conditions at ground surface.

The temperature probe V.3.5 (1.10 m deep in the ground) was more affected by the variations in environmental conditions and therefore it was subjected to fluctuations. The minimum temperature recorded at the end of February was the same (6 °C) in both 2012 and 2013, although the energy exploited during winter 2012 was lower in comparison with winter 2013. The minimum temperature was achieved a month in advance in winter 2014. The months of January and February 2014 were effectively characterized by a warmer climate than other periods. The ground was significantly warmer in 2015 due to the large amount of thermal energy released to the ground until the last December. The air temperature followed similar trends in the months of May and June for all the years. In the same way, the ground temperature had similar values for each year, regardless of the previous winter tests. In addition, the relative differences between the different years appeared to be related to the differences in the air temperature. The quick increase in the ground temperature following the beginning of a test in heating mode is evident for all three years (24/07/2012, 14/08/2013 and 12/06/2014). The maximum temperature of 2014 was measured on 16th August 2014.
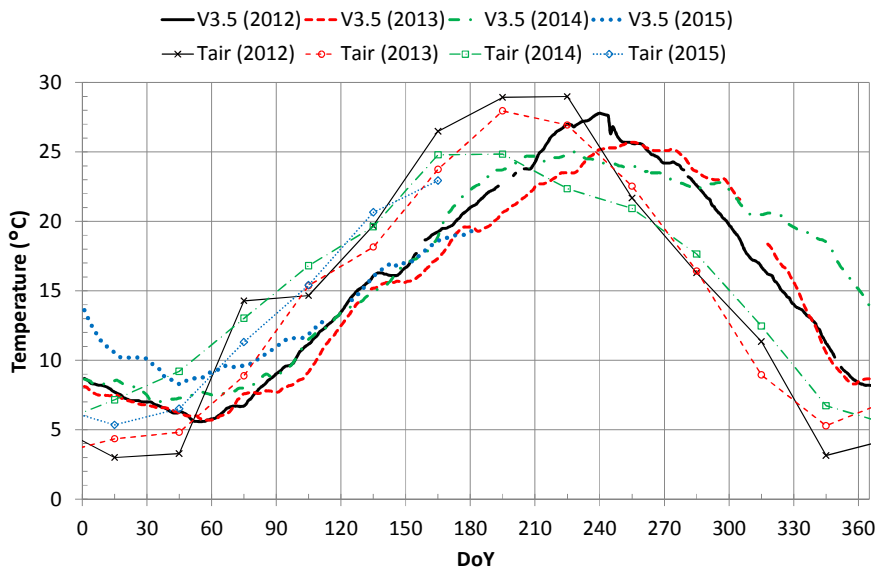
Fig. 2.44 Time series for the sensor V.3.5 (1.11 m deep) close to the HGHEs.
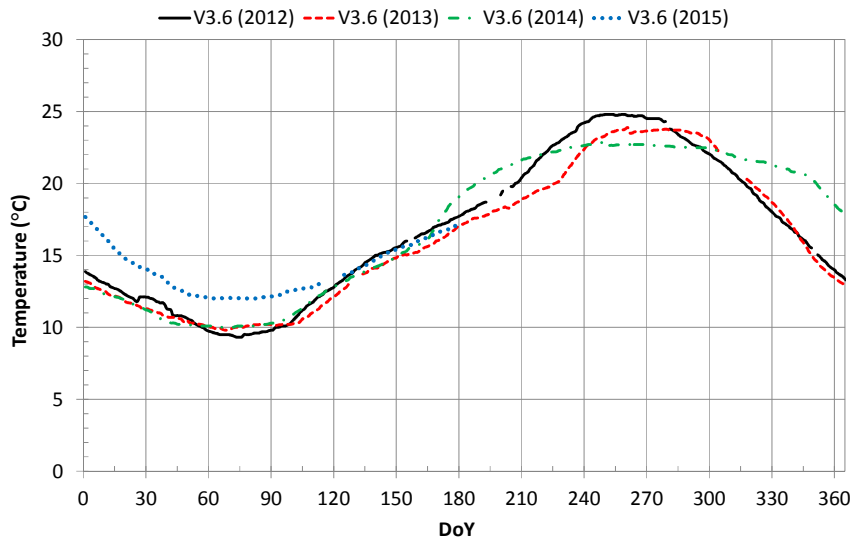
Fig. 2.45 Time series for the sensor V.3.6 (2.03 m deep) close to the HGHEs.

The latter did not reach the high values of previous years, although the test was brought forward to the 12th June and the large amount of energy transferred in the following 2 months. This could be explained by looking at the average monthly air temperature in the summer of 2014, which was on average more than 3 °C lower than in 2012 and 2013. In 2014 in fact, the system worked for 6 months in heating mode and was shut down on 12th December 2014. At that time, the ground temperature measured by probe V.3.5 was 8 °C higher than in previous years (in which a test in cooling mode had already been started). The thermal anomaly was cancelled in the following spring, despite the different winter conditions. Finally, the ground temperature time series for the sensor V.3.6 (depth of 1.65 m) are shown in Fig. 2.45. In this case the effect of the variations occurred in air temperature was reduced due to the greater depth considered. Consequently, the effect of the summer tests in heating mode was clearly highlighted. On the contrary, the differences in terms of ground temperature were reduced between winter tests.

The lines of sensors allowed the recreation of the vertical profiles of the ground temperature and their evolution over time. The graphs 2.46-2.51 show the vertical profiles of the average daily temperature of the ground for two lines of sensors (V.3 and V.7), placed in parallel and in front of the Flat-Panels, respectively. The temperature values were measured monthly, on the fifteenth day of the month. Each graph compares temperature profiles measured in the various years of experimentation on the same day. In addition, the vertical temperature profiles of thermally undisturbed soil have been included in the graphs and taken as a reference (measurements were available for 2014 and 2015 only). Any deviation in the tem-

perature at shallow depths between the two probe lines (V.3, V.7) and the reference one have been related to the different conditions of installation (position e.g.). However, a detailed reconstruction of the temperature profiles has been made from the data recorded by the available probes at different depths. With a relative comparison it was possible to distinguish the different tests performed and their effect on the ground temperature. Moreover, thanks to the different positions of the probes, the thermal gradient has been analysed laterally (V.3) and in front of the HGHE (V.7), and the presence of an "edge effect" due to the thin cross section (0.02 m thick). The shape of the Flat-Panel in fact, was designed to maximize the heat transfer area along the exchanger.

For better readability of the following figures 2.46-2.51, the tests performed with the experimental setup in heating, cooling and free mode have been summarized in table 2.10. The days in which the measurements were recorded are also displayed.

The figures 2.46, 2.47 and 2.48 show the vertical profile of the average daily ground temperature of the line of sensors V.3, located near FP2 (distance of 0.54 m). The temperature was measured at a depth of 0.3 m, 1.1 m, 2 m and 3 m. On 15th January, the profiles of 2012, 2013 and 2014, had a negative variation compared to the reference profiles (2014 and 2015). The difference was about 2°C at the depth of 1.1 m and it decreased with the depth. The values of the temperature to a depth of 3 m in all profiles were contained in a range of 1 °C, except for year 2015. The difference was related to the cooling of the ground performed by the exchanger. During previous periods, prior to the measurement and in all the three cases, the system was turned on at mid-November approximately, albeit with different operating modes. The temperature difference was significantly higher in 2012 (-3 °C) and 2013 near the surface (V3.4 at a depth of 0.3 m). The thermal profiles had similar trends to a greater depth.

The temperature of the shallow ground was naturally influenced by the environmental conditions (which varied every year), and in this case partially by the geothermal system. Consequently, the relative difference observed between the years was related to a superposition of different heat transfer processes, and therefore it was not a direct effect of the system operation.

Tab. 2-10 Operating modes

Heating (red) / Cooling (blue) / Free (green)	Jan.	Feb.	Mar.	Apr.	May	Jun.	Jul.	Aug.	Sep.	Oct.	Nov.	Dec.
2011			Heating	Heating	Heating	Free	Heating	Heating	Heating		Free	Free
2012	Free	Cooling	Cooling	Cooling				Heating	Heating		Cooling	Cooling
2013	Cooling	Cooling	Cooling					Heating	Heating	Free	Cooling	
2014	Cooling	Cooling	Cooling	Cooling			Heating	Heating	Heating	Heating		
2015												

For this reason, a perfect match between the reference profile (natural temperature) and the other profiles was not expected near the surface.

On the contrary, the ground temperature near the surface was comparable to the reference one in almost all the periods. On 15th January in fact, there was a good agreement between the temperature measured by the probe V.3.4 and the reference of 2014 and 2015. In contrast to previous years, the 2015 profile for V.3.4 had values higher than the reference (+ 2 °C) with an increasing depth. This thermal anomaly is related to the long test in heating mode, performed from 12th June to 12th December. No data were recorded in this period of 2011.

In the second graph (15th February), the values are lower in the profiles of 2012, 2013 and 2014 in comparison with the reference one (2014). The system operated in cooling mode before the measurement in all the years considered. Moreover, in 2014 the temperature measured in shallow ground (probe V.3.4, depth of 0.28 m) was 2 °C lower than the reference one. Therefore, the thermal anomaly reached the layers of topsoil, with a lag of about 75 days with respect to the beginning of the cooling test. As regards the year 2015, there was a significant agreement between the values of the profile of V.3 and the reference one at all depths. This means that the effect of the intense test in heating mode carried out in 2014 and clearly visible on 15th December, was cancelled after two months. Also in this case no data were recorded in this period of 2011.

After a month (on 15th March), the ground temperature dropped in profiles of 2012, 2013, and 2014 as expected, due to the cooling activity. On the contrary, the negative trends were reversed near the surface where a rise in ground temperature was recorded in all years. During the winter both the external environmental conditions and the cooling effect of the system, contributed to the lowering of the temperature in the shallow ground. Starting from the second half of February, the effect of the external environment became increasingly prevalent.

The ground temperature on 15th April 2011 had values 2 °C higher than the reference at the average depths (-1.1 m), as expected after about one month of heating activity. On the contrary, the profiles of 2012, 2013 and 2014, were colder than reference one due to the tests performed before in cooling mode. The 2013 profile was the coldest, with a difference of 5 °C compared to the reference one and 2 °C compared to 2012 and 2014. This difference was related to the long cooling test (about a month longer than the others) carried out between November 2012 and April 2013. The plant data analysis supported these considerations, in particular the assessment of the energy extracted/given from/to the ground.

Periods of inactivity ranging from about 30 (2013) to 45 days (2012, 2014) preceded the profiles reported for the month of May. The exception was the 2011 profile, which followed two months of ground heating and consequently it was significantly warmer than the reference. The temperature in the former profiles had good agreement, with a relative difference of 1 °C. The gaps with the reference profiles were ranging between 1 °C and 2 °C at a depth of 1.1 m and 2 m, respec-

tively. Therefore, the thermal anomaly was significantly reduced from 15th April to 15th May. Finally, there is a good agreement in the temperature values measured in 2013 and 2014 at a depth of 1.1 m and 2 m. After 30 days (15th June), an increase in ground temperature ranging from 2.5 °C (2013) to 4 °C (2014) for sensor V.3.5 (1.1 m deep) was recorded. The profile for 2011 had a small variation in comparison with the previous month and consequently the thermal anomaly, clearly visible in May, was reduced.

Looking at the profiles on 15th July, the ground temperature in 2014 was 2 °C higher than the natural one at a depth of 1.1 m and 2 m. A test in cooling mode started on 12th June. Conversely, a good agreement was recorded for the shallow and the deep probes (V.3.4 and V.3.7).

In August, the experimental setup was operating in heating mode in all years considered so the ground was warmed up by the Flat-Panels. As a consequence the ground temperature was higher than the natural one for all the profiles. The exception was 2013, whose trend was comparable to the reference one because the system was turned on only two days before the starting of the measurement. The profiles of 2011 and 2012 are significantly warmer (from 3 °C to 4 °C higher than the reference) and they followed similar trends. The effect was lower in 2014, when a uniform difference of 2 °C was measured at all the depths. The 2014 profile was colder than that of 2011 and 2012, even though it was preceded by a test of two months in heating mode. This was related to the different environmental conditions of summer 2014, as highlighted by the differences in the temperature of the shallow ground. At the end of summer, the natural decreasing supply of energy at the ground surface led the temperature of topsoil to a decrease, as shown in 15th September. At the average depth of the Flat-Panels (between -1 m and -2 m) the ground was still warm, in all the years considered. As regards the year 2014, it was on average colder than the others.

The thermal anomaly described above was clearly visible even at the end of the heating season (15th October), when the ground temperature was significantly higher than the natural temperature, in all the cases. However, significant differences between the profiles were recorded at a depth of 0.3 m, because of the environmental conditions which were different for each year. The decrease in ground temperature was more pronounced in 2011 and 2012, with a lag of 15 days from the end of the tests. The profile of 2013 was still affected by the two months of heating performed in the previous summer. As regards the year 2014, there was a good agreement with the reference values. The ground was on average 1 °C colder than in 2013, even though preceded by almost four months of heating.

In November the thermal anomaly for 2011 and 2012 was significantly reduced by the environmental conditions and after a period of inactivity 45 days. A similar descending trend was recorded in 2013, although the temperature was still 1 °C higher than the natural one. The experimental setup was still working in heating mode on 15th of 2014 and consequently the ground warming effect was clearly
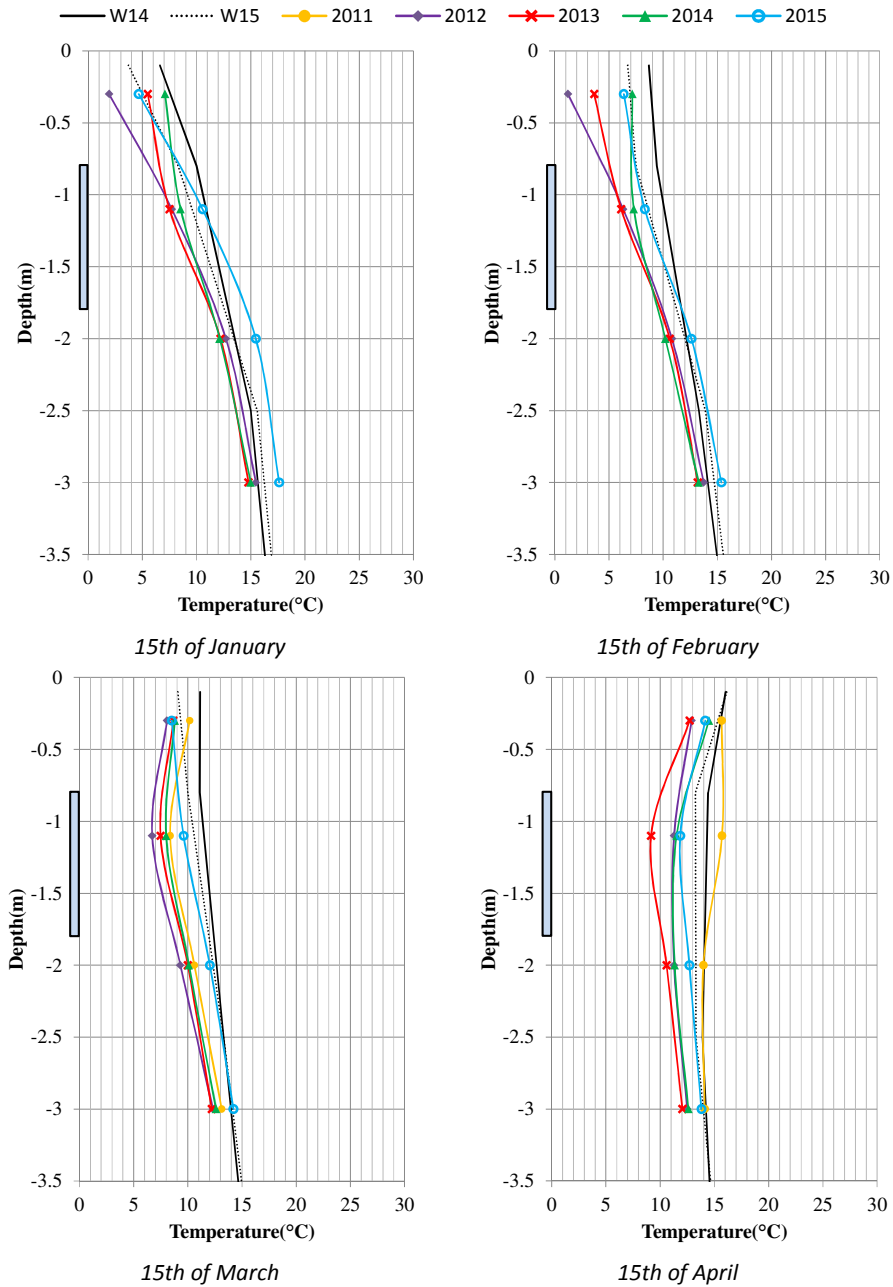
Fig. 2.46 Temperature profiles in the ground measured at vertical probe V.3 and undisturbed ground temperature.
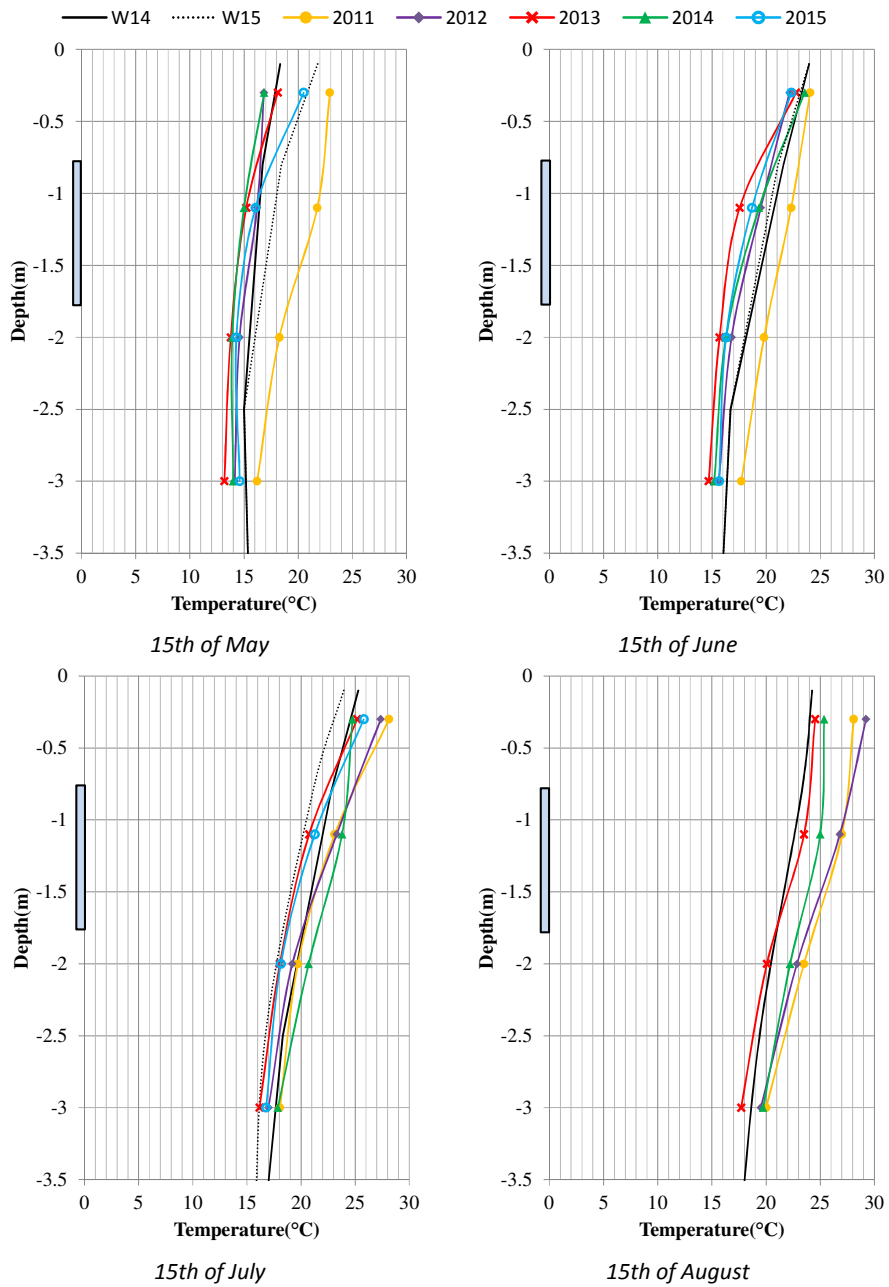
Fig. 2.47 Temperature profiles in the ground measured at vertical probe V.3 and undisturbed ground temperature.
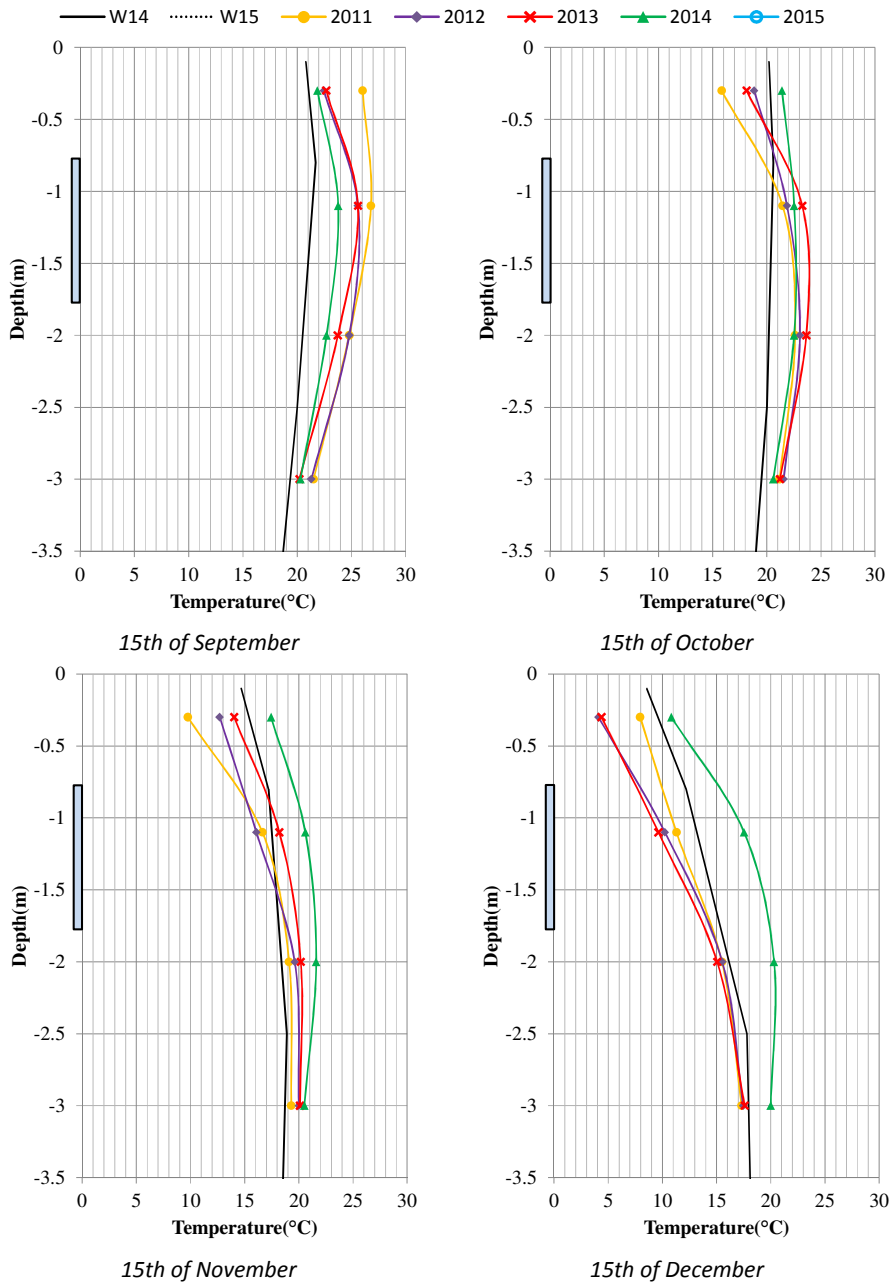
Fig. 2.48 Temperature profiles in the ground measured at vertical probe V.3 and undisturbed ground temperature.

visible, with an increase of 3 °C compared to the reference. In this case, the thermal anomaly had spread to the probe V.3.4 (+2 °C) located to a depth of 0.3 m, in analogy with what was observed during a cooling test on 15th February. However, the temperatures decreased also in 2014 from 22.5 °C to 20.6 °C and from 22.5 °C to 21.6 °C at a depth of 1.1 m and 2 m, respectively, according to the natural cooling of the ground and despite the heat transfer performed by the system.

The last graph in Fig.2.48 shows the ground temperature profile on 15th December. Tests in cooling mode (and different time scheduling for each year) were started in December 2012 and 2013. As a result the corresponding profiles were colder than the reference one. The temperature profiles of 2012 and 2013 are similar. In 2011 the ground temperature was higher of 1.5 °C at a depth of -1.1 m and 3 °C near the surface. In that winter, in fact, the system had worked in free-cooling mode (only the supply pump was operating). The flow temperature was about 11 °C. Finally, contrary to previous years, the ground temperature in December 2014 was higher than the natural one at all the depths, due to the long and heavy test in heating mode extended until the 12th of December. The maximum measured difference is more than 4 °C at a depth of 1.1 m.

In comparison with the previous Fig. 2.46- 2.48, other vertical profiles of the average daily ground temperature are shown in the following Fig. 2.49, 2.50 and 2.51. Profiles are referred to the probe line V.7, placed in front of the second Flat-Panel (FP2) at a distance of 0.9 m from it. This line was equipped with 5 temperature sensors at the depth of 0.21 m, 0.96 m, 1.79 m, 2.79 m and 3.68 m. At shallow depths (0.21m), the temperature profiles for the line V.7 are consistent with those of the V.3, previously analysed. As for V.3, temperature differences (more than 5 °C in some cases) were recorded in the same period for each of the years considered. On the contrary, the temperature measured by the sensor V.7.3 in the years 2014 and 2015 and the corresponding reference were comparable in all instants, with small variations of 1.5 °C. These differences could be related to the different location of lines V.7 and WLK (the reference), which may result in different soil properties. In this case, the variation in the ground thermal field due to the Flat-Panels was clearly detectable only at medium depths (probes V.7.4 and V.7.5). Furthermore, the deviation between the altered temperature and the natural one was reduced in comparison with that recorded for the line V.3.

Looking at the profile of 15th March 2015, there is very good agreement at all the depths with the natural profile. The system was turned off three months before and the ground near the Flat-Panels had cooled during winter. In the previous year, after about 90 days of cooling, the temperature at a depth of 1 m was 1.5 °C lower than the reference one. In the same period and depth, this deviation was more than 3.5 °C for probe V.3.

At the end of the cooling season, the temperature values are once more comparable to the reference (15th May). Therefore the thermal anomaly caused by the cooling tests was cancelled a month after the end of the each test.
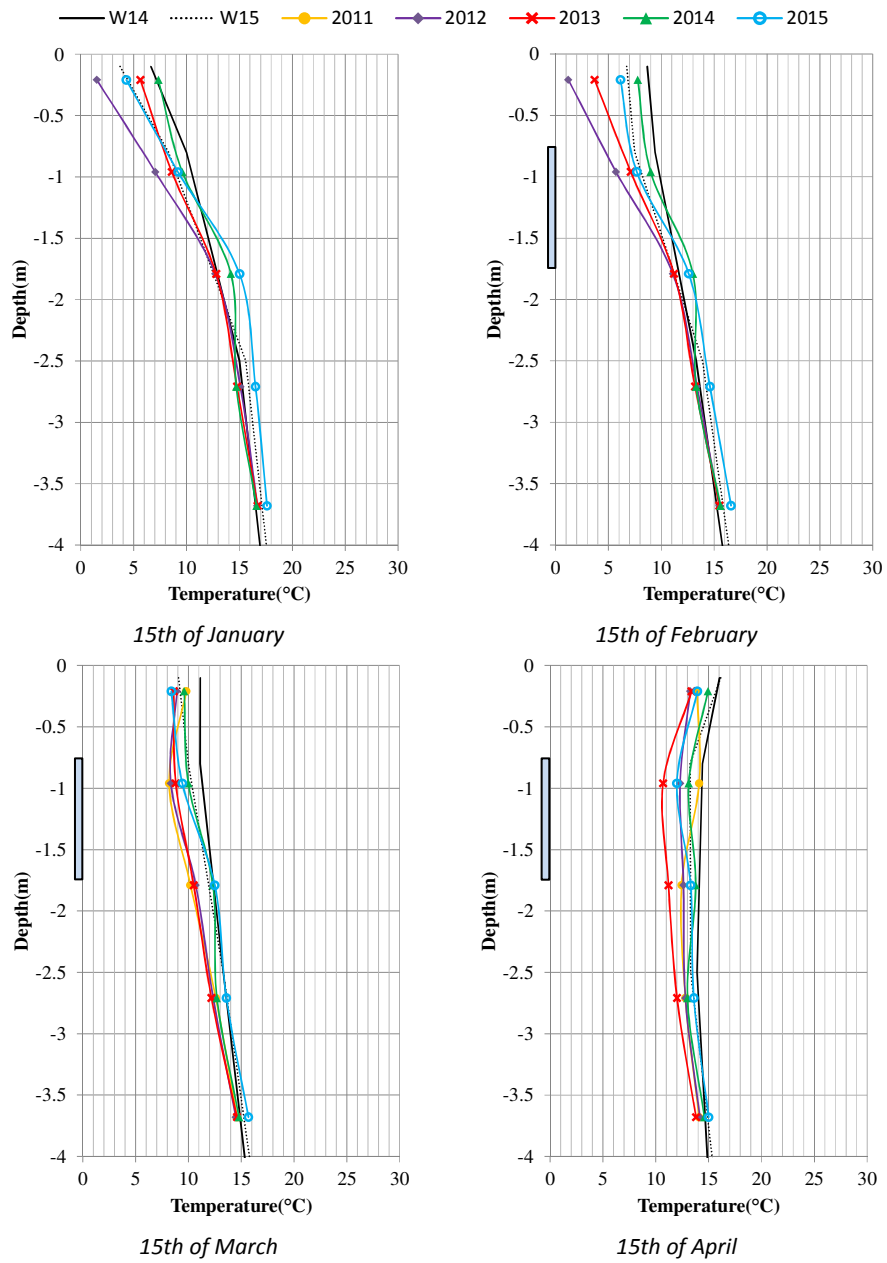
Fig. 2.49 Temperature profiles in the ground measured at vertical probe V.7 and undisturbed ground temperature.
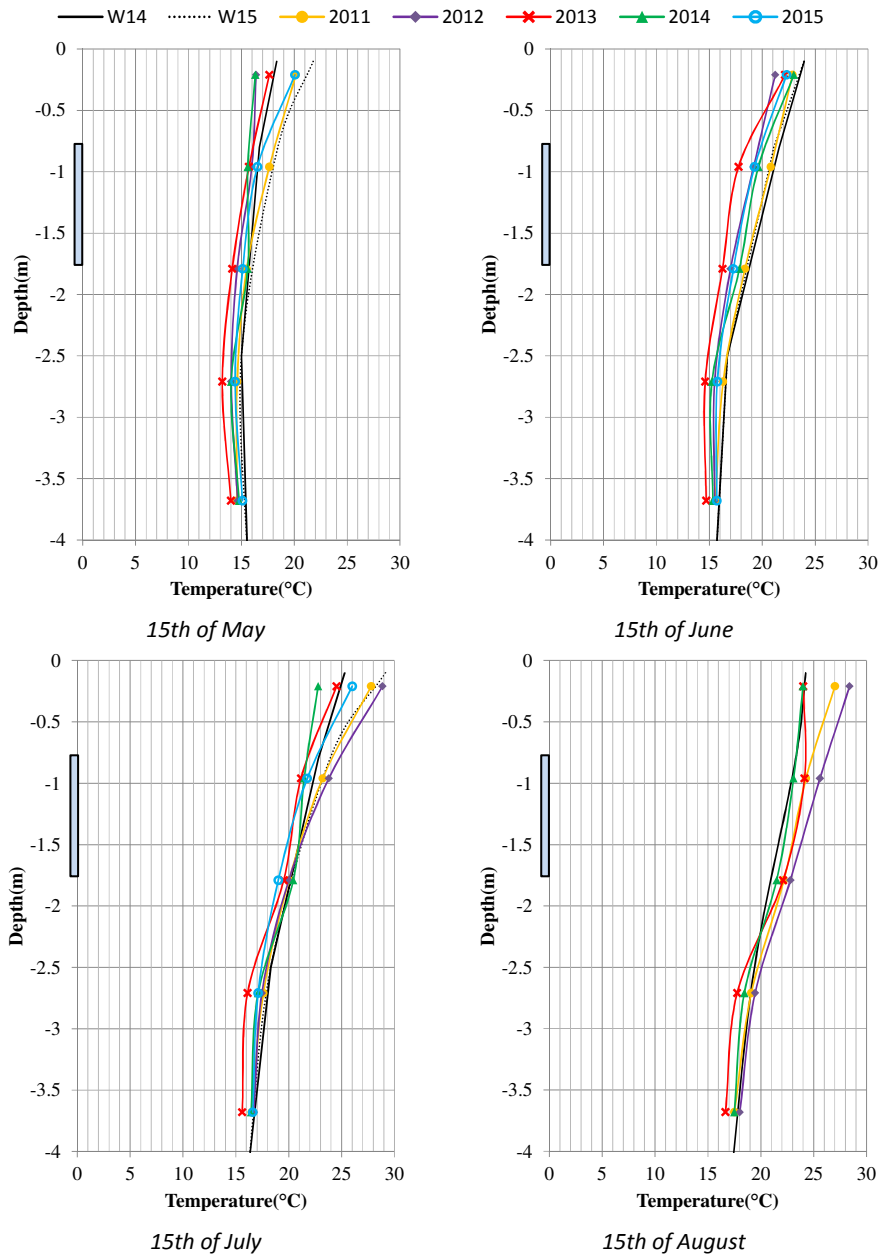
Fig. 2.50 Temperature profiles in the ground measured at vertical probe V.7 and undisturbed ground temperature.
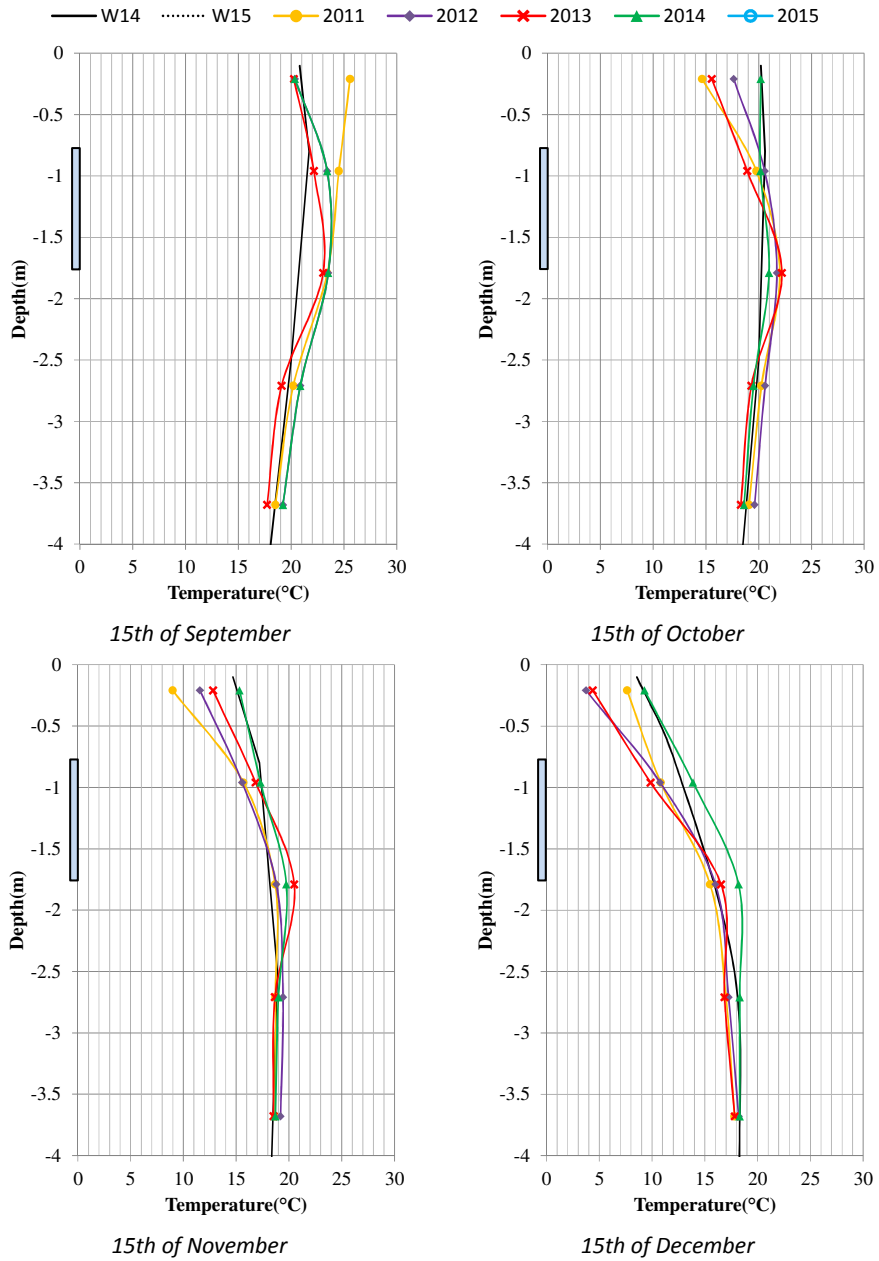
Fig. 2.51 Temperature profiles in the ground measured at vertical probe V.7 and undisturbed ground temperature.

Similarly to the end of winter, the deviation between V.7 and the reference (WLK) were small at the end of the summer season. Since 12th June 2014 e.g., the system had worked in heating mode and the inlet temperature had been maintained to 35 °C for the whole test. Two months after the beginning of the test, on 15th August 2014, the profile of V.7 was still comparable with the reference one, on the contrary to what was shown for V.3. After 30 days, however, the ground temperature was 2 °C higher than the reference one, and it was equal to that in V.3 in the same period. Therefore, the thermal anomaly reached a distance of 0.9 m from FP2 after 90 days of continuous heating. The delay of approximately 2 months in comparison with V.3 was related to both distance and the position of the line V.7, which was only partially exposed to the heat transfer area.

The ground remained warm at the average depth of the Flat-Panels until December 2014. The effect is no longer detectable on 15th January 2015, just 30 days after the system shutdown and about one month earlier than for the probe line V.3. Finally, below 2.5 m the variations among different years and periods are negligible.

2.4   Summary

The experimental analysis of the Flat-Panel ground heat exchanger has been illustrated in this chapter. A number of tests were conducted by means of a dedicated experimental setup, in different operating conditions (heating and cooling) and for different operating modes (continuous, discontinuous and pulsed). Tests were performed for different flow rates, in the range of 80 l/h and 260 l/h. In any case the flow regime was always laminar.

Two tests were carried out in cooling mode (i.e. cooling the ground) simulating long-term seasonal operation. The temperature of the working fluid was controlled in order to maintain a high rate of heat exchange for the whole duration of the tests, which lasted 148 days/1267 h and 120 days/2858 h for Test I and Test III, respectively. In both cases, the minimum flow temperature was about 1.5 °C. The specific energy extraction for unit length of trench was about 60 kWh/m and 80 kWh/m. These values are consistent with the recommended specific extraction for traditional configuration of HGHE (not in the trench) for the whole heating season, which typically lie between 50 kWh/m^2 and 70 kW/m^2 for unit of ground surface (VDI, 2001). Overall, the HGHE showed very good performance in terms of heat transfer rate, according to the operating conditions. Under discontinuous operation (daily energy extraction 2.48 kWh/m) the RHT was significantly high, with an average value of 48.3 W/m. As expected, the RHT was approximately the 40% lower under continuous operation (daily energy extraction 4 kWh/m) and amounted to 28.1 W/m, which is still a good performance.

The performance of the Flat-Panels have been analysed in heating mode with the Test II and Test IV, in continuous and discontinuous operation. Contrary to cooling tests, the flow temperature was set between 31 °C and 35 °C. The first one

started in late summer and lasted for 70 days only, whereas the second was extended to 182 days, from June to December. In addition, during Test IV the experimental setup was set to perform On/Off cycle of 30 min, with a run and off time of 15 min each. The rate of heat transfer was significantly higher compared to the winter tests, because of the higher difference between the fluid temperature and the undisturbed soil temperature. During continuous operation in fact, the average RHT was of 58.6 W/m for a daily energy transfer of 8.3 kWh/day. The RHT was even higher (120 W/m on average) for discontinuous and pulse operation, although in the summer months (from July to September) on average it was of about 80 W/m. The high performance recorded during Test IV are due to the lower daily energy transfer (5 kWh/day).

Overall, these are very good performance for a HGHEs, in both heating and cooling operation. The flat geometry has been designed to enhance the heat transfer due to a larger surface in contact with the ground for the unit length of trench (2 m^2/m) in comparison to common HGHE configurations based on straight pipes and slinky coils (in order to have the same heat transfer area over 30 m/m of DN20 tube would be needed). Consequently, for a given heat load, the overall size of the HGHE can be reduced. On the other hand, for a given HGHEs size, the ground thermal load will be lower, therefore more favourable working conditions are achievable for a GCHP.

According to other studies, the performance of the HGHE are strongly affected by the environmental conditions at the ground surface. In view of this, it is interesting to note that the rate of heat transfer may even increase in late heating/cooling season, independently from energy extracted/released from and to the ground.

In addition, the effect on soil temperature of heat transfer due to HGHEs was analysed. The operation of the HGHE produce a significant variation in the temperature of the ground. During the tests, the thermal anomaly in the shallow soil was extended to a distance of 1.4m, where a variation of about 2 °C was measured in comparison to the undisturbed soil temperature. However, the soil temperature tends rapidly to the undisturbed value after a few months of HGHE inactivity, according to the environmental conditions. These results are in accord with recent studies indicating that any seasonal thermal drift in the soil is expected for HGHEs, after long-term operations. This aspect is otherwise very important in the design process of the VGHEs.

3. NUMERICAL SIMULATION OF THE FLAT-PANEL

3.1 Introduction

This chapter is dedicated to the numerical simulation of Flat-Panel horizontal ground heat exchangers, which are the object of this thesis. The simulations have been conducted by means of a commercial finite element numerical code COMSOL Multiphysics, by solving the heat transfer problem in a bi-dimensional domain.

Applications of analytical and numerical models for HGHEs have been reviewed in Chapter 1. A number of studies followed a detailed approach, explicitly simulating the complex geometry in 3D domains. This approach offers a more general and accurate representation of both mass and heat transfer processes but it is rather complex therefore, high computational resources are required. However, solving the 3D thermo-fluid dynamic problem within the Flat-Panel is beyond the scope of this study, which is focused on the temperature distribution in the ground induced by localised heat sources (i.e. the Flat-Panels) and by the heat transfer process at the ground surface. In view of this, only the heat transfer problem has been solved in a bi-dimensional domain, which is representative of a 3D geometry with the assumptions that no heat transfer occurs along the length of the HGHE. This simplification allows unsteady state long term simulations, due to the low computational time.

Some interesting issues have emerged from the literature review dedicated to this topic and from the analysis of the experimental data, in Chapter 1 and 2, respectively. Therefore, this analysis is intended to investigate some aspects of innovative Flat-Panels and more in general of horizontal ground heat exchangers. In more detail, the study deals with the heat transfer in the soil due to the thermal energy extraction or release from and to the ground with Flat-Panels.

Firstly, it has been found that the performance of horizontal exchangers are closely related to daily and seasonal variations of the soil temperature, due to the energy balance at the ground surface, which depends on weather variables. Moreover, the thermal anomaly induced by HGHEs can reach the ground surface and as a consequence change the natural energy balance. This aspect cannot be taken into account with simplified boundary conditions (e.g. temperature or equivalent heat flux). As a consequence, the proper assignment of the boundary condition to the ground surface is important in order to carry out an accurate simulation of HGHEs. With this in mind, an energy balance equation at the ground surface has been developed and implemented in the numerical code as the boundary condition. Moreover, the reliability of the proposed energy balance has been tested against experimental data.

Secondly, this chapter illustrates a simplified and flexible method that has been developed to define the thermal load (for both heating and cooling) at the ground heat exchanger.

Finally, the complete model has been used to simulate and evaluate the Flat-Panel operation in heating and cooling mode. In addition, different boundary conditions at the ground surface (equivalent to BC of the first, second and third kind, have been compared) has been analysed in order to understand their effect on the solution.

3.2   Numerical thermal modelling of a Flat-Panel ground heat exchanger

Numerical modelling of geothermal exchangers involves many aspects. Although the considerable computing power available today allows the use of advanced numerical codes, the real physical phenomena must be inevitably simplified in simulation.

Modelling Flat-Panels is similar to the modelling of other traditional horizontal ground heat exchangers. However, solving the thermo-fluid dynamic problem within the full geometry of a Flat-Panel is a rather complex task, and would be costly in terms of calculation time. Since this study focuses upon the thermal process in the ground, the thermal and fluid transport processes within the Flat-Panel are not discussed here.

The analysis is intended to evaluate the evolution of the thermal field in the ground due to heat extraction/release by Flat-Panels under various conditions. The heat extraction is affected by the available temperature difference between the working fluid and the undisturbed ground temperature. The overall efficiency of GCHPs in fact, depends mainly on the temperature of the ground as a heat source or sink. In addition, the thermal analysis may also provide a basis to investigate new design options for Flat-Panels.

The commercial software COMSOL Multiphysics V5.0 based on the finite-element method has been used to solve the heat transfer problem in solids, thus, only conductive heat transport is considered. By applying the law of conservation of energy, the model solves within a domain the heat equation, which can be expressed in the form:

$$\rho c \frac{\partial T}{\partial t} - \nabla \cdot (k \nabla T) = Q \tag{3.1}$$

where:
ρ = density of soil (W/m^3)
c = heat capacity of soil (J/kg/K)
k = thermal conductivity of soil (W/m/K)
Q = heat source term (W/m^3)

This approach is based on the assumption that the soil is homogeneous and its thermal properties are independent of temperature (thermal conductivity, density, heat capacity). The assumption of average and constant soil properties may seem an excessive simplification. In general in fact, this is not the case at any geological

site. Often the soil properties are supposed to be constant and homogeneous (Simms, et al., 2014), but the shallow soil is commonly characterized by different compositions and layers, especially in urban areas. Moreover, the heat capacity and conductivity of soils vary in a non-linear manner with soil moisture (Roth, 2012).

However this assumption is widely applied because a detailed mapping of the soil properties is not feasible and would be too expensive. Furthermore, the groundwater table usually lies at a greater depth compared to those typical of HGHEs installation, so the effect of the groundwater flow is negligible. In absence of groundwater flow, most of the heat is transferred by conduction.

The precise assessment of the soil properties is beyond the scope of this thesis. Values of thermal conductivity and thermal capacity are available in the literature and in the national regulations for different types of soil. Nevertheless, a preliminary field survey was carried out at the experimental site in order to take into account the local conditions in the numerical model. The excavation made for the HGHE installation showed the irregular composition of the shallow soil, which is mixed with rubble, bricks (ancient wall foundations) and pottery up to a depth of 2 m, as shown in Fig. 3.1. Moreover, a piezometer was built in order to observe the site conditions and the depth of the water table. The groundwater table is at a depth of 6 m, in a sandy geological unit.

Some samples were taken in order evaluate the soil properties. Overall, the soil was found to be a mixture of silt, sand and clay, with a large component of organic matter. The heterogeneity of the soil increase significantly the uncertainties of the properties assessment. Together, these components affect the soil's texture, water holding capacity and heat capacity and thermal conductivity. The sand has the highest heat capacity and thermal conductivity while litter/organic matter the lowest, when dry.

The soil density of three samples were experimentally estimated to be on average of 1720 kg/m^3. A rough estimate of the overall specific heat capacity of the ground (2 kJ/kgK) was carried out according to Bottarelli, (2013). The effective soil thermal conductivity was calibrated indirectly by applying an analytical solution of the 1D transient heat conduction in a homogeneous semi-infinite solid.

Fig. 3.1 Different soil compositions at the construction site.

Given the flat shape of the Flat-Panel, the ground around it may be idealised as a semi-infinite solid. For short periods of time, the heat conduction in this idealised body, and thus the temperature variation in the region close to the flat surface (the Flat-Panel) is closely related to the thermal boundary condition at the surface. Therefore, the heat transfer is assumed to be only in the direction normal to the surface. The analytical solution in the case of constant temperature on the surface is reported in Çengel & Ghajar (2015). For a specified surface temperature T_s applied to a body at uniform temperature T_i and maintained constant, the temperature variation at a distance x from the surface cab be determined as:

$$\frac{T(x,t) - T_i}{T_s - T_i} = erfc\left(\frac{x}{2\sqrt{\alpha t}}\right)$$

(3.2)

The soil thermal conductivity has been calibrated against experimental data, given the estimated values of density and specific heat capacity. A test was conducted by means of the experimental setup, circulating the fluid at a constant temperature (28 °C) in only one Flat-Panel (FP1). The measured temperature variation in the ground near the HGHE was compared with the temperature trend calculated with the 1-D analytical solution for a semi-infinite body.

In order to obtain the same temperature trend monitored with the temperature sensor (H.2.2), the thermal conductivity in the model was calibrated, as shown in Fig. 3.2. The sensor is close the border between the ground within the trench (sifted) and the ground outside, to 0.40 m from the surface of the heat exchanger, at a depth of 1.15 m, and 0.15 m from the median axis of the surface. The comparison between simulated and measured temperature of the ground was repeated for the sensor H.1.3, which is closer to the heat exchanger (0.2 m) and located at a greater depth (-1.65 m), as shown in Fig. 3.3. In this case the estimated thermal conductivity was significantly lower (0.6 W/mK than 1.4 W/mK). This could be partially explained by the position of the temperature probe, which is close to the lower corner of the ground heat exchanger. In addition, the sensor H.1.3 is located 0.15 cm over the sand bed at the bottom of the trench, which prevents the water rising by capillarity. Consequently, the surrounding soil might have a low moisture content, and therefore a worse thermal diffusivity. The soil properties are listed in the following Tab. 3-1.

Tab. 3-1 Soil properties.

Density	1720 kg/m^3
Porosity	0.36
Specific heat	2.00 kJ/kgK
Thermal conductivity	1.40 W/mK (H.2.2)
	0.60 W/mK (H.1.3)
Thermal diffusivity	4.069 10^{-7} m^2/s (H.2.2)
	1.744 10^{-7} m^2/s (H.1.3)

Given the great variability in soil composition, the accurate estimation of thermos-physical properties is difficult. Furthermore, the properties can vary significantly throughout the year due to the variation in moisture content. Therefore, the properties estimated are approximated and should be treated carefully.
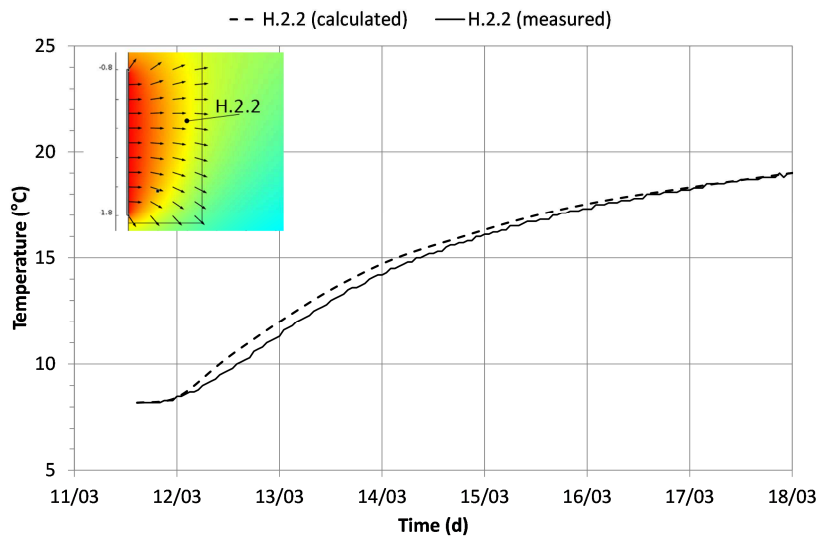

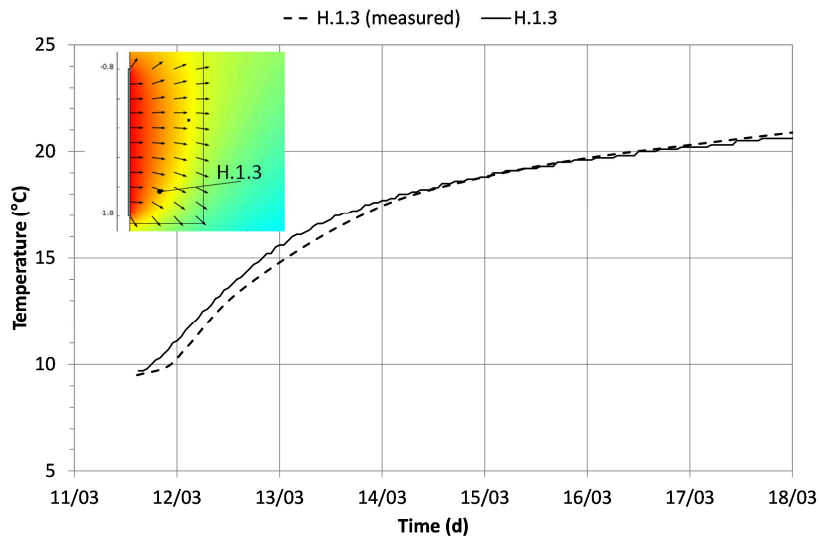Fig. 3.2 Measured and calculated temperature change for sensor H.2.2.

Fig. 3.3 Measured and calculated temperature change for sensor H.1.3.

According to a bi-dimensional approach to the modelling of HGHEs, the Flat-Panel shape may be considered as a cold/hot plate, to and from which heat flows from the surrounding soil mainly by heat conduction. In the 2D domain the Flat-Panel has been modelled as a boundary condition. From this point of view, it is reasonable to follow a two-dimensional approach where the soil domain is in the plane perpendicular to the heat exchanger. Consequently, the two-dimensional model is representative of a three-dimensional geometry in the hypothesis that there is no heat flux along the length of the Flat-Panel:

$$\frac{\partial T}{\partial z} \equiv 0 \tag{3.3}$$

This assumption is reasonable in the case where the temperature variations along the exchanger are small (i.e. a reduced temperature difference between inlet and outlet) and when the effect of the corners is unimportant (i.e. the length of the HGHE is significantly greater than the other dimensions).

3.2.1   Model domain and material properties

The FEM model has been solved for a 2D model domain which comprises a Flat-Panel and a wide part of the surrounding soil. The domain was configured according to the experimental setup. A representation of the numerical domain is shown in Fig. 3.4. The domain is 10 m long and 10 m deep. The extent of the domain has been selected so that it is large enough to approximate an infinite medium.

The properties of the soil domain have been set according to paragraph 3.2 to be representative of a mixture of silt, sand and clay, with a large component of organic matter. In order to solve the energy balance equation at the ground surface, the surface albedo α and emissivity ε (in the infrared) have been considered. When calculating the radiation balance components, the magnitudes of α and ε are
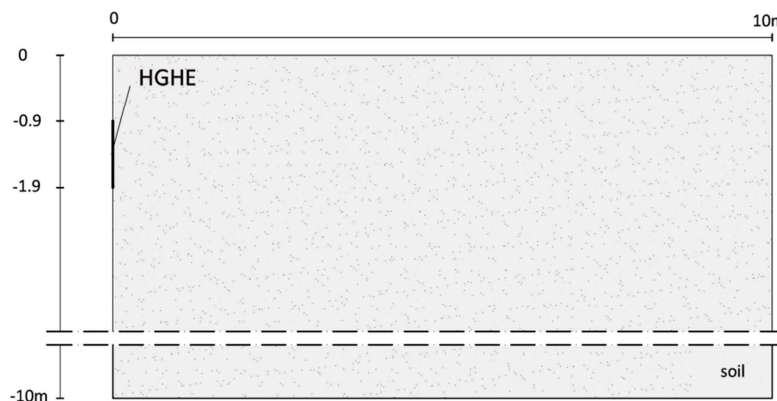

Fig. 3.4 Model domain

different, since the spectral distribution and the angular structure of atmospheric radiation and of the black body are different. The values, which are typical of bare soil and have been taken from the literature (Best, 1998). The material properties are summarised in the Table 3-2.

Tab. 3-2 Material properties

Thermal conductivity	Density	Specific heat	Surface albedo	Surface emissivity (infrared)
(W/mK)	(kg/m^3)	(J/kgK)	(-)	(-)
1.40	1720	2000	0.15	0.95

3.2.2 Grid generation and preliminary verification

The partial differential equation Eq. 3.1 is discretized spatially by the finite element method using triangular elements with quadratic weighting functions. COMSOL Multiphysics provides dedicated meshing algorithms, which automatically create a free grid. Parameters such as the number of elements, the dimension of the elements and their growth rate can be specified for each domain and boundary. The distribution of the elements should be set to obtain a higher mesh resolution where higher temperature gradients are expected, e.g. close to Flat-Panel wall, and less and bigger elements in the outer part of the domain.

In order to check the grid independence, a preliminary analysis has been carried out. A benchmark model has been set up, on the basis of the 2D geometry of the flat panel, as shown in Fig.3.5. The model domain is a portion 3 x 3 m of soil. Temperatures of 30 °C and 20 °C have been assigned to the upper and lower boundary respectively. A pulsed heat flow, which varies from 0 to 100 W/m^2 at intervals of 900 s (i.e. 15 min), has been assigned at the heat exchanger boundary.
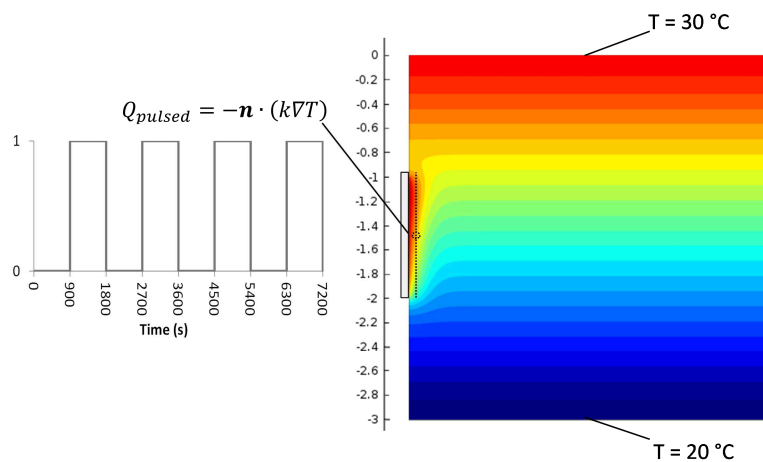

Fig. 3.5 Geometry of benchmark model and boundary conditions.

Such a boundary condition was chosen in agreement with the experimental activi-ty. The high value of the heat flow and the frequency cause large temperature gra-dients in the vicinity of the heat exchanger. Four grid refinements have been simu-lated, progressively increasing the number of elements in the vicinity of the source as well in the whole domain, as shown in Fig. 3.6.

Moreover, the simulations were conducted by optimizing the time-step for the direct solver (maximum 150 s) according to the pulse duration. Clearly, as the number of degrees of freedom increases, the times of calculation increase as well. The statistics of the four tested meshes and the calculation time required for a simulation of 86400 s (i.e. one day) are shown in Table 3-3. In order to monitor the grid independence, the temperature trend has been calculated in a point 5 cm far from the source (0.05 m; -1.5 m). Moreover, the normal component of the average heat flux (W/m^2) passing on a section of 1 m and positioned 5 cm far from the source has been calculated. The measuring points are reported in Fig. 3.5.

The solutions are very similar for the meshes c) and d) in terms of temperature trend; differences are visible for the meshes a) and b), as shown in Fig. 3.7. The difference between c) and d) is minimum also in terms of heat flux, as shown in Fig. 3.8. On the contrary, the solutions are significantly different for a) and b). Further analysis has been carried out with the full domain for different simulations.

Tab. 3-3 Mesh analysis statistics

	Degrees of freedom	No. of elements	Solution time (s)
Mesh a)	3396	1645	59
Mesh b)	4663	2268	73
Mesh c)	6315	3082	96
Mesh d)	14811	7296	226

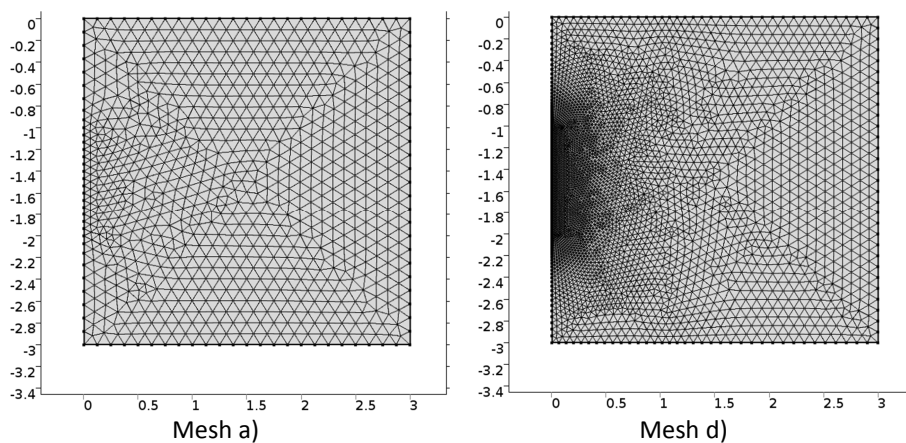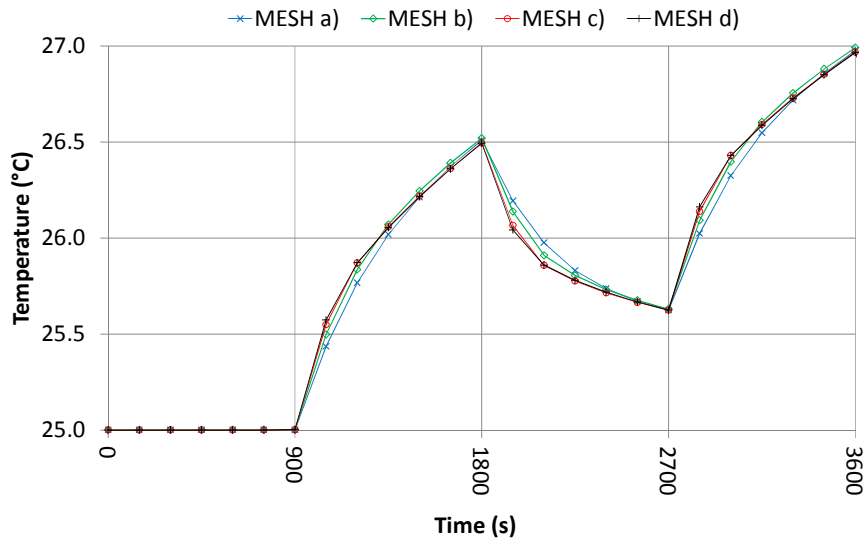
Fig. 3.6 Different mesh resolutions.

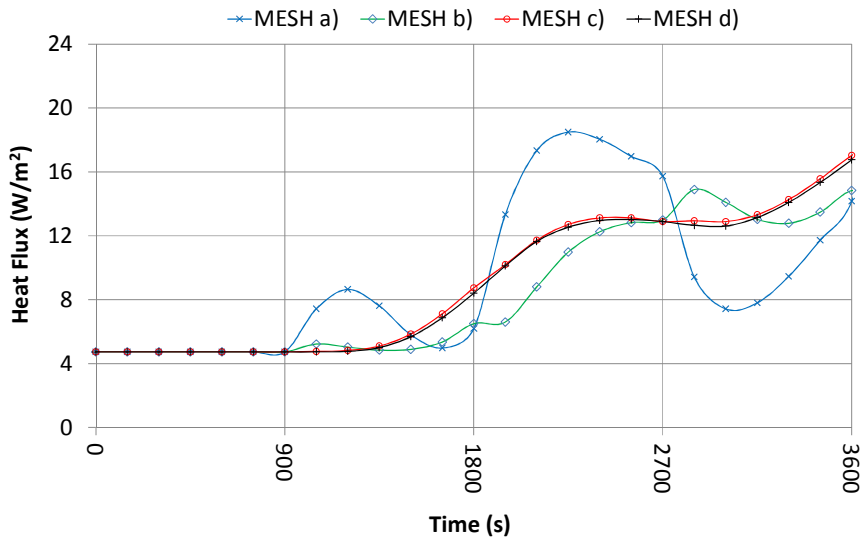Fig. 3.7 Temperature evolution at a point 5 cm far from heat source.

Fig. 3.8 Normal average heat flux passing thorough a section 5 cm far from the heat source.

3.3   Boundary conditions

The lower and vertical boundaries in the soil domain are assumed to be adia-batic. On the left vertical side this is due to the condition of symmetry. At the top

boundary, representing the ground surface, a 3rd kind boundary condition (BC) has been assigned by means of an in-house ground surface energy balance equation (GSEB). The Flat-Panel is treated as a time-dependent boundary condition by means of a heat flux time series, representing the heating and cooling demand. In Chapter 4, dedicated to a comparison between simulations and measurements, the Flat-Panel BC has been improved to an equivalent 3rd kind boundary condition, since time series for the bulk temperature of the working fluid were available. Full details of the BCs at the ground surface and of the energy demand at the HGHE are given in Section 3.5 and 3.6, respectively.

3.4   Soil heat flux

Physical, chemical and biological processes in soil are strongly influenced by soil temperature. As a consequence, the knowledge of soil temperature and heat flux are key factors in several scientific disciplines. These two factors depend mainly on climatic conditions on the earth surface (which are related to local climate) and on the properties of the ground surface that controls the reflection of the incident solar radiation, the magnitude of sensible and latent heat flux. Moreover, the velocity at which the temperature changes within the shallow soil on a daily or seasonal basis, is determined by the soil properties and depth. The energy balance at the ground surface and the energy fluxes in the soil (soil thermal regime) are linked in the soil heat flux, defined as the amount of thermal energy that moves through an area of soil in a unit of time in Sauer & Horton, (2005).

Soil heat flux has been studied in depth in the last decades, mainly in micro-meteorology and agricultural applications. This knowledge can be applied in a different scope, according to the recent and renewed interest in GCHPs with horizontal exchangers. The performance of such GCHP systems in fact, depends mainly on the thermo-kinetics coupling between the ground heat exchanger and the shallow soil. HGHEs use the ground as an unsteady source/sink of energy storage, which is mainly related to the soil thermal regime due to energy balance at the ground surface. Therefore, the correct estimation of soil temperature and heat flux is a key parameter in designing and numerical modelling of horizontal ground heat exchangers, where attention should be paid to the correct assignment of the boundary condition at the ground surface, in order to treat realistically the effect of the environmental conditions. The temperature in the soil is driven by the energy fluxes at the ground surface: the rate at which the energy is stored in the shallow layer is equal to the difference between the net incoming energy flux and the net outgoing energy at the surface. The major heat transfer processes at the outer surface are three.

A first process is the radiative heat transfer which is critically influenced by the surface characteristics and cover. The net radiation consists in the net shortwave radiative flux and in the net longwave radiative flux. The first depends on the inci-

dent solar radiation (in its direct and diffuse components) which is transmitted through the atmosphere and partially reflected to the sky by the soil/vegetation surface. The second is the difference between the down-welling thermal radiation from the sky (and potentially from other surfaces) and the upwelling thermal radiation from the soil or canopy surface.

Secondly, the convective heat flux, which occurs by turbulent convection due to the wind above the surface.

Finally, the latent heat flux which depends on the evaporation and plant transpiration.

Consequently, the energy balance equation for an ideal surface in its general form may be written as:

$$R - H - LE - G = \frac{\partial W}{\partial t}$$
(3.4)

where:
R = net radiative energy flux (W/m^2)
H = sensible energy flux (W/m^2)
LE = latent energy flux (W/m^2)
G = soil heat flux (W/m^2)
∂W/∂t = rate of energy storage per unit of ground area

The magnitude of each term in the surface energy balance equation has a daily and a seasonal variation, as reported in Fig. 3.6. As a general rule, during daylight periods, the solar radiation is the major component, therefore the soil heat flux is positive. Latent and sensible heat fluxes, also referred to turbulent fluxes, follow the diurnal cycle of solar radiative energy supply. During the night the energy balance at the ground surface is different, and the net energy flux is usually away from the soil. Moreover, the incidence of each individual component may vary significantly according to the soil surface finish. A number of observations for different surfaces and canopies are available in the literature, as reported in (Garratt, 1992) and in (Brutsaert, 2005).
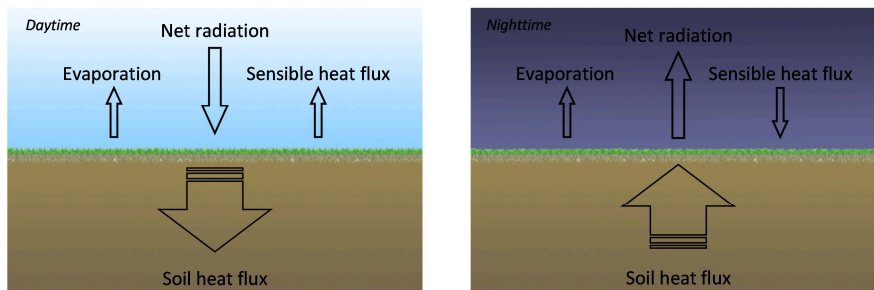

Fig. 3.9 Typical surface energy budget during daytime and night-time

The energy budget over a paved surface or bare ground is mainly affected by solar radiation both for daytime and night-time. During the day, the surface is heated up rapidly by incident solar radiation. As a consequence, a large part of the energy absorbed is conducted down into the soil. The heat flux due to evaporation is usually limited and negligible for paved surfaces. Moreover, since the temperature at the surface can be very high in comparison to the air temperature, the sensible heat flux is usually significant. On the contrary, the sensible heat flux is low at night-time due the lower difference between air and surface. However, during the night, the ground cools down due to the radiative cooling. The energy budget at the surface is different in the case of partial or total vegetation cover, which shades and insulates the soil beneath. Radiative heating of the surface is further reduced by the latent heat flux due to evapotranspiration (i.e. the sum of evaporation from the soil surface and transpiration from the plant leaves). Moreover, canopies shelter the soil surface from wind, thus also reducing the sensible heat flux. As a consequence the daily variation in soil temperature is reduced in comparison to that in bare soil.

The recent developments in the instrumentation have allowed the taking of detailed measurements of the heat flux at the ground surface and of its components. Nowadays, a considerable amount of experimental data for a large variety of soils and surface covers is available in the literature, as well as a number of models for the estimation of the ground surface temperature. However, all the available research attest to the complexity of heat and mass transport processes at the surface and there are still many unresolved issues in the study of their mutual relationship which is affected by several factors.

When measures are not available the simplest approach is to use empirical correlations. Then, the heat flow in soil is considered proportional to other terms of the energy balance of the ground. A number of studies have demonstrated that soil heat flux is strongly correlated with net radiation, Rn. Soil heat flux typically represents 10 % of the net radiation for growing crops (Sauer & Horton, 2005) and a value of around 30 % for bare soil or sparse canopies (Brutsaert, 2005). Anyway, these values are only indicative and are subject to inaccuracies due to the seasonal cycles of natural surfaces. Moreover, several studies demonstrate that this ratio is not constant. As reported in (Kustas, et al., 1993), it can range from 0.05 to 0.50 according to the time of day, soil moisture content and vegetation cover. The relationships between the ratio G/R_n and vegetation cover, soil conditions and time of day has been investigated by Santanello & Friedl (2003). The soil heat flux can be higher than 50 % of the net radiation, for sparse vegetation. As vegetation cover increases (Leaf area index = 5) the maximum G/R_n decreases, but it can even be up to 20%.

A number of mathematical models have been developed for an efficient prediction of ground temperature for these types of surface, with different level of detail. These models use available weather data and are usually calibrated against field

experimental measurements. A method for predicting both surface moisture and temperature was presented by Deardorff (1978), which considered a layer of vegetation above the soil. This layer is parametrised including both radiative heat transfer between vegetation and soil, and the turbulent transfer of heat and moisture within the canopy. Based on a simplified version of Deardorff's one-level canopy method, a model to predict the temperature of different surfaces (vegetation, bare soils and roads) has been proposed by Best (1998). A statistical uncertainty of about 2 °C was found in the predicted surface temperature in comparison with the observed temperature. Analytical models for the prediction of ground temperature on a monthly basis have been proposed by Krarti, et al. (1995) and Mihalakakou, et al. (1997). Both models are based on energy balance equations at the ground surface (for bare and grass cover) and on the heat conduction equations. In a further study of Mihalakakou (2002) an analytic deterministic model, which uses a ground surface energy balance equation, was compared with a data-driven neural network model. A comprehensive description of a surface energy balance mathematical model for bare soil has been provided by Qin, et al. (2002). The model solves both variations in surface temperature and surface moisture content. In recent years complete and detailed models have been also released such as the COUP model (Jansson & Karlberg, 2001) and the FASST model (Frankenstein & Koenig, 2004), that allow the calculation of the soil energy and water budget in order to assess both the heat flux and moisture flow within the soil. The second one has been recently implemented within the software EnergyPlus, dedicated to energy simulations. Although those are very complex models for the purpose of this thesis, they provide a comprehensive overview of methods for estimating weather variables in the case of missing data. A complete set of equations to estimate the magnitude of radiative, convective, conductive and evaporative heat fluxes have been provided by Herb, et al. (2006) and in Herb, et al. (2008). The model has been developed to calculate the soil temperature to a depth of 10 cm, by coupling the surface energy balance to 1-D unsteady state heat diffusion equation and applies to different surfaces, both dry and wet. The canopy effect has been considered according to the previous works of Best (1998) and of Deardorff (1978). The simulated temperature has been calibrated by means of appropriate coefficients of each surfaces, resulting in a good agreement of simulated and measured values (in the case of vegetation-covered surface, a statistical uncertainty of 1-3 °C has been found).

Other researchers have instead performed experimental measurements in order to identify simplified correlations to determine the temperature of the soil. Based on 10 years of records of the daily average temperature of the ambient air and ground at different depths in Northern Greece, Tsilingiridis & Papakostas (2014) have recently proposed a correlation between air and ground temperature. In order to develop a reliable method for determining the undisturbed ground temperature (usually this is constant to a depth of 10 m) to be used as parameter in vertical ground heat exchangers, a further correlation is presented by Ouzzane,

et al. (2015). The correlation has been determined using filed data from several thermal response tests (TRTs) and is a function of ambient air temperature, wind velocity, global solar radiation and sky temperature.

The numerical simulation of horizontal coupling techniques for GCHPs requires the knowledge of the temperature of shallow soil and its daily and seasonal variation, according to the soil surface cover (usually bare ground or vegetated surface). In modelling horizontal ground heat exchangers, a temperature trend at the ground surface is the most simple and used boundary condition (i.e. 1st kind boundary condition). The correlation developed by Kusuda & Achenbach (1965) is still widely applied to calculate the surface temperature and the undisturbed ground temperature as a function of time and depth:

$$T(z,t) = T_s - \Delta T_s \cdot e^{-z\sqrt{\frac{\pi}{\alpha \cdot 365}}} cos\left(\frac{2\pi t}{\alpha t} - \theta\right) \tag{3.5}$$

where:
T_s = average annual soil surface temperature (°C)
ΔT_s = amplitude of the soil temperature change throughout the year (°C)
Θ = phase shift, or day of minimum surface temperature
α = thermal diffusivity of the ground (m²/s)

Equation 3.3 requires the knowledge of the soil surface temperature amplitude throughout the year, which is not always available. Consequently, the annual amplitude of ambient air temperature is often considered. Unfortunately, this simplification adds an extra margin of uncertainty in modelling HGHEs.

In a study by Lee & Strand (2008) on earth tube systems, a ground surface energy balance similar to Krarti, et al. (1995) approach, is applied to calculate the amplitude of surface ground temperature and thus deduce the sinusoidal temperature trend (assigned to the ground surface as boundary condition). A recent work by Fujii, et al. (2013) proposed the use of sol-air temperature (SAT) as 1st kind boundary condition, which is calculated using weather data. A similar surface temperature trend has been numerically converted to an equivalent overall heat flux (i.e. 2nd kind boundary condition) in Bottarelli, et al. (2014), with the aim of considering the effect of the energy exploitation on the ground surface temperature. Despite the long computational time required, other numerical studies have been carried out including the mass transfer to take into account the effects of the soil moisture, as presented in the previously mentioned Piechowsky (1999). A 3rd kind boundary condition at the ground surface has been recently introduced in Gan (2013), where the convective heat fluxes were considered. On the other hand, the influence of radiation and evaporation heat transfer under vegetation in heating seasons has been neglected. Similarly, Kupiec, et al. (2015) considered only the convective heat flux between air and ground. The environmental conditions are included in the model developed by Demir, et al. (2009). Energy balance equation was validated against experimental data, taking into account the effect of solar radiation, latent

and sensible heat transfer. A paved surface heat balance is also used to study the performance of building foundations as a heat exchanger in Nam & Chae (2014).

For more detailed models a considerable amount of data is required as input, and they are not always available. Furthermore, excessive detail would result in a long computational time. In order to treat the boundary conditions at the ground surface a simplified model of energy balance has been developed (Bortoloni, et al., 2015). The use of such a boundary condition (third kind) would allow taking into account the possible variation of the surface temperature due to the heat exchanger. Therefore, a specific analysis has been dedicated to the comparison of the different boundary conditions which are commonly assigned to the soil surface (surface temperature or equivalent heat flux) in modelling the HGHE.

3.4.1 Numerical modelling of heat transfer at the ground surface

The equation of energy balance at the ground surface has been developed and implemented in the FEM numerical code COMSOL Multiphysics. Although, this is a simplified model, the use of such a boundary condition would allow a better prediction of soil temperature variations. As a result, a higher accuracy is expected in numerical simulation of the Flat-Panel and more in general of horizontal ground heat exchangers.

The temperature in the shallow soil depends on the energy fluxes at the ground surface. Depending on the nature of the surface, the soil heat flux is defined by the ground surface energy balance equation (GSEB) for the infinitesimally thin surface layer (i.e. the interface between the ground and atmosphere), which can be written in his general form as a function of time and the surface temperature:

$$G(t, T_s) = R - H - LE \tag{3.6}$$

where:
G is the soil heat flux (W/m^2)
R is net radiative energy flux (W/m^2)
H = sensible energy flux (W/m^2)
LE = latent energy flux (W/m^2)

The magnitude of each component is a time-varying function, which depends on weather conditions, therefore, a complete set of weather data including solar radiation, wind speed, air temperature, atmospheric pressure and relative humidity is required as an input for Equation 3.4. Moreover, the soil heat flux is strongly affected by the properties of the surface. In the case of ground heat exchangers installed horizontally, the surface is usually covered with grass or at most is bare soil. The vegetation covers in fact, are optimal for HGHEs, as the shallow ground is subjected to smaller temperature fluctuations on both a daily and seasonal basis. As a consequence, the GSEB is developed for grassy surfaces in this task. Moreover, this

has been made to calibrate and compare the model results with the available measurements of soil temperature at different depths. The experiment described in Chapter 2, taken as a reference, is covered by a wild meadow which is not subjected to regular watering and mowing.

However, the introduction of a vegetated layer has a major effect on the surface heat transfer, and consequently is a major issue in modelling the GSEB. A detailed modelling of the effect of vegetation would require an additional equation to solve the energy balance in the foliage layer firstly and secondly that between vegetation and soil as reported in (Alexandri & Jones, 2007) and (Sailor, 2008). However, these models are quite complex and require the knowledge of several parameters related to the type of vegetation, cutting cycles and irrigation, which are difficult to find. Therefore, given the purpose of this work, a simplified approach has been adopted. To reduce the computational time, a simplification in modelling the vegetation layer has been introduced by neglecting a separate energy balance equation for vegetation and the underlying soil. The effect of the former one was introduced in each component of the GSEB by means of appropriate correlations.

The surface temperature is mainly driven by the radiative component, especially during the summer. The net radiative flux R (W/m^2) depends on absorption and reflection of the incident shortwave solar radiation into its direct and diffused components and on the longwave radiation received and emitted by the surface. The amount of shortwave and longwave solar radiation reaching the ground surface and the outgoing longwave radiation as well, are reduced by the shading due to the foliage layer. Moreover, the plant canopy absorbs long-wave radiation from the sky and re-radiates to the underlying soil surface. Consequently, a coefficient of shading (s_f=0.50) has been introduced similarly to FASST model (Frankenstein & Koenig, 2004). This accounts for the actual surface coverage and for the mutual radiative heat transfer between vegetation and soil, which has not been solved here, contrary to the FASST model. The net radiative energy flux at the ground surface is given by:

$$R = s_f\big((1 - \alpha)R_s + R_{ld} - \sigma\varepsilon_s T_s^4\big) \qquad (3.7)$$

where:
s_f = calibration coefficient of shading
α = surface albedo
R_s = shortwave solar radiation (W/m^2)
R_{ld} = downward longwave solar radiation (W/m^2)
σ = Stefan-Boltzmann constant (W/m^{2}K^4)
ε_s = surface emissivity
T_s = surface temperature (K)

The use of weather data is preferable for better accuracy. The time series at an hourly scale of the short-wave solar radiation incident on the horizontal surface are

usually provided by the local meteorological services. Anyway, if the weather data is not available, the literature provides a number of models dedicated to the calculation of solar radiation. A comprehensive dissertation of the subject is provided by Duffie & Beckman (2013). Measurements of the downward longwave radiation are more difficult to find. However, the development of models for estimating the thermal radiation from above has a long history. Among the others, Swinbank (1963), Brutsaert (1975) and Prata (1996) proposed a formulation of the long-wave radiation from clear skies. The effect of cloud cover was included in (Sugita & Brutsaert, 1993). A work from Choi, et al. (2008) compared different formulations for both clear and cloudy sky thermal radiation in order to identify the best one.

An important component of the energy balance at the ground surface is the convective heat flux. In recent decades, several correlations of varying complexity have been proposed for estimating the convective heat transfer coefficient. A comprehensive survey has been carried out by Palyvos (2008). The linear correlations proposed by Jürges (1924) for a plane wall and by McAdams (1954) for smooth surfaces, have been widely applied in numerical modelling of ground heat exchangers such as (Nam, et al., 2008) and (Fujii, et al., 2012), despite its shortcomings. However, the wind speed is significantly reduced within vegetation, as reported by Scott (1978). Scott carried out empirical measurements of air velocity within six different types of vegetation. Consequently, a specific approach, albeit simplified, is required to take into account the reduction in convective heat flux at ground surface due to the wind sheltering by the foliage layer. According to Antonopoulos (2006) this component of the GSEB can be calculated as:

$$H = \rho_a c_a \frac{(T_a - T_s)}{r_a} \tag{3.8}$$

where:
ρ_a = density of air (1.205 kg/m^3)
c_a = specific heat of air (1005 J/kg/K)
T_s = surface temperature (°C)
T_a = air temperature (°C)
r_a = aerodynamic resistance to heat transfer (s/m)

The parameter aerodynamic resistance, r_a (s/m), is function of wind speed and canopy properties (Allen, et al., 1998):

$$r_a = \frac{\ln\left(\frac{z_m - d}{z_{om}}\right)\ln\left(\frac{z_h - d}{z_{oh}}\right)}{k^2 u_z} \tag{3.9}$$

where:
z_m = height of wind measurements (m)
z_h = height of humidity measurements (m)
d = zero plane displacement height (m)

z_{om} = roughness length for momentum transfer (m)
z_{oh} = roughness length for transfer of heat and vapour (m)
k = von Karman constant (0.41)
u_z = wind speed at height z (m/s)

Assuming as a reference a grass cover with a constant height of 0.12 m and a standardised height for wind speed, temperature and humidity of 2 m according to Allen, et al. (1998), Eq. 3.7 becomes:

$$r_a = \frac{208}{u_2}$$

(3.10)

where:
u_2 = wind speed at 2 m (m/s)

Usually, the wind speed is measured at the standard height of 10 m in meteorology. As a consequence, the wind speed data should be adjusted (Allen, et al., 1998) using a logarithmic profile of wind speed above grassed surfaces:

$$u_2 = u_z \frac{4.87}{\ln(67.8z - 5.42)}$$

(3.11)

where:
u_z = wind speed at z m above the ground surface (m/s)
z = height of measurement above the ground surface (m)

The last component of Eq.3.4 is the latent heat flux, which depends on several weather variables and clearly on the water availability at the ground surface, which is not directly calculated in this model. The latent heat flux at the ground surface is given by:

$$LE = K_c ET_0 l_h$$

(3.12)

where:
K_c = crop coefficient
ET_0 = reference crop evapotranspiration (mm/day)
l_h = latent heat of evaporation (kJ/kg)

The evapotranspiration is defined as the sum of two separate processes: the water evaporation from the soil surface and the water transpiration from plants. The Food and Agricultural Organisation of United Nations (FAO) developed a reliable methodology for ET_0 calculation, also referred as the FAO Penman-Monteith model that proved to be reliable for different climates and time step (Allen, et al., 1998). The original FAO-PM requires weather data (e.g. solar radiation, relative humidity, wind speed, air temperature) to be used. A complete discussion of the model is available on-line at (FAO, s.d.).The evapotranspiration for a reference grass crop

ET_0 (mm/day), well irrigated and completely shading the ground, using standard climatic parameters, can be derived from the FAO-PM equation as follow:

$$ET_0 = \frac{0.408(R_n - G) + \gamma \dfrac{900}{T + 273} u_2(e_s - e_a)}{\Delta + \gamma(1 + 0.34u_2)} \qquad (3.13)$$

where:
R_n = net radiation at the crop surface (MJ/m^2/day)
G = soil heat flux density (MJ/m^2/day)
γ = psychrometric constant (kPa/°C)
T = mean daily air temperature at 2 m height (°C)
u_2 = wind speed at 2 m (m/s)
e_s = saturation vapour pressure (kPa)
e_a = actual vapour pressure (kPa)
Δ = slope vapour pressure curve (kPa/°C)

Some of the weather data is available directly from local weather services; other can be calculated by means of direct or empirical relationship. Appropriate methods for estimating missing data are provided in (FAO, s.d.).

In calculating the latent heat flux at the ground surface with Eq.3.10, the reference ET_0 has been multiplied by a single crop coefficient K_c in order to take into account the characteristics of the vegetated layer, which is a not irrigated wild meadow. Typical values are listed in (FAO, s.d.) for different agricultural crops and crop growth stages. For natural vegetated surfaces in fact, the evapotranspiration is significantly reduced compared to the agricultural crops, therefore, K_c has been taken equal to 0.25 (constant). Changes in vegetation and ground cover mean that the crop coefficient K_c varies during the growing period. Anyway, these variations have not been considered in this model due to the objective difficulties in knowing the different stages of a wild meadow.

The GSEB equation (Eq.3.4) has been properly implemented in COMSOL Multiphysics as a model variable. This represents the overall heat flux at the ground surface G (t, T_s), which is a function both of time and surface temperature.

The GSEB has been subsequently assigned as a boundary condition at the upper layer of the calculation domain, which has been previously described in paragraph 3.2.1 in order to carry out the numerical analysis of the Flat-Panels.

3.4.2 Comparison of simulation results and field data

The reliability of the model has been preliminary tested with a dedicated simulation. This was run using the model domain and soil properties described in the previous paragraph 3.2.1, for a whole year using a time step of 60 min. In this simulation, the heat load at the ground heat exchanger has been neglected; therefore,

the variation in the soil thermal field has been only determined by the environmental conditions.

A comprehensive data set of 2014 has been managed to obtain several hourly scale time series that are needed as input in each component of Eq.3.3. Several weather variables (solar radiation, air temperature, relative humidity, atmospheric pressure and wind speed) have been measured by means of the Davis Vantage Pro2 Plus weather station that was installed at the end of 2012 at the Department of Architecture in Ferrara, Italy. Missing data, such as the downward longwave radiation, have been kindly downloaded from (ARPA-EM, s.d.), the meteorological service of the Emilia Romagna region.

The simulated ground temperature trend has been compared with the measured values at different depths. The weather station in fact has been equipped with four temperature probes since 2014, to monitor the soil temperature at different depths (0.1, 0.8, 2.5 and 4.2 m).

A soil temperature profile for the 1st day of 2014 has been obtained from the available soil temperature data; this profile was set as the initial condition for simulations.

The daily average simulated values of soil temperature are reported against measure values in Fig. 3.7. Three temperature probes have been considered (T1, T2 and T3) at three different depths (0.1, 0.8, 2.5 m respectively).
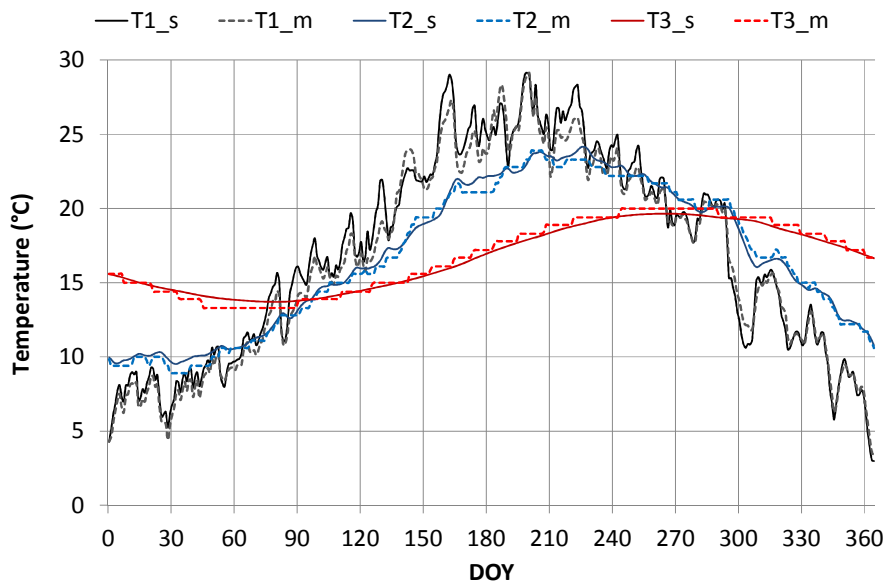

Fig. 3.10 Daily average temperature at different depth (0.1, 0.8, 2.5, 4.2 m): simulated (s) and measured (m).

Deviations are detectable mainly for the shallow probe T1, where fluctuations in temperature are greater. The relationship between measured and simulated temperature is more stable in winter for shallow probes, when the radiative heat flux is low and the latent heat flux is nearly zero. The model showed less accuracy in estimating shallow soil temperature in summer, with a maximum error of 3 °C at a depth of 0.1 m.

The analysis of simulated and measured temperature time series shows that the model both over and under-predicts peak daily temperature near the surface, during different periods of the season. This could be related to variation in heat flux at the ground surface due to the natural growth cycle of the meadow and associated mowing cycles, which are not considered in the model. Moreover, deviations may also be caused by the large rainfall events and the resulting water infiltration. However, horizontal ground heat exchanger is usually installed at a depth between 1 and 2 m, where the daily fluctuations in soil temperature are reduced. As a consequence, a precise estimate of the soil temperature near the surface was not the objective of the model. Contrary to probe T1, the soil temperature values are in good correspondence with measurements, for both the deeper probes (T2 and T3) for the entire period of simulation.

The statistical uncertainty has been calculated for the entire simulation period. For 2014, it was 0.44 °C at a depth of 0.8 m. Table 3-3 summarises the accuracy of temperature simulation for each temperature probes.

Scatter plots of the simulated soil temperatures versus the equivalent measured are shown in Fig. 3.8 for probe T1 (depth 0.1 m) and in Fig. 3.9 for probe T2 (depth 0.8 m). In these graphs, the central line represents a perfect correlation between measured and simulated values, and the two others a span of 2 °C. In both cases the slope of the relationship is close to 1:1, although slight dispersion occurs when the soil temperature is higher than 20 °C.

Fig. 3.10 shows the heat fluxes related to each component of the GSEB equation, for 3 days in winter and summer. Both in winter and in summer, the conductive heat flux in soil (G) shows a strong dependence on the net radiation (R) because the ground surface was supposed to be only partially shaded by the vegetation above. The average convective heat flux (H) is low due to the sheltering effect by the vegetated layer. Moreover, the convective heat flux is further reduced due to the low wind speed, here representative of an urban area. H is relatively stable and varies between +75 and -25 W/m^2 depending on the temperature difference between air and surface.

Tab. 3-4 Soil temperature simulation accuracy at different depths.

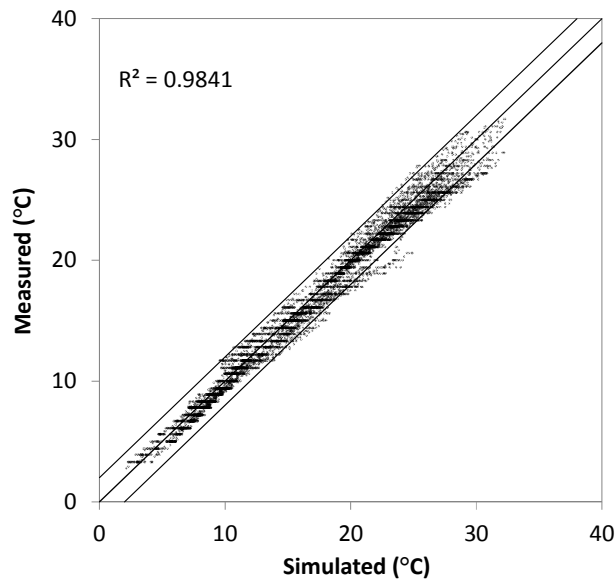| Depth (m)	0.1	0.8	2.5
RMSE (°C)	0.99	0.44	0.35

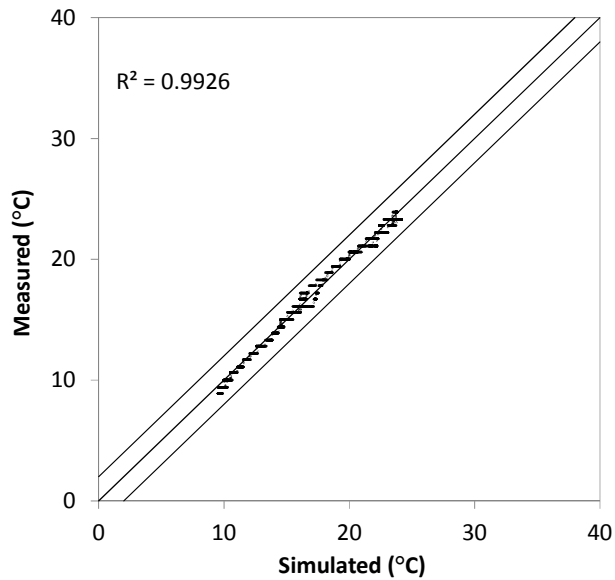Fig. 3.11 Scatter plot of the simulated and measured hourly temperature 0.1 m deep in soil.

Fig. 3.12 Scatter plot of the simulated and measured hourly temperature 0.8 m deep in soil.
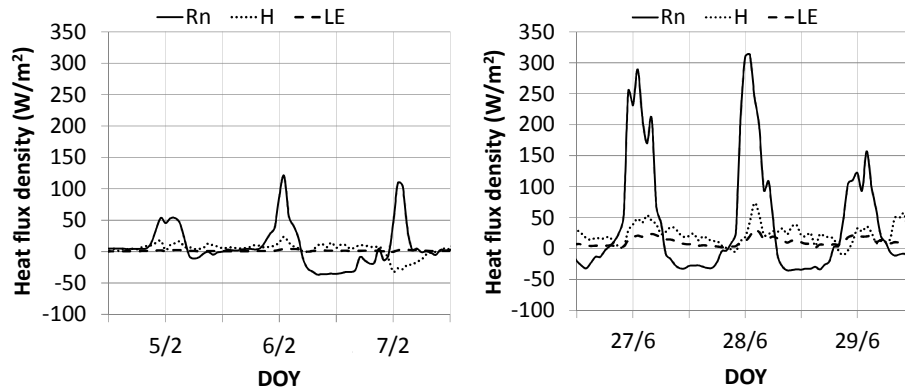
Fig. 3.13 Components of ground surface energy balance during winter and summer.

As expected, the heat loss from the surface due to the latent heat flux (LE) is nearly zero in winter. It is related to the air temperature and soil heat flux, thus an increase is observed in summer, with a daily oscillation between 25 and 5 W/m2 during daytime and night-time, respectively.

A further verification has been done by simulating the soil temperature in 2013. Since in that year the Soil Station had not yet been installed, the simulated soil temperature has been compared with that measured at a depth of 1.65 m by the sensor V.6.5. This is 1.4 m away from the heat exchanger therefore, the soil is thermally affected by effect of the heat transfer. For this reason, a period of 6 months is selected, between the Test I and the Test II. The soil temperature simulated and measured are shown in Fig. 3.14, together with the air temperature.

In the graph, the simulated values represent the soil temperature under undisturbed conditions. The thermal anomaly was caused by the test carried out in cooling mode (Test II), which lasted until 10th April (the red line in the graph). Initially in fact, a significant difference (more than 2 °C) is visible between simulated (undisturbed) and measured soil temperature.

After the end of the Test I, the measured soil temperature slowly returns to undisturbed conditions and resembles the simulated one (undisturbed) around the middle of May.

In undisturbed conditions there is a good correspondence between the simulated and measured temperature, with a maximum difference of 0.4 °C. Therefore, the model predicted suitably the temperature of the soil of 2013, although the calibration had been made on the basis of 2014 data which were acquired by means of different sensors.

Test II was started on 14th August, in the heating mode. The measured temperature at a distance of 1.4 m starts to increase with about a one week delay. On the contrary, the undisturbed soil temperature (simulated) decrease from the second half of August, according to the air temperature.
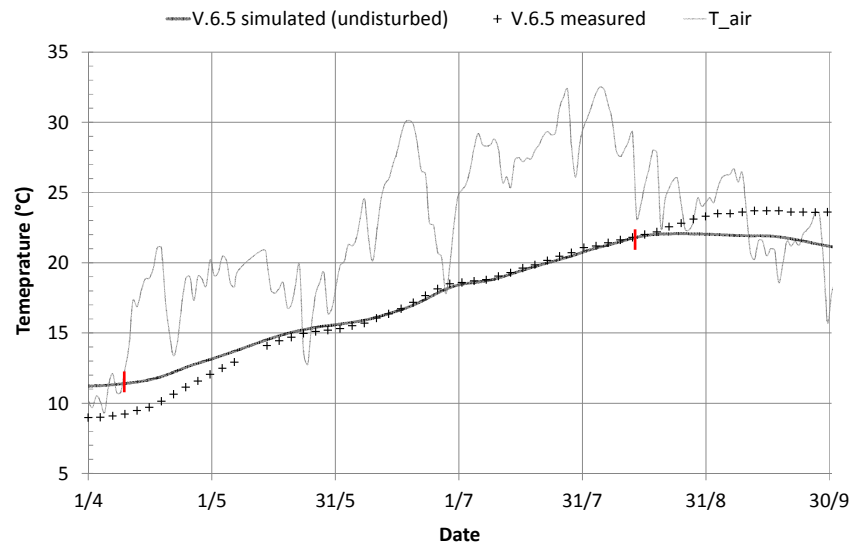
Fig. 3.14 Simulated and measured temperature at a depth of 1.65 (probe V.6.5) in 2013.

3.5   Energy loads calculation for the ground heat exchanger

The energy requirement for space heating and cooling may be defined as the amount of energy needed to maintain a constant target value of the buildings indoor temperature. In GCHP systems, the thermal energy is extracted/released from/to the ground by means of the ground heat exchanger. Since the 1970s, several studies have been carried out on the thermal modelling of buildings aiming to provide techniques for building design and energy demands for heating and cooling. Among the other methods for thermal modelling of buildings (e.g., the impulse factor method, the finite difference method) the lumped parameter method is certainly the simplest and most efficient from a computational point of view (Gouda, et al., 2002). The lumped capacitance method provides simplification in solving transient heating and cooling problems assuming that temperature gradients within a solid body are negligible during the transient heat transfer process. Consequently the temperature of such a solid is nearly spatially uniform at any instant and it can be considered to be a function of time only T (t).

The modelling of the thermal behaviour of a building can be simplified with a lumped parameter approach by reducing the building to a resistance-capacitance model and taking into account the heat transfer through the walls, the thermal inertia of the building and the energy contribution by HVAC systems (Morini & Piva, 2007). In view of this, the building can be described as a lumped thermal circuit, as shown in fig. 3.15, where R_i and R_e are the indoor and outdoor lumped thermal resistances, respectively. This approach is commonly has been widely applied to assess the dynamic behaviour of a building instead of static models.
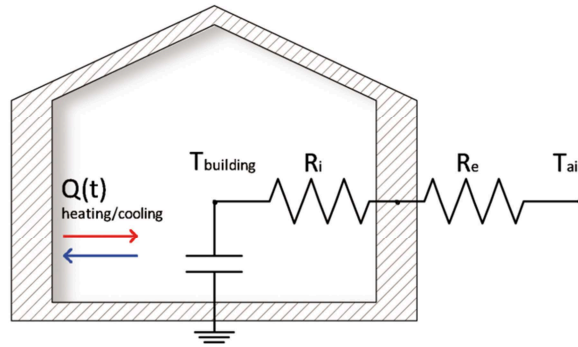
Fig. 3.15 Homogeneous lumped system.

However, not all heat transfer process involved in building performance are ac-counted, as well as a number of features of a real building (Wilson, et al., 2015).

A simplified model, based on a lumped resistance-capacitance method, is pro-posed in order to define an hourly energy requirement (both for heating and cool-ing) to be used in numerical simulation of Flat-Panels (Bortoloni & Bottarelli, 2015). The transient temperature response of the building is determined by formulating an overall energy balance on the entire solid by relating the variation of the inter-nal energy to the rate of heat loss at the surface, according to the difference be-tween the outdoor air temperature and indoor temperature of the building. The overall energy balance of the building can be written as:

$$rV \cdot \rho c \cdot \frac{dT}{dt} = -\widehat{U}S\big(T_{building} - T_{air}\big) \tag{3.14}$$

where:
r = ratio of the plenum to the total building volume
V = total building volume (m^3)
ρ = average density of the solid (kg/m^3)
c = effective heat capacity of the solid (J/kg/K)
$\widehat{U}$ = overall equivalent transmittance (W/m^2K)
S = heat transfer surface (m^2)
T = temperature of the solid (°C)
T_{air} = ambient air temperature (°C)

The overall equivalent transmittance has been defined by Bottarelli & Gabrielli (2011), where it was related to the standard for energy performance of buildings, local climate (degree-days) and the building shape ratio as:

$$\widehat{U} = \frac{EP}{\left(\frac{S}{V}\right) \cdot DD \cdot hh} \tag{3.15}$$

where:
EP = standardised energy requirement (W/m^3)
S/V = building shape ratio (m^{-1})
DD = degree days
hh = daily operating hours of heating/cooling system

In this model, it is assumed that the ambient air temperature T$_{air}$ is constant in the chosen time step (1 h). This assumption is sufficiently accurate for this purpose to which the above formulation would be applied to assess the building heat loss in relation to an hourly average time series of T$_{air}$. In view of this, the term dT equals d(T-T$_{air}$), therefore Eq. 3.15 can be rearranged as:

$$\frac{rV \cdot \rho c}{\widehat{U}S} \frac{d\left(T_{building} - T_{air}\right)}{dt} = -\left(T_{building} - T_{air}\right)$$

(3.16)

The ambient air temperature variation is independent from the temperature of the solid, therefore by separating variables the previous Eq. 3.16 can be integrated in time, from the initial condition when t$_i$=0 and T=T$_i$ (T$_i$ initial temperature) to a time t when T=T(t):

$$\frac{rV \cdot \rho c}{\widehat{U}S} \int_{\theta_i}^{\theta} \frac{d\theta}{\theta} = \int_{t_i}^{t} \theta$$

(3.17)

where:
$\Theta \equiv T_{building} - T_{air}$ (°C)
$\Theta_i \equiv T_i - T_{air}$ (°C)

Evaluating the integrals, the indoor temperature of the building at some time t can be calculated as:

$$T_{building}(t) = T_{air} + (T_i - T_{air}) \cdot e^{-b \cdot t}$$

(3.18)

where b is a positive quantity (s^{-1}) is defined in Eq. 3.16:

$$b = \frac{\widehat{U}S}{rV \cdot \rho c}$$

(3.19)

which is the reciprocal of the time constant of the building.

In the model, the hourly average ambient temperature is calculated by means of a yearly sinusoidal trend (i.e. the seasonal temperature variation) and by superimposing a daily sinusoidal oscillation ranging between the daily minimum and maximum air temperatures (night/day) in winter and in summer, as reported in (Bottarelli & Di Federico, 2010) and shown in Fig. 3.16.

The trends of day (T$_d$) and night (T$_n$) ambient air temperature are expressed as function of the annual maximum temperature of day and night (T$_{y,d}$^{max} and T$_{y,n}$^{max},

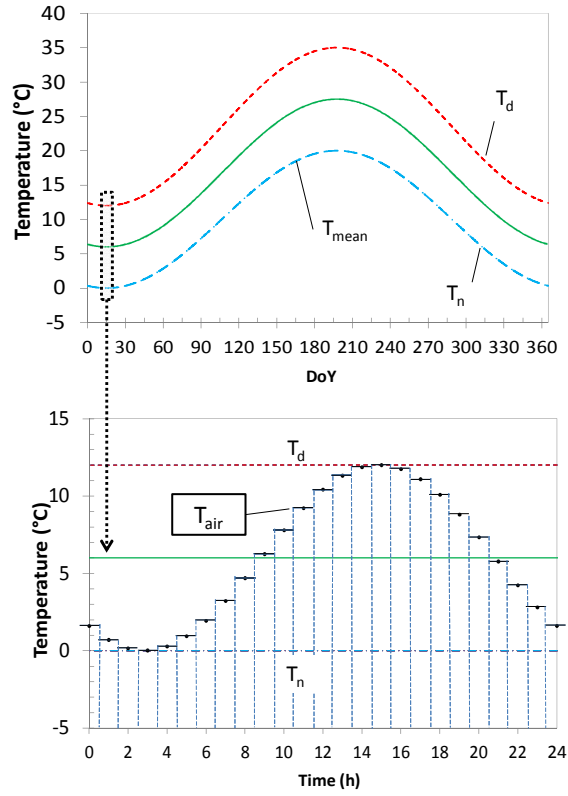Fig. 3.16 Time series of the hourly average air temperature.

respectively) and the annual minimum temperature of day and night ($T_{y,d}^{min}$ and $T_{y,n}^{min}$, respectively), with a seasonal time shift of 365 days (t_{365}^{d} and t_{365}^{n}):

$$T_d = T_{y,d}^{\min} + \left(T_{y,d}^{\max} - T_{y,d}^{\min}\right)\cdot\left[1 + \sin\left(\frac{2\pi}{365}\cdot\left(t_{365} + t_{365}^{d} - \frac{365}{4}\right)\right)\right] \qquad (3.20)$$

$$T_n = T_{y,n}^{\min} + \left(T_{y,n}^{\max} - T_{y,n}^{\min}\right)\cdot\left[1 + \sin\left(\frac{2\pi}{365}\cdot\left(t_{365} + t_{365}^{n} - \frac{365}{4}\right)\right)\right] \qquad (3.21)$$

Therefore, the hourly mean ambient air temperature T_{air} varies between T_d and T_n according to a sine curve with a daily time shift t_{24}^{d}:

$$T_{air} = \frac{\left(T_d + T_n\right)}{2} + \frac{\left(T_d - T_n\right)}{2}\cdot\sin\left(\frac{2\pi}{24}\cdot t_{24} + t_{24}^{d}\right) \qquad (3.22)$$

In the model, a heating/cooling system has been supposed to be an internal heat source, which balances the heat loss/gain through the heat transfer surface of the solid, when it is turned ON. Moreover, two values of set-point temperature (one for heating and one for cooling mode) and a time schedule has been introduced to control the system operation.

Therefore, at time step t_i, when the heating/cooling system is turned OFF, the indoor air temperature $T_{building}$ is supposed to be equal to an initial temperature T_i. After initial time step, if the system is turned OFF, the indoor air temperature is allowed to vary according to the overall thermal transmittance $\hat{U}$, the thermal inertia and ambient air temperature.

On the contrary, when the system is turned ON, the indoor temperature $T_{building}$ approximates the set-point temperature T_{sp} in a single time step set equal to one hour, due to the thermal energy generation or extraction by the internal heat source. To determine the heating or cooling power q (W/m^3) at each single step is:

$$q(t) = r\rho c\left(T_{sp} - T_i\right) + \hat{U}\frac{S}{V}\left(T_{building} - T_{air}\right)\Delta t \qquad (3.23)$$

where the first term accounts for the power needed to raise or lower the temperature of the building from a different initial value, until this reaches the set-point temperature. The second term is the power needed to balance the heat transfer through the building envelope due to the difference between the indoor and outdoor temperature. Moreover in the model, a time scheduling can be set to control the heating/cooling system operation as well as the start date and the end of the heating season and cooling respectively.

The method described above has been developed to obtain the thermal load at the ground heat exchanger with significant flexibility, and is therefore based on some simplifying assumptions. For example, solar gains have not yet been included in the calculation. Consequently it has some limitations of applicability.

3.6   The Effect of the Boundary Condition at the Ground Surface Layer

This study aims to compare the effect on the solution of 1st, 2nd and 3rd kind boundary conditions when assigned at the ground surface in modelling HGHEs. The FEM code has been applied by solving the unsteady-state heat transfer problem in a 2D domain.

A preliminary simulation was run using the GSEB model as the boundary condition at ground surface, therefore the equivalent heat flux and the equivalent temperature have been obtained. As for the preliminary analysis, a complete set of weather data of Ferrara for 2014 has been used. The operation of the HGHE has been simulated with the different kinds of boundary conditions. The simulations were run for two consecutive years in each case.

3.6.1 Boundary conditions

At the top of the domain, boundary conditions of 1st, 2nd and 3rd kind have been imposed at the ground surface in three different simulations. The GSEB model was firstly used as the 3rd kind BC in a preliminary model to assess equivalent heat flux (2nd kind BC) and equivalent ground surface temperature (1st kind BC). In order to calculate the GSEB and to determine the HGHE heat flux at an hourly scale, a complete set of 2014 weather data of Ferrara was used in simulations. An adiabatic condition was assigned to the side and bottom boundaries of the domain, according to paragraph 3.3.

The building energy demand has been calculated with a lumped system analysis by simplifying the actual ambient air temperature of Ferrara for 2014 with two sinusoidal trends; on an annual and daily basis, respectively, as shown in Fig 3.16 together with the hourly heat load profile during winter. The energy demand has been calculated for a building with an overall transmittance of 0.5 W/m^{2}K, and a volumetric heat capacity of 100 kJ/m^3. The heating season is supposed from October 15th to April 15th; the cooling from May 5th to the end of September. In the model, the heating/cooling system was set to operate to maintain a set point indoor temperature (20 °C in winter and 24 °C in summer). A time schedule was assumed to simulate actual working conditions for a residential building in a mild climate: 4 - 11 AM and 6 - 12 PM during working days, and 6 AM to 12 PM on the weekends. Furthermore, it has been assumed that the heating and cooling power of the system could not exceed 50 W/m^3 of the building when it is turned ON. The daily energy demand is reported in Fig. 3.17. Under the assumed conditions, the space heating/cooling system worked for a total of 2728 h in heating mode; only 792 h in cooling mode.
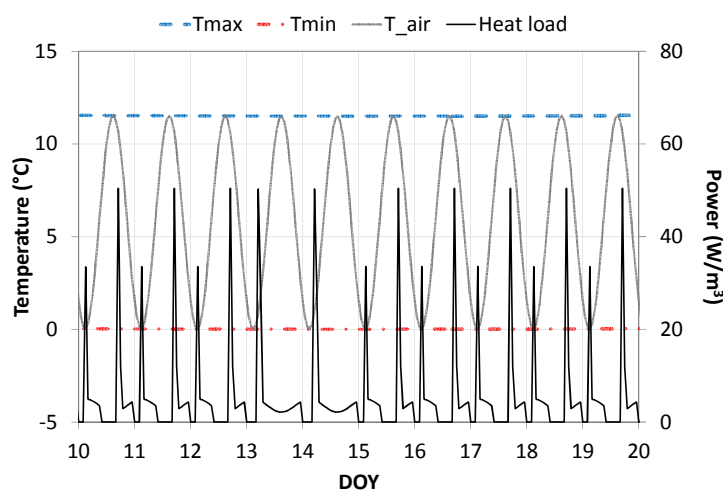

Fig. 3.17 Hourly ambient air and building heating power time series.
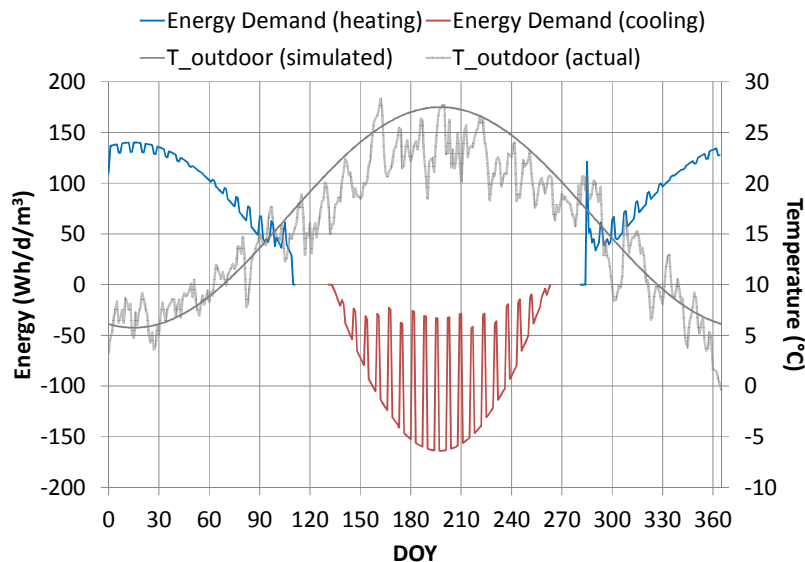
Fig. 3.18 Daily average outdoor air temperature and daily energy requirements for space heating and cooling.

The calculated energy demand for 2 m^3 of building has been supposed to be the full energy requirement for the closed loop, therefore the resulting heat flux time series (W/m^2) has been directly applied as the boundary condition at the FP in the numerical model. As a result, the maximum heating and cooling heat flux at the ground heat exchanger was 100 W/m2. On overall terms, during the heating season a total amount of 36.4 kWh (i.e. 72.8 kWh according to the symmetrical domain) for each metre of FP have been extracted from soil for 190 days; during cooling season it was 21.8 kWh (43.6 kWh) 145 days. These values are comparable with those recorded during the experimental tests.

3.6.2 Results

The results are compared in terms of the average temperature at the HGHE wall surface, according to the simplifications and assumptions considered. This may be considered as the temperature at the Flat-Panel surface, and therefore it is representative of the HGHE performance with the different boundary conditions at the ground surface. Moreover, the temperatures in the surrounding soil have been calculated by means of point probes within the domain at different depths in order to discuss the evolution of the thermal field.

The resulting time series for each BCs of the daily average temperature at the HGHE wall are shown in Fig. 3.19. In the graph, a whole year is presented, starting in May, when the cooling season begins.
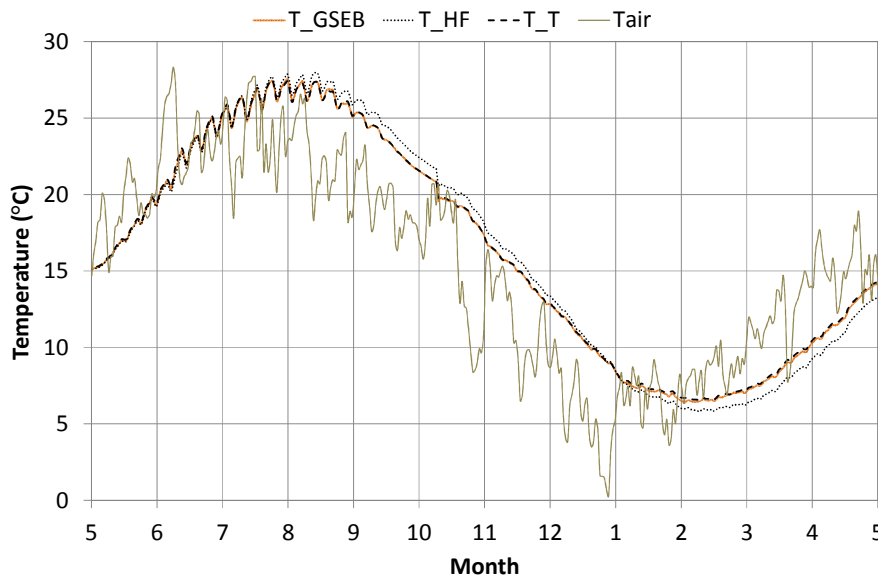
Fig. 3.19 Daily average temperature on the Flat-Panel surface.

The initial average temperature is around 15 °C, and then it rapidly increases according to heat released to the ground. After two months of operation, the temperature at the HGHE surface is up to 5 °C higher than the equivalent undisturbed. The maximum temperature is reached in all three cases in August. The temperature follows a similar trend in the case where the GSEB and the equivalent temperature are assigned as BC. However, as expected in the first case the temperature at the ground surface is slightly higher just above the heat exchanger. Contrary to previous cases, with the equivalent flux the Flat-Panel surface has a maximum 1.2 °C higher. Moreover, in this case, the thermal drift continues until the beginning of the winter season. The minimum temperature is reached in all three cases in the second half of February, with a lag of 45 days in comparison with the temperature at the ground surface and of air. The temperature drops more rapidly with the equivalent heat flux assigned to the surface (case HF) and shows a maximum difference of 1.2 °C compared to the other two cases on a daily average basis. Moreover, unlike the other cases (GSEB and T), a thermal drift of 1 °C is detected after a year in HF, because the equivalent heat flux does not balance the heat demand of HGHE operating. On the contrary, a negligible discrepancy is observed between the case GSEB and T. Therefore the use of 1st kind boundary conditions could be considered an acceptable simplification.

In Fig. 3.20 weekly detail of the hourly HGHE operation, when the minimum temperature at the Flat-Panel surface is reached in the heating period. In comparison with the above considerations, temperature values are significantly different in
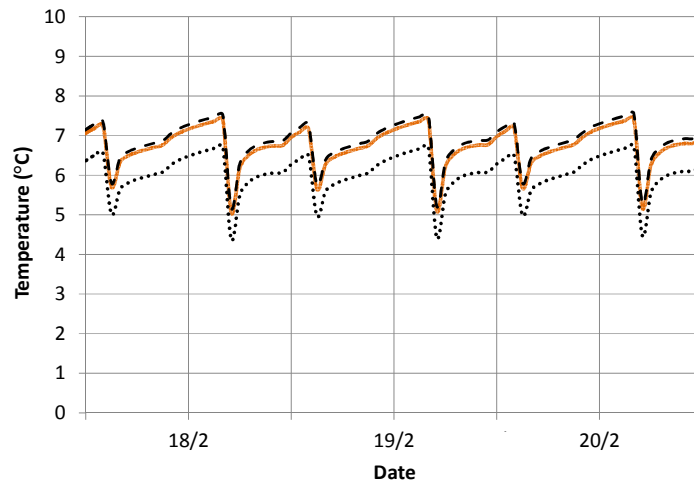
Fig. 3.20 Three operating days with hourly average temperature in winter.

the case of equivalent heat fluxes; therefore the effect of energy extracted or re-leased is over-estimated. In the other two cases the differences, though present, are negligible.

Finally, Fig.3.21 shows the hourly time series of soil temperature at two differ-ent points in the soil domain. The first temperature probe is above the HGHE, 0.8 m deep in soil.
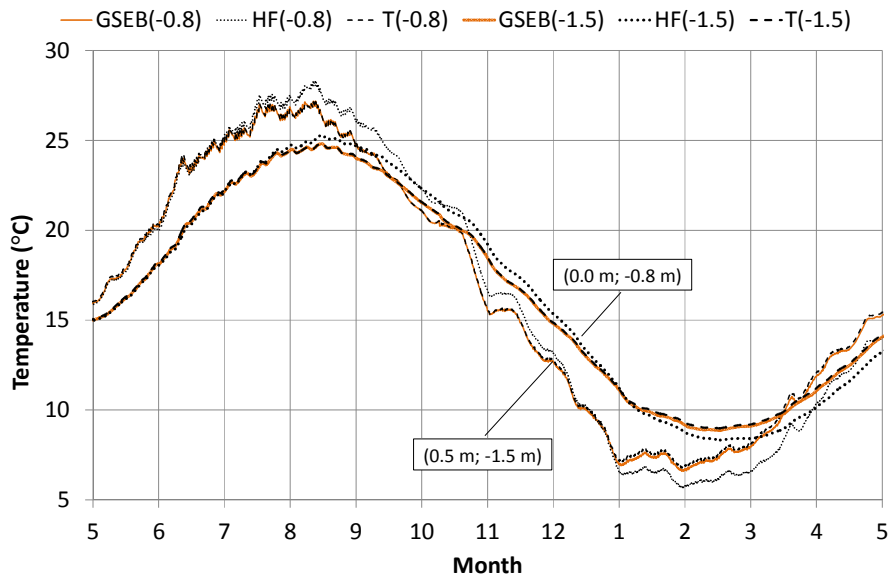

Fig. 3.21 Average temperature in the soil for three boundary conditions.

The second probe is positioned at the average depth of the HGHE (-1.5 m) and 0.5 m far from it. In the former one, the maximum difference between the case HF and the two other cases is 1.4 °C. Moreover, a significant thermal drift is maintained over the entire year. As for the temperature at the HGHE wall, the soil thermal field is comparable for GSEB and T.

3.6.3 Discussion

The effect on numerical solutions of different boundary conditions at the ground surface was analysed in modelling HGHEs. The commercial software COM-SOL Multiphysics was used to solve the unsteady heat transfer problem in a 2D computational domain. A model of the energy balance at the ground surface (GSEB) based on the ground surface properties and weather variables was developed, and implemented in COMSOL to be tested as boundary condition at ground surface. For a realistic simulation of the environmental conditions, weather data sets based on experimental data were used for simulations. The GSEB model was validated with the observed soil temperature data at different depths in 2013 and 2014, proving to accurately predict the temperature in the soil.

Simulations were carried out to test the HGHE energy performance in heating and cooling, under the same environmental conditions. The GSEB model, the equivalent heat flux and temperature at the ground surface were used as boundary conditions (BC) of the 1st, 2nd and 3rd kind in simulations.

The solution of the equivalent heat flux at the ground surface is significantly different from the other two cases, and appeared as a precautionary approach. On the other hand, when a boundary condition of the first kind (i.e. equivalent surface temperature) is used, a significant constraint is imposed to the surface temperature, which is not allowed to vary due to the HGHE heat transfer. Consequently, a 3rd boundary condition in modelling HGHE is preferable approach to the problem, not affecting the calculation time. However, the correct estimation of the surface temperature is of great importance also in this case, and a preliminary simulation with a GSEB could be required.

4.   MODEL COMPARISON WITH EXPERIMENTAL DATA

4.1   Introduction

The validation of a numerical application is an important step. The comparison against experimental measurements in fact, provides indications on the reliability of the approach followed and also highlights any weaknesses.

In Chapter 3, the simulated and the measured ground temperature were compared, when no heat transfer occurs between the ground and the heat exchanger. This comparison allowed a validity check of the modelling of the several heat transfer mechanisms occurring at the ground surface and within the ground by means of the proposed GSEB model.

The aim of this chapter is to validate the Flat-Panel numerical model against a selection of experimental dataset. As the analysis of fluid flow and heat transfer in the working fluid within the GHE is beyond the scope of this study, the comparison is focused on the temperature variation in soil, due to the combined effect of the Flat-Panel operations and the natural heat transfer process at the ground surface. In view of this, the numerical model has been tested against the available experimental data, which was measured during the tests at the Dept. of Architecture in Ferrara. Among these, three tests were selected for the comparison, in order to evaluate the model under different operating conditions: heating mode and continuous operation (Test II, summer 2013); cooling mode and continuous operation (Test III, winter 2013-2014); heating mode and discontinuous operation (Test IV, summer 2014).

4.2   Methodology

The heat transfer in solids has been solved in a two-dimensional domain, likewise in Chapter 3. Here, the computational domain represents a symmetrical cross section of the ground heat exchanger. In view of this, the boundary representing the Flat-Panel is placed on the axis of symmetry of the model domain, between a depth of 0.8 m and 1.8 m, according to the experimental setup layout, as shown in Fig.4.1. The domain consists of a wide portion of soil (10 x 10 m) in order to approximate the soil to an infinite medium. Therefore, the far-field distance (in horizontal and vertical direction) ensures that the far-field boundary conditions would not have any effect over the duration of the simulations.

The soil is considered to be homogeneous with constant thermal properties (thermal conductivity, density, heat capacity), which are chosen according to the previous model (Chapter 3). The thermal conductivity was calibrated to obtain the same temperature variation of the sensor H.2.4, which is located at the boundary between the soil and the trench. In view of this, this value is taken as the reference

because of the thermal field at that point is less affected by the edge effect. The soil properties are listed in Table 4-1.
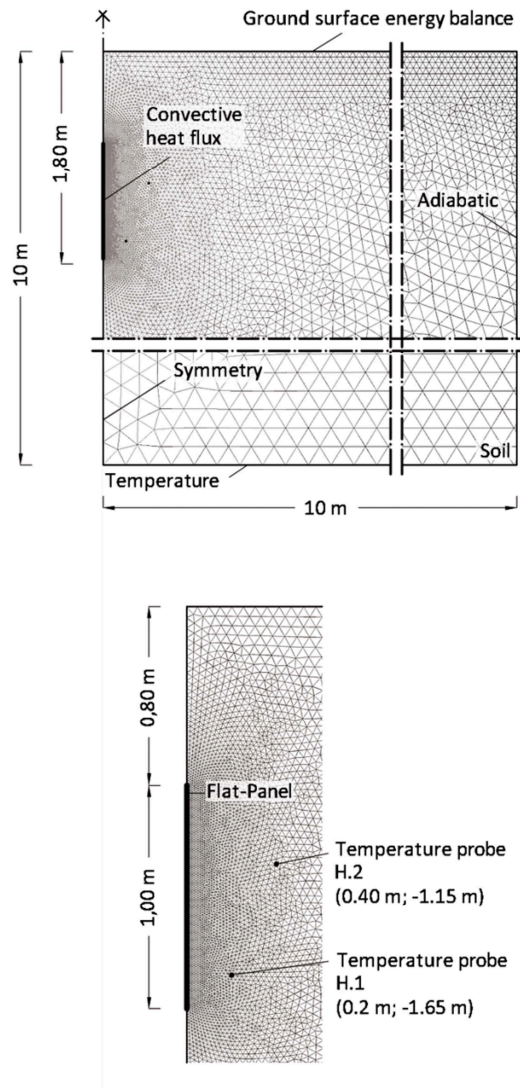

Fig. 4.1 Model domain, mesh and boundary conditions.

Tab. 4-1 Material properties

Thermal conductivity	Density	Specific heat
(W/mK)	(Kg/m^3)	(J/kgK)
1.40	1720	2000

The ground surface energy balance equation (Eq. 3.6) is assigned at the top soil boundary condition, with weather data of 2013 and 2014 as input. At the bottom boundary (-10 m) a constant temperature of 16.6 °C is given, equal to the annual mean temperature of deep soil at the experimental site. Symmetry and adiabatic condition are assigned at the vertical edges, at the HGHE side and far-field side respectively.

Finally, the Flat-Panel has been modelled as a 3rd kind thermal boundary condition in the 2D domain. The heat flux at the interface between the Flat-Panel and soil is defined as a function of the temperature difference between the interface HGHE/soil (T) and the working fluid temperature (T_{wf}):

$$-\mathbf{n} \cdot (-k\nabla T) = h \cdot \left(T_{wf} - T\right)$$

(4.1)

where the convective heat transfer coefficient (h) is equal to 120 W/m²K. The convective heat transfer coefficient has been estimated in (Battarra, 2013), where a detailed analysis focused on the fluid dynamics of the Flat-Panels under the same operating conditions.

The temperature of the working fluid is the average temperature in the ground loop at each time step. Although the use of the term "average" can be misleading, however, here it is used to indicate the average between the measured values of fluid temperature entering and exiting the ground loop (i.e. inlet and outlet sections, respectively) during each test. Unfortunately some records have been missed during the experimental activity and the large dataset related to the heat meter measurements was initially incomplete. Therefore, a procedure has been applied to manage and calculate the missing data thus obtaining a complete temperature time series for each simulated test.

The initial temperature profile of the soil is obtained from the experimental data set, in order to account for thermal anomalies caused by previous tests.

The finite element grid resolution is higher at the FP boundary and within the trench area where large temperature variations are expected and coarse in the outer domain. The full mesh consisting of 23,000 elements (41,200 degrees of freedom) is shown in Fig. 4.1.

Preliminary simulations have been carried out to check the mesh independence by increasing the number of the elements without relevant difference in numerical solution. The simulations are conducted for different periods (from 20 days to two months), with different time steps according to the different operating conditions.

Finally, the comparison is made in terms of soil temperature as measured by sensors H.1.3 and H.2.4, which are positioned at a distance of 0.20 m and 0.40 m from the HGHE. The two sensors are at a depth of 1.65 m me 1.15 m, respectively. Although other soil temperature sensors were available, the soil thermal field at their position could be affected by the edge effect. Therefore, they were considered to be unsuitable for the purpose of the comparison between the measured

and calculated temperature by means of a 2D model, which is representative of a median section of the HGHE.

4.3   Simulation of heating mode and continuous operation

The heat transfer in soil is a period of 30 days of Test II, which began in August of 2013. Test II was conducted in heating mode (i.e. heating the ground) in continuous operation, in order to simulate the operation of the GCHP in cooling mode. The HGHE was supplied continuously (seven days a week, 24 hours a day) with a fluid temperature between 33.5 °C and 35.0 °C.

As discussed in Chapter 2, the measured return temperature showed a daily oscillation, due to heat gains along the horizontal piping, which was not involved in the soil heat transfer process due to HGHE operations. In test II in fact, the temperature of the working fluid increased up to 0.5 °C during warm and sunny days in comparison with the return temperature measured night-time. As a consequence, the estimation of the mean temperature of the working fluid, between the inlet and outlet sections of the HGHE, is affected by these fluctuations.

At the beginning of Test II, the effect of the heat transfer due to HGHE operation during Test I was still detectable. Figure 4.2 shows the comparison between the calculated vertical temperature profile in undisturbed conditions and the temperature measured at various depths.
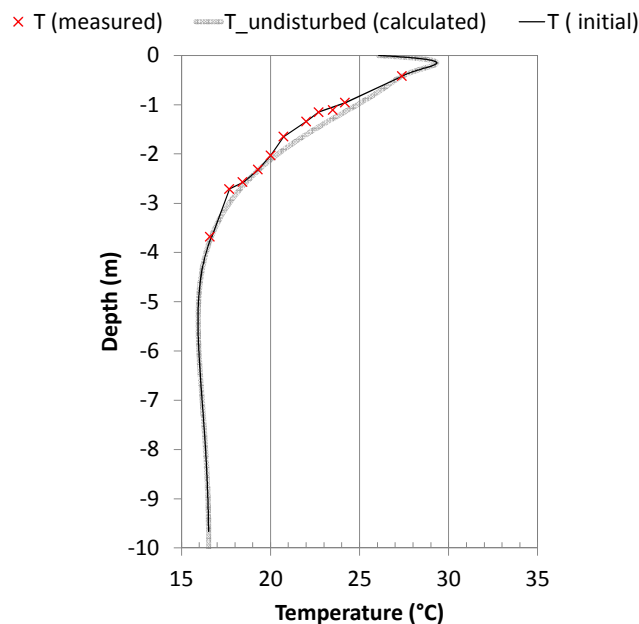

Fig. 4.2 Calculated and measured temperature profile at 14th August 2013.

On average, the initial ground temperature was 1 to 1.5 °C lower in comparison with the initial undisturbed conditions at the depth of the probes H.1 and H.2, respectively. However, there is a good agreement between the measured and calculated soil temperature, near the surface (-0.4 m) and deeper (-3.7 m). In order to obtain a reliable initial condition for the simulation, the temperature profile (black line in the graph) is calculated by linear interpolation between the values of soil temperature, measured at different depths. As regards the remaining part, between the ground surface and 0.4 m, and below 3.7 m, the undisturbed profile previously calculated is used, as shown in Fig. 4.2.

A comprehensive weather dataset has been used as input for the GSEB model. In addition, the time series (on an hourly basis) of the mean temperature of the working fluid has been calculated as the average between the measured temperature at the inlet and outlet sections of the closed-loop. Unfortunately, some plant data has been missed due to unresolved problems of communication with the heat meter, therefore a second dataset collected with the RTDs has been used to manage and calculate the missing data.

In order to complete the heat meter records, the data collected by the heat meter and the RTDs (i.e. the network) has been compared in terms of DT (difference inlet/outlet), as shown in Fig. 4.3. In this graph, the red line represents a perfect relationship between the two datasets. In this case, the interval between 1.5 °C and 3 °C included most of the values of DT. Overall, the correlation is good (R^2 is equal to 0.97). The RTDs show the tendency to slightly over-estimate DT in comparison to
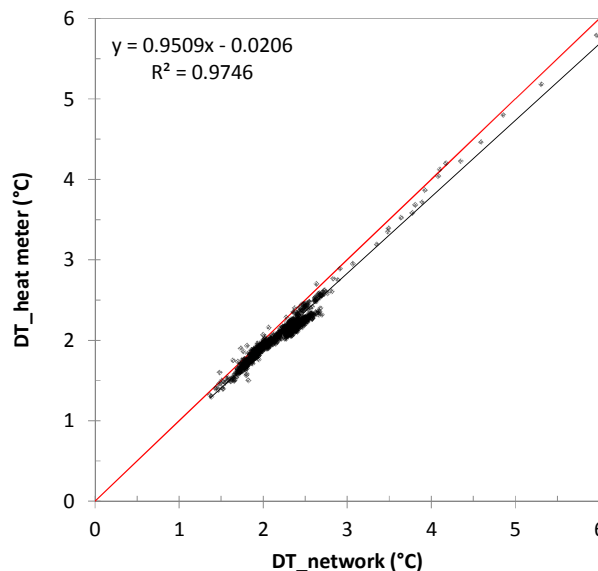

Fig. 4.3 Scatter plot of the difference of temperature between inlet and outlet as measured by the plant probe line (y axis) and the heat meter (x axis).

the heat meter and the standard deviation is 0.15 °C. In order to obtain a complete time series of the mean fluid temperature to be used in the simulation, a linear regression (reported also in Fig. 4.3) has been used to calculate the missing values on the basis of the RTDs dataset.

4.3.1 Comparison between simulated and measured soil temperature distributions

The heat transfer to the ground was simulated over a 30-day period, from 14th August to 12th September 2013.

The comparison between the measured and simulated soil temperature is shown in Fig. 4.4 and 4.5 for the temperature probes H.1 and H.2, respectively. In addition, Fig. 4.4 shows the calculated average temperature of the fluid (T_{wf}) used as input in the model. Finally, the undisturbed temperature of the ground (calculated) at the same depth of the two sensors (-1.15 m and -1.65 m, respectively) is reported in the graph. In Test II, the fluid temperature was initially set at 33.5 °C, and subsequently increased to 35 °C to enhance the performance of the ground heat exchanger. The test was temporarily interrupted on the 2nd of September for a maintenance intervention.

The probe H.1, which is closer to the heat exchanger and deeper than H.2, has a significant difference between calculated and observed temperature. Although the initial condition may be considered consistent with the actual soil thermal field, the measured and calculated soil temperature rapidly differentiate from each other, up to a maximum of about 1.4 °C, as shown in Fig. 4.4. The model over-predicts the initial temperature increase in soil temperature due to the HGHE operation. Subsequently (after about two day), the difference stabilizes until the end of the period.

The difference between calculated and measured soil temperature can be explained by an excessively large value of the soil thermal diffusivity, as used in the model. In particular, the soil thermal conductivity (1.4 W/mK) within the domain is calibrated to temperature distribution measured by sensor H.2 (paragraph 2.3) and is significantly different from that calibrated for sensor H.1 (0.6 W/mK).

On the other hand, the ground temperature is better calculated for the probe H.2, as expected. However, there is an average difference of 0.7 °C between the measured and predicted temperature. Also in this case the model overestimates the temperature increase in the initial phase.

The difference between the calculated and measured temperature could be due to a wrong estimate of thermal conductivity, which was carried out in late winter when the soil water content is typically higher than in summer.

After a month of simulated operation, the effect of the heat transfer due to the HGHE is significant. The undisturbed ground temperature is about 8 °C and 6.5 °C colder than the calculated ones at the measuring points H.1 and H.2, respectively.
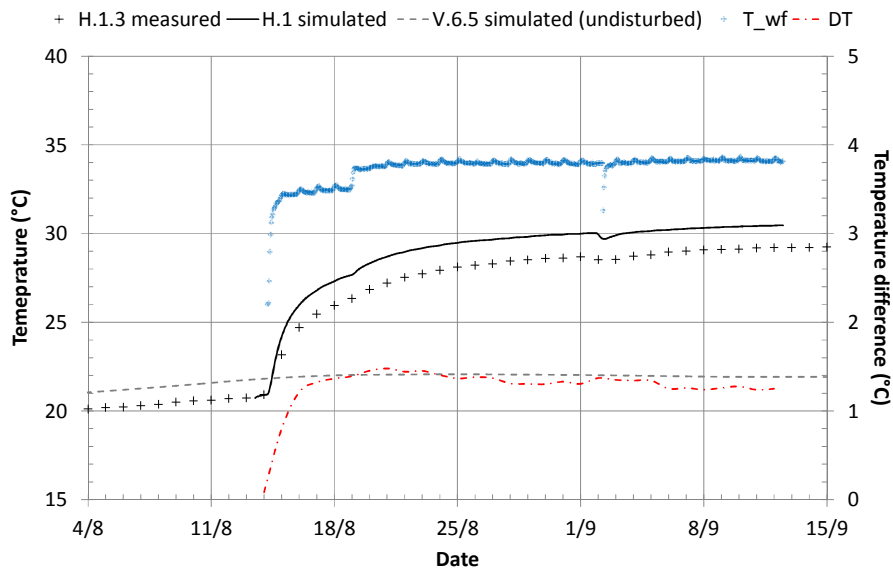
Fig. 4.4 Measured (daily average) and simulated ground temperature at sensor H.1.
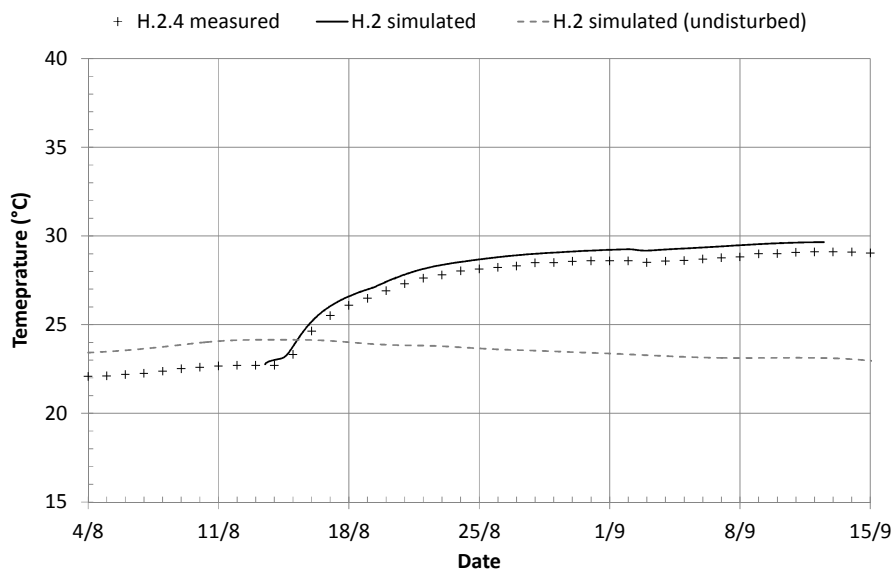

Fig. 4.5 Measured (daily average) and simulated ground temperature at sensor H.2.

Finally, using the numerical model under the same boundary conditions, a sensitivity study has been performed to evaluate the effect of soil thermal conductivity on temperature trend at measurement points. The simulations are carried out for two further values of thermal conductivity: 1.0 W/mK and 0.6 W/mK, respectively. In particular, the first is calculated as the average of the values calibrated for sensors H.2.4 and H.1.3; the second was calibrated to obtain the same temperature variation of the sensor H.1.3, (as described in Paragraph 3.2). These variations produce a significant change in the soil thermal diffusivity, equal to a reduction of 28% and 57%, respectively. As a consequence, the lower the thermal diffusivity, the slower the increase in the soil temperature, as expected.

The temperature distributions calculated at the two measurement points are shown in Fig. 4.6 and Fig. 4.7. In the figures, the range of temperature is reduced from 25 °C to 15 °C in comparison to Fig. 4.4-5, to highlight the differences between the cases. For a thermal conductivity value of 0.6 W/mK, (the one estimated for the probe H.1.3), there is a good agreement between the measured and predicted temperature in the initial phase, as shown in Fig.4.6. However, there is a difference of 0.7 °C at the end of the simulation. Finally, the use of the average value (1.0 W/mK) produces a slight reduction of the difference between the measured and calculated temperature of the soil.

On the other hand, a reduction in thermal conductivity (to 1.0 W/m) results in a better agreement between measured and calculated values at the point H.2, as shown in Fig. 4.7. The model predicts correctly the initial temperature increase.
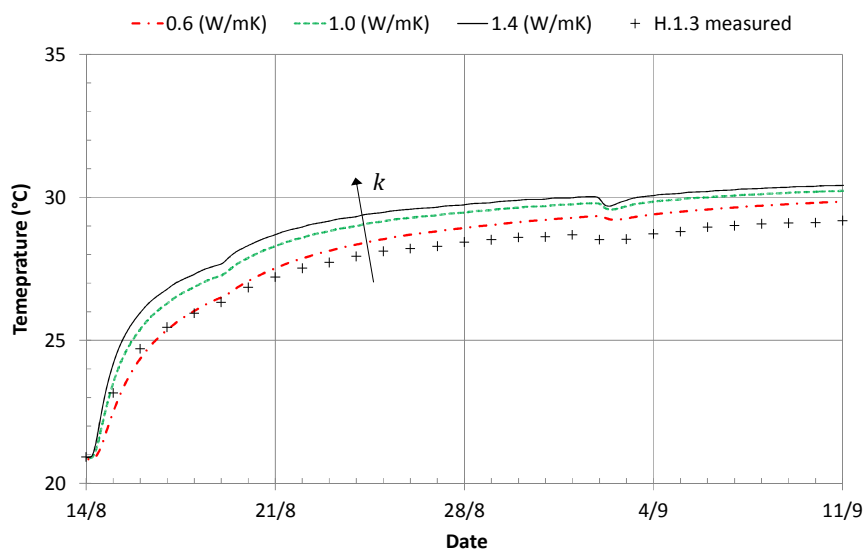

Fig. 4.6 Soil temperature at measurement point H.1 (0.2 m; 1.65 m) for different values of soil thermal conductivity (0.6; 1.0; 1.4).
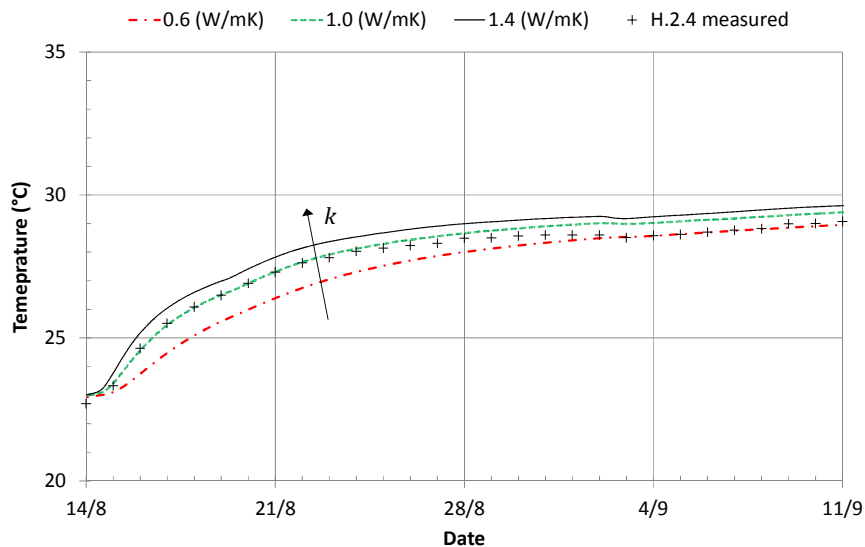
Fig. 4.7 Soil temperature at measurement point H.2 (0.2 m; 1.65 m) for different values of soil thermal conductivity (0.6; 1.0; 1.4).

After 30 days of simulation the difference is 0.3 °C. Although the average value of soil thermal conductivity is significantly different from the value initially estimated for this sensor (1.4 W/mK), it should be noted that it allows a better simulation of temperature distribution for H.2.

The thermal conductivity calibration (section 3.2) was done with reference to a dedicated experimental test, which was carried out in the middle of March. During winter and spring the shallow soil has high water content, contrary to summer when it dries out, as shown in Figure 2.16. Variations in water content could occur also at the depth of 1.15 m (probe H.2.3) due to water filtration; therefore seasonal variations in soil diffusivity are reasonably expected, and they should be taken into account for a further model development.

Overall, a 57% variation in soil diffusivity produces a difference in the final value of temperature of about 1 °C, for both the measuring points.

4.4   Cooling mode and continuous operation

In this section, the model predictions are compared with the experimental data of Test III, which started on 4th December 2013. However, the experimental setup was tested on the previous day for a few hours, after some improvements. The test was carried out in cooling mode (i.e. cooling the ground) and under continuous operation. The initial set point temperature of 8 °C was lowered to 5 °C on 5th De-

cember, and further reduced to 2 °C on 14th January in order to maintain a signifi-
cant temperature difference between the working fluid and the ground (undis-
turbed). In view of this, the simulation begins on 3rd December. The heat extraction
from the ground has been simulated over a 2-month period, from 4th December
2013 to 4th February 2014.

After the end of Test II in heating mode on 23rd October, the experimental setup
had been operating in free mode (i.e. according to the ambient air temperature),
until the beginning of December. Although the soil temperature had recovered, a
sudden fall in ambient air temperature caused the cooling of the ground in the sec-
ond half of November. Consequently, the available soil temperature data has been
managed (according to section 4.3) to calculate the soil temperature profile to be
used as the initial condition in this simulation, as shown in Fig. 4.8.

The dataset collected by the heat meter was incomplete also in this case. The
missing data has been managed with the method used for the Test II, where a ded-
icated linear regression has been used to calculate the missing values of DT. The
time series of DT measured by the heat meter and by the RTDs has been compared
in Fig. 4.9. The difference between inlet and outlet temperature is negative be-
cause the fluid warms up along the exchanger and thus the outlet temperature is
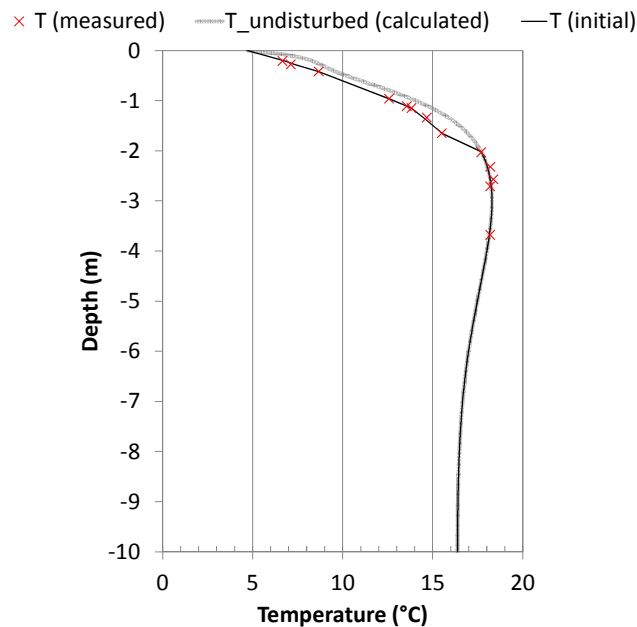higher than the inlet one. The red line in the graph represents a perfect correlation

Fig. 4.8 Simulated and measured temperature profile at 3rd December 2013.
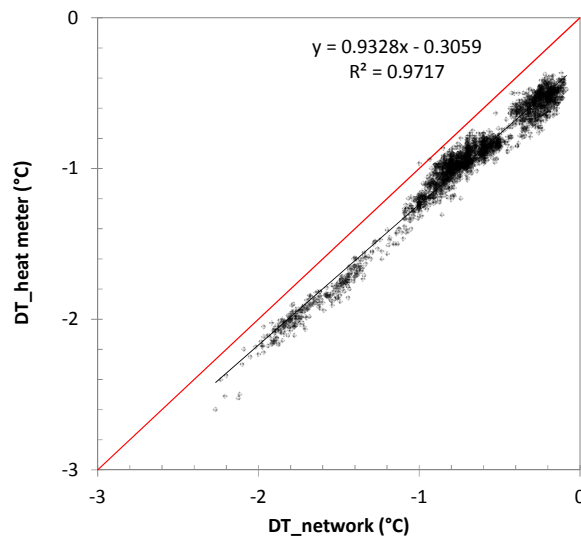
Fig. 4.9 Scatter plot of the difference of temperature between inlet and outlet as measured by the plant probe line (y axis) and the heat meter (x axis).

between the two data sets. There is a good correlation between the two data sets. The RTD network over-estimates the temperature difference in comparison to the heat meter, due to the different installation. The standard deviation is 0.27 °C.

Finally, the complete mean working fluid temperature has been used as the input in the model, to simulate Test III conditions (continuous operation in cooling mode).

4.4.1 Comparison between simulated and measured soil temperature distributions

The heat transfer to the ground has been simulated over a 2-month period, starting from 3rd December 2013.

The distribution of the average working fluid temperature T_{wf} and daily average ground temperature measured by probes H.1 and H.2 during the whole period in cooling mode operation are shown in Fig. 4.10 and 4.11. Similarly with the previous simulation, the simulated soil temperature has been reported in graphs on an hourly basis.

According to these figures, the model over-predicts the effect of the heat transfer in the initial phase, for the probe H.1. The negative difference between measured and simulated soil temperature rapidly increases, up to a maximum of -1.5 °C, and then reduces over the period simulated (the average difference is -1.2 °C).

Contrary to the measurement point H.1, a very good agreement is obtained for the sensor H.2, 0.4 m away from the heat exchanger.
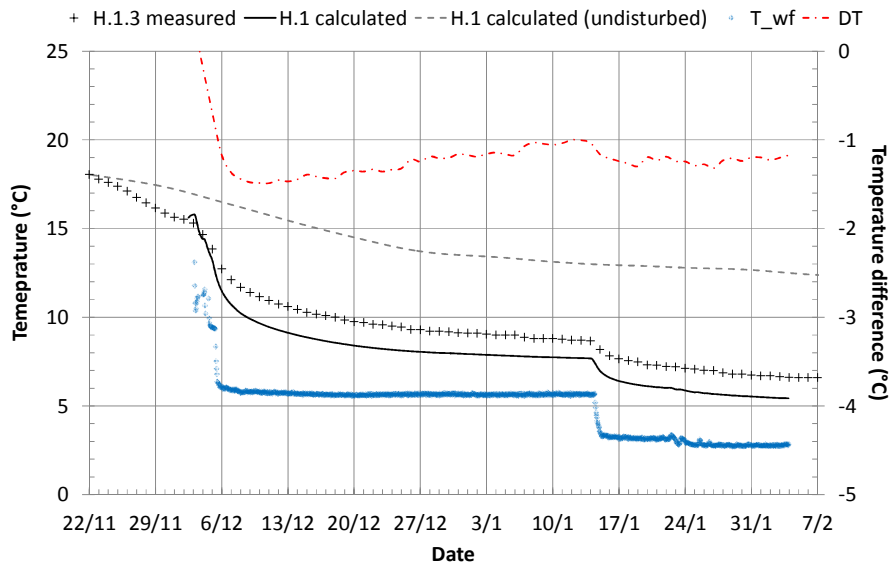
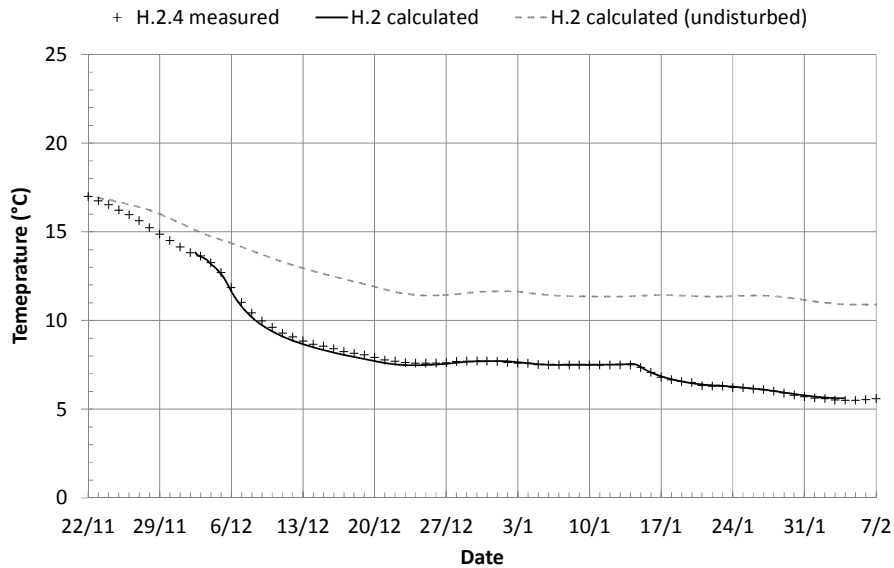Fig. 4.10 Measured (daily average) and simulated ground temperature at sensor H.1.

Fig. 4.11 Measured (daily average) and simulated ground temperature at sensor H.2.

As regards this measurement point, the reference thermal conductivity allows the correct simulation of soil temperature distribution. Contrary to the previous case in fact, this test was carried out in similar conditions to the calibration test (in winter).Therefore, the calculated thermal conductivity is appropriate in this case. The thermal properties of shallow soil are subject to significant seasonal variation, because of the change in water content. Finally, the soil temperature for both the measuring points is significantly lower than the undisturbed temperature as it is predicted by the model (up to 6.5 °C lower).

Similarly to what done for the Test II, a sensitivity study has been performed to evaluate the effect of soil thermal conductivity on heat transfer under cooling operating conditions. The simulations are conducted for two different values of thermal conductivity, with a reduction of 0.4 and 0.8 W/mK from the reference value, as shown in Fig. 4.12 and Fig. 4.13.

The difference between measured and calculated temperature (point H.1) decreases according to the thermal conductivity, as expected. The maximum difference is of about 0.5 °C with a thermal conductivity of 0.6 W/mK, which was estimated for the probe H.1.3.

A reduction of the thermal conductivity to 1 W/mK produces a slight variation in the calculated temperature trend at the point H.2. A difference of about 0.4 °C is shown at the end of the simulated period. A significant difference is visible for a further reduction to 0.6 W/mK.
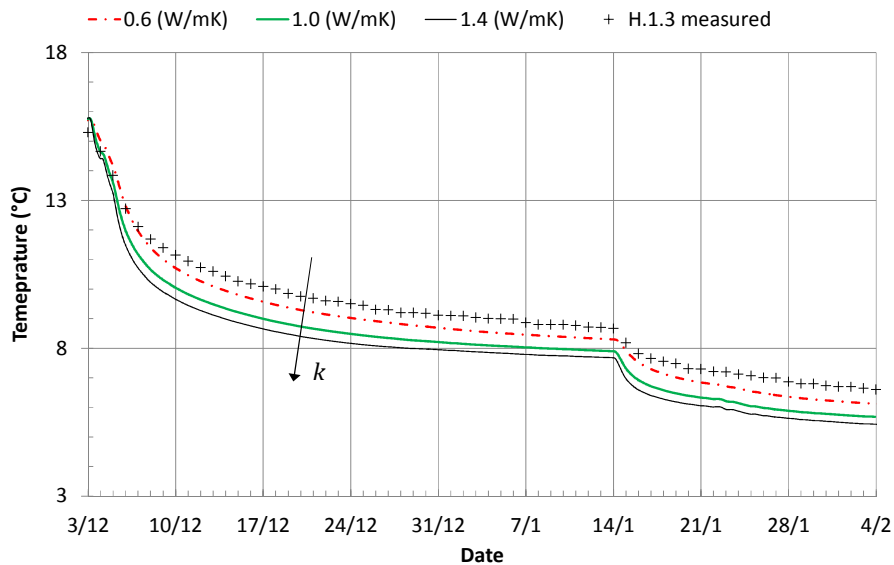

Fig. 4.12 Soil temperature at measurement point H.1 (0.2 m; 1.65 m) for different values of soil thermal conductivity (0.6; 1.0; 1.4).
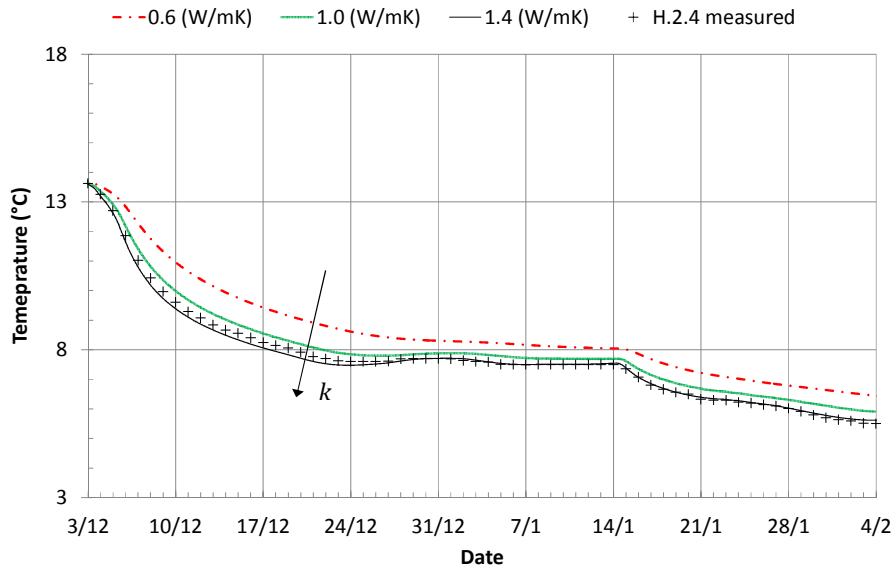
Fig. 4.13 Soil temperature at measurement point H.2 (0.2 m; 1.65 m) for different values of soil thermal conductivity (0.6; 1.0; 1.4).

4.5   Heating mode and discontinuous operation

The numerical model has been finally tested and validated in heating mode and discontinuous operation, in comparison with the experimental data-set of Test IV (summer 2014).

During this test, the experimental setup operated under a discontinuous time scheduling; therefore the ground heat exchanger was supplied from 10 AM to midnight only. Moreover, the circulator was programmed to perform an On/Off cycle of 30 min (28 cycles a day), with a run and off time of 15 min each.

In order to simulate this operating mode, a dedicated step function has been set in the model. This function varies from 0 to 1 with a period of 900 s (i.e. 15 min) and controls the boundary condition at the ground heat exchanger, within the time interval 10 AM - 12 PM, as shown in Fig. 4.14. For this reason, in the numerical model the maximum time-step of the solver has been reduced to 300 s.

The M-Bus network, which suffered communication problems during the previous experimental activities, has been finally optimized for Test IV and therefore, a comprehensive database has been available without the need for integration.

A complete weather dataset has been used. In addition, the time series of the average hourly temperature of the working fluid (as it was measured when the system was switched on) has been included as input in the model. The 20-day period of simulation begins on 12th June, according to Test IV.
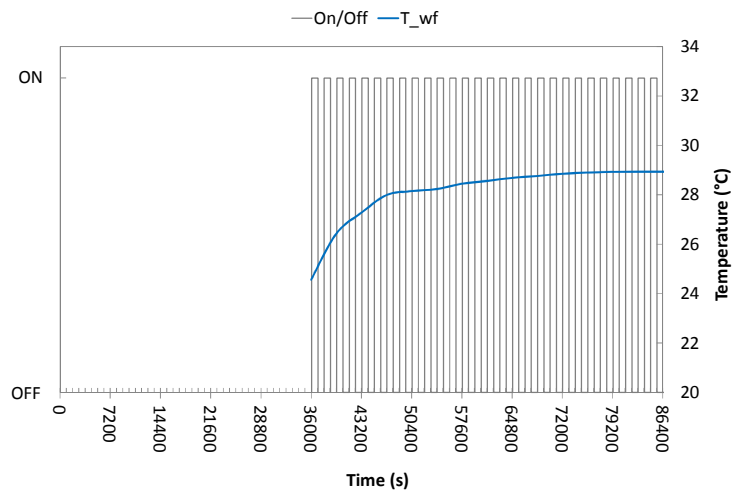
Fig. 4.14 Daily time scheduling and temperature of the working fluid at the GHE.

Similarly to the two previous simulations, the ground temperature around the ground heat exchanger was even lower by about 1 °C in comparison to the undisturbed one, due to the ground cooling of the system during the previous test, which was concluded 2 months before. Consequently, the initial temperature profile has been calculated by interpolating the available data of soil temperature at the different depths, as shown in Fig. 4.15.

Fig. 4.15 Simulated and measured temperature profile at 12th June 2014.

4.5.1 Comparison between simulated and measured soil temperature distributions

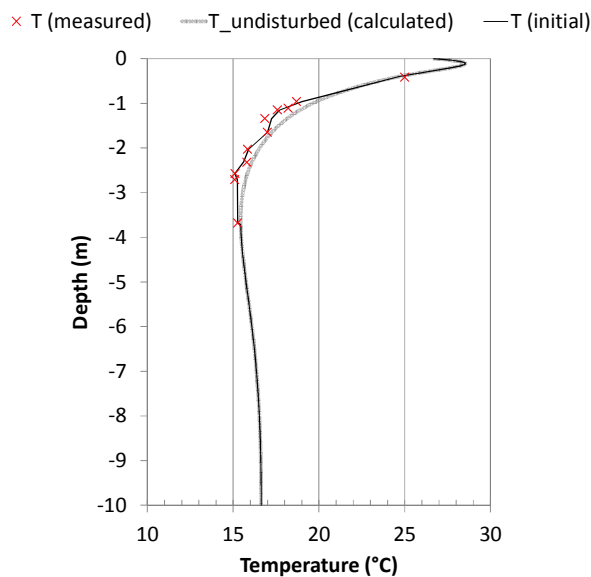Figures 4.16 and 4.17 compare the measured and calculated ground temperatures at point H.1 (-1.65 m) and H.2 (-1.15 m), respectively, during the period of simulation. The temperature for both the measurement points increases in a comparable way. Close to the HGHE, at the measurement point H.1, the temperature shows daily oscillations due to the daily switch-off of 10 h.

Contrary to the previous comparison, in the case of discontinuous and pulsed operations (as an actual GCHP system) the model allows a better estimation of the soil temperature trend. The model over-predicts the initial temperature increase in soil temperature due to the HGHE operation.

The difference between measured and calculated soil temperature is on average of about 0.6 °C and 0.4 °C at the points H.1 and H.2, respectively. In analogy with the simulation of summer 2013, the difference between the calculated and measured temperature at the point H.2 could be due to an overestimate of the soil thermal conductivity, which was carried out in different environmental conditions. Moreover, after 15 days the undisturbed ground temperature is about 5.5 °C and 4.5°C colder than the calculated ones at the measuring points H.1 and H.2, respectively.

A sensitivity study has been performed to evaluate the effect of soil thermal conductivity on temperature trend at measurement points under the same boundary conditions, as shown in Fig. 4.18 and 4.19, respectively.
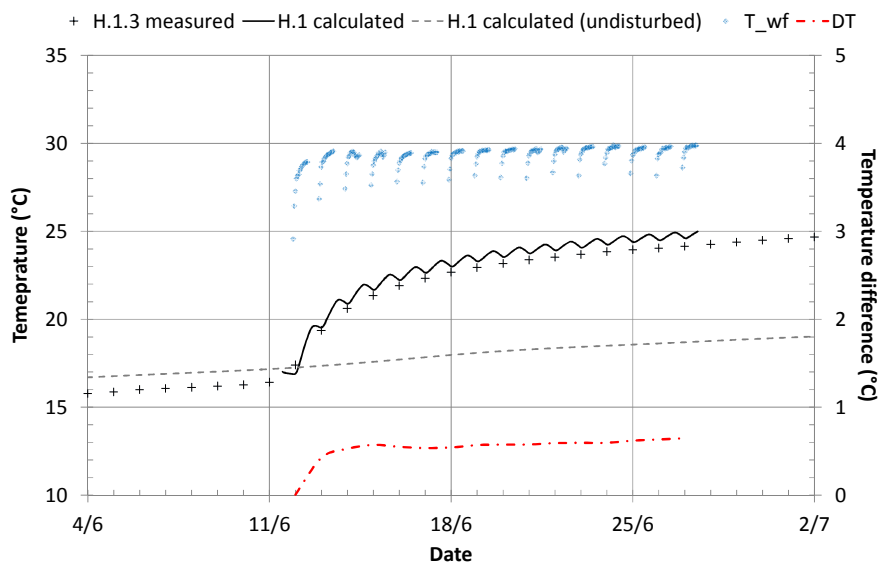

Fig. 4.16 Measured (daily average) and simulated ground temperature at sensor H.1.
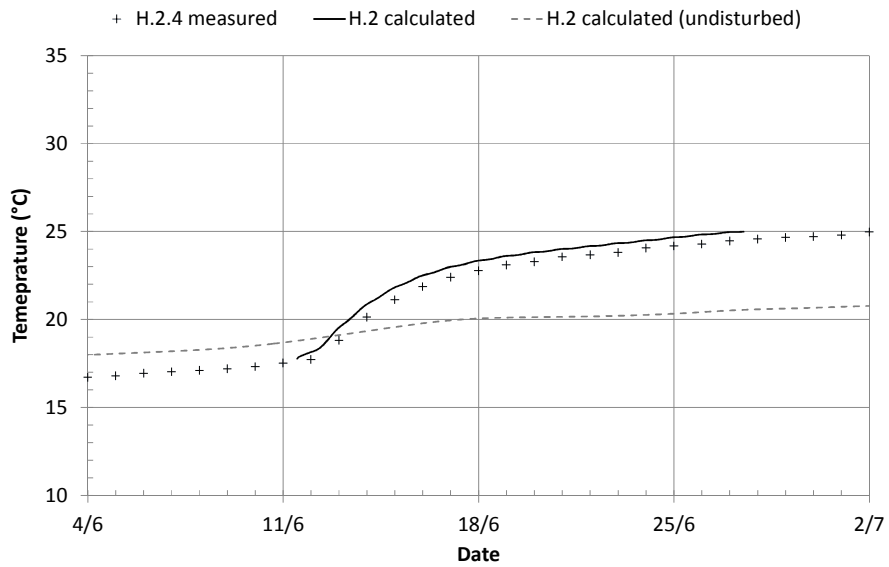
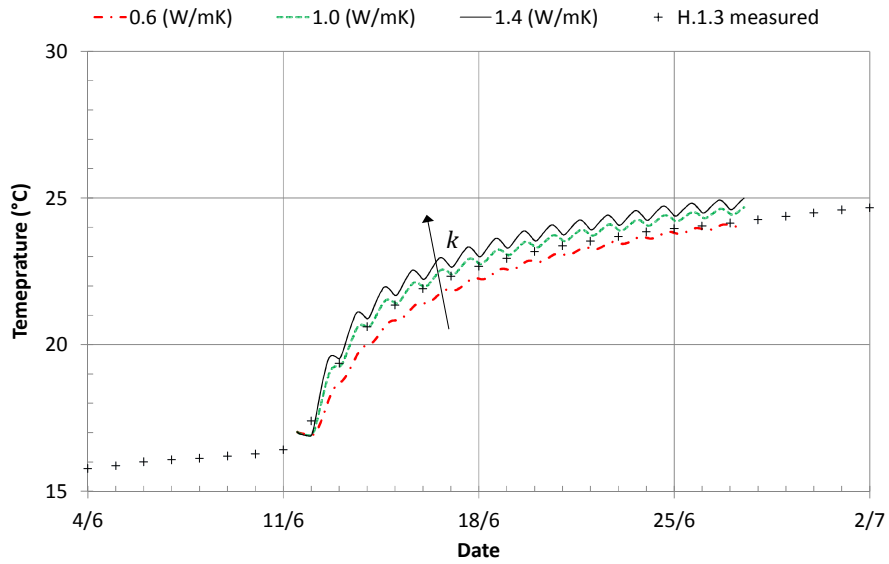Fig. 4.17 Measured (daily average) and simulated ground temperature at sensor H.2.

Fig. 4.18 Soil temperature at measurement point H.1 (0.2 m; 1.65 m) for different values of soil thermal conductivity (0.6; 1.0; 1.4).
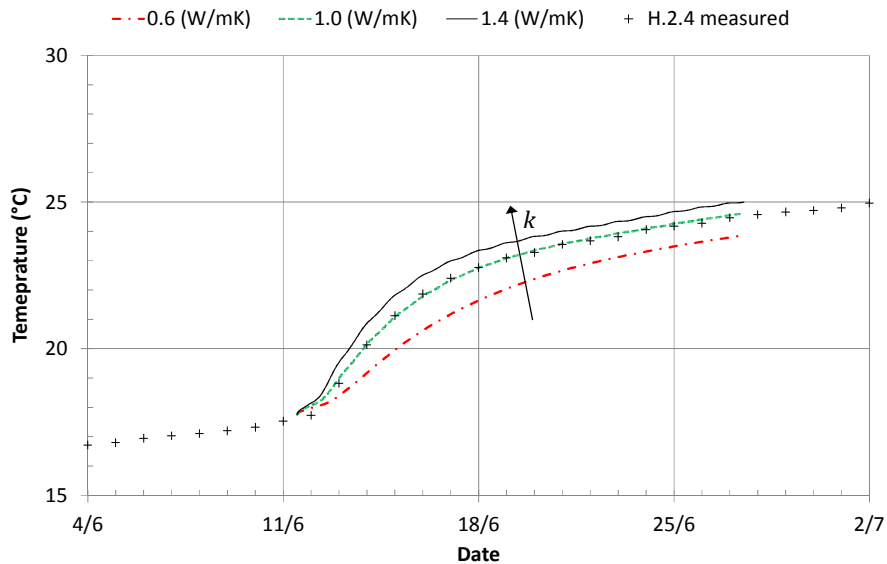
Fig. 4.19 Soil temperature at measurement point H.2 (0.2 m; 1.65 m) for different values of soil thermal conductivity (0.6; 1.0; 1.4).

Similarly to the previous simulations, two further values of thermal conductivity have been tested: 1.0 W/mK and 0.6 W/mK. The temperature fluctuations due to the daily On/Off cycle are reduced significantly as the thermal diffusivity decreases, as expected.

A reduction in thermal conductivity to 1.0 W/m produces an improvement in the agreement between measured and calculated temperature in both cases. A good correlation is obtained at point H.2. However, a significant difference is visible for a further reduction to 0.6 W/mK (0.7 °C after 15 days).

4.6   A further sensitivity analysis on soil thermal conductivity.

A further analysis is carried out in order to evaluate the effect of using two distinct values of soil thermal conductivity, one for the area around the heat exchanger and one for the surrounding ground. This study is based on the assumption that the soil filling the trench has different properties than the soil outside, although it was excavated on site.

In the model, the HGHE is placed on the axis of symmetry of the domain, at an average depth of 1.30 m, according to experimental setup. Contrary to the previous model, here the domain is divided into two parts: the installation trench (where the soil was sieved), which is 0.50 m wide and 1.85 m deep, and the ground outside, as shown in Fig. 4.20. The soil in the outer domain has the reference thermal properties, as the previous model (section 4.2).
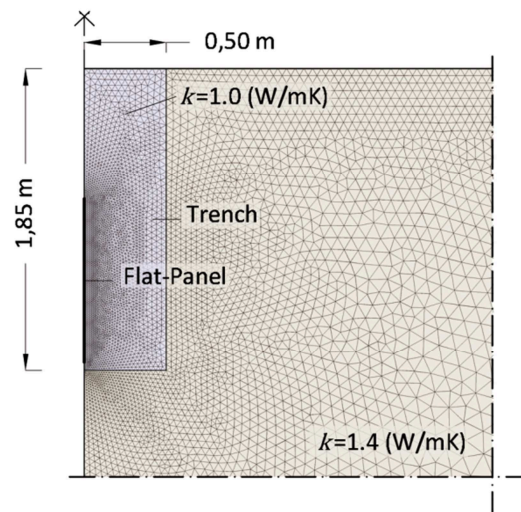
Fig. 4.20 Model domain, mesh.

The soil thermal conductivity within the trench is the average of the values calibrated for sensors H.2.4 and H.1.3, 0.60 W/mK and 1.40 W/mK, respectively. A summary of the soil properties for the simulations is reported in Table 4-2.

The simulations are repeated for Test II and Test III with the same boundary conditions, in heating and cooling mode (i.e. heating and cooling the ground), respectively. The temperature distribution for the points H1 and H.2 is compared with the case of benchmark (i.e. the whole domain with a thermal conductivity of 1.4 W/mK), as shown in Fig. 4.21. Moreover, the trend of the measured and the simulated soil temperature (with thermal conductivity of 1.0 W / mK) are reported.

Overall, a significant improvement in the calculation of soil temperature is visible, for both probes. The probe H.1, which is closer to the heat exchanger and deeper than H.2, has slightly larger differences between calculated and observed temperature. In simulating Test II conditions, the model over-predicts the initial temperature increase in soil temperature due to the HGHE operation, with a mean difference is 0.7 °C at the point H.1. On the other hand, the ground temperature is well simulated for the probe H.2, with a maximum difference of 0.2 °C between the measured and simulated temperature.

Tab. 4-2 Material properties

	Thermal conductivity	Density	Specific heat
	(W/mK)	(Kg/m^3)	(J/kgK)
Trench	1	1720	2000
Outer domain	1.40	1720	2000

+ H.2.4 measured   —— domain: k=1.4   ----- domain: k=1.0   — — trech: k=1.0; domain: k=1.4

H.1 Summer 2013
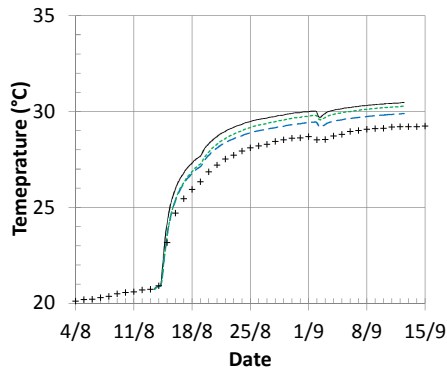
H.2 Summer 2013
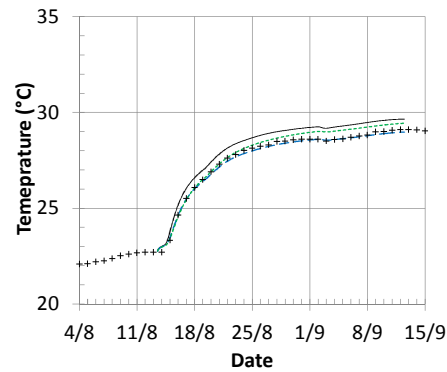
H.1 Winter 2013-2014
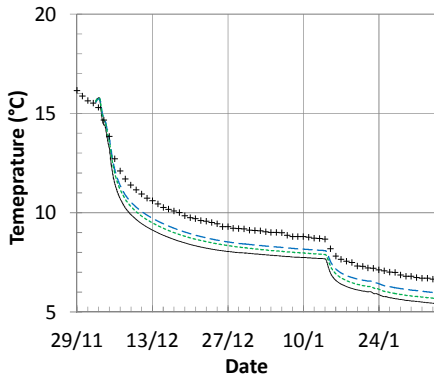
H.2 Winter 2013-2014
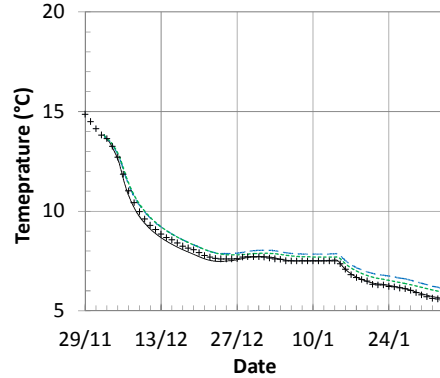
Fig. 4.21 Soil temperature at measurement point H.1 and H.2.

According to the previous simulations of Test III, the model over-predicts the effect of the heat transfer due the HGHE in the initial phase, at the point H.1. The maximum negative difference between measured and calculated soil temperature is -0.8 °C. Although a slight increase in the difference is observed at the point H.2, the temperature distribution is still well calculated in comparison with the measurements. However, the positive difference is 0.5 °C after 2 months. In view of this, the use of two different values of thermal conductivity, allows a better calculation of the temperature.

4.7   Final remarks

The bi-dimensional numerical model for Flat-Panels has been extensively tested in comparison with the experimental data collected during the tests between 2013

and 2014. The comparison has been made both in heating and cooling and for different operating modes (continuous and discontinuous).

Although with some limitations, the model allows an accurate medium term simulation of the soil temperature variation due to the GHE operation and the complex heat transfer process at the ground surface.

Overall, the difference between the predicted and measured ground temperature is small, with a maximum difference of about 1.4 °C with the reference thermal conductivity and therefore it has been retained as satisfactory. However, a more precise calculation of the soil temperature distribution can be obtained by means of a more precise estimate of the soil thermal properties, especially in the vicinity of the HGHE, as confirmed with the sensitivity analysis.

Deviations may be attributed to a number of factors. Firstly, the soil properties that control heat transfer in soil (density, thermal conductivity and specific heat capacity) are assumed to be constant in the model. Although these have been measured on soil samples collected on-site and calibrated on the basis of experimental data, significant variations could occur in time due to the migration of water vapour and water infiltration. Moreover, the shallow soil is usually inhomogeneous in urban areas.

Secondly, the two-dimensional approach is based on the assumption of small variations in the temperature of the fluid along the HGHE. Although this approach is acceptable and commonly applied, it showed a few limitations in predicting the heat transfer process during the start-up phase, when the process is highly transient.

It can be concluded that the proposed numerical approach allows reproduction of the thermal response of the ground, for different operating conditions. In view of this, this model is useful for further investigations into ground-coupled heat pumps with Flat-Panel type HGHE. Moreover, in the absence of a reliable data-set of the fluid temperature, the model provides suitable information about the trend of the temperature at the interface between fluid/soil for assigned heat load.

5.   SUMMARY AND CONCLUSIONS

Renewable energy technologies have received considerable attention in recent years as a key sector in environmental research and innovation policies. Among these, ground-source heat pumps (GSHPs) are regarded as a viable solution for space heating and cooling applications. GSHPs are applied as an alternative to conventional heating systems which offer significant energy savings.

Several typologies of GSHPs have been developed to use the ground, ground water or surface water as heat source and sink. In ground-coupled heat pump (GCHP) systems, the heat pump is thermally coupled with the ground by means of a ground heat exchanger. In widespread application, the ground heat exchanger consists of a piping system installed in vertical deep boreholes or in shallow horizontal diggings, a few meters below the ground surface. The ground thermal mass is used as a heat source or sink, without underground water extraction.

The ground heat exchanger is recognised as the least efficient component of these systems; therefore research efforts are focused on its potential development. Although vertical ground heat exchangers (VGHEs) usually have a higher performance, the horizontal installation holds some advantages in terms of costs and installation. Strengths and weaknesses of the technology have been widely discussed in Chapter 1.

The performance of horizontal ground heat exchangers (HGHEs) are strongly dependent on climatic conditions, due to the low installation depth, therefore the shallow soil is mainly used as seasonal unsteady source/sink of heat. Consequently, HGHEs are particularly effective in regions with a temperate climate, which are characterised by the absence of extremes of temperature in both winter and summer.

Chapter 1 has presented a detailed review of the current status of research on HGHEs. In last decades a considerable amount of studies have dealt with the design and performance optimization of GCHP systems. More recently, a part of this research effort has been focused on the development of innovative and more efficient concepts of HGHEs, and progress is still ongoing. This thesis fits into this context as part of these efforts. Two approaches have emerged from the literature review:

• New arrangements and configurations have been proposed for HGHEs based on conventional round pipes, such as Baskets, Helical, and Slinky Coils.

• New shapes of HGHEs have been designed and tested. Contrary to VGHEs in fact, the installation at shallow depth allows considerable freedom in the design of HGHE geometry.

In view of this, an innovative HGHE, called Flat-Panel, has been recently invented and developed at the University of Ferrara. The original geometry consists in a thin and flat shape, which is designed to enhance the performance by widening the heat transfer surface for unit length of trench in comparison to common HGHE configurations based on straight pipes.

This study has dealt with the experimental analysis and numerical simulation of Flat-Panels, with the aim of providing guidance on the operation and performance of these novel HGHEs. Overall, this thesis has intended to gain additional knowledge about the behaviour of HGHEs and the challenges related to their design. These depend primarily on the multiplicity of processes that control the heat transfer in soil.

Chapter 2 presented the experimental analysis of a ground heat exchanger equipped with Flat-Panels. Two hand-crafted prototypes were initially built and installed in an experimental setup dedicated to the study of their behaviour and performance by simulating the operation of a GCHP. Tests were conducted in different operating conditions (heating and cooling) and for different operating modes (continuous, discontinuous and pulsed).

Overall, the HGHE showed very good performance in terms of heat transfer rate both in cooling and heating operations. In winter, the average rate of heat transfer was about 28 W/m under continuous operation; approximately 48 W/m under discontinuous operation due to the lower daily energy extraction. The rate of heat transfer was significantly higher in heating mode due to the higher temperature difference between the working fluid and the undisturbed soil. In summer in fact, the average RHT was about 58 W/m and 80 W/m (from July to September) under continuous and discontinuous/pulsed operation, respectively.

Consequently, the land area requirement for HGHE can be reduced for a given heat load by employing the Flat-Panels. On the other hand, for a given HGHEs size, the ground thermal load per unit of heat transfer surface is lower; therefore more favourable working conditions are achievable for a GCHP.

The performance of the HGHE was affected by the available temperature difference between the working fluid and the undisturbed ground temperature. Moreover, the rate of heat transfer slightly increased in late heating/cooling season, independently from energy extracted/released from and to the ground. Overall, these results strengthens the idea of a strong relationship between the performance of HGHEs and the natural heat transfer process at the ground surface.

Finally, the heat transfer due to the HGHEs operation produced an extended thermal anomaly in the shallow soil. However, according to the environmental conditions the undisturbed soil temperature was naturally achieved after a few months of HGHE inactivity, regardless of the amount of energy exchanged. As a consequence, according to recent studies, any seasonal thermal drift in the soil is expected for HGHEs, also after long-term operations.

The third section of the thesis dealt with the numerical simulation of the Flat-Panel. Applications of analytical and numerical models for HGHEs were reviewed in Chapter 1. Numerical modelling of HGHE exchangers involved many aspects. This analysis was intended to evaluate the evolution of the thermal field in the ground due to heat extraction/release by Flat-Panels. A 2D approach was considered a reasonable simplification of the problem of studying the temperature distribution in the ground induced by localised heat sources (i.e. the Flat-Panels). The simulations were conducted by means of a commercial finite-element numerical code COMSOL Multiphysics, by solving the unsteady-state heat transfer problem in a 2D domain. According to this approach, the Flat-Panel shape was considered as a cold/hot plate, to and from which heat flows from the surrounding soil mainly by heat conduction, therefore the Flat-Panel was modelled as a boundary condition.

The heat transfer processes at the ground surface were included in detail in the numerical model. The energy balance at the soil surface has a decisive role in determining the temperature of the soil, therefore the proper assignment of the boundary condition to the ground surface is important in modelling HGHEs.

In view of this, a model of the energy balance at the ground surface (GSEB) based on the ground surface properties and weather variables was developed, and implemented in the numerical model to be tested as a boundary condition at ground surface. The use of such a boundary condition would allow a better prediction of soil temperature variations, therefore an higher accuracy was expected in the numerical simulation of the Flat-Panel. The GSEB model was validated with the observed soil temperature data at different depths, proving to accurately predict the temperature in the soil.

In addition, the effect on numerical solutions of different boundary conditions when assigned at the ground surface was analysed in modelling HGHEs. The GSEB model, the equivalent heat flux and temperature at the ground surface were used as the boundary condition of the 1st, 2nd and 3rd kind, respectively. Simulations were carried out to test the HGHE energy performance in heating and cooling, under the same environmental conditions.

The results of this study indicate that the use of an equivalent heat flux at the ground surface should be considered as a precautionary approach. On the other hand, when a boundary condition of the first kind (i.e. equivalent surface temperature) is applied, a significant constraint is imposed to the surface temperature, which is not allowed to vary due to the HGHE heat transfer. Anyway, this approach can be considered as a reasonable simplification, which can be useful for preliminary analysis. However, the correct estimation of the surface temperature is a major issue and a preliminary simulation with a GSEB could be required. Consequently, a 3rd boundary condition (e.g. the ground surface energy balance) in modelling HGHEs is a preferable approach to the problem, not affecting the calculation time.

Chapter 4 provided a comparison between the simulated and the measured ground temperature. The comparison was focused on the temperature variation in

soil, due to the combined effect of the Flat-Panel operation and the natural heat transfer process at the ground surface. The numerical model was tested with data collected during tests between 2013 and 2014 from the experimental setup at the Dept. of Architecture in Ferrara. The comparison was performed both in heating and cooling and for different operating modes (continuous and discontinuous). A comprehensive dataset of weather variables and of mean temperature of the working fluid was used as input in the model.

Overall, the models produced reasonable matches to the measured ground temperature variation due to the HGHE operation and the complex heat transfer process at the ground surface. Deviations may be attributed to the soil properties that were assumed to be constant in the model although, significant variations could occur in time and space due to the migration of water vapour, water infiltration and soil heterogeneity. The generalisability of these results is subject to certain limitations. The thermal properties of the soil in fact, were measured on soil samples collected on-site and calibrated on the basis of experimental data. In view of this, a sensitivity analysis was performed to evaluate the effect of variations in the soil thermal conductivity.

The proposed numerical approach could be useful for further investigations on ground-coupled heat pumps with Flat-Panel type. Moreover, in the absence of a reliable data-set of the fluid temperature, the model provides suitable information about the trend of the temperature at the interface between fluid/soil for the assigned heat load.

REFERENCES

Ingersoll, L. & Zobel, O., 1954. *Heat Conduction with Engineering, Geological, and other Applications.* New York: McGraw-Hill.

Adamovsky, D., Neuberger, P. & Adamovsky, R., 2015. Changes in Energy and Temperature in the Ground Mass with Horizontal Heat Exchangers-The Energy Source for Heat Pumps. *Energy and Buildings,* Issue 92, pp. 107-115.

Alexandri, E. & Jones, P., 2007. Developing a one-dimensional heat and mass transfer algorithm for describing the effect of green roofs on the built environment: Comparison with experimental results. *Building and Environment,* Volume 42, pp. 2835-2849.

Allen, R. G., Pereira, L. S., Raes , D. & Smith, M., 1998. *Crop evapotranspiration-Guidelines for computing crop water requirements No 56,* Rome: Food and Agricolture Organisation.

Antonopoulos, V., 2006. Water Movement and Heat Transfer Simulations in a Soil und Ryegrass. *Biosystems Engineering ,* Volume 95, pp. 127-138.

ARPA Emilia-Romagna, Servizio Idro-Meteo-Clima, 2009. *Atlante Idroclimatico dell'Emilia-Romagna 1961-2008,* s.l.: ARPA Emilia-Romagna.

ARPA-EM, s.d. *Sistema dexter.* [Online]
Available at:
http://www.arpa.emr.it/dettaglio_generale.asp?id=3284&idlivello=1625

ASHRAE, 1999. *ASHRAE Handbook: HVAC Applications.* Atlanta: ASHRAE Inc..

ASHRAE, 2007. *2007 ASHRAE Handbook - Heating, Ventilating, and Air-Conditioning Applications.* s.l.:ASHRAE.

Battarra, M., 2013. *Analisi numerica delle prestazioni energetiche di una sonda geotermica piana.* s.l.:Università degli Studi di Ferrara, Dipartimento di Ingegneria.

Beier, R. & Holloway, W., 2015. Changes in the Thermal Performance of Horizontal Boreholes with Time. *Applied Thermal Engineering,* Issue 78, pp. 1-8.

Benazza, A. et al., 2011. Numerical Investigation of Horizontal Ground Coupled Heat Exchanger. *Energy Procedia,* Issue 6, pp. 29-35.

Best, M. J., 1998. A Model to Predict Surface Temperatures. *Boundary Layer Meteorology,* Volume 88, pp. 279-306.

Bortoloni, M. & Bottarelli, M., 2015. On the sizing of a flat-panel ground heat exchanger. *International Journal of Energy and Environmental Engineering,* 6(1), pp. 55-63.

Bortoloni, M., Bottarelli, M. & Yuehong , S., 2015. *A Study on the Effect of Ground Surface Boundary Conditions in Modelling Shallow Ground Heat Exchangers.* Nottingham, s.n.

Bottarelli, M., 2013. A preliminary testing of a flat panel ground heat exchanger. *International Journal of Low-Carbon Technologies ,* 8(2), pp. 80-87.

Bottarelli, M. & Bortoloni, M., 2013. *Field behaviour of a Flat Panel ground heat exchanger.* Qwara, Malta, s.n.

Bottarelli, M. & Di Federico, V., 2010. *Adoption of flat panels in soil heat exchange.* Abu Dhabi, s.n.

Bottarelli, M., Fujii, H. & Di Federico, V., 2014. *Performance of a drainage trench employed as ground heat exchanger.* Kyoto, s.n.

Bottarelli, M. & Gabrielli, L., 2011. Payback period for a ground source heat pump system. *Internation Journal of Heat and Technology,* 29(2), pp. 145-150.

Boughanmi, H., Lazaar, M., Bouadila, S. & Farhat, A., 2015. Thermal Performance of a Conic Basket Heat Exchanger Coupled to a Geothermal Heat Pump for Greenhouse Cooling Under Tunisian Climate.. *Energy and Buildings,* Issue 104, pp. 87-96.

Brutsaert, W., 1975. On a Derivable Formula for Long-Wave Radiation From Clear Skies. *Water Resources Research,* 11(5), pp. 742-744.

Brutsaert, W., 2005. *Hydrology, An Introduction.* Cambridge: Cambridge University Press.

CANMET Energy Technology Centre, 2005. *Ground-Source Heat Pump Project Analysis.* s.l.:Minister of Natural Resources Canada.

Carslaw, H. & Jaeger, . J., 1947. *Heat conduction in solids.* Oxford: Claremore Press.

Cauret, O. & Bernier, M., 2009. *Experimental validation of an underground compact collector model..* Stockholm, s.n.

Çengel, Y. A. & Ghajar, A. J., 2015. *Heat and Mass Transfer - Fundamentals and Applications.* 5th a cura di New York: McGraw-Hill Education.

Chiasson, A., 2006. *geothermalcommunities.* [Online]
Available at:
http://www.geothermalcommunities.eu/assets/elearning/6.25.chiasson0306_4.pp
t.

Chiasson, A. D., 1999. *Advances in modelling of ground source heat pump system.*
s.l.:Oklahoma State University.

Choi, M., Jacobs, J. M. & Kustas, W. P., 2008. Assessment of clear and cloudy sky
parametrizations for daily downwelling longwave radiation over different land
surfaces in Florida, Usa. *Geophysical Resarch Letters ,* Volume 35, pp. 1-6.

Congedo, P., Colangelo, G. & Starace, G., 2012. CFD Simulations of Horizontal
Ground Heat Exchangers: A Comparison Among Different Configurations. *Applied
Thermal Engineering,* Issue 33-34, pp. 24-32.

Dasare, R. R. & Saha, S. K., 2015. Numerical Study of Horizontal Ground Heat
Exchanger for High Energy Demand Applications. *Applied Thermal Engineering,*
Issue 85, pp. 252-263.

Deardorff, J. W., 1978. Efficient Prediction of Ground Surface Temperature and
Moisture, with Inclusion of a Layer of Vegetation. *Intenational Journal of
Geophysical Research,* 83(C4), pp. 1889-1903.

Demir, H., Koyun, A. & Temir, G., 2009. Heat Transfer of Horizontal Parallel Pipe
Ground Heat Exchanger and Experimental Verification. *Applied Thermal
Engineering,* Issue 29, pp. 224-233.

DOE, 2001. *Ground-Source Heat Pumps Applied to Federal Facilities,* s.l.: Energy,
The US Department of.

Duffie, J. A. & Beckman, W. A., 2013. *Solar Engineering of Thermal Processes.*
Fourth Edition a cura di Hoboken: Wiley.

Esen, H., Inalli, M. & Esen, M., 2007. Numerical and Experimental Analysis of a
Horizontal Ground Coupled Heat Pump. *Building and Environment,* Issue 42, pp.
1126-1134.

Eskilson, P., 1987. *Thermal Analysis of Heat Extraction Boreholes.* s.l.:University of
Lund.

FAO, s.d. *FAO Document Repository.* [Online]
Available at: http://www.fao.org/documents/en/

Frankenstein , S. & Koenig, G. G., 2004. *Fast All-season Soil Strenght (FASST).* Washington, D.C.: U.S. Army Corps of Engineers.

Fujii, H., Nishi, K., Komaniwa, Y. & Chou, N., 2012. Numerical Modelling of Slinky-Coil Horizontal Ground Heat Exchangers. *Geothermics,* Issue 41, pp. 55-62.

Fujii, H., Okubo, H., Cho, N. & Ohyama, K., 2010. *Field Tests of Horizontal Ground Heat Exchangers.* Bali, s.n.

Fujii, H., Yamasaki, S. & Maehara, T., 2013. *Numerical Modelling of Slinky-Coil Horizontal Ground Heat Exchangers Considering Snow Coverage Effects.* Stanford, s.n.

Fujii, H. et al., 2013. Numerical Simulation and Sensitivity Study of Double-Layer Slinky-Coil Horizontal Ground Heat Exchangers. *Geothermics,* Issue 47, pp. 61-68.

Gan, G., 2013. Dynamic Thermal Modelling of Horizontal Ground-Source Heat Pumps. *International Journal of Low-Carbon Technologies,* Issue 8, pp. 95-105.

Garratt, J. R., 1992. *The Atmospheric Boundary Layer.* Cambridge: Cambridge University Press.

Gouda, M. M., Danaher, S. & Underwood, C. P., 2002. Building thermal model reduction using nonlinear constrained optimization. *Building and environment,* Issue 37, pp. 1255-1265.

Grant, M. A., Donaldson, I. G. & Bixley, P. F., 1982. *Geothermal Reservoir Engineering.* New York: Academic Press, Inc..

Hart, D. P. & Couvillion, . R., 1986. *Earth-coupled Heat Transfer.* s.l.:National Water Well Association.

Herb, W. R., Janke, B., Mohseni, O. & Stefan , H. G., 2008. Ground surface termperature simulation for different land covers. *Journal of Hydrology,* Volume 356, pp. 327-343.

Herb, W. R., Janke, B., Mohseni, O. & Stefan, H. G., 2006. *All-Weather Ground Surface Temperature Simulation,* Minneapolis: Minnesota Pollution Control Agency.

Hughes, P. & Im, P., 2012. *Foundation Heat Exchanger Final Report: Demonstration, Measured Performance and Validated Model and Design Tool,* s.l.: s.n.

Hwang Kwang-il, et al., 2007. A Study on the Seasonal Performances Evaluation of the Horizontal-Type Geothermal Heat Exchanger Installed in the Foundation Slabs

of a Complex Building. *Journal of the Korean Solar Energy Society,* Volume 27, pp. 11-17.

IGSHPA, 1991. *Closed-Loop/Ground-Source Heat Pump - Design and Installation Standards.* s.l.:International Ground Source Heat Pump Association, Oklahoma State University.

IGSHPA, 2009. *Ground Source Heat Pump residential and light commercial design and installation guide.* s.l.:s.n.

Ingersoll, L. R. & Plass, H. J., 1948. Theory of the ground pipe heat source for the heat pump. *Heating, Piping & Air Conditioning,* 20(7), pp. 119-122.

Jansson , P.-E. & Karlberg, L., 2001. *Coupled heat and mass transfer model for soil-plant-atmosphere systems.* Stockholm: Royal Institute of Technology, Dept. of Civil and Enviromental Engineering.

Jones, F., 1994. *Closed-Loop Gethermal Systems - Slinky Installation Guide.* s.l.:IGSHPA.

Jürges, W., 1924. Der Wärmeübergang an einer ebenen Wand. *Gesundheits-Ingenieur,* Volume 19, pp. 1227-1249.

Kavanaugh, S. P., 1984. *Simulation and Experimental Verification of Vertical Ground-Coupled Heat Pump Systems.* s.l.:Oklahoma State University.

Kavanaugh, S. & Rafferty, K., 1997. *Ground Source Heat Pumps - Design of Geothermal Systems for Commercial and Institutional Buildings.* s.l.:ASHRAE.

Koyoun, A., Demir, H. & Zakir, T., 2009. Experimental Study of Heat Transfer of Buried Finned Pipe For Ground Source Heat Pump Applications. *International Communications in Heat And Mass Transfer,* Issue 36, pp. 739-743.

Krarti, M., Lopez-Alonzo, C., Claridge, D. & Kreider, J., 1995. Analytical Model to Predict Annual Soil Surface Temperature Variation. *Journal of Solar Energy Engineering ,* Volume 117, pp. 91-99.

Kupiec, K., Larwa, B. & Gwasdera , M., 2015. Heat Transfer in Horizontal Ground Heat Exchangers. *Applied Thermal Engineering,* Issue 75, pp. 270-276.

Kustas, W. P., Daughtry, C. S. & Van Oevelen, P. J., 1993. Analytical Treatment of the Realationships Between Soil Heat Flux/Net Radiation Ratio and Vegetation Indices. *Remote Sensing Environment ,* Volume 46, pp. 319-330.

Kusuda, T. & Achenbach, P., 1965. Earth Temperatures and Thermal Diffusivity at Selected Stations in the United States. *ASHRAE Transactions,* Issue 71, pp. 61-74.

Lee, K. H. & Strand, R. H., 2008. The cooling and heating potential of an earth tube system in building. *Energy and Buildings,* Volume 40, pp. 486-494.

Luo, Z. & Asproudi, C., 2015. Subsurface urban heat island and its effect on horizontal ground-source heat pump potential under climate change. *Applied Thermal Engineering,* Volume 90, pp. 530-537.

McAdams, W. H., 1954. *Heat Transmission.* 3rd a cura di s.l.:McGraw-Hill.

Mei, V., 1986. *Horizontal Ground Coil Heat Exchanger. Theoretical and Experimental Analysis,* s.l.: ORNL.

Mihalakakou, G., 2002. On estimating soil surface temperature profiles. *Energy and Buildings,* Volume 34, pp. 251-259.

Mihalakakou, G., Santamouris, M., Lewis, J. & Asimakopoulos, D., 1997. On the Application of the Energy Balance Equation to Predict Ground Temperature Profiles. *Solar Energy,* Volume 60, pp. 181-190.

Morini, G. L. & Piva, S., 2007. The simulation of transients in thermal plant. Part I: Mathematical model. *Applied Thermal Engineering,* Issue 27, pp. 2138-2144.

Naili, N., Attar, I., Hazami, M. & Farhat, A., 2012. Experiemental Analysis of Horizontal Ground Heat Exchanger for Northern Tunisia. *Journal of Electronics Cooling and Thermal Control,* Issue 2, pp. 44-51.

Nam, Y. & Chae, H.-B., 2014. Numerical Simulation for The Optimum Design of Ground Source Heat Pump System Using Building Foundation as Horizontal Heat Exchanger. *Energy,* 73(C), pp. 933-942.

Nam, Y., Ooka, R. & Hwang, S., 2008. Development of a numerical model to predict heat exchange rates for a ground-source heat pump system. *Energy and Buildings,* Volume 40, pp. 2133-2140.

Ouzzane, M., Eslami-Nejad, P., Bedache, M. & Aidoun, Z., 2015. New correlations for the prediction of the undisturbed ground temperature. *Geothermics,* Volume 53, pp. 379-384.

Palyvos, J. A., 2008. A survey of wind convection coefficient correlations for building envelope energy systems modeling. *Applied Thermal Engineering,* Volume 28, pp. 801-808.

Piechowski, M., 1998. Heat and Mass Transfer Model of a Ground Heat Exchanger: Validation and Sensitivity Analysis. *International Journal of Energy Research,* Issue 22, pp. 965-979.

Piechowsky, M., 1999. Heat and Mass Transfer Model of a Ground Heat Exchanger: Theroretical Development. *International Journal of Energy Research,* Issue 23, pp. 571-588.

Ping, C., Hongxing , Y. & Zhaohong, F., 2006. Heat transfer analysis of ground heat exchangers. *Applied Thermal Engineering,* Volume 26, p. 1169–1175.

Popiel, C., Wojtkowiak, J. & Biernacka, B., 2001. Measurements of temperature distribution in ground. *Experimental Thermal and Fluid Science,* 25(5), pp. 301-309.

Prata, A., 1996. A new long-wave formula for estimating clear-sky radiation at the surface.. *Quarterly Journal of the Royal Meteorological Society,* Volume 122, pp. 1127-1151.

Qin, Z., Berliner, P. & Karnieli, A., 2002. Numerical solution of a complete surface energy balance model for simulation of heat fluxes and surface temperature under bare soil enviroment. *Applied Mathematics and Computation,* Volume 130, pp. 171-200.

Raymond, J., Mercier, S. & Nguyen, L., 2015. Designing coaxial ground heat exchangers with a thermally enhanced outer pipe. *Geothermal Energy,* 3(7).

Reuss, M. & Sanner, B., 2001. *Design of Closed-Loop Heat Exchangers.* s.l., s.n., pp. 147-156.

Roth, K., 2012. *Soil Physics. Lecture Notes..* s.l.:Institute of Environmental Physics, Heidelberg University.

Sailor, D., 2008. A green roof model for building energy simulation programs. *Energy and Buildings,* Volume 40, pp. 1466-1478.

Santanello, J. A. & Friedl, M. A., 2003. Diurnal Covariation in Soil Heat Flux and Net Radiation. *Journal of Applied Meteorology,* Volume 42, pp. 851-862.

Sauer, T. J. & Horton, R., 2005. Micrometeorology in Agricultural Systems. In: Madison: American Society of Agronomy, Crop Science of America, Soil Science Society of America.

Scott, D., 1978. Air movements within six vegetations. *New Zealand Journal of Agricoltural Research,* Volume 21, pp. 651-654.

SIA, 1996. *Grundlagen zur Nutzung der untiefen Erdwärme.* s.l.:s.n.

Simms, R., Haslam, S. & Craig, J., 2014. Impact of Soil Hetereogeneity on the Functioning of Horizontal Ground Heat Exchanger. *Geothermics,* Issue 50, pp. 35-43.

Sofyan, S., Hu, E. & Kotousov, A., 2015. A New Approach to Modelling of a Horizontal Geo-Heat Exchanger with an Internal Source Term. *Applied Energy.*

Spitler, J. D., Marshall, C., Delahoussaye, R. & Manicham, M., 1996. *Users Guide of GLHEPRO.* Stillwater: Oklahoma State University.

Sugita, M. & Brutsaert, W., 1993. Cloud Effect in the Estimation Of Instantaneous Downward Longwave Radiation. *Water Resources Research,* 29(3), pp. 599-605.

Swinbank, W., 1963. Long-wave radiaton from clear skyes. *Quarterly Journal of the Royal Meteorological Society,* Volume 89, pp. 339-348.

Tsilingiridis, G. & Papakostas, K., 2014. Investigating the relationship between air and ground temperature variations in shallow depths in northern Greece. *Energy,* Volume 73, pp. 1007-1016.

UNI 11466, 2012. *Heat pump geothermal systems - Design and sizing requirements,* s.l.: s.n.

UNI/TS 11300, 2012. *Prestazioni energetiche degli edifici - Parti 1 e 2,* s.l.: s.n.

VDI, 2001. *VDI 4640 Blatt 2,* Dusseldorf: s.n.

Wärnelhöf, J. & Kronström, U., 2007. *Ground Source Heat Pump With a New Compact Collector.* [Online]
Available at: www.cres.gr/kape/pdf/geotherm/23.pdf

Wilson, M. B., Rogelio, L. & Pedro, J. M., 2015. A Firs-Order Study of Reduced Energy Consumption via Increased Thermal Capacitance with Thermal Storage Management in a Micro-Building. *Energies,* Issue 8ù, pp. 12266-12282.

Wu, Y. et al., 2010. Experimental Measurement and Numerical Simulation of Horizontal-Coupled Slinky Ground Source Heat Exchangers. *Applied Thermal Engineering,* Issue 30, pp. 2574-2583.

Xiong, Z., Fisher, D. & Spitler, J., 2015. Development and Validation of a Slinky Ground Heat Exchanger Model. *Applied Energy,* Issue 141, pp. 57-69.

Yoon, S., Lee, S.-R. & Go, G.-H., 2015. Evaluation of Thermal Efficiency in Different Types of Horizontal Ground Heat Exchangers. *Energy and Buildings,* Issue 105, pp. 100-105.

Zoelly, H., 1912. *Heizverfahren.* Zürich, Patent n. Nr. 59350.

Sezioni

Dottorati di ricerca

Il tuo indirizzo e-mail

marco.bortoloni@unife.it

Oggetto:

Dichiarazione di conformità della tesi di Dottorato

Io sottoscritto Dott. (Cognome e Nome)

Bortoloni Marco

Nato a:

Este

Provincia:

Padova

Il giorno:

02/04/1984

Avendo frequentato il Dottorato di Ricerca in:

Scienze dell'Ingegneria

Ciclo di Dottorato

28

Titolo della tesi:

Experimental analysis and numerical simulation of a Flat-Panel ground heat exchanger

Titolo della tesi (traduzione):

Analisi sperimentale e simulazione numerica di uno scambiatore geotermico di tipo Flat-Panel

Tutore: Prof. (Cognome e Nome)

Piva Stefano

Settore Scientifico Disciplinare (S.S.D.)

ING-IND/10

Parole chiave della tesi (max 10):

Ground source heat pumps, Horizontal ground heat exchangers, Flat-Panel
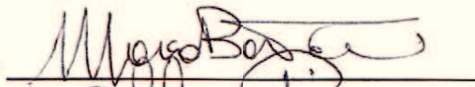
Consapevole, dichiara

CONSAPEVOLE: (1) del fatto che in caso di dichiarazioni mendaci, oltre alle sanzioni previste dal codice penale e dalle Leggi speciali per l'ipotesi di falsità in atti ed uso di atti falsi, decade fin dall'inizio e senza necessità di alcuna formalità dai benefici conseguenti al provvedimento emanato sulla base di tali dichiarazioni; (2) dell'obbligo per l'Università di provvedere al deposito di legge delle tesi di dottorato al fine di assicurarne la conservazione e la consultabilità da parte di terzi; (3) della procedura adottata dall'Università di Ferrara ove si richiede che la tesi sia consegnata dal dottorando in 2 copie di cui una in formato cartaceo e una in formato pdf non modificabile su idonei supporti (CD-ROM, DVD) secondo le istruzioni pubblicate sul sito: http://www.unife.it/studenti/dottorato alla voce ESAME FINALE –

disposizioni e modulistica; (4) del fatto che l'Università, sulla base dei dati forniti, archivierà e renderà consultabile in rete il testo completo della tesi di dottorato di cui alla presente dichiarazione attraverso l'Archivio istituzionale ad accesso aperto "EPRINTS.unife.it" oltre che attraverso i Cataloghi delle Biblioteche Nazionali Centrali di Roma e Firenze; DICHIARO SOTTO LA MIA RESPONSABILITA': (1) che la copia della tesi depositata presso l'Università di Ferrara in formato cartaceo è del tutto identica a quella presentata in formato elettronico (CD-ROM, DVD), a quelle da inviare ai Commissari di esame finale e alla copia che produrrò in seduta d'esame finale. Di conseguenza va esclusa qualsiasi responsabilità dell'Ateneo stesso per quanto riguarda eventuali errori, imprecisioni o omissioni nei contenuti della tesi; (2) di prendere atto che la tesi in formato cartaceo è l'unica alla quale farà riferimento l'Università per rilasciare, a mia richiesta, la dichiarazione di conformità di eventuali copie; (3) che il contenuto e l'organizzazione della tesi è opera originale da me realizzata e non compromette in alcun modo i diritti di terzi, ivi compresi quelli relativi alla sicurezza dei dati personali; che pertanto l'Università è in ogni caso esente da responsabilità di qualsivoglia natura civile, amministrativa o penale e sarà da me tenuta indenne da qualsiasi richiesta o rivendicazione da parte di terzi; (4) che la tesi di dottorato non è il risultato di attività rientranti nella normativa sulla proprietà industriale, non è stata prodotta nell'ambito di progetti finanziati da soggetti pubblici o privati con vincoli alla divulgazione dei risultati, non è oggetto di eventuali registrazioni di tipo brevettale o di tutela. PER ACCETTAZIONE DI QUANTO SOPRA RIPORTATO

Firma del dottorando

Ferrara, li 07/03/2016 Firma del Dottorando _____

Firma del Tutore

Visto: Il Tutore Si approva Firma del Tutore _____